CHAPTER ONE

INTRODUCTION

1.1 Background to the Study

Honey is a sweet fluid produced by honey bees (*Apis Mellifera*) from the nectar of flowers (White, 1992). It is composed of mainly carbohydrates such as monosaccharides (glucose and fructose) and oligosaccharides like sucrose, maltose, melezitose, raffinose to mention a few. Pure honey also contains proteins, fats, water, vitamins and minerals. It is reputed to have a diverse set of nutritional and medicinal benefits. This and honey's pleasant taste of universal appeal ensure a sustained high demand for the product. The supply of honey is, however, quite constrained and hardly ever matches the demand. Consequently, the product always commands a relatively high price and is exposed to adulteration and imitation. Sugar based products such as fructose, glucose, sucrose, and starch are used by unscrupulous vendors to adulterate honey. Some bee keepers even feed their insects with the aforementioned to enhance the volume of "honey" produced and, hence, to maximize profit at the expense of the product's quality. Experienced fake honey vendors add honey flavor to caramels to mimic honey. Adulterated or fake honey would not be expected to have the potency of the genuine product as they would contain little or none of the constituents that impart nutritional and medicinal values to the latter. There is, thus, a strong imperative to constantly ascertain the quality of what is sold in the market as honey for public consumption, to hospitals for medicinal applications and to the industry for commercial purposes.

This need is presently met by means of time consuming and expensive procedures based on physicochemical characterizations of the product. In view of the wide and varied use to which honey is put and in view of the varied scale of its utilization a simple inexpensive

characterization of the integrity of fluids passed off as honey is called for. This study explores the efficacy of a rheological characterization method to answer this need.

Rheology is the study of deformation and flow of fluids. Its goal is to understand and predict the behaviour of fluids undergoing deformation. The rheological responses of fluid materials are obtained in terms of the dependence of their apparent viscosities on shear rate, and shear stress. A good understanding of rheology is essential to understanding many processes in engineering and to other areas of research. All materials are made up of molecules under relative motion. These molecular motions are influenced by interaction potentials arising from the presence of the molecules. The same molecular motions and interactions are responsible for rheology (Bird *et al.,* 2006).

There are many types of fluids: pure substances, mixtures, dispersions and solutions, which fall into categories of either simple or structured fluids (Franck, 2004). Each has its own unique behaviour when subjected to shear. In general, when a material such as a solution or pure substance has a uniform phase, it is referred to as a simple fluid. The viscosities of pure substances and simple fluids are independent of shear rate and are independent of deformation history. Such fluids are referred to as Newtonians. Materials which are made up of more than one phase, such as solid particles dispersed in a liquid, gas particles in a foam or emulsion of immiscible liquids are termed structured fluids which do not follow Newtonian behaviour. Honey and most food materials belong to this class of fluids (Rao and Steffe, 1992).

Structured fluids, unlike Newtonians, do not obey simple linear relationship between applied shear stress and shear rate. Nearly all these materials have their viscosities decreasing with increasing rate of shear. This phenomenon of shear thinning becomes progressively larger as the volume concentration of oligomers increases. The observed rheological responses reflect

the macroscopic state. They are, however, affected by the changes and properties at the molecular or microscopic levels. A major challenge is to establish links between macroscopic rheological properties with changes at the molecular and microscopic levels (Rao, 2006). Rheological data on honey together with data on its composition and structure should lead to understanding the relationship between them (Nwalor *et al.,* 2014). In turn such knowledge should lead to the improvement in the assessment of the integrity of honey presented for consumption through the development of cheap rheological methods.

1.2 Statement of the Problem

The world honey production capacity in 2010 was 1,500,000 tons while the demand in the same year was 2,000,000 tons (FAO*,* 2012). Little wonder, therefore, that honey attracts the illicit attention of fraudsters who adulterate or fake the product for quick money and to meet up with huge gap between the demand and the supply of the product. For this reason there is a strong imperative to constantly screen for quality, what is sold in the market as honey for public consumption and to industry for commercial purposes. This requires an understanding of known methods of honey adulteration and faking on the one hand and on the other, the development of cheap procedures for assessing the degree of corruption. Presently, honey is characterized using its physicochemical properties by tedious and expensive procedures. An alternative non destructive economical method based on rheology is worthy of study and of development into a tool for differentiating pure from adulterated or imitation honey. Collateral to the required development process is the rheological characterization of this valuable natural product, in its own right, an important technical information.

1.3 Aim and Objectives of the Study

The aim of this study is to develop a test method based on rheology that can differentiate pure from adulterated honey.

The objectives are to:

i. explore the efficacy of utilizing honey rheology to assess its purity.

ii. extract structural and compositional information from the rheological data.

iii. establish rheological characterization as a testing method for honey quality.

1.4 Significance of the Study

The uses of honey cannot be over emphasized. It span across nutritional, medicinal and industrial uses. These three major areas of honey applications lead to its high demand in its pure form. The high demands for honey and low supply of the product promotes adulteration and imitation. Existing methods for honey quality assessment are tedious, time consuming and expensive. The rheological method for quality assessment of fluids will be desirable being economical and simple. This study seeks to establish the efficacy of rheological assessment for honey. A test method deriving from this study will find application in the quality assessment of other fluids.

CHAPTER TWO

LITERATURE REVIEW

This section, anticipatory of the value of rheograms as reflective of fluid composition and structure, reviews the literature on rheological characterization of fluids. The prevailing methods for the assessment of honey quality are also covered, as are special characteristics of honey. The latter which includes the antibacterial property of honey would be tested for possible correlation with deductions derived from this study's rheological assessment of quality.

2.1 Theory of Viscosity

For Newtonian fluids, viscosity is defined as the constant of proportionality between the tangential stress component and the velocity gradient (Yung-Yi, 1974). In the case of non-Newtonian fluids, a complex relationship exists between the tangential stress and the velocity gradient (rate of shear). It is a fact that the viscosity of a fluid will increase if another material in the form of small particles, either solid, liquid or gases are dispersed randomly throughout the fluid. The effect of suspended particle concentration by volume on the fluid-viscosity change was studied and expressed quantitatively by Einstein in 1906. It can be expressed as follows:

$$\lim_{\phi \to 0}\left(\frac{(\eta/\eta_o)-1}{\phi}\right)=\frac{\eta_{sp}}{\phi}=\frac{5}{2} \qquad (2.1)$$

Where η is the viscosity of pure fluid, η is the viscosity of dilute suspension fluid and ø is the volume fraction occupied by the spherical particles. The quantity $(\eta/\eta_o)-1$ is of frequent occurrence in the theory of viscosity and is known as specific viscosity, η_{sp}. This equation

implies that the viscosity change of fluid relates to the size and density of suspended particles.

Staudinger (1930) called attention to the utility of viscosity measurements of dilute polymer solutions as a method of determining the molecular weight of a linear polymer. However, Staudinger then arrives at the conclusion that a direct proportionality exists between the intrinsic viscosity and the molecular weight. Hence

$$\eta = (\frac{\eta_r - 1}{c})_{c \to 0} = KM \qquad (2.2)$$

In equation (2.2), η_r is the relative viscosity of a polymer solution of concentration c, K is a constant characteristic of a given polymer series, M is the molecular weight and η is defined as the intrinsic viscosity of the solution. The application of Staudinger's formula was found to generally yield low values of molecular weights – sometimes low by factors of ten or more. This situation was not fully rectified until Mark-Houwink's equation had been introduced in the mid 1940's (Story, 1953):

$$\eta = KM^{a} \qquad (2.3)$$

K and a are constants and M is the molecular weight of the fluid from the deformation data.

The Mark-Houwink equation above was found useful, in chapter three of this work, to amend the Carreau Yasuda Model (CYM – an empirical model found to give excellent fit to this study's honey rheograms) and in the structural kinetic analysis, to extract average molecular weight data from time resolved constant rate of shear data.

2.2 Properties and behaviour of fluids

The shear viscosity of a fluid expresses its resistance to shearing flows, where adjacent layers move parallel to each other with different speeds. It can be defined through the idealized situation known as a Couette flow, where a layer of fluid is trapped between two horizontal

plates, one fixed and one moving horizontally at constant speed, u. The plates may be assumed to be very large, so that one need not consider what happens near their edges, as seen in Figure 1 below.

The elements of fluid immediately adjacent to the solid plates assume the velocities (u and 0 respectively) of the solid plate surfaces. This is the so called non-slip boundary condition of fluid dynamics. The layers of fluid in between are forced to move at velocities between u and 0 by the transmission of momentum or shear stress, τ, from the moving plate toward the stationery plate aided by the viscosity between adjacent layers of fluid. Each layer of fluid will move faster than the one just below it (as seen in figure 1 below), and friction between them will give rise to a force resisting their relative motion. In particular, the fluid will apply on the top plate a force in the direction opposite to its motion, and an equal but opposite one to the bottom plate. An external force is therefore required in order to keep the top plate moving at constant speed.

The magnitude, F of this force is found to be proportional to the speed, u and the area, A of each plate, and inversely proportional to their separation, y:

$$F = A\eta\frac{u}{y} \tag{2.4}$$

The proportionality factor, η in this formula is the viscosity of the fluid. The ratio u/y is called the rate of shear deformation or shear rate, and is the derivative of the fluid speed in the direction perpendicular to the plates. Isaac Newton expressed the viscous forces by the differential equation:

$$\tau = \eta\frac{\partial u}{\partial y} \tag{2.5}$$

where $\tau = F/A$ and $\partial u/dy$ is the local rate of shear.

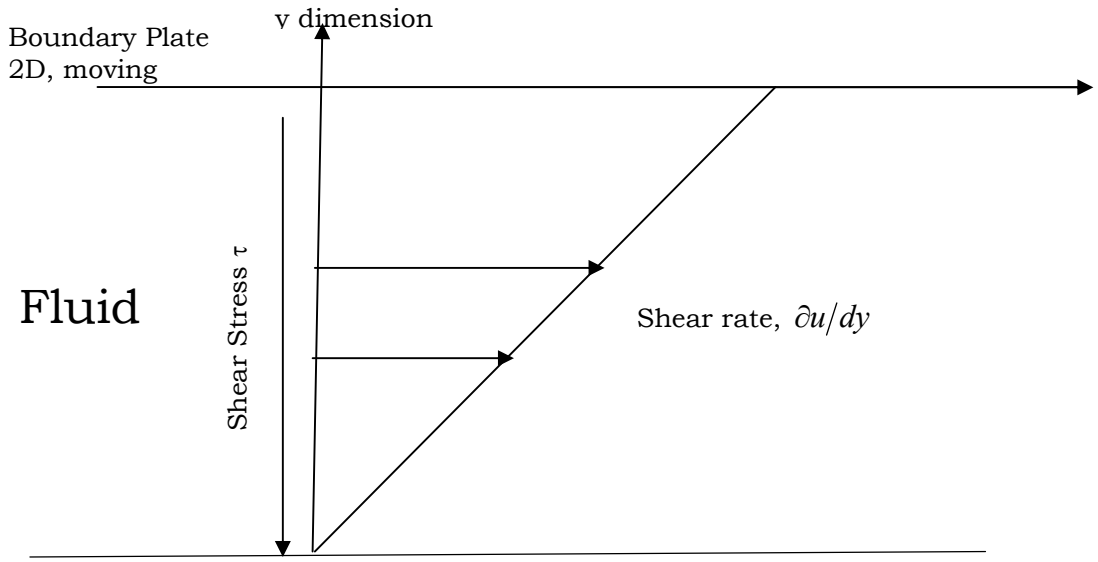

Figure 1. Laminar shear of fluid between two plates. Friction between the fluid and the moving boundaries causes the fluid to shear. The force required for this action is a measure of the fluid's viscosity.

2.3 Types of Flow

The figures below explains the different types of flow.

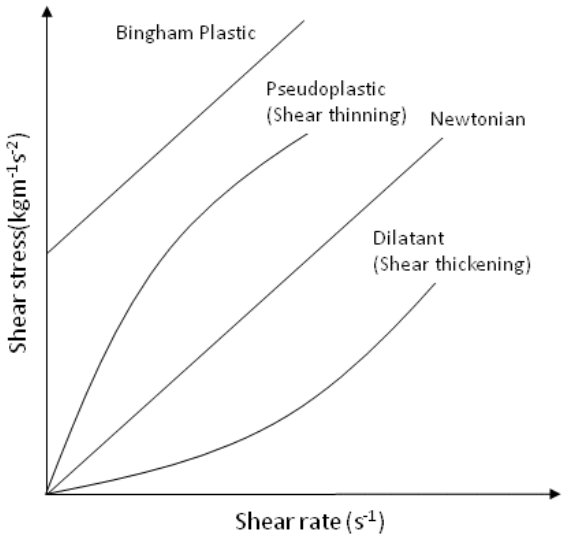

Figure 2a Time Independent flow

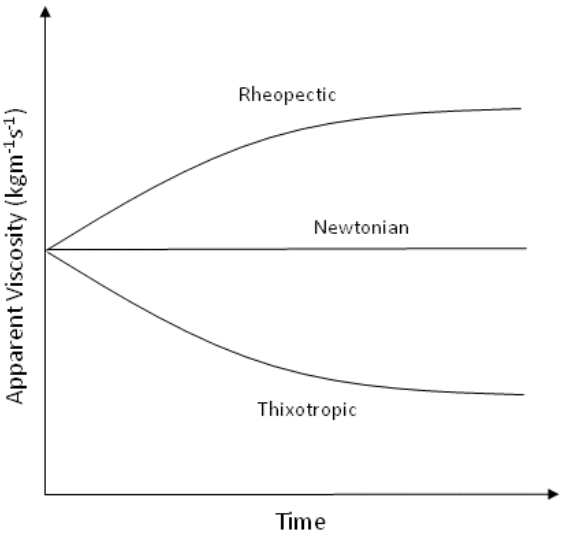

Figure 2b Time dependent flow

Figures 2a and 2b above are the graphical representation of different types of flow. In the Figure 2a, a plot of shear stress versus shear rate, describes time independent flow wich include: a Bingham plastic, a Shear thinning fluid, a Shear thickening fluid, and a Newtonian

fluid. The Figure 2b above shows time dependent flow which incled a thixotropic and a rheopectic fluid.

Time Independent Fluids

2.3.1 The Newtonian fluids

These fluids are, which have a constant viscosity with change in shear stress and shear rate. The viscosity of this type of fluid is independent of the shear history of the fluid. This implies that at a given temperature, the viscosity remains constant regardless of the viscometer model, spindle size and speed that were used to measure it.

2.3.2 The Bingham Plastics

Eugene Bingham, a colloid chemist, first coined the term "Rheology". He also showed that for many real fluids , a critical level of stress must be attained in order to initiate flow. Once the threshold of critical stress has been reached, the material yields to flow, hence the term, yield stress. The yield stress is the reason, why one needs to shake or tap a bottle to make the ketchup flow. Materials which exhibit Newtonian flow beyond the yield bear the name Bingham Fluids.

2.3.3 The Dilatant Fluid

They are also known as shear thickening fluids, is an unusual phenomenon whereby the viscosity of material increases upon stirring or shearing. In some cases these are dense suspensions of solid particles in a fluid medium, which develop greater spacing between particles during shearing or agitation. This behavior is infamous in quick sand, moist-beach sand and certain pharmaceuticals such as a suspension of penicillin. Shear thickening often result from material instability and structural rearrangements or phase separation during flow.

2.3.4 The Psuedoplastic Fluid

Fluids of this nature display decreasing viscosity with increasing shear rate. This type of

fluid is commonly referred to as Shear thinning fluids. Polymeric solutions exhibit pseudoplastic flow as does bread dough and many paints and cosmetics.

Time Dependent Fluids

2.3.5 The Thixotropic Fluid

In this type of fluid, materials become less viscous over time when shaken, agitated, or otherwise stressed. For many fluid materials, viscosity is mostly independent of time, and is only a function of the shear rate and temperature. For concentrated dispersions their viscosity does not reach a steady value for some time upon application of stress, or shear. The fluid's steady state is dependent on the stabilization of internal network structures that can be broken down by shearing, and requires time to rebuild. A steady state plateau in viscosity is reached if equilibrium has been established between structure break-down and rebuilding. Upon ceasing the shear rate which caused the breakdown, the material reforms its internal network, and the viscosity recovers. The term used to describe this phenomenon is Thixotropy. In studying such materials it can be beneficial to destroy the network structure by deforming or shearing the material, giving a clean-slate for examination of the path by which the viscosity rebuilds. The viscosity of thixotropic materials does not follow the same path on structure breakdown and recovery. In most cases, when the shear rate is slowed, the stress path lags forming a hysteresis loop, which then returns to a point lower than the initial critical shear stress. The area within the hysteresis loop represents the energy consumed in structural breakdown.

2.3.6 The Rheopectic Fluid

Materials become more viscous over time when shaken, agitated, or otherwise stressed. A rheopectic fluid such as a dense suspension of latex particles or plastisols will gel when agitated. If allowed to rest, a rheopectic fluid will return to its original lower viscosity. The viscosity-shear rate curve forms a hysteresis loop and the hysteresis can be repeated indefinitely. This is a way to distinguish between true and apparent rheopectic behavior.

Apparent rheopectic fluids change physically or chemically (gelling, solvent evaporation) while shear is imposed. It also experiences a viscosity increase. These changes, however, will not be reversible and therefore do not represent true rheopexy.

2.4 Rheological Characterization of Honey

Rheology is expected to lend itself to fluid characterization since flow behaviour reflects fluid properties such as composition, average molecular weight and molecular weight distribution (Bakier, 2007). The composition of a material is a key determining factor of its viscosity. When composition is altered, either by changing the proportion of the component substances, or by the addition of other materials, a change in rheological properties is quite likely to occur (Bera *et al.,* 2008). Non-Newtonians like honey should be expected to express a greater sensitivity in their rheological behaviour to compositional changes.

Bera *et al.,* (2008) investigated the effect of gamma radiation on the viscosity of honey and on other selected physicochemical properties. They concluded that gamma radiation had little or no influence on these properties. Significantly, they reported Newtonian rheological behaviour for their samples. This is contrary to the overwhelming prevailing consensus on this matter which sees honey as a non-Newtonian fluid (Witczak *et al.,* 2011). It has been suggested that pure honey owes its non-Newtonian behavior to its Oligomer content.

Results like those reported in Bera *et al.,* (2008) above limit the discriminating value of rheological profiling to viscosity enhancement or reduction. As already suggested, Non-Newtonian behavior promises an even wealthier resource for tracking compositional changes including changes due to adulteration. The results reported by James *et al.,* (2009) who worked on the physical characterization of some honey samples from North-Central Nigeria also suggested Newtonian behavior for these samples. Like Bera *et al.,* (2008), these workers utilized a simple viscometer for the measurements. The simple viscometer would hide the

non-Newtonian character of a fluid if replicate determinations of viscosity allowed sufficient relaxation time.

DaCosta and Pereira, (2012) used a rheometer to carry out rheological analyses of honey and propolis mixtures. They reported shear rate independent viscosities for their samples. It is very likely that these authors' results could have suggested Non-Newtonian behavior had they extended their analyses to the low rates of shear end of the deformation spectrum.

El-Bialee and Sorour, (2011) studied the effect of adulteration on honey properties. In that study, honey was adulterated to different adulterant compositions by adding amounts of starch, glucose, molasses, and distilled water. They employed the Brookfield Programmable rheometer but worked at high shear rates of 12.5-125 s^{-1} and at a temperature of 30^0C. Their results suggested that honey exhibited Newtonian behavior while adulterated honey exhibited non-Newtonian pseudoplastic behaviour. The present study (spanning rates of shear in the range 0.01-2.45 s^{-1}) would suggest that care must be taken in choosing the range of rates of share, in order to obtain meaningful rheological characterizations of honey. A judicious choice of rates of shear would span low to modest rates of shear.

The rheological characterization of polymers and polymers in dilute solutions are well established and so could be adopted to characterize honey since honey contains some oligomers. It has been reported that honey contains as high as 11% Melezitose which is an oligomer (Lazaridou *et al.,* 2004; Sopade *et al.,* 2004; Rao and Steffe, 1992; and Rao 1997, and 2006). This Melezitose content, therefore, easily supports rheological profiling required here since threshold for reflection of non-Newtonian behaviour starts from about 2% (De Laney and Reilly, 2000 and Sunthar, 2008).

2.5 Molecular Interpretation of Honey Rheograms

Franck, (2004) recorded rheogram line shapes for solutions of polymers which resemble those of pure honey obtained in the preliminary experiments conducted for the present study. A maximum (peak) was observed between the shear thickening and the shear thinning features. Triantafillopoulos, (1988) had a model for interpreting rheograms of polymers. He suggests that at rest or under low rates of shear, particles of the fluid fit into voids of adjacent layer of flow. As flow progresses, the particles begin to predominantly slide over the adjacent layers as against adjacent layer void filling. Under this circumstance, resistance to flow increases in a manner that causes the fluid to behave in a solid-like manner, thereby precipitating the shear thickening behaviour at the beginning of the rheological signature. Likewise, suspensions and colloidal mixtures resist deformation and sometimes cease to flow until reversible change of internal network of particle arrangement is completed (Franck, 2004). The peak exists at the point at which the structural build up due to shear thickening effect is in equilibrium with the structural breakdown leading to shear thinning effect (Franck, 2004).

At higher shear rates, Triantafillopoulos' model explained the shear thinning behaviour to be as a result of isothermal and reversible breaking of structures in the fluid. The clusters and aggregates of particles originally present in colloids and suspensions are destroyed by shear. The specific mechanisms responsible for this kind of rheological behaviour are structural-breaking due to hydrodynamic effects where the rate of particle dissociation is greater than the rate of their association, favourable orientation of macromolecules or dispersed asymmetric particles in the flow field and diminution or removal of the absorbed film (solvation layer) surrounding the particles due to hydrodynamic effects. The origin of non-Newtonian flow phenomena in fluids is attributed to various kinds of solids and liquid particles suspended in the liquid phase and/or polymeric molecules stabilizing it. The main

effect is that, upon flow, momentum transfer through the bulk fluid changes because particles translated and rotated under the influence of superimposed flow, in addition to the fluid motion. Bulk rheological properties depend on a net potential energy manifested by the superposition of secondary forces (i.e., electrostatic, Van der Waals, steric, and solvation) and mechanical effects due to hydrodynamic phenomena. A flow structure of complex nature develops within non-Newtonian fluids, as an effect of all the above interactions. Thus, the equilibrium between association and disassociation of particles that form this structure controls rheology under shear. When the particles are asymmetric, orientation plays an additional role.

Suspension rheology at low solid concentration is primarily dictated by particle-liquid interfacial interactions. Under shear, there is enough liquid phase between particles to lubricate them, and the interaction between particles is mainly conducted by the liquid. With increasing solid content, however, the mean distance between particles decreases and drastic interaction such as particle-particle hydrodynamic effects influence the flow. The degree of shear thinning depends on the structural state of the dispersion or colloid prior to shearing and the composition of the dispersing phase.

Triantafillopolous' model may be adapted to explain the rheology of honey (a solution of oligomers to which may be applied mathematical models previously developed for polymeric fluids).

2.6 Rheological Characterisation of Polymers

DeLaney and Reilly, (2000) worked on a new application to polymer rheology. They used rheological data obtained under defined conditions of temperature and shear to assess the quality of resins. Chenlo *et al.,* (2006) studied the effect of glucose content and temperature on steady-shear flow curves of Aqueous Guar gum solutions. Genovese *et al.,* (2007) studied

the rheology of colloidal and non colloidal food dispersions. The conclusions from these studies shall enhance the understanding of honey rheology since it has been established that honey contains oligomers and thus should behave like polymeric fluids.

2.6.1 Honey as a Polymeric Liquid

Honey contains oligomers including melezitose, raffinose, sucrose, maltose, turanose,erlose and polymerized monomers which has been found to be as high as 11%. (Lazaridou *et al.,* 2004; Sopade *et al.,* 2004; Rao and Steffe, 1992; and Rao 1977, and 2006). These oligomers content in honey, therefore, qualifies it to be a polymeric fluid since the threshold for reflection of non-Newtonian behaviour which is a major character of polymers starts from about 2% concentration (De Laney and Reilly, 2000 and Sunthar, 2008).

Polymeric liquids contain long chain molecules and some short chain oligomers which flow when subjected to shear. The conventional definition used to define simple liquid which states that they do not support shear stress at rest cannot be used to define the liquid state of polymeric liquid. They exhibit both liquid and solid like behaviour. One of the rheological properties of polymeric fluids as alluded to in section 2.3 is that their viscosity is a function of shear rate and change with time (Sunthar, 2008).

2.6.2 Chemical Nature of Polymeric Liquid

The common feature of most polymeric liquids is that they have long chains of monomers joined by chemical bonds. They could even, like honey, be oligomers of short chains. Their molecular weights are from 1000g/mol upwards (DeLaney and Reilly, 2000).

2.6.3 Physical Nature of Polymers

The physical properties of a polymer are determined by the configuration of the constituent atoms, and to some extent by the molecular weight. The configuration is

partly dependent on the main chain, and partly on the various side groups. The chief physical property of a polymer that distinguishes it from other fluids is that it exhibits complex behaviour which is the linearity of the chain. It is not the high molecular weight that leads to the peculiar phenomenon but how the chains are arranged linearly. The length along the chain is much larger than the other dimensions of the molecules (Sunthar, 2008). For example, a suspension of polystyrene beads (in solid state) may have high molecular weight per bead. But it may exhibit rheological properties of a suspension rather than a polymer solution. This is because for most properties, such as viscosity; it is the beads' spherical diameter that matters, and not the molecular weight per bead (DeLaney and Reilly, 2000). Honey may not have high molecular weight but the length of structure of the oligomers (Melezitose) content, greatly influence its behaviour (Sabato, 2004). Chain branching hinders free rotation and raises the softening point of the polymer. Even a small number of crosslinks may, however, cause a major hindrance to the free rotation of the internal carbon bonds of the chain, resulting in a sharp increase in stiffness of the resulting product. Many side chain groups cause steric hindrance and restrictions in the free rotation about the double bonds. These principles suggest that rheograms would reflect the physical and chemical characteristics of a fluid and are likely to lend themselves to the objective of assessing the quality of honey.

2.7 Physicochemical Characterisation and Antibacterial Properties of Honey

This section seeks to review the literature on the test methods approved by the international honey commission and Codex Alimentarius for the characterisation of honey. These tests serve to differentiate pure from adulterated honey and shall be explored here to assess the efficacy of this study's rheological evaluation of honey quality.

2.7.1 Hydroxyl Methyl Furfural (HMF) Content

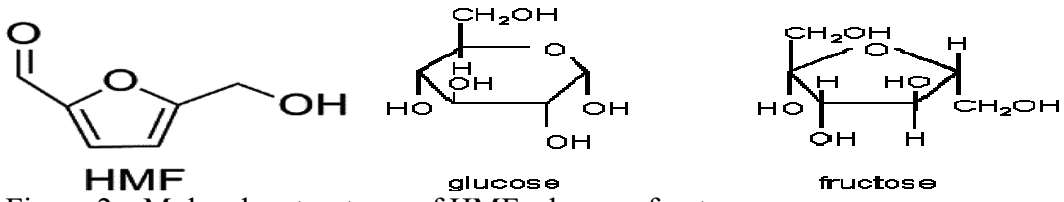

Figure 2c. Molecular structures of HMF, glucose, fructose.

5-hydroxyl methyl furfuraldehyde (HMF) content in honey is measured to assess the quality of honey. This compound is generally not present in fresh well processed pure honey. It is obtained from acid catalised thermal dehydration of hexoses, glucose and fructose. Figure 2c shows the molecular structure of HMF and its constituents hexoses, fructose and glucose. Its content increases during temperature conditioning to dissolve crystallized fragments, in storage and upon adulteration (Kalabova *et al.,* 2003). Some Nigerian harvesters, to facilitate honey harvesting, use smokers during harvesting to drive the bees away or to render the insects less active (Fallico *et al.,* 2004). This process may lead to elevated concentrations of HMF in honey. This compound is also formed in honey during acid-catalyzed thermal dehydration of hexoses (fructose and glucose) (Belitz and Grosch, 1999). Second and third diagrams in figure 3 above are the molecular structure of glucose and fructose. The high concentration of saccharides and the good acidic medium in the sweetener occasioned by low pH and the presence of oxalic and amino acids and numerous other acids lead to easy formation of 5-hydroxyl methyl furfuraldehyde in adulterated honey (Lewkowski, 2001).

The Codex Alimentarius (Alinorm 01/25 2000) established that the hydroxyl methyl furfural content of honey after processing or blending must not be higher than 80 mg/kg. The European Union (EU Directive 110/2001) fixed HMF limit in honey to be 40mg/kg with the following exceptions: 80mg/kg for honey coming from countries or regions with tropical temperatures, and 15 mg/kg for honey with low enzymatic level. Kamal *et al.,* (2002) reported the HMF content of Pakistan honey to be 0 - 42.896 mg/kg. These values are

within the standard regulation of 80mg/kg. Kalabova *et al.,* (2003) also reported the values of 24.8 - 66.1mg/kg in Czech honeys. Similarly, Zappal *et al.,* (2005) reported values of 0.03-0.061 for the Italian honeys. On the other hand, Makawi *et al.,* (2009) reported the values of 0 - 900mg/kg for the Sudanese honey. They inferred that the high temperature of the region, above 35°C during the summer influenced higher production of HMF in some honeys produced in Sudan. Owayss, (2005) reported the average HMF value of 4.61 mg/kg for the Libyan honey. Ayansola and Banjo, (2011) in their work: Chemical evaluation of the authenticity of honey marketed in southwestern Nigeria recorded hydroxylmethylfurfural content of 66.68 - 143.05 mg/kg with a mean value of 98.61mg/kg for honey samples they collected from the open market. This suggests that many of the samples from the open market are adulterated or that the high temperature at which those honeys are exposed in the market spurred the excessive formation of the furfural. On the other hand, Lawal *et al.,* (2009) recorded HMF values of 3.8-12.9 mg/kg for the Nigerian honeys suggesting that those samples are pure. The best way for HMF determination is the use of High Performance Liquid Chromatographic (HPLC) method developed by Jeuring and Kuppers, (1980). A Zappala *et al.,* (2005) compare this HPLC method with two Spectrophotometric methods after White (1979) and after Winkler (1955). They concluded that they obtained better, repeatable and reasonable results using the HPLC method.

2.7.2 Carbohydrates Content

Sugars are the major constituents of honey, comprising about 95 wt% of its dry weight (Bognadov, 2008). The main sugars are the monosaccharides hexoses: fructose and glucose, which are the products of hydrolysis of the disaccharide sucrose. It also catalyses many other sugar conversion and is mainly responsible for honey's sugar pattern (Kaskoniene *et al.,* 2010). The principal oligosaccharides in honey are disaccharides: sucrose, maltose, turanose,

erlose and trisaccharides: melezitose and raffinose (De la Fuente *et al.,* 2007). Trace amounts of tetrasaccharides and pentasaccharides have also been isolated (Bognadov, 2008). The relative amounts of the monosaccharides glucose and fructose, disaccharides sucrose and turanose or maltose and turanose may be used to assess possible adulteration of honey with glucose or high-fructose syrup (White, 1975). Bognadov *et al.,* (2008) suggested that for pure honey, the standard for fructose is 30-45% while that of glucose is 24-40%. The sucrose content should be 0.1-4.4% while trisaccharides melezitose is about 1% and erlose should be around 0.8%. Some researchers focused on carbohydrate profiling as a means of ascertaining the quality of honey. Kaskoniene *et al.,* (2010) worked on carbohydrate composition and electrical conductivity of different honeys from Lithuania origin. De la Fuente *et al.,* (2007) worked on volatile and carbohydrate composition of rare unifloral honeys from Spain. Also De la Fuente *et al.,* (2011) studied carbohydrate composition of Spanish unifloral honeys. Sugar composition can be determined by diverse methods, which include HPLC with refractometric detection (Bogdanov, 2004), HPLC with pulse amperometric detection (Nozal *et al.,* 2005), ion exchange chromatography with pulse amperometric detection (Bogdanov, 2004). It can also be determined by gas chromatography with flame ionization detection (Cotte *et al.,* 2004), gas chromatography-mass spectrometry (Sanz *et al.,* 2004), nuclear magnetic resonance, Fourier transform infrared and dispersive Raman spectroscopy (Batsoulis *et al.,*2005) etc.

2.7.3 Protein Content

The amounts of amino acids and proteins are relatively small in honey, at most 4.0 wt.%. However, these components are highly important in judging the quality of honey. The amino acid, which is added to honey through the bees is an indicator of honey quality. Its content in honey should be more than 1.25 wt.%. A value below 1.12 wt.% means that the honey is probably adulterated (Von De Ohe *et al.,* 1991). Owayss, (2005) used protein

content as an index of quality in Libyan honey. Bogdanov *et al.,* (2008) suggested a standard of 1.25 - 2.5 % protein content for every pure honey. In this report, the protein content of the samples was determined using Kjeldahl analysis outlined by AOAC (1990).

2.7.4 Minerals, Trace Elements and Vitamins Content

The mineral content is determined as a quality criterion for honey. It is possible to differentiate between unifloral honeys by measuring the magnesium, calcium, aluminum, iron, manganese, zinc, barium, copper, cobalt, chromium, nickel, cadmium and lead content of honey (Bognadov *et al.,* 2008). Nozal *et al.,* (2005) classified honeys from Soria province of Spain using trace metal and mineral content of honey. Blossom honeys (honey from the nectar of flowers) have mineral content of between 0.1 and 0.3%, while that of honey dew (honey derived from the sap of plants) can get to a total content of 1%. Bognadov *et al.,* (2008) suggested a standard of 0.1-0.5% for total percentage minerals for pure honey.

Drawing from the depth of their experience on the subject, Bognadov *et al.,* (2008) suggested the model distribution of trace elements in honey given in the table below.

Table 1. Elemental Composition of Trace Metal Constituents of Honey

Element	Range (mg/100g)
Sodium	1.6 - 17.0
Calcium	3.0 - 31.0
Potassium	40.0 - 3500.0
Magnesium	0.7 - 13.0
Phosphorus	2.0 - 15.0
Zinc	0.05 - 2.0
Copper	0.02 - 0.6
Iron	0.03 - 4.0
Manganese	0.02 - 2.0
Chromium	0.01 0.3
Selenium	0.02 0.01

The vitamin content of honey is always in trace amounts. Every honey contains some amount of vitamins from the nectar of the original plant. Whenever a sample does not contain vitamins even in trace amount, the imitation product is inferred. Adulterated products would still contain vitamins in trace amounts (Bognadov *et al.,* 2008).

2.7.5 Moisture Content

The water content of honey is an index of quality. Codex Alimentarius specified that the water content of good honey should not be above 21%. Adebiyi *et al.,* (2004) obtained the moisture content of Nigerian honey to be 18-30%. Lawal *et al.,* (2009) from their study of the Nigerian honey obtained the water content of 16-20%. Also Ayansola and Banjo, (2011) concluded that the moisture content of honey from southwest Nigeria is 13.32 -18.12%. Likewise, Owayss, (2005) obtained a value of 18% for the Libyan honey. Also Rehman *et*

al., (2008) obtained values between 14.11 and 19.09% for the Pakistani honey while Kamal *et al.,* (2002) corroborated his results.

2.7.6 Antibacterial Activities of Honey

This section seeks to review the literature on the antibacterial / healing properties of honey. In current medical practice, honey is gaining acceptance for use as a therapeutic agent for treatment of ulcers and bed sores, for surface infections resulting from burns and wounds, and for non-surface infections. For over 2000 years, even before bacteria were discovered to be the cause of many infections, honey has been in use for treatment of some of these diseases (Gunther, 1959). More recently, honey has been reported to have an inhibitory effect of around 60 species of bacteria, including aerobes and anaerobes, gram-positive and gram-negative organisms (Alqurasi *et al.,* 2013). Honey has been found to be effective against microorganisms isolated from the urinary tract infection and in the treatment of infantile gastro-enteristis (Chavez and Decker, 2008). In many cases honey has been used with success on the treatment of infections not responding to standard antibiotics and antiseptic therapy. The current prevalence of antibiotic-resistant microbial species has led to a re-evaluation of the therapeutic use of ancient remedies, including those based on honey. Different aspects of antibacterial properties of honey have been extensively reviewed (Molan, 1992).

Dustmann, (1979) noted that the antibacterial effect of honey was first reported in 1892 by Van Ketel. The antibacterial properties of honey were often assumed to be entirely due to osmotic effect of its high sugar content (Bose, 1982; Green, 1988 , Candon, 1993). Honey as a saturated sugar has osmolarity property sufficient to inhibit microbial growth (Chirife *et al.,* 1983). However, it has been shown that wounds infected with *Staphylococcus aureus* and *Pseudomonas aeruginosa* are quickly rendered sterile by honey (Efem, 1988). *Staphylococcus aureus* is one of the major human pathogens that cause hospital and

community-acquired infections (Chavez and Decker, 2008). This bacterium is the most prevalent pathogen isolated from hospitalized patients. It is a very common bacterium that can live on the skin or on the anterior side of healthy individuals and a common cause of skin lesions including pimples and boils. It can sometimes cause more serious infections in the skin and other sites on the body, such as legs, arms, eyes, bones and nose (Kavanagh *et al.,* 2014). Some S. *aureus* infections are more difficult to treat because the organism has become resistant over time to the antibiotics usually used to treat such infections (Klevens *et al.,* 2007).

Pseudomonas aeruginosa is a very opportunistic pathogen that can induce life threatening infections that result in hospitalization (and are very often life-threatening) (Mullai and Menon, 2007). This bacterium exhibits innate resistance to many antibiotics and can adapt when exposed to antimicrobial agents as a result develops resistance to these as well (Chauhan *et al.,* 2010). Infection typically starts with some type of bacterial attachment to an open wound for instance or from a simple exposure coupled with a weakened immune system (Cooper *et al.,* 2002). Honey, being hygroscopic because of its low water content extracts the water and nutrient in the organism thereby inhibiting its growth. As such, while honey may not kill the organism, it renders it dormant by its activity – the so called bacteriostatic effect. Complete inhibition to growth maintained over a long period is obviously an important feature in controlling infections. When bacteria are kept in a state of bacteriostasis for a long enough period, their capacity to recover is lost. This feature rules out the development of resistance by the pathogen. Undiluted or full strength honey exhibits its antibacterial properties mainly through this mechanism. The water in honey promotes the production of hydrogen peroxide which is generated by the action of the enzyme glucose oxidase . Hydrogen peroxide is an antioxidant and also kills bacteria through its bactericidal effect. As an antibacterial agent, hydrogen peroxide in moderate to high concentrations ran

out of favour by causing inflammation and damage to tissues (Saissy *et al.,* 1995 and Salahudeen *et al.,* 1991). However, the hydrogen peroxide concentration produced in honey has concentrations typically around 1mmol/l (Molan,1992), about 1000 times less than in the 3% solution commonly used as an antiseptic. This infinitesimal quantity of hydrogen peroxide produced may not after all, be the potency behind the antibacterial property of any honey. This suggests that the antibacterial properties of some honey could as well be as a result of non-peroxide components of honey as reported in the case of Manuka honey (Allen *et al.,* 1991). Ajibola *et al.* (2012) found that hydrogen peroxide is not the only bacteria inhibiting compound in honey. In fact, inhibitors in honey include many other compounds, two important classes of which are flavonoids (Havsteen, 1983) and phenolic acids (caffeic acid and ferulic acid). Honey has low pH ranging from 3.2 to 4.8 (Nwalor *et al.,* 2014). This low pH is attributed to the presence of gluconic acid, which also causes inhibitory effects to bacterial growth (White, 1975). This pH is considerably lower than the optimum pH required for the growth of most bacteria, which is around 7.0 (Molan, 1992). Evidently, from the foregoing, much research focus has been directed on the antibacterial properties of honey. As earlier noted, the present study seeks to correlate antibacterial activities of purported honey sample with their rheological behaviour in the expectation that such correlation would align with sample's honey content or quality.

2.8 Rheological Modeling of Complex Fluids

The rheological modeling of honey is expected to connect the rheograms to the integrity of the fluid. By extension, therefore, information might be extracted from the rheograms to differentiate pure honey from the adulterated or fake honey.

In most complex food materials apparent viscosity decreases with increasing shear rate. This type of fluids is regarded as thixotropic. Thixotropy means that the change in the material

properties (caused and also maintained by shear load) is just temporary. The properties of the material return to their original values upon elimination of the load (Kokuti *et al.,* 2011). The recovery of the microstructure can take a long time though, after the removal of shear load. As long as the microstructure has not fully recovered, the fluid would yield again if exposed to further shear stress, even at a lower level than the original yield stress. Previous researchers tried to derive models to explain this memory effect.

Razavi *et al.,* (2010) worked on modeling of the time dependent rheological properties of pistachio butter. Khoni, (2001) studied the kinetics of irreversible structural relaxation and rheological behaviour of metallic glasses under quasi-static loading. He derived a model that describes, within a common framework, a number of mechanical relaxation phenomena induced by irreversible structural relaxation of metallic glasses under quasi-static loading. Also, Coussot *et al.,* (1992) studied the rheological modeling and peculiar properties of some debris flow. They took cognizance of the inter-particle links and microstructure in developing a model that describes the behaviour of clay-water mixtures. Abu-Jdayil, (2003) worked on modeling the time dependent rheological behaviour of semisolid foodstuffs. He used the structural kinetic model (SKM) to characterize the thixotropic behaviour of three different kinds of food products. His model was for structural decay with time at constant shear rate which assumes n^{th} order kinetics for the decay of material structure. The model inspired the adoption of the structural kinetic analysis in the present study. The n^{th} order kinetics accounts for n principal participants in the structural configuration that determines observed rheology.

In the present study the SKM shall be derived for honey rheology. It shall be applied to the experimental rheolgical data of the study. The Mark Houwink equation would be incoorated into the model to permit the extraction of average molecular weight information from the samples' rheological data. The CYM shall be also modified, again by incorporating the

Mark Houwink Equation. The amended version of the model shall be used to extract compositional information. The PLM shall be also used as a good tracker of adulteration and imitation in honey .

CHAPTER THREE

MATERIALS AND METHODS

The collection, preparation and demographic location of honey samples analyzed in this study are presented in this chapter. The experimental methods for the rheological characterization of these samples and of their adulterated versions are also discussed. Validity checks were made on the inferences derived from the rheological analyses using the results of established confirmatory tests and by attempting correlations of the rheological data with accepted characteristics of honey. The chapter also covers the principles that led to the extraction of the SKM parameters from the time resolved, constant rates of shear rheolgical data on pure and adulterated honey samples. Finally, the procedure for upgrading the Carreau-Yasuda Model (CYM) to enable the extraction of the molecular weight of samples is presented.

3.1 Sample Collection and Preparation

A total of thirty-seven samples were analyzed by rheological characterization. Control samples (reference pure honey samples) A1, A2 and A4 were harvested and processed as representatives of pure honey. Sample A3 was the “natural” honey produced by Forever Living Product, Texas USA. Sample A1 was collected from a bee farm at Afao 15km from Ado-Ekiti. Sample A2 was harvested and processed from the Apiculture Unit, Entrepreneurship Development Center, Federal Polytechnic Ado-Ekiti. Sample A4 was harvested and processed at Imuwen Ijebu Mushin in Ogun State. It was necessary, in this study, to ensure the authenticity of these reference pure honey standards by the direct harvesting and processing steps.

Sample E1 (100% Imitation) was produced by heating 2.5 kg of table sugar to melt. To this brownish liquid product was added an amount of distilled water that gave a final product viscosity close to that of Sample A1 at room temperature of 27 °C. Membership in the Bee Farmer's Association Ekiti State afforded this study access to knowledge of this adulteration method considered by members as harmless to health. The adulteration of honey with sucrose is not new, though, as it was reported by White, (1992). Obtained from mixtures of E1 and pure honey are samples E2, E3, E4 and E5 at 10%, 50%, 70% and 90% mass levels of adulteration, respectively. Likewise solutions of, glucose G1 (produced by dissolving three parts of glucose in one part of distilled water), fructose F1 (produced by dissolving three parts of fructose in one part of distilled water) and then distilled water, H0, were used to serially adulterate the control sample A4. Samples G2, G3, G4 and G5 are 10%, 50%, 70% and 90% adulteration with sample G1 while Samples F2, F3, F4 and F5 are 10%, 50%, 70% and 90% adulteration with sample F1. Also Samples H1, H2, H3, H4, H5 and H6 are 5%, 10%, 15%, 20%, 30% and 50% adulterated with H0. Samples B1-B7 were collected from the open market in Northern part of Nigeria in 2011. Samples C1-C6 were collected from different parts of southern Nigeria between 2010 and 2011.

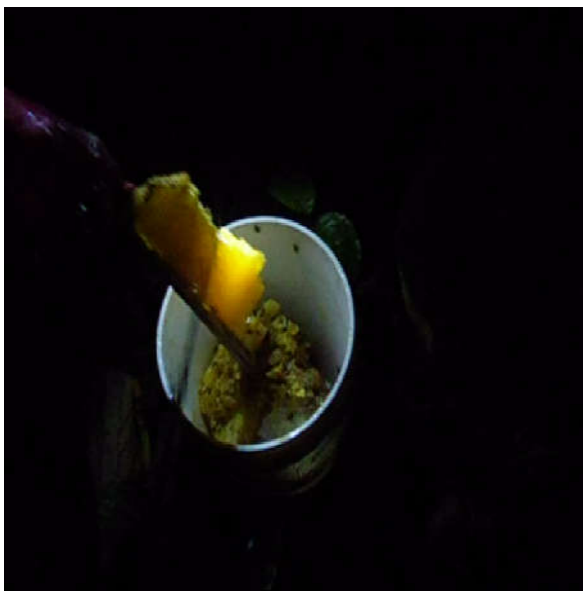

Plate 1. Honey Harvesting Proper by 8:00pm 29-11-12

Plate 2. Apis Melifera bees in a Farm at Imuwen Ijebu Mushin

Plate 3. Honey Ladden Comb

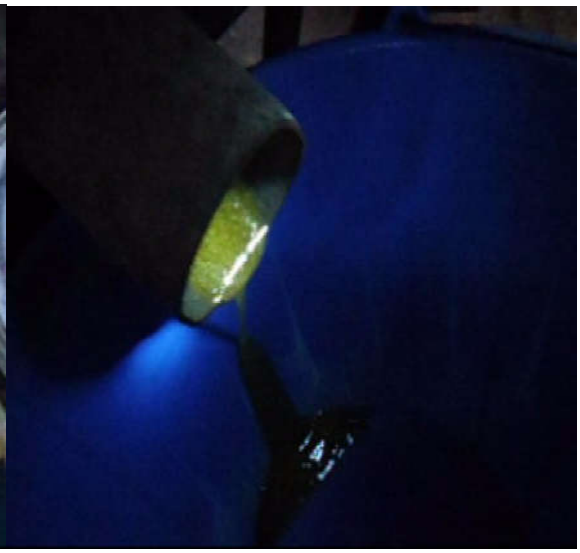

Plate 4. Expressed Honey from the Combs

Harvesting is conducted at night in the local belief that violent African *Apis Melifera* bees are less active at night. Plate 1 captures the actual harvesting. Wooden bars on which the combs are supported are carefully removed and the combs containing the honey detached into the harvesting cans. Plate 2 is the picture of *Apis Melifera* bees. A hive is populated by a single queen, a sizable number of drones and thousands of worker bees. The queen, which is a female with developed reproductive organs, is the largest in size and also the leader of the pack. It spreads a hormone called pheromones on other bees for identification and coordination in the hive. The work of the male drones is to fertilize the queen. The worker bees are females with undeveloped reproductive organs. Their work is to take care of the hive, gather nectar from outside of the hive, deposit them in the combs for honey production, and feed the queen in the hive. Plate 3 is the honeycomb out of which honey is expressed using an extraction device. The expressed honey is shown in plate 4.

The table below shows the details of the locations, in geographical coordinates, of sample collection points.

TABLE 2.DETAILS OF SAMPLES COLLECTION AND LOCATION PARAMETERS

S/N	Sample	Location	Location Coordinates	Collection Date	Production Date
1.	A1	Afao Ekiti	7.7167°N, 5.300°E	3-12-2011	4-12-2011
2.	A2	Federal Poly Ado-Ekiti	7.6211°N, 5.2214°E	14-01-2012	15-01-2012
3.	A3	Forever , Texas USA	31.0000°N, 100.0000°W	16-03-2011	
4.	A4	Imuwen, Ijebu Mushin	6.7379°N,4.1605°E	29-11-2012	30-11-2012
5.	B1	Gauraka, Niger	9.2000°N, 7.2167°E	June,2011	
6.	B2	Yola, Adamawa	9.2300°N, 12.4600°E	May,2011	
7.	B3	Zuru, Kebbi	11.5000°N, 4.0000°E	May,2011	
8.	B4	Orolu, Kwara	6.3833°N, 4.1833°E	May,2011	
9.	B5	Keffi, Nasarawa	8.8486°N, 7.8736°E	May,2011	
10.	B6	Lokoja, Kogi	7.8167°N, 6.7500°E	February,2011	
11.	B7	Kabba, Kogi	7.8333°N, 6.0667°E	May,2011	
11.	C1	Sunshine, Ondo	7.2500°N, 5.1950°E	May,2010	
12.	C2	Real Oasis, Iworoko Ekiti	7.7267°N, 5.2667°E		15-03-2011
13.	C3	Blessed, Ado-Ekiti	7.6211°N, 5.2214°E	February,2010	
14.	C4	Nsukka, Enugu	6.8567°N, 7.3958°E	November,2010	
15.	C5	Abba Igbira Ekiti	7.6211°N, 5.2214°E	February,2011	
16.	C6	Lagos	6.4351°N, 3.3958°E	March,2012	
17.	E1	Sucrose melt			28-03-2012
18.	E2	10% Adulteration			29-03-2012
19.	E3	50% Adulteration			29-03-2012
20.	E4	70% Adulteration			29-03-2012
21.	E5	90% Adulteration			29-03-2012
22.	F1	Fructose Syrup			01-12-2012
23.	F2	10% Adulteration			01-12-2012
24.	F3	50% Adulteration			01-12-2012
25.	F4	70% Adulteration			01-12-2012
26.	F5	90% Adulteration			01-12-2012
27.	G1	Glucose			01-12-2012
28.	G2	10% Adulteration			01-12-2012
29.	G3	50% Adulteration			01-12-2012
30.	G4	70% Adulteration			01-12-2012
31.	G5	90% Adulteration			01-12-2012
32.	H1	5% Adulteration with H_2O			01-12-2012
33.	H2	10% Adulteration with H_2O			01-12-2012
34.	H3	15% Adulteration with H_2O			01-12-2012
35.	H4	20% Adulteration with H_2O			01-12-2012
36.	H5	30% Adulteration with H_2O			01-12-2012
37.	H6	50% Adulteration with H_2O			01-12-2012

SAMPLE DEMOGRAPHY

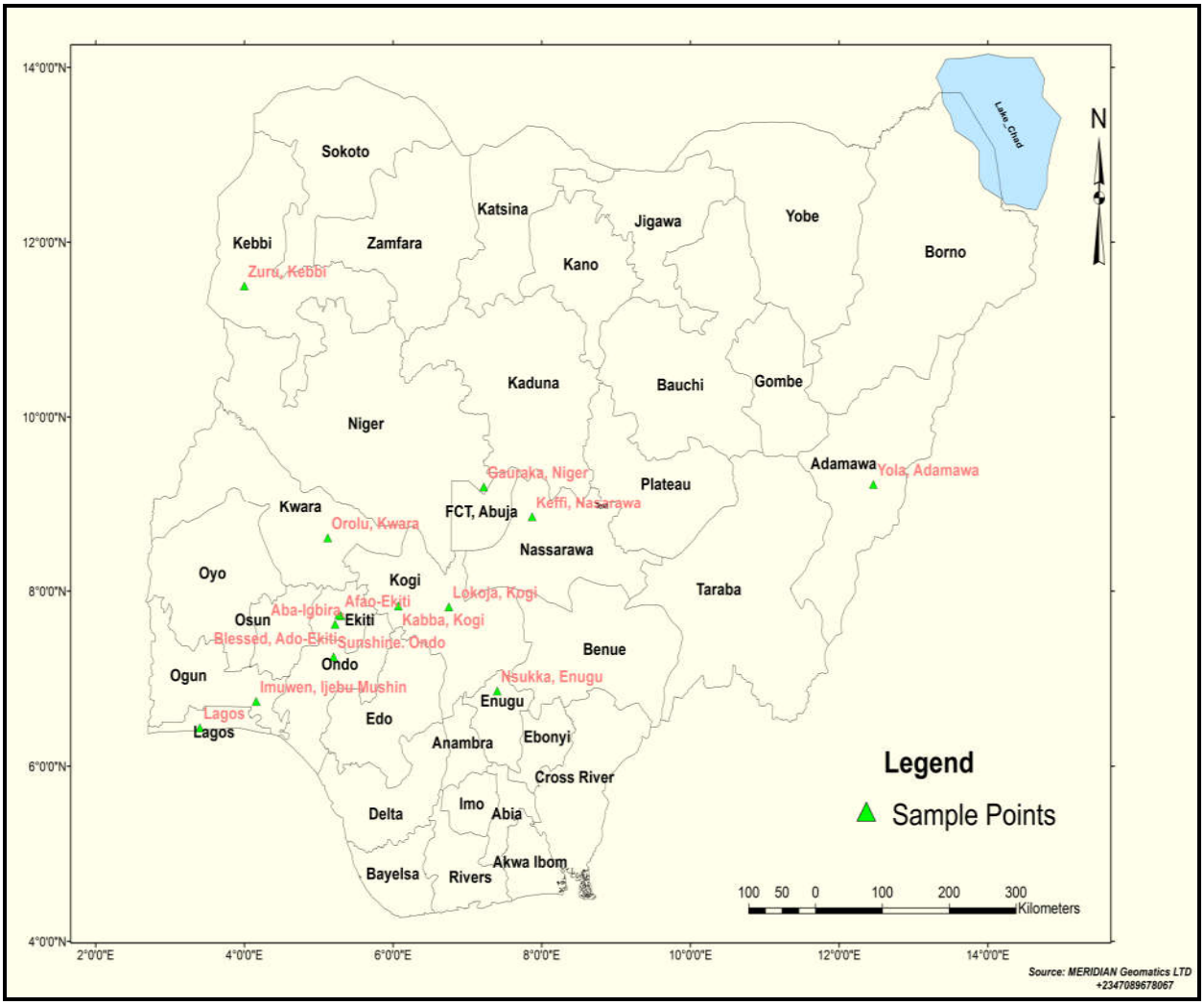

Figure 3 Demography of sample Collection Points in Nigerian Map

Figure 3 is the demography and distribution of all the sample collection points on the map of Nigeria.

3.2 Procedure for Rheological Characterisation

The rheology of the samples was carried out using the Brookfield RV DV-III Ultra Programmable Rheometer. The analyses were carried out at 27°C and at 35°C to study

the effect of sucrose adulteration on honey rheology and only at 27°C to study of the effects of fructose, glucose and water adulteration on honey rheology.

The Rheometer was auto zeroed upon each power-on. Since the samples were viscous, slow speed and biggest co-axial spindle were as most appropriate for the rheology of the viscous non-Newtonian samples. Coaxial cylinder geometries are suitable for this application which required well-defined rate of shear and shear stress. The spindle number "00" was chosen, enabling the Rheometer to calculate the shear stress (N/m^2), viscosity (mPa.s), and torque (%) for every shear rate (s-1). The equipment's thermometer was dipped inside the fluid before the start of each analysis for appropriate temperature control. The DV III Program mode was used. The speeds of: 0.0 to 1.0 at incremental steps of 0.1 and at 2.0 revolutions per minute were chosen. The program was run in reverse order from 2.0 to 0.0 without allowing a step time while studying the effects of sucrose adulteration on honey. During the study of the effects of glucose, fructose and water adulteration on honey, the speeds of 0.0 to 3.4 at incremental steps of 0.01 were used. The time interval on each speed was sixty seconds, also step time was disabled to prevent the sample recovery from shearing at earlier speeds. The samples were made to stand in the container for at least 30 minutes before the analysis to allow for the complete structural buildup induced by flow into the container.

The results of the analyses were exported as Microsoft Excel tables for subsequent analyses. Each experimental determination was repeated after 24 hours to verify reproducibility of results.

3.3 Data Reduction – Theoretical Consideration

Rheological experiments produce data (rheograms) which, immediately *albeit* qualitatively, strongly suggest the validity of the assumption that they contain information

on the quality of the samples. As suggested in section 2.5, rheological modeling of the rheograms would yield information on degree of departure from purity of honey sample.

This section discusses the Power law and the Carreau-Yasuda models traditionally applied to characterizing rheograms. It is desired to determine the information content of the parameters of these models and to explore their sensitivity to the quality of honey samples. By the same token, the SKM is applied to obtain a link between observed rheograms and the structural and molecular characteristics of the samples under the conditions that produced the rheograms. It is hoped that an objective assessment of rheograms may be obtained from this exercise.

3.3.1 Power Law Model (PLM)

In most polymeric fluids, the coefficient of viscosity is not constant, but varies with shear rate. Such fluids can be modeled by means of the power law equation (Turian and Bird, 1963). The Power law equation is given as:

$$\tau = \eta \gamma^{n} \tag{3.1}$$

Where, η is the consistency coefficient or dynamic viscosity (mPa.s)

τ is the shear stress of the fluid (N/m^2)

n is the behaviour index (Dimensionless)

If the behaviour index, $n = 1$, the power law equation reduces to the Newtonian model. If n is less than 1, the fluid is shear thinning and, if n is greater than 1, the fluid is shear thickening.

The simplest empiricism of the two-parameter power law expression was derived by Turian and Bird, (1963):

A two parameter power law model is obtained when the shear stress, τ, is eliminated as follows:

Replace τ in equation (3.1) with $\eta\gamma$, where η is the apparent viscosity, while changing η of the equation to the zero shear rate viscosity, η_o, gives equation (3.2)

$$\eta\gamma = \eta_o \gamma^n \tag{3.2}$$

Making η the subject,

$$\eta = \eta_o \gamma^{n-1} \tag{3.3}$$

Taking the natural logarithm of equation (3.3)

$$\ln\eta = \ln\eta_o + (n-1)\ln\gamma \tag{3.4}$$

A plot of $\ln\eta$ against $\ln\gamma$ will give a straight line graph with slope and intercept *(n-1)* and $\ln\eta_o$ respectively.

3.3.2 Carreau-Yasuda model (CYM) (Yasuda, 1979):

The Carreau-Yasuda Model (Equation 3.5 below) is an empirical model with five adjustable parameters, α, λ, *n,* η_0 and η_∞.

$$\eta(\dot{\gamma}) = \eta_\infty + (\eta_o - \eta_\infty)\left[1 + (\dot{\gamma}\lambda)^a\right]^{\frac{n-1}{a}} \tag{3.5}$$

This model describes a non-Newtonian time dependent flow with apparent viscosities of η_0 and η_∞ at zero and infinite rates of shear, respectively, and without a *yield stress*. The parameter λ is the viscous relaxation time that defines the location of the transition from shear-thickening to shear-thinning behaviour – $(1/\lambda)$ marks the critical shear rate at which viscosity begins to decrease. The power-law slope is $(n-1)$. The value of n, changes with the composition of the fluid. The parameter, "α" is a dimensionless parameter (sometimes called "the Yasuda constant") introduced by Yasuda to the Carreau equation. It is related to the breath of the transition region between η_o and the power-law region.

The Mark-Houwink's equation (2.3) is introduced in equation (3.5) by replacing the zero rate of shear viscosity with a term reflecting the average molecular weight of the fluid. Thus,

$$\eta(\dot{\gamma}) = \eta_\infty + \left(\mathrm{KM}^{\mathrm{A}} - \eta_\infty\right)\left[1 + (\dot{\gamma}\lambda)^a\right]^{\frac{n-1}{a}} \tag{3.6}$$

Equation 3.6 is regarded as an Amended Carreau-Yasuda Model (ACYM) that would be used to estimate the molecular weight of honey. Also a comparison shall be made on the molecular weight obtained using (3.6) and that obtained from the adaptation, in the next section, of the Structural Kinetic Model to honey rheology.

3.3.3 The Structural Kinetic Model (SKM) on the Nigerian Honey

The structural kinetic approach assumes that the change in the rheological behaviour is associated with shear-induced breakdown of internal structure of pure honey (Nguyen *et al.,* 1998). The analogy of chemical reaction to express the structural breakdown process in the following form(Abu-Jdayil, 2003) :

$$\text{Structured state} \rightarrow \text{Non Structured state} \tag{3.7}$$

This model will assume, in accordance with the above equation, that the structure of honey changes under the effect of imposing shear but restores itself upon the withdrawal of shear.

Earlier in this report, it was suggested that pure honey exhibits thixotropic time dependent flow behaviour. The structured state of the thixotropic structure at any time, *t,* and under applied shear rate γ, can be represented by a dimensionless structural parameter:

$$\theta = \theta(\gamma, t) \tag{3.8}$$

This may be defined, following Abu-Jdayil, (2003) as

$$\theta(\gamma, t) = \frac{\eta - \eta_\infty}{\eta_o - \eta_\infty} \tag{3.9}$$

Here η_o is the initial apparent viscosity at $t = 0$ (structured state) and η_∞ is the equilibrium apparent viscosity as the fluid tends to the non-structured state (as $t \rightarrow \infty$). As the fluid may be yet to reflect the exposure to the constant rate of shear in a typical SKM experimental analysis, η_o may be assumed to independent of the rate of shear. Conversely, extended time exposure of the fluid when η_∞ would be determined suggests that this parameter must be a function only of the applied shear rate.

The dimensionless structure variable, θ assumes the following values as boundary conditions: at the fully structured state, at t = 0, $\theta = \theta_o = 1$ and at non-structured state, as $t \rightarrow \infty$, $\theta = \theta_\infty = 0$

The rate of structural break down can be expressed as:

$$-\frac{d\theta}{dt} = k(\theta - \theta_\infty)^n \tag{3.10}$$

Where $k=k(\ )$ is the rate constant, and n (expected to take values in the range, 1 - 4) is the order of the structure breakdown process. Equation (3.10) may be solved subject to the boundary conditions noted above to give,

$$\eta = \eta_\infty + (\eta_o - \eta_\infty)\left[k(n-1)t + 1\right]^{1/(1-n)} \tag{3.11}$$

Equation 3.11 may be designated as the Structural Kinetic Model for honey samples in this study if the time resolved constant shear rate data obtained on these samples may be well correlated by it. This equation should answer the need to have a model that can give an insight into the composition of honey. One way to make this connection is through an appropriate introduction of the average molecular weight of the honey sample. A good relationship has been found for polymeric materials in the Mark Houwink relation (equation 2.3) discussed earlier in Chapter 2.

In that equation reproduced below,

$$\eta = KM^A \tag{2.3}$$

η is η_o which is the zero shear viscosity which as argued earlier in this section may be approximated to the zero time viscosity of the SKM experiment. K and A = are Mark Houwink Constants while M is the average molecular weight of the fluid. A is generally in the range of 0.5 to 0.8 (Launay *et al.,* 1986).

Putting equations (2.3) into equation (3.11) gives:

$$\eta = \eta_\infty + (KM^A - \eta_\infty)\left[kt\ (n-1) + 1\right]^{1/(1-n)} \tag{3.12}$$

As the SKM of a honey sample, equation 3.12 would produce the fluid's average molecular weight of the sample. Analyses for different rates of shear, γ, would yield, *k,* the rate constant of sample deformation as directly proportional to γ.

$$k=k(\gamma) \tag{3.13}$$

The remaining model parameters determined from data of apparent viscosity versus time at constant rate of shear contain interesting information on the fluid as well. These are,

η_∞ — Infinite shear viscosity which would throw up curious negative values

n — order of structural breakdown reaction which may be related to the number of active components participating in deformation induced interactions.

The most important value of the SKM applied to honey and cognate to this study is the variation of the SKM parameters with adulteration.

3.3.4 RHEOLOGICAL CURVE FITTING

3.4.1 The Power Law Model

The curve fitting for the two parameter power law model (**PLM**) was carried out using linear least squares error regression analyses on the semi-log tables of the rheological data. The details of the calculations on the PLM are presented in the Appendix1.

3.4.2 The Structural Kinetic Model

For the five parameter structural kinetic model (**SKM**), the order of break down kinetics was assigned numbers to ascertain which one will give the least error. In this study integers 1 to 3, 3.5 and 4 were tested. The preset shear rate, experimental apparent viscosities and time of deformation from the experiment were utilized, leaving as

unknowns the zero and infinite shear viscosities (η_0 and η_∞) which are not practicable to measure, and the rate constant of deformation (*k*) to be determined from the time versus apparent viscosity data. By extrapolation of the data to the *t = 0* line, η_0 is estimated. With this latter determination and a guess of η_∞, *k* may be explicitly determined for each data point from equation (3.11) which gives,

$$k = \frac{\theta^{(1-n)} - 1}{(n-1)t} \tag{3.14}$$

$$\text{Since } \theta(\gamma, t) = \frac{\eta - \eta_\infty}{\eta_o - \eta_\infty}$$

This scheme seeks a solution which will yield the minimum coefficient of variation (CV) of *k.* This decision is justified by the reasonable assumption that *k* should be a constant at the constant rate of shear condition of the SKM data. The combination of η_∞, *n*, and *k* which produces this optimum CV is utilized, along with the η_0 and the corresponding average molecular weight, *M* as the parameters of the SKM of the fluid for the (experiment's) preset rate of shear.

3.4.3 The Carreau-Yasuda Model

The curve fitting on **CYM** was carried out by the method of Morrison, (1999). A Solver Add-in of Microsoft Excel was used for this case. The initial guess parameters of this model were values obtained from the PLM. The data were arranged in an Excel spreadsheet. Two columns were used, one for shear rate the other one for viscosity. A column was created for the correlated values of viscosities calculated from the amended CYM. The Error column contained the square of the difference between the estimated viscosity and experimental viscosity divided by square of the experimental viscosities.

The sum of the Errors is an indicator of how well the fitting was done. The smaller the sum of errors, the better the fits for the models and vice versa.

3.5 Honey Quality Assessment Tests

Established Honey Quality Assessment tests approved by Codex Alimentary and the International Honey Commission were carried out to independently assess the conclusions derived from the new Rheological Method of honey Characterization. Correlation of the results of these tests with the conclusions of the rheological evaluation was employed to validate the new method. Most of these tests were carried out at the laboratory of the National Agency for Food and Drug Administration and Control (NAFDAC) in Oshodi, Lagos.

3.5.1 Hydroxyl Methyl Furfural Determination

HMF content of samples was determined using the High Performance Liquid Chromatography (HPLC) following the technique of Jeuring and Kuppers, (1980).

Principle

The HMF contents of samples were determined from the reverse phase HPLC (Agilent 1200, Califonia-US) equipped with a Diode Array Detector (DAD). Peak areas of chromatograms of the clear, filtered, aqueous solutions of the samples were translated to HMF concentrations of the samples by reference to an HMF content calibration curve prepared for the analyses.

Reagents

Mobile Phase: Water-methanol (90:10 by volume), both of HPLC qualities. Standard Solution: 5-hydroxyl methyl- furan-2-carbaldehyde (H40807) from Sigma-Aldrich, Milan. All other reagents used were of HPLC standard.

Determination of Standard for HMF-Content

The absorbance, *A*, of the prepared standard solution was determined with a DAD spectrophotometer set at 285 nm. The samples were charged in 1cm quartz cells with water in the blank reference cell. The HMF concentration of the standard solutions can be calculated from the literature value for molar absorbtivity, $a^{1\%}_{1cm}$=133.57. Thus,

$$\text{Concentration in mg/L} = \frac{A}{1 \times 133.57} \times 1{,}000 .$$

The calculated content must correspond to the specifications given by the supplier. The standard was stored at 4-8 ^{o}C under dry nitrogen since it is extremely hygroscopic.

Equipment

The HPLC (Agilent-Califonia,US) equipped with a DAD detector and an integrator

Colum: The HPLC column was a Merck Lichrospher, RP-18, 5 in, 12.5 x 4 mm, fitted with a guard cartridge packed with the same stationary phase (Merck, Milan).

Membrane filter, 0.45 µm (Dynargard).

Procedure

Ten grams of honey sample was accurately weighed into a 50 ml beaker. The sample was dissolved in approximately 25 ml of distilled water and transferred quantitatively to a 50 ml volumetric flask. It was then diluted to 50ml with distilled water. The resulting sample was made chromatography-ready by filtration through a 0.4 µm membrane filter at a flow rate of 1.0 ml/minute. Each chromatographic analysis had 20 µl of a sample as injected volume. The detection was carried out using DAD 285 nm and the range is 0.2UAFS.

Calculation and Expression of Results:

The HMF content was read off a calibration curve prepared from a table of standard solutions concentrations versus areas of HMF peaks from the HPLC chromatograms. The values obtained were corrected for sample dilution and reported as HMF content in mg/kg.

Proximate Analyses of Honey

This section gives a detailed procedure for determination of the proximate composition of samples**.**

3.5.2 Determination of Carbohydrate

The carbohydrate content of honey was determined by the method of Dreywood, 1946 outlined by AOAC, 1990 using an Agilent UV-VIS 8453 spectrophotometer.

Procedure for Extraction

1g of the sample was weighed into 5 ml of 72% of H_2SO_4 and the mixture was shaken and filtered. 1 ml of the filtrate was pipetted into a conical flask. 5 ml of anthrone reagent (produced by adding of Anthrone reagent in 200 ml of H_2SO_4) was added and shaken. 30 ml of the anthrone reagent was added to reduce its concentration and shaken. It was heated for 10 minutes and cooled to room temperature and the absorbance measured at 620 nm.

Standard

D glucose(0.01g) was weighed into a 100 ml of volumetric flask. Distilled water was used to make up to the 100 ml mark. This gave the stock solution 0.1, 0.2, 0.3, and 0.4 ml each, the solution was pipetted into a conical flask and was made up to 1ml with water. 5

ml of the anthrone reagent was added to the solution and the mixture heated for 10 minutes, cooled to room temperature. The absorbance was measured at 620 nm.

Carbohydrate =0.9 x Starch

3.5.3 Protein Analysis

Scope

Kjeldal method was used. The method is applicable to the determination of nitrogen occurring in the trinegative state in food and raw materials. It does not apply to N-N and N-O linkages (e.g. oxides, nitrates, nitrites, nitro groups, etc.).

Basic Principle

The method consists of three steps:

1. DIGESTION of the sample in sulphuric acid with a catalyst (3.5 g K_2SO_4 + 0.0035 g Se). The nitrogen contained in the sample is converted to ammonia and ammonium sulphate.
2. DISTILLATION of ammonia released from ammonium sulphate by addition of an excess of sodium hydroxide; ammonia being trapped in a trapping solution (sulphuric acid).
3. BACK-TITRATION of the excess of the trapping solution.

Equipment

1. Digestion unit Tecator 2006 (Foss-Hilleroed,Denmark).
2. Distillation unit Kjeltec 2100 (Foss-Hilleroed,Denmark).

Procedure

Digestion

Two mixed catalyst digestion tablets were placed into a digestion tube. Approximately 1.0 g of honey samples was weighed using a weighing boat. The sample was quantitatively transferred into the digestion tube using 12ml of concentrated sulphuric acid.

The acid was first poured into a beaker. Then 12 ml was measured from the beaker into a cylinder. The sample was transferred to the digestion tube such that the walls stay clean. Any residue of the sample was rinsed off using sulphuric acid from the cylinder. After it was shacked in a circular fashion, the tube was placed in a digestion stand. A vapour exhauster was attached; water vacuum aspirator was switched on and the recommended digestion temperature was set at 420 $^{\circ}$C. After the required temperature was attained (approximately 15 minutes), the sample was digested for 40 minutes. The digestion unit was switched off and left to cool down (for approximately 20 minutes). The digestion tubes were placed in the digestion unit and the unit switched on. Digestion was shortened for the purpose of this exercise to enable the digestion of resistant compounds (Lysin, Tyrosin). An additional 60 minutes of digestion would be necessary after clearing up the tube´s contents.

Distillation using the distillation unit KJELTEC 2100

Preparation of the Distillation Unit

A clean digestion tube containing the sample (half filled with distilled water) and an Erlenmayer flask were placed into the distillation unit, and the safety window was closed. By pressing the handle labeled "STEAM", the steam generator was started up and it was allowed to run for 5 minutes to clean and preheat the whole unit. After 5 minutes the steam generation was stopped by pulling the handle "STEAM" to the upper position. The safety

window was opened; the tube and Erlenmayer flask were also removed. Their contents were discarded into the sink with cold water running.

Sample Distillation

The cool digest was carefully diluted by adding 30 ml of distilled water. It was placed into the distillation unit. A titration (receiver) flask containing 25 ml of 0.05 M sulphuric acid and a few drops of Tashiro indicator were placed into the unit and the platform was lifted. It was ensured that the end of the cooler was under the surface of the unit; if not, a small amount of distilled water was added. The safety window was closed and the "ALKALI" handle pressed all the way down and dispensed 45 ml 45 % (w/w) sodium hydroxide solution. The steam valve was opened and the timer set to 3.5 minutes. After the signal was heard, the platform was lowered with the receiver flask so that the end of the cooler was above the surface. The "STEAM" valve and the safety window were opened. The tube was removed and the content was discarded into the sink with cold water running. The contents of the receiver flask were ready for titration.

Final Cleaning of the Unit

The unit was rinsed with distilled water and a wet cloth was used to clean all the parts (especially the rubber adapter) that were in contact with hydroxide or acid. The drain trough at the bottom of the unit was removed and cleaned with water. The unit was wiped to remove any spillage. The digestion tube and a receiver flask were emptied and were placed into position, and close the safety window.

Closing Down

The water tap was closed and power switched off, and the valve labeled "DRAIN" at the back of the unit opened and all the water in the expansion vessel and steam generator flew out.

Blank Titration

Blank titration was carried out to test the colour change of Tashiro indicator. Tashiro indicator is a mixture of methylen blue and methyl red. The colour changes depend on pH are as follows: acidic range: violet; neutral range: colourless; greyish tinge basic range: green. The endpoint (equivalence point) was then identified by the decolorisation of an originally violet solution by adding one more drop of titrant, the solution then turns green (i.e. over-titrated). Using a burette, 10 ml of 0.05M sulphuric acid was added into a titration flask containing approximately 10 ml of water and a few drops of Tashiro indicator. This solution was titrated using 0.1M sodium hydroxide , the volume of added titrant should be 10 ml.

Sample Titration

The contents of the receiver flask was titrated with 0.1M sodium hydroxide solution to the neutral endpoint. The volume of hydroxide required was recorded.

Calculation of results

The chemical reactions involved in the whole procedure are summarised as follows:

Sample digestion

$$\text{Organic N} + H_2SO_4 \rightarrow CO_2 + H_2O + (NH_4)_2SO_4$$

Neutralisation of digestion mixture and release of ammonia

$$(NH_4)_2SO_4 + 2NaOH \rightarrow 2NH_3 + Na_2SO_4 + 2H_2O$$

Reaction of ammonia with trapping solution (H_2SO_4)

$$2NH_3 + H_2SO_4 \rightarrow (NH_4)_2SO_4$$

Back titration of the excess of trapping solution

$$H_2SO_4 + 2NaOH \rightarrow Na_2SO_4 + 2H_2O$$

With respect to stoichiometry, and taking into account the concentration of titrant (NaOH, c = 0.1 mol/l) and trapping (H_2SO_4, c = 0.05 mol/l) solution, the volume of sodium

hydroxide needed to titrate the sample (VNaOH) corresponds to the excess of sulphuric acid in the trapping solution ($VEx H_2SO_4$).

To calculate the amount of nitrogen in the sample it is necessary to determine the amount of sulphuric acid (trapping solution) that reacted with ammonia to form ammonium sulphate ($V_{React\ H2SO4}$), That is to subtract the excess of sulphuric acid from the total (original) amount of sulphuric acid in the trapping solution ($V_{TotH2SO4}$):

$$\mathbf{V_{React\ H2SO4} = V_{TotH2SO4} - V_{ExH2SO4}\ (ml)} \qquad \mathbf{V_{ExH2SO4} = V_{NaOH}}$$

The amount of nitrogen is then calculated according to the following equality:

1 mL of 0.05 mol/L H_2SO_4 corresponds to 1.4 mg of nitrogen. The result should be expressed in g of nitrogen per 100 g of sample, and also in g of crude protein per 100 g of sample. To calculate the crude protein, multiply the amount of nitrogen by factor F (*Fhoney = 5.70).*

3.5.4 Determination of Vitamin A

Apparatus

1. Spectrophotometer (UV-VIS 8453 , Agilent-Califonia,US)

Procedure

Two grams of the sample was weighed into a beaker. 10ml of distilled water was added. It was shacked carefully to form a paste. 25ml of alcoholic KOH (produced by dissolving 4g of KOH in 50ml of water and make up to 100ml with alcohol) was added to the solution. It was heated in a water bath for 1 hour with frequent shaking. The mixture was cooled rapidly and 30ml of water was added. The mixture was transferred into a separating funnel. 250ml of chloroform was used for the extraction three times. 2g of anhydrous Na_2SO_4 was added to the extract to remove any trace of water. The mixture

was then filtered into 100ml of volumetric flask and made up to mark with chloroform. The absorbance was read at 328nm.

Standard (100ppm) stock

B-carotene, 0.003g, was weighed and dissolved in 100ml of chloroform working standard. From the 100ppm stock, 5ml, 10ml, 15ml, 20ml and 25ml were each pipetted into 50ml flasks. They were made to mark with chloroform.

Vitamin A (mg/100g) = Absorbance of sample x dilution Factor/ Weight of sample.

3.5.5 Determination of Vitamin C (Ascorbic Acid)

Method presented in Revanasiddappa and Veena, 2008 was used.

Apparatus

1. Spectrophotometer (UV-VIS 8453, Agilent-Califonia, US)

Standard Ascorbic Acid

1. 0.1g of ascorbic acid was weighed into a 100ml flask. It was made up to mark with distilled H_2O (Stock).
2. Working Standard: 0.05ml, 0.1ml, 0.15ml, 0.2ml, 0.25ml, 0.3ml, and 0.35ml of standard ascorbic acid solutions was pipetted each into 50ml flasks to represent 1ppm, 2ppm, 3ppm, 4ppm, 5ppm, 6ppm, 7ppm.
3. Procedure for Standard Preparation

From the 50 ml flasks above for the various standards, 1ml for each of the standard was pipetted into a 50 ml flask. 0.8 ml of (10 ppm $K_2Cr_2O_7$) solution was added into it. 1ml of 1M H_2SO_4 was added after 10 minutes. 1ml of 0.25% Chloroform was also added. It was

filled to mark with distilled H_2O. The absorbance was measured at 550 nm. Note, the absorbance of the blank was equally read and standard subtracted from it. The UV/VIS was blanked with distilled water.

Procedure for Sample Preparation

One milli-liter of sample was pipetted into 500ml flask (when the vitamin c is low) 100ml flask (when the vitamin c is high). 1ml was pipetted into a 50 ml flask and 0.8 ml of (10 ppm $K_2Cr_2O_7$) solution was added into it. 1ml of 1M H_2SO_4 was added after 10mins. 1ml of 0.25% Chloroform was added to make up with distilled water.

Vitamin C (µg/100g) *= Absorbance of sample x dilution Factor/ Weight of sample.*

3.6 Determination of Refractive Index

The Abbe refractometer (Abbe 60 Refractometers,UK) was used for this process. A drop of sample was placed on the sample space of the refractometer and covered with the lid. Through the eye piece, the equipment was observed to read. The calibration was also adjusted. After adjusting to a clear vision, the reading was noted.

3.7 Determination of pH

The pH meter (215 Denver-Colorado,USA) was calibrated using buffer 4 and buffer 9 before taking the readings of the samples. 10 g of the honey sample was dissolved into 75 ml carbon dioxide-free water in a 250 ml beaker. The mixture was stirred with magnetic stirrer and the electrodes were immersed and recorded the pH (AOAC, 1990).

3.8 Determination of Density

The 50 ml density bottles were used in this process. The density bottles were weighed and weight noted. The bottles were filled with samples and reweighed. The weights of only honey were obtained from where the densities were obtained (AOAC, 1990).

3.9 Determination of Water Content

The water content of the honey samples was calculated from the respective refractive index values. Hence, the water content was determined by adopting the expression below from (Abu-jdayil *et al.,* 2002).

% water = 608.277 – 395.743 n_D

Where, n_D =refractive index.

3.10 Determination of Antibacterial Properties of Honey

Preparation of Media

The culture media employed in this study was Nutrient Agar. It was prepared according to the manufacturers' specification. Except otherwise stated, all the media used were sterilized by autoclaving at 121°C for 15mintes, and in the case of solid media, it was allowed to cool to temperature of 50°C, dispensed aseptically into sterile Petri dishes and allowed to set. An un-inoculated plate was always incubated alongside inoculated plates to test for sterility.

Sterilization and Aseptic Technique

All glassware used were first washed with detergent, rinsed first with tap water and finally with distilled water and allowed to air-dry before sterilization by dry heat in the oven at 160^{o}C for two hours. The surface of working bench was thoroughly cleaned and disinfected before and after each experiment to prevent contamination.

Preparation of Test Organism

Stocked cultures of *Staphylococcus aureus* and *Pseudomonas aeruginosa* used in this study were obtained from the Microbiology Laboratory Unit, University Teaching Hospital Ado-Ekiti State. The isolates were identified based on standard microbiological techniques, and sub-cultured in nutrient agar slope at 37°C for 24hrs.

Isolation and Identification of Bacteria

Isolation and identification of Staphylococcus *aureus* and *Pseudomonas aeruginosa* was based on their cultural, morphological and biochemical characteristics employing standard procedures (Cheesbrough, 2006).

Antimicrobial Assay

Antibacterial activity of different honey samples and a reference antibiotic, against *Staphylococcus aureus* and *Pseudomonas aeruginosa* isolated from infected wounds, obtained from University Teaching Hospital Ado-Ekiti was tested by an agar diffusion method (CLSI, 2012). Honey samples were prepared by diluting each honey in sterilized, double distilled water at different dilution (concentration) ranging 20%, 40%, 60%, 80% and Net honey (100% honey) and then with sucrose, glucose and fructose. The earlier serially adulterated samples were also tested (see sec 3.1). The plates were prepared with 20 ml of sterile nutrient agar and the surface of the plates was inoculated using a 100 µl of 0.5 McFarland standardized inoculums suspension of bacteria which are allowed to dry. Wells, 6.0 mm in diameter were cut from the culture media using sterile metal cylinder, and then filled with test "honey" samples. The plates were incubated at 37°C and observed after 24 hours for clear, circular inhibition zones around the wells which were measured with the use of a vernier caliper.

3.11 Heavy metal analysis of honey samples

The analysis of heavy metals in honey samples was carried out using atomic absorption spectroscopy (AAS) standard method (Tuzen and Soylak, 2005). One gram of each honey sample from each region was mixed with magnesium acetate (1 mg/mL). The mixture was placed in a porcelain crucible. After drying at 100 °C for 2 hours, the samples were ashed at 600°C. Care was taken during heating so that no excess foaming took place. The ash was extracted with nitric acid (HNO_3) and was diluted to

30 ml. The contents of heavy metals were determined directly in the ash solution using atomic absorption spectroscopy (GF 3000 model AAS, Graphite Furnace GF 3000, Auto Sampler GBC PAL 3000, GBC Scientific Equipment Pty Ltd, Australia). The results were read three times and the mean values were computed.

CHAPTER FOUR

RESULTS AND DISCUSSION

4.1 Rheological Characterization of Honey

This section presents and discusses this study's rheological curve fitting results using PLM, CYM, ACYM and SKM. The data on the rheological profiling of pure honey and on the effects of sucrose, glucose, fructose, and water adulteration on honey rheology are presented. The effect of honey adulteration was used to classify other samples gathered from different locations in Nigeria. Also presented are the results of tests which aimed at correlating rheological profiling with the results of chromatographic, proximate, elemental compositions and antibacterial activities analyses of the same samples.

4.1.1 Rheology of Honey at 27°C and 35°C

This subsection presents and discusses the rheological characterization of reference pure honey at room temperature of 27°C and at 35°C.

Figure 4 is the rheograms of pure samples at 27°C . The two pure honey samples exhibited very close characteristics, producing nearly identical rheograms. The samples first exhibited shear thickening behaviour at the inception of flow and at low shear rate but later assumed an essentially shear thinning behaviour at higher rate of shear. Kurzberck *et al.,* (1999) suggested that the presence of chain branches gave rise to strain hardening a necessary property of stability for polymers undergoing deformation. The present data follow the flow behavior whose mechanistic interpretation by Triantafillopoulos, (1988), was presented in section 2.5. This kind of flow behaviour was also reported by Fan *et al.,*(2009) in their work on the numerical simulation of pulsatile non-Newtonian flow in the Carotid artery bifurcation.

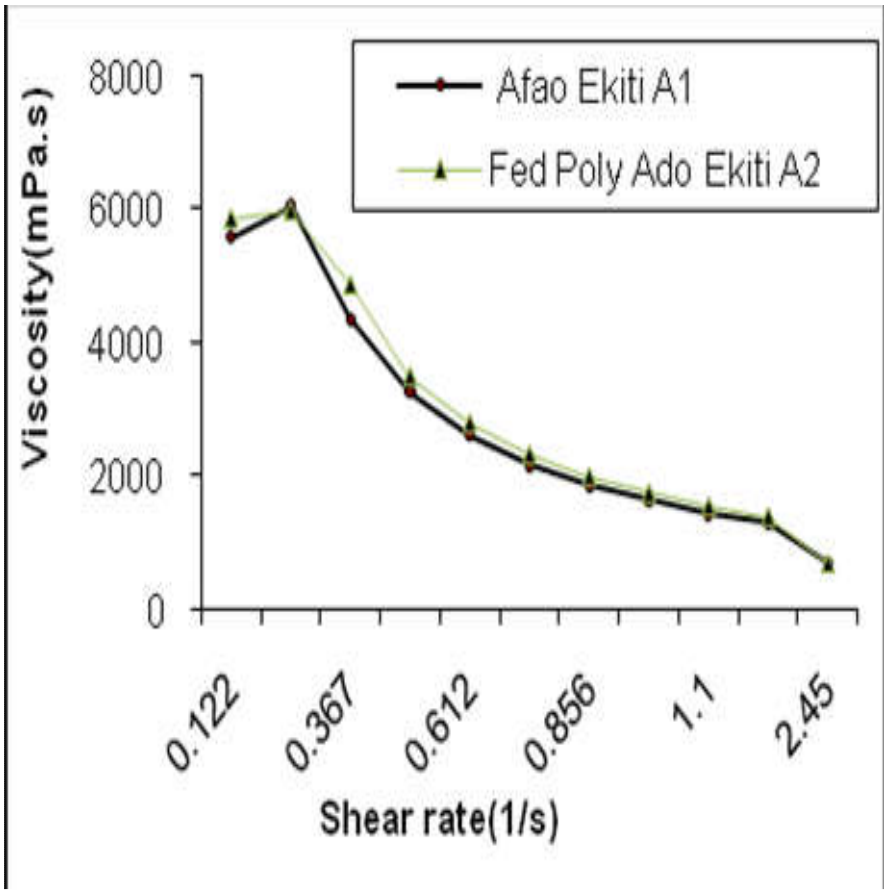

Figure 4. Rheology of Pure Honey at 27˚C

They suggested that at low shear rate, blood exhibits shear thinning behaviour but as shear rate increases, the non-Newtonian behaviour gradually diminishes. It might be suggested from the forgoing observations that the low shear rheology under which honey displayed in this work was governed by the molecular interactions of the structures and particles of the fluid. At higher rates of shear, the hydrodynamic effect takes over, resulting in Newtonian behaviour since the fluid may have been fully stretched.

Figure 5 shows the rheogram of the samples A1 and A2 at a temperature higher than that employed in generating Figure 4.

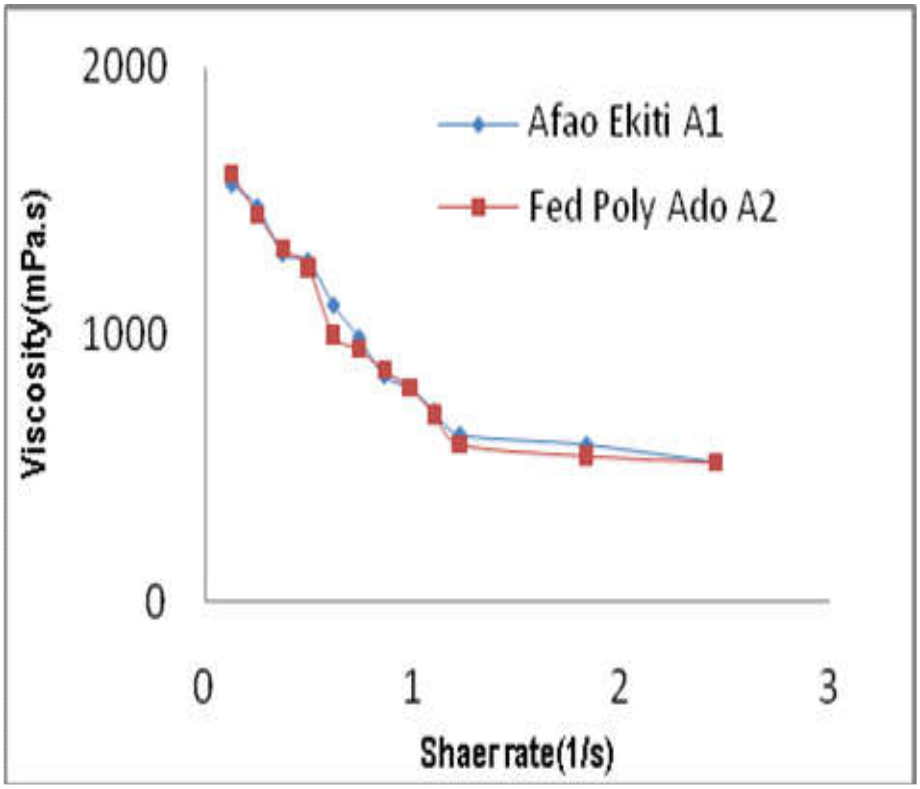

Figure 5. Rheology of Pure Honey at 35˚C

The two data sets, therefore, reflect the effect of temperature on pure honey rheology. The apparent viscosities of Nigerian honey samples decrease with increasing temperature as would be expected. It may, however, also be observed that at a shear rate of 1.22 s^{-1} and viscosity of 589 (mPa.s) the pure honey samples from Nigeria display a breaking point at which the viscosity of honey tends towards Newtonian. This justified the choice of the low rate of shear zone of the shear rate "spectrum" for the present study – a choice made in the hope that observed rheology will reflect molecular interactions of the fluid during deformation. The logic here is that intrinsic properties of the samples are best captured at the inception of fluid deformation.

4.1.2 Rheology of Forever Honey

A slight variation was observed for the Forever Honey (A3), in Figure 6 below. This sample of honey is observed to follow a similar rheological line shape with the two Nigerian pure honey samples at room temperature (see Figure 4 above) though the Nigerian honeys had higher viscosities.

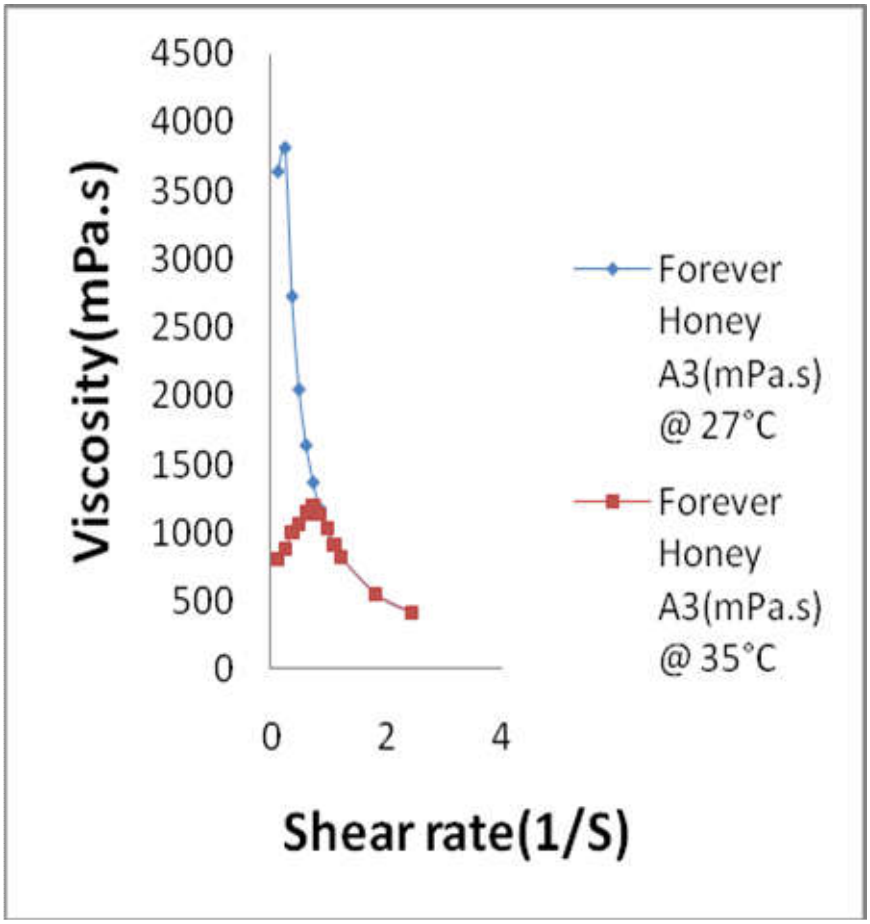

Figure 6. Rheology of Sample A3 at 27 and 35 °C

At a higher temperature of 35°C, however, the American honey still continued to mimic the room temperature rheogram of the sample, with shear thickening behaviour at the inception of deformation and shear thinning as shear rate increased. This might suggest that this sample contains more or heavier oligosaccharides and HMF than does the Nigerian Honeys, perhaps on account of geographical origin or as a reflection of adulteration. This study had indeed opted to carry out the rheological analyses of samples at two different temperatures on the assumption that a fake or adulterated sample of

honey, successfully formulated to mimic pure honey rheological behavior at a given temperature, will show disparity at a different temperature. Also it is note-worthy that at higher rates of shear, the viscosity dependence on temperature is minimized leading to merging of both rheograms. This might be attributed to vaporization of volatile components as temperature increases.

4.1.3 The Effect of Adulteration on the Rheology of Honey

This subsection discusses the effect of adulteration on the rheology of honey**.** Figures 7, 8, 9, and 10, respectively, show the effects of sucrose, glucose, fructose, and water adulteration on honey rheology.

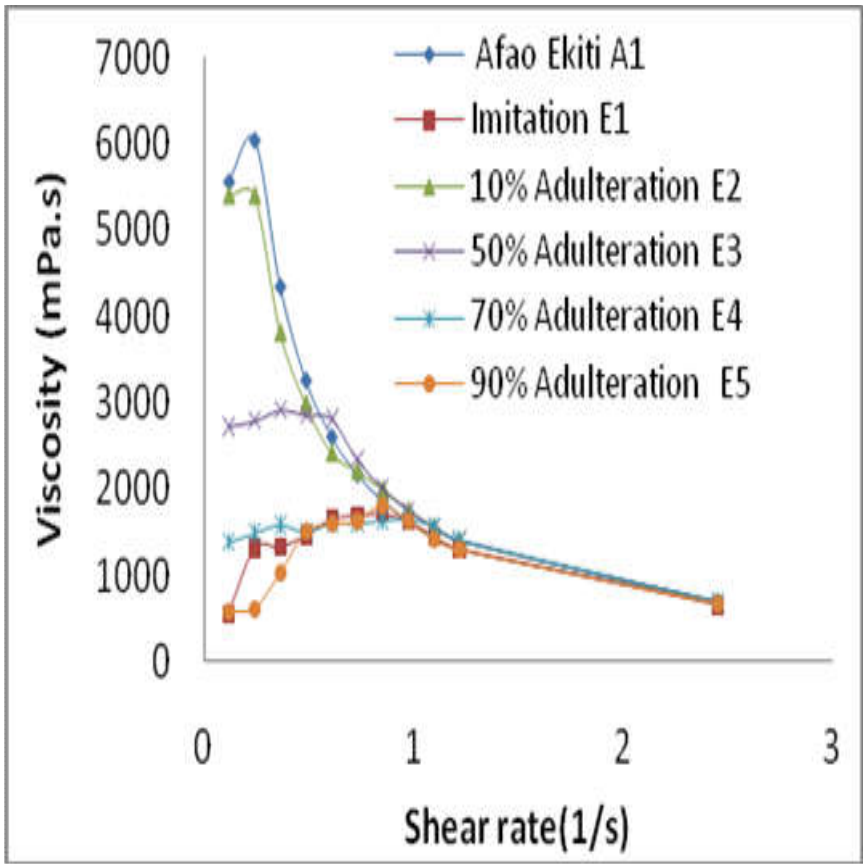

Figure 7. Effect of Sucrose Adulteration on Honey Rheology at 27˚C

It can be inferred from Figure 7 that addition of different percentages of sucrose melt (E1) to pure sample A1 lead to decrease in the viscosity of the resulting samples up to sample E5. This simply suggests that rheology is dependent on composition (Bakier, 2007 and Bera *et*

al., 2008). The rheograms suggests that the viscosity of sample E1 changes minimally with increase in shear rate. This implies that the rheology of sucrose tends towards Newtonian.

Likewise, similar results were observed in the use of glucose and fructose in honey adulteration in Figures 8 and 9.

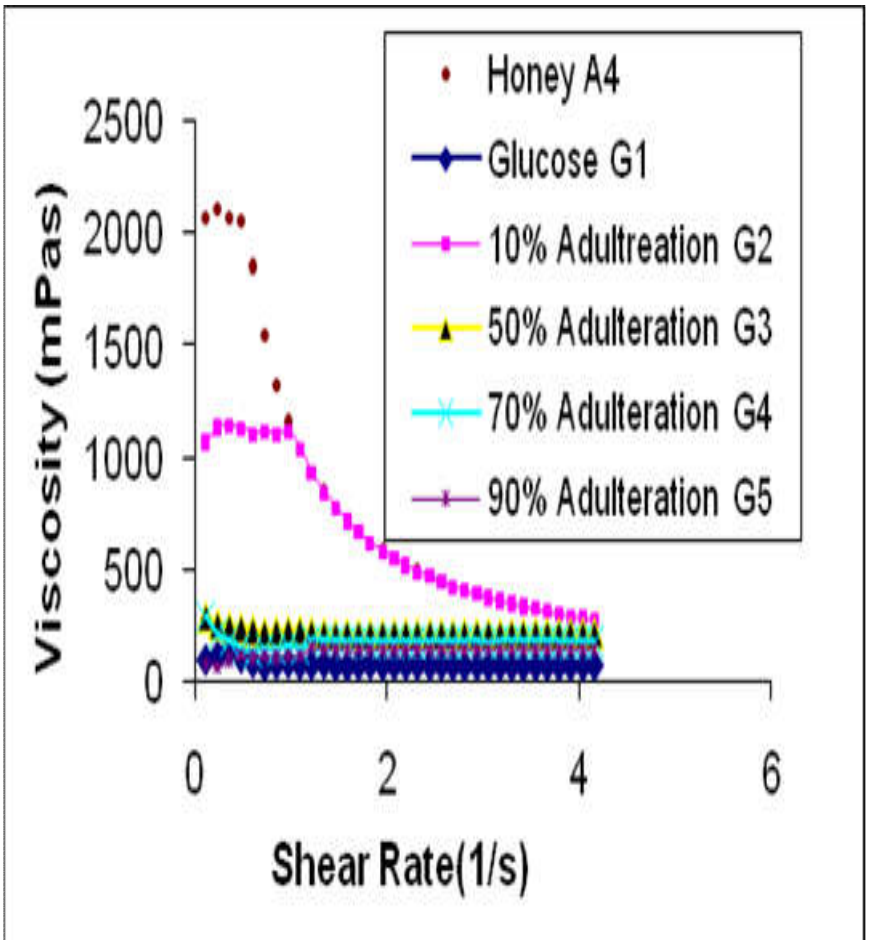

Figure 8. Effect of Glucose Adulteration on Honey Rheology at 27˚C

It has been suggested that the colloidal materials, polymerized monosaccharides, melezitose, raffinose and some oligosaccharides are responsible for honey's non-Newtonian behaviour (Sopade *et al.,* 2004). The substitution of these heavy or high molecular weight materials with the lower molecular weight adulterants lead to sequential decrease in the viscosity of the resulting adulterated fluids.

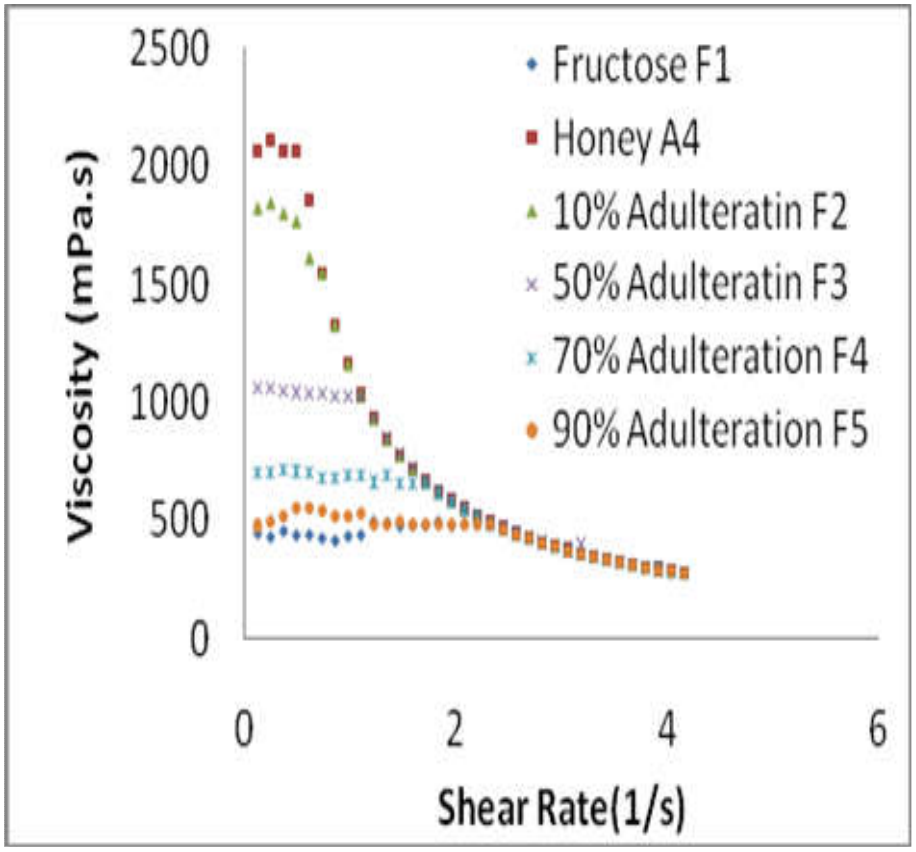

Figure 9. Effect of Fructose Adulteration on Honey Rheology at 27˚C

Figure 10 shows the rheological signatures of honey adulterated with distilled water. In some parts of Nigeria (like North East region) where the usual adulterants are inaccessible or are considered uneconomical on account of high levels of poverty, some honey vendors resort to adulteration of honey with water.

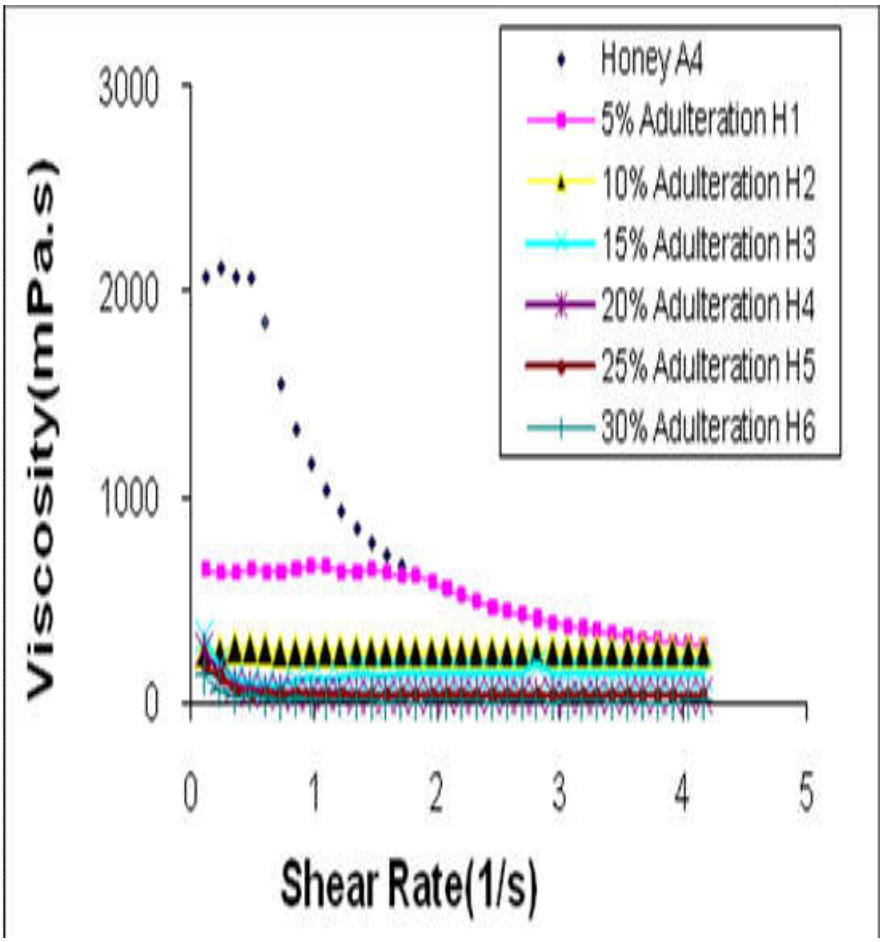

Figure 10. Effect of Water Adulteration on Honey Rheology at 27˚C

The plots show that water is not a good adulterant for honey as only 5% adulteration drags the viscosity of the resulting adulterated sample close to Newtonian behaviour. Upon further adulteration of honey with water, above 10%, the resultant fluids exhibited Newtonian flow behaviour. Sucrose adulterated samples were heated and analyzed rheologically at temperature of 35°C.

Figure 11 is the effect of temperature treatment on the rheology of sucrose adulterated honey. There is need to use models to better analyze the rheogram.

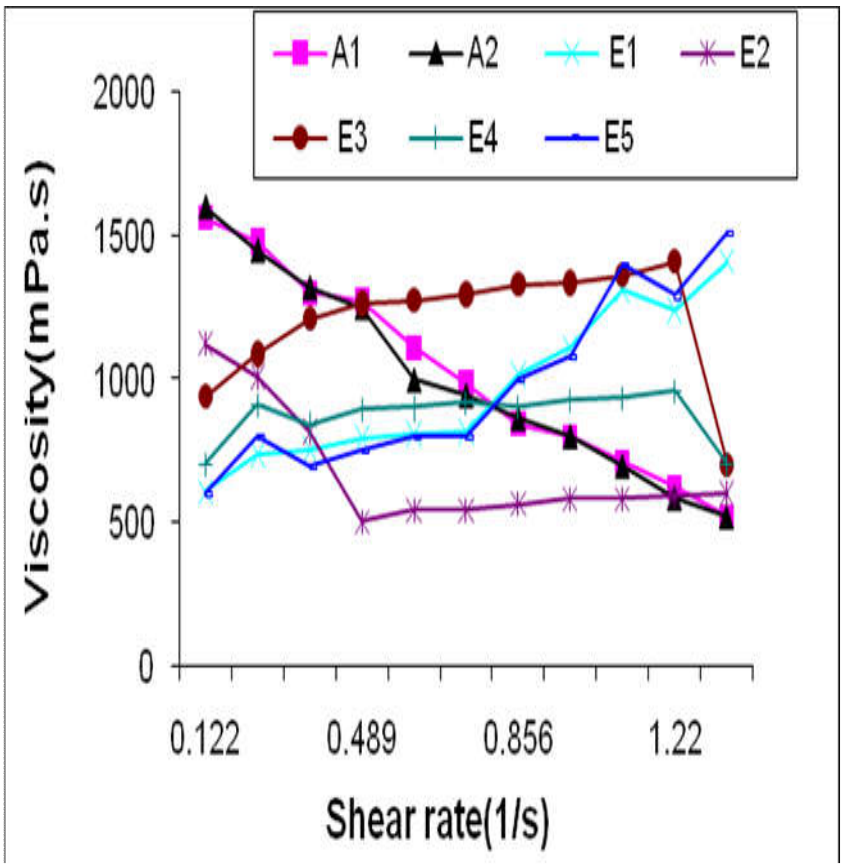

Figure 11. Effect of Sucrose Adulteration on Honey Rheology at 35˚C

4.1.4 Rheology of Samples from Different Locations in Nigerian

Figure 12 is the rheology of honey from Northern Nigeria at 27°C. It can be seen that the rheograms of sample B1 (Gauraka) and sample B7 (Kabba) bear strong semblance to that of pure honey in Figure 4. This shall be confirmed using the rheological models, PLM and CYM (see section 4.1.5). Likewise, sample B2 (Yola) exhibited an entirely shear thinning behaviour, without the initial shear thickening characteristic earlier established for pure honey. This behaviour could be attributed to lower contents of protein, colloidal materials, crystallized or polymerized monosaccharide.

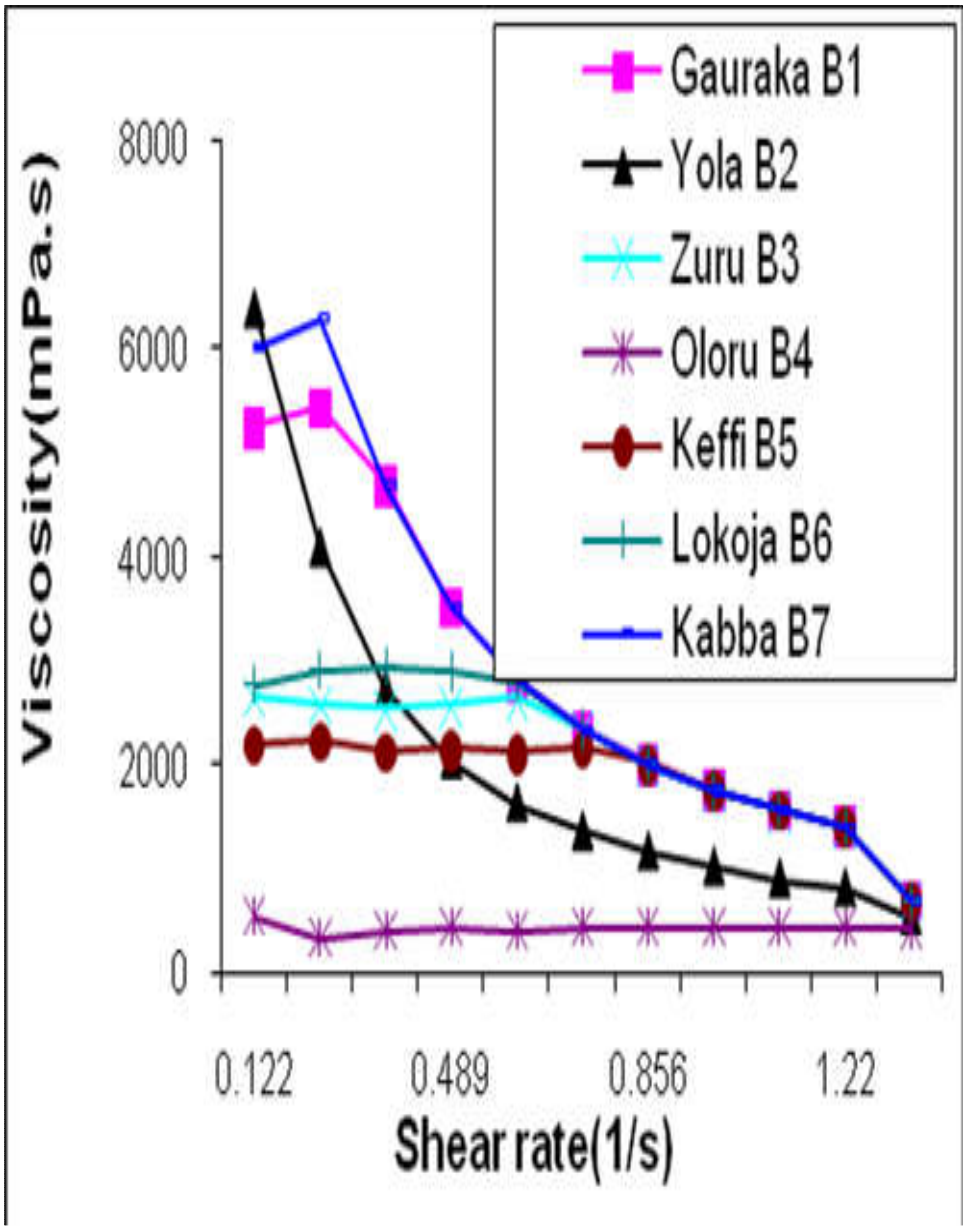

Figure 12. Rheology of Honey from Northern Nigeria at 27° C

A close inspection of the proximate composition of this sample showed that sample B2 is leaner in protein content than the other pure honey samples as further elaborated upon in section 4.3. Likewise and worthy to note, is the rheogram of sample B4 (Oloru, Kwara) in Figure 12. This sample exhibited essentially Newtonian behaviour at all shear rates, leading to its eventual classification as a fake honey.

Figure 13 presents rheological profiles of honey samples from Southern Nigeria. The high viscosities of sample C1 (Sunshine, Ondo) and to a lesser extent that of C3 (Blessed Ado) dwarfed the rheograms of other samples.

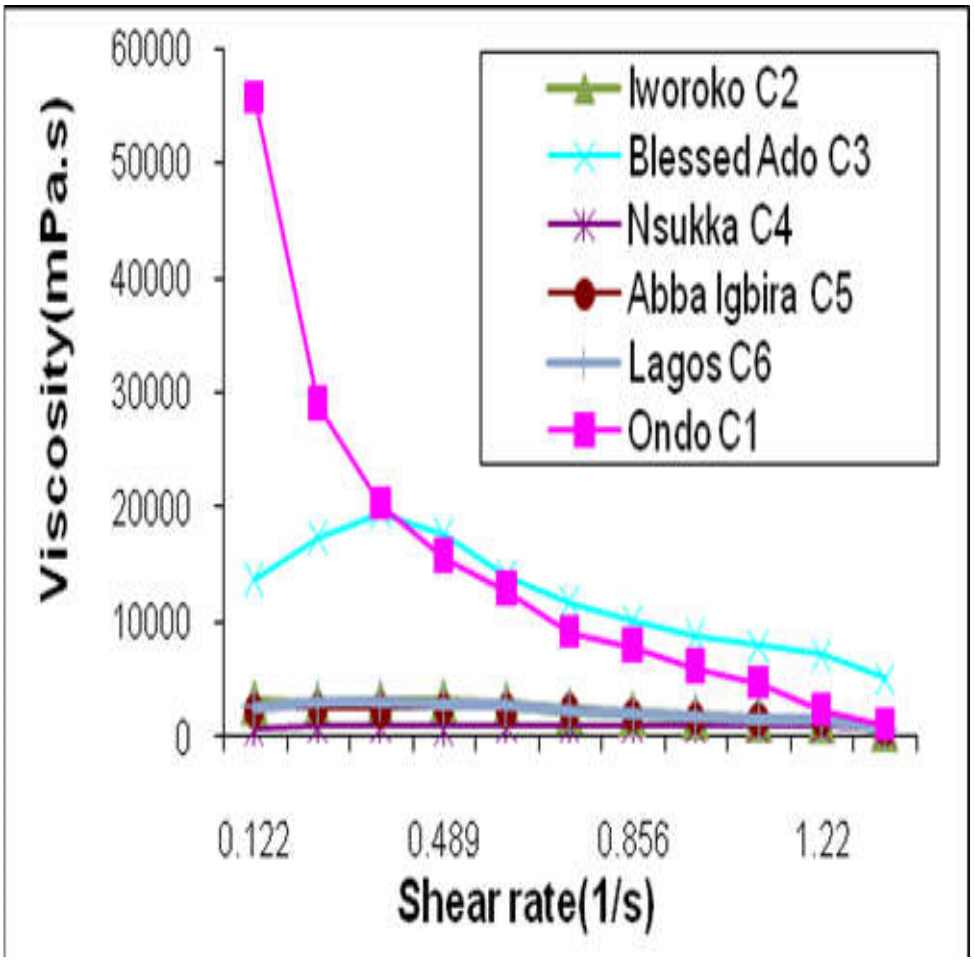

Figure 13a. Rheology of Honey from Southern Nigeria at 27˚C

Figure 13b is the rheograms of samples from Southern Nigeria without samples C1 and C3. The rheogram of sample C4 from Nsukka in Enugu State has the characteristic shear thickening and shear thinning behaviour of pure honey which will eventually lead to its classification as pure honey.

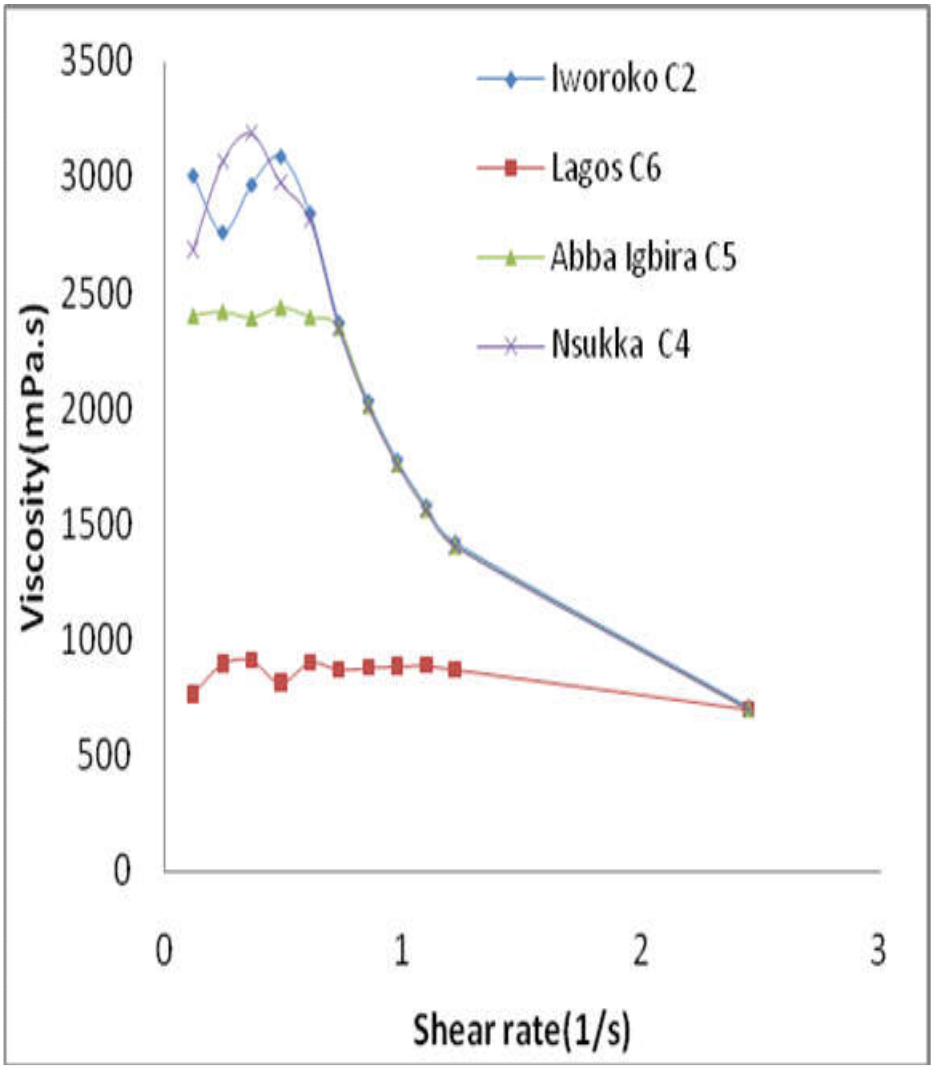

Figure13b. Rheology of Honey from Southern Nigeria at 27˚C without Samples C1 and C3

However, rheological models shall be useful to extract the compositional and structural properties of the fluids. The rheograms of other samples in Figure 13b showed disparities from that of honey were classified (see section 4.1.6).

Figure 14 is the rheology of honey from Northern Nigeria measured at 35˚C. At the higher temperature, the rheograms were stretched as a result of high temperature and may require rheological models for interpretation.

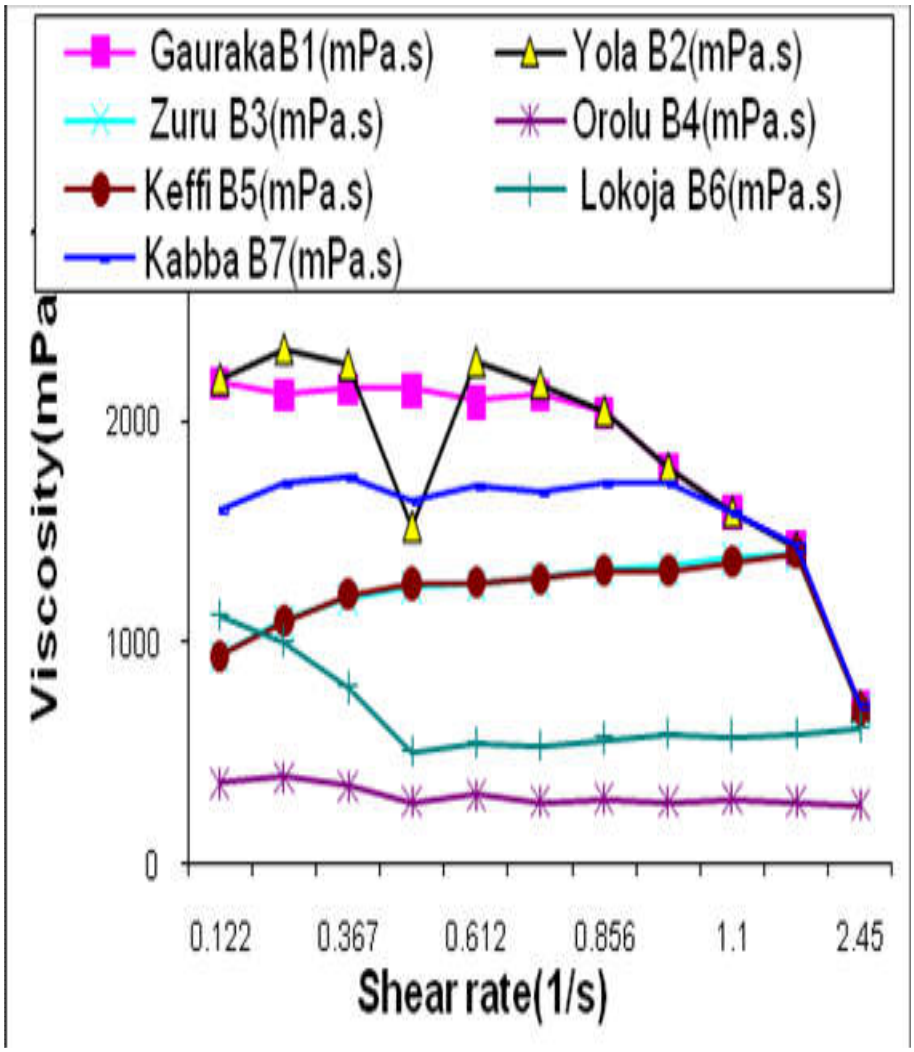

Figure 14. Rheology of Honey from Northern Nigeria at 35°C

Figure 15a represents rheological data of honey from southern Nigeria. Here, the Blessed honey sample from Ekiti state are seen to possess relatively high viscosities such that its rheograms, on the same scale, obscure those of the other samples at this temperature as was the case at room temperature.

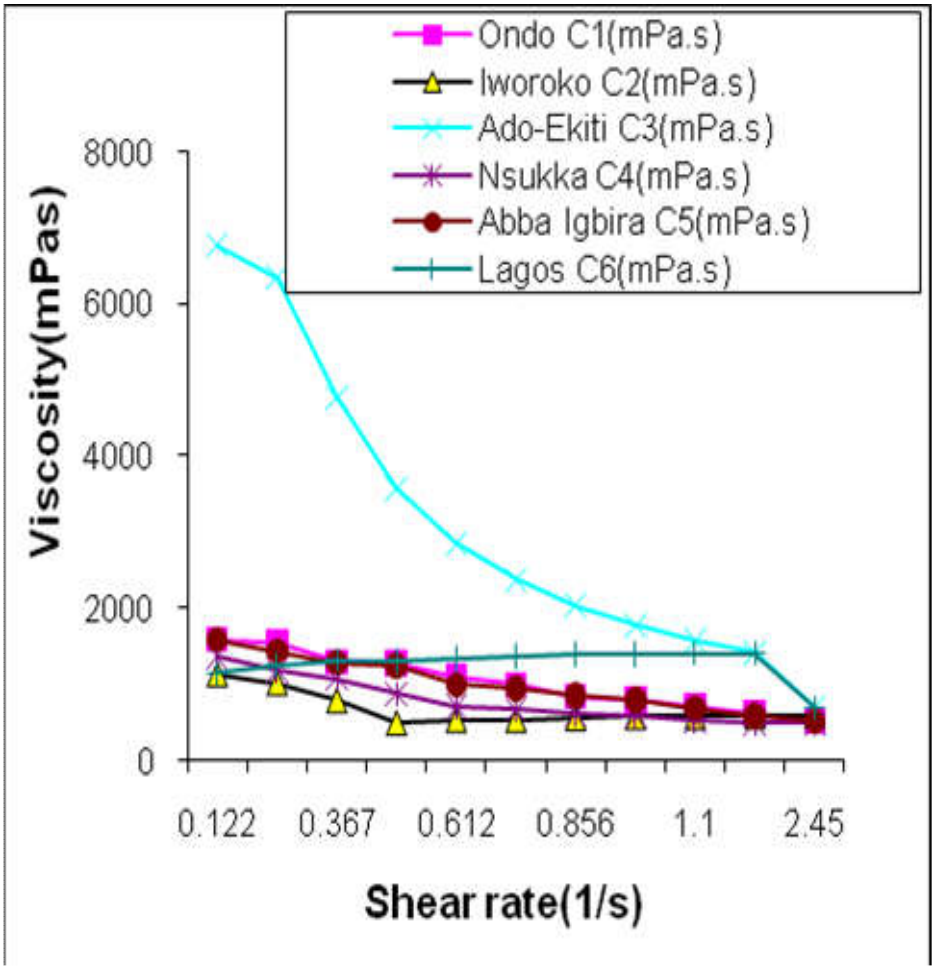

Figure 15a. Rheology of Honey from Southern Nigeria at 35°C

Figure 15b was plotted without the sample from Ekiti. In the plot, the rheogram of sample from Enugu resembles that of honey at elevated temperature. While samples from Lagos and Iworoko came nothing close to honey. Like the rheograms for samples from Northern Nigeria, rheological models may also be required to analyze the Southern Nigerian honey data.

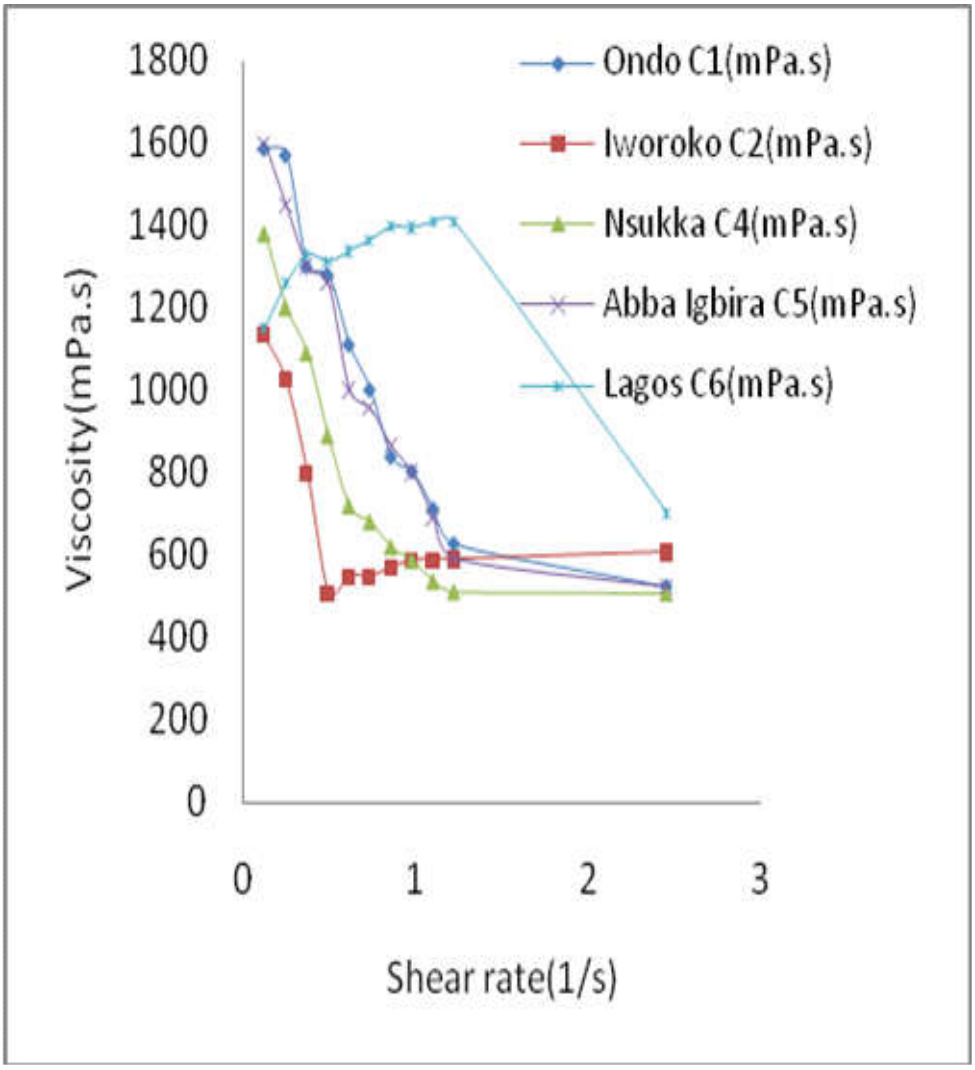

Figure 15b Rheology of Honey from Southern Nigeria at 35˚C without C3

4.1.5 Extraction of Compositional Information from Rheological Data Using Power Law Model and Carreau-Yasuda Model

In the preceding subsection 4.1.4, the rheograms were employed for the qualitative assessment of the samples. Emerging from this assessment is that changes in the purity of honey reflected in their rheograms. In this subsection, however, quantitative analyses of samples by the use of models are sought. The PLM and CYM were used to extract

compositional information and to assess the level of purity of honey from rheological data. The data on samples obtained from the graduated dilution of an established pure honey specimen with typical adulterants were used for calibration to determine the levels of purity of other Nigerian honey samples. Figures 16 and 17 are the PLM curve fit of pure honey sample A1 at 27˚C and 35˚C. In the PLM, the two most important parameters of this model are the behaviour index , n, and zero shear viscosity, $\eta_{0.}$

These parameters correlate with the compositional and molecular orientation of samples (DeLaney and Reilly, 2000) and have been employed, here, as distinguishing factors for purity or authenticity of samples in this study.

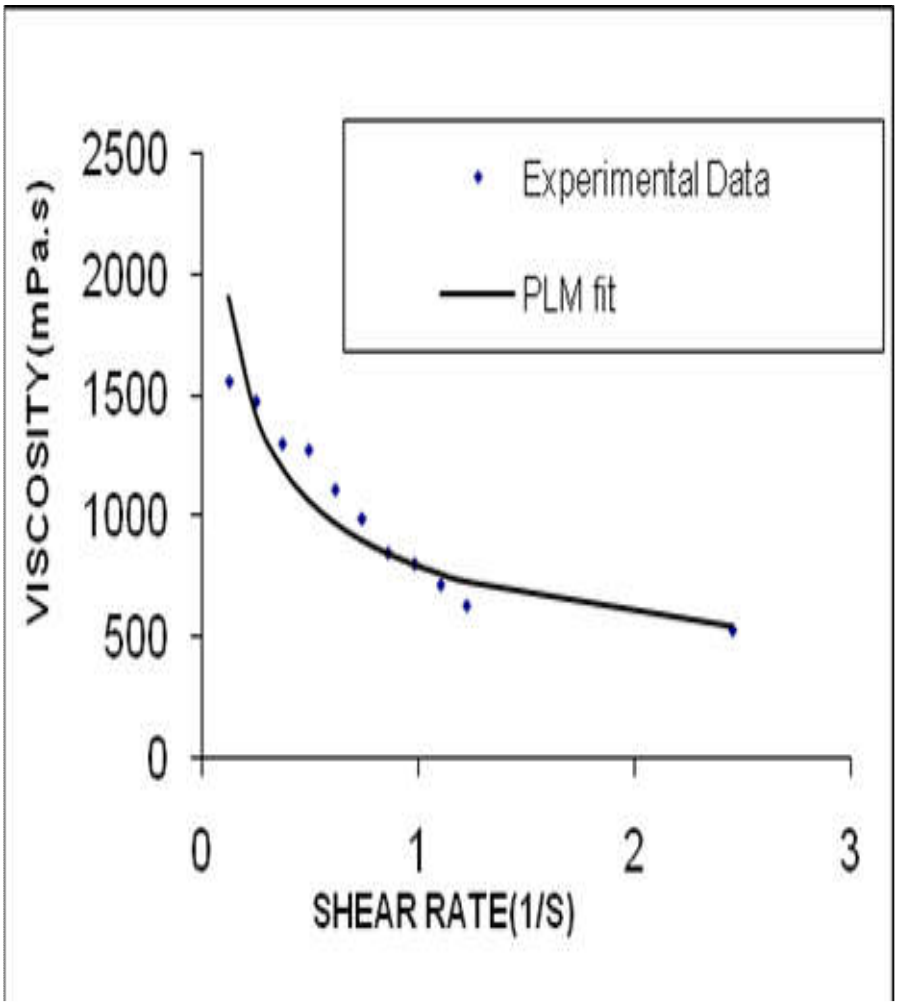

PLM Curvefit of Afao-Ekiti Sample A1 (Afao-Ekiti)at 35˚C

The behaviour index correlates closely with composition while the zero shear viscosity correlates closely to the molecular weight of honey. For a shear thinning fluid, the value of behaviour index is less than one, greater than one for when a fluid is shear thickening and one for a Newtonian fluid. The behaviour indices values of 0.23 and 0.30, respectively, were obtained for pure samples A1 and A2 at 27 °C. These results suggest that at room temperature, honey exhibited shear thinning behaviour. The corresponding zero shear viscosity were 1746.33 and 1856.76 mPa.s respectively. The close values obtained for both consistency indices and zero shear viscosities of the two samples suggest similarities in their composition and structure.

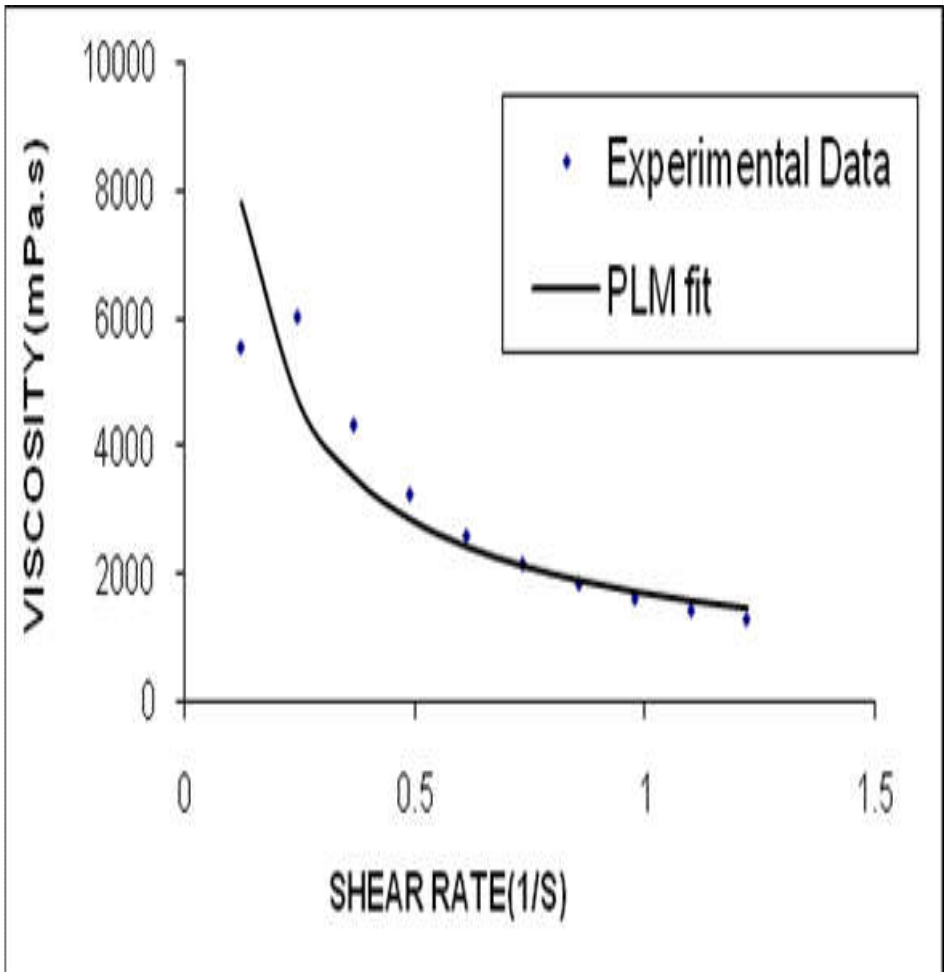

Figure 16.PLM curvefit of Sample A1(Afao-Ekiti)at 27°C Figure 17

The zero shear viscosity has a relationship with the average molecular weight of honey in the Mark Houwink equation as earlier observed. It was deemed unfit to use in the PLM to obtain the molecular weight of honey. This is because of palpably large discrepancies at the inception of deformation between this model's estimate and the experimental zero shear viscosities. The Mark Houwink equation will, however, be later explored while working with the CYM and SKM models for the extraction of average molecular weight estimates. The observed discrepancies pointed out earlier were typified in the error factor of 0.27 between the experimental and calculated viscosity for this sample. This discouraged the further use this model to calculate the average molecular weight of samples. This is so because the zero shear viscosity which Mark Houwink relation replaces in the equation has to do with viscosity at the inception of flow. Figure 17 is the PLM curve fit of sample A1 at 35°C. The behaviour index increased to 0.59 at 35°C from 0.23 at 27°C. It suggests that increasing the temperature further drew the structures of the fluid apart. Perhaps the colloidal materials and other heavy protein based components responsible for the viscous nature of honey were altered by high temperature. However, the error factor decreased to 0.1409 but the deviation of correlated viscosities at the inception of the deformation was still showing large discrepancies with the experimental data at this temperature. The details of the PLM curve fitting can be found in Appendix 1.

Figure 18 is the CYM curve fit of pure sample A1. The behaviour index in CYM depends also on the compositon of the fluid. The value of 0.00 which suggests a shear thinning behaviour was obtained for pure Sample A1 at 27°C.

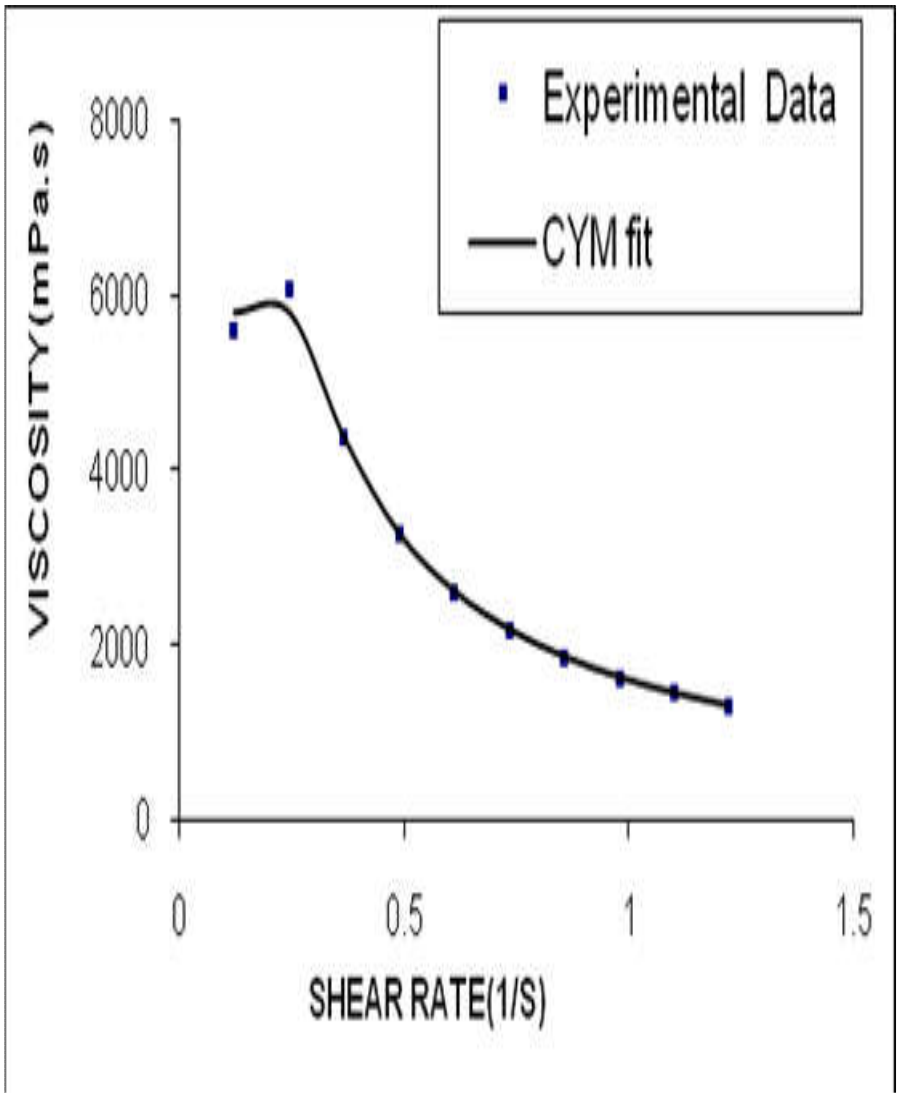

Figure 18.CYM Curvefit of Sample A1 (Afao-Ekiti) at 27°C

A look at the plot shows that the difference between the experimental and correlated viscosities at the inception of deformation was infinitesimal suggesting this model as a good tool to calculate the average molecular weight of samples from the rheological data . Figure 19 is the CYM curve fit of sample A1 at 35°C. The behaviour index increased to 0.68 as a result of increase in temperature. Similarly, increasing the temperature of the fluid further stretched the structures of the fluid apart. Also, the error factor decreased to 0.093775 and the deviation of correlated viscosities at the commencement of the structural breakdown showed negligible discrepancies with the experimental data.

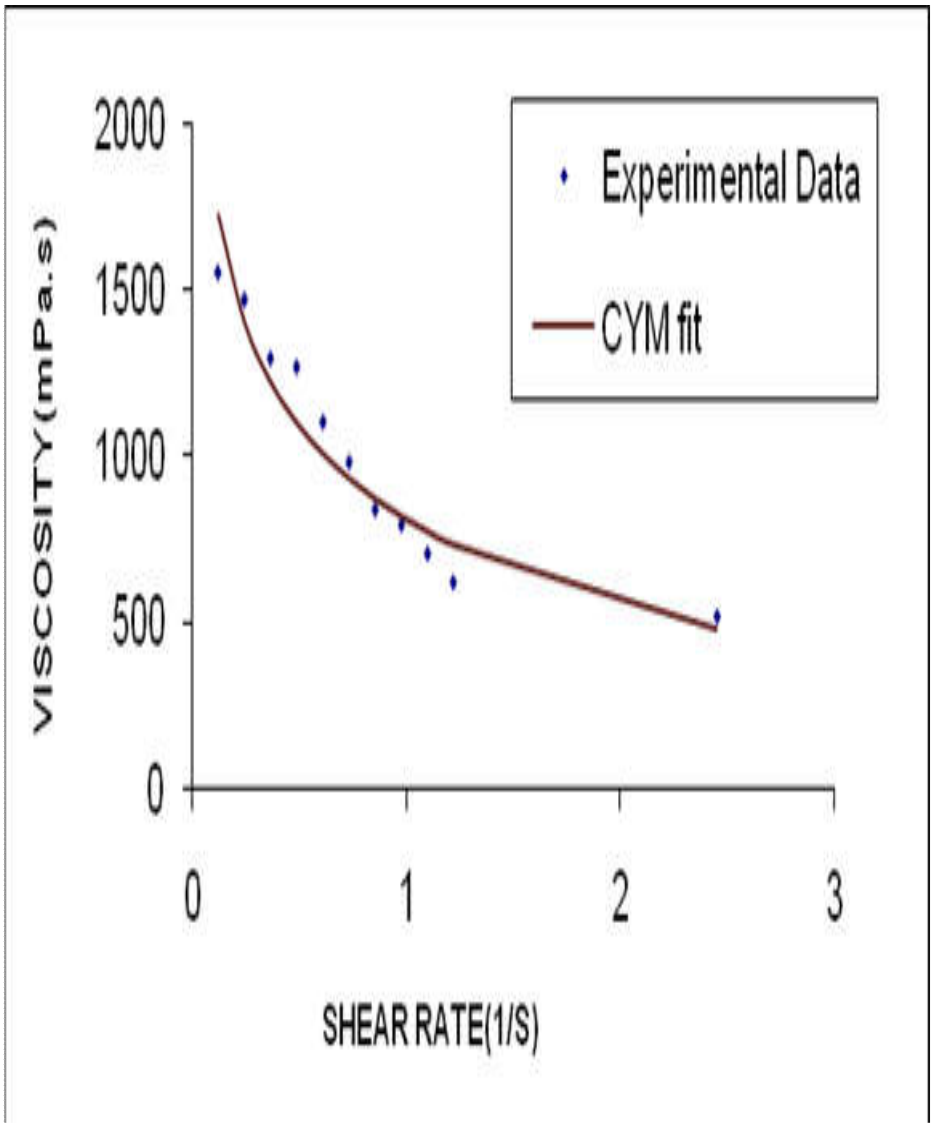

Figure 19. CYM Curvefit of Sample A1 (Afao-Ekiti)at 35˚C

Comparing, the error factor of sample A1 for PLM and CYM, it suggests that since at room temperature of 27°C, the PLM yielded an error factor of 0.27 while the CYM produces a factor of 0.003412, the CYM correlated the experimental data better. On the other hand, at 35°C error factor for the CYM was 0.093775 compared to 0.14 for PLM. The smaller is the error factor, the better the curve fit. The CYM therefore fits better than the PLM at this temperature also.

Figures 20 and 21 are the PLM curve fits of sample A2 at 27°C and 35°C. This sample has behaviour index and zero shear viscosity values close to those of sample A1. These similarities, naturally, derive from the close match of the rheograms of the two samples.

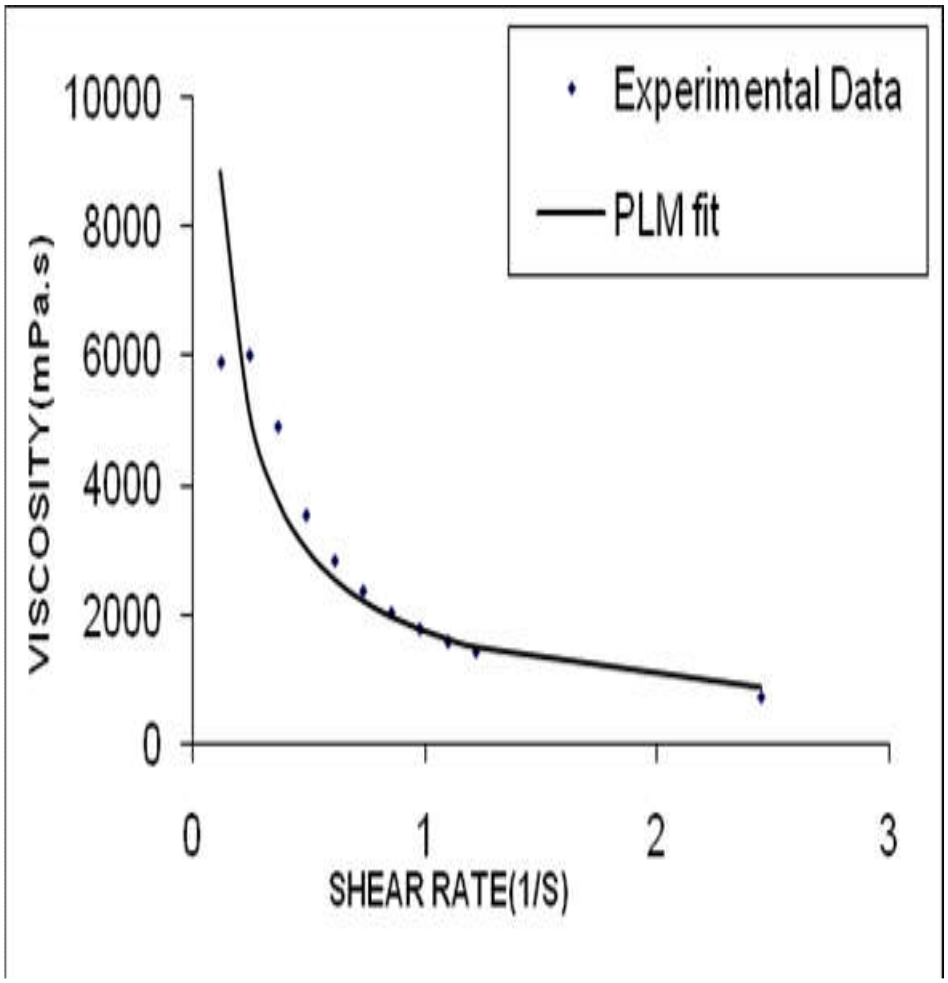

Figure 20.PLM Curvefit of Sample A2(Ado-Ekiti) at 27˚C

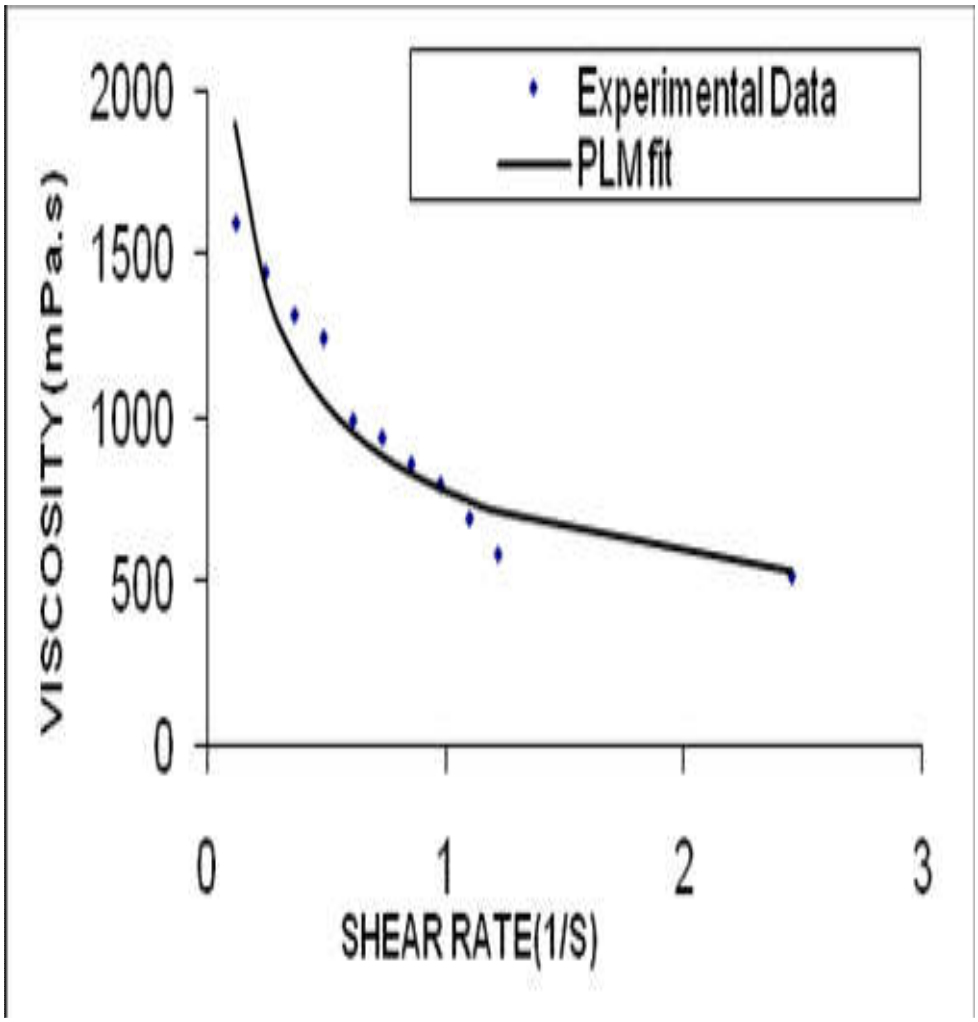

Figure 21.PLM Curvefit of Sample A2(Ado-Ekiti) at 35˚C

Figures 22 and 23 are the CYM curve fits of sample A2 at 27°C and 35°C – reflecting the same observation made on sample A1 from Figures 18 and 19. This should be expected, again, on account of the close similarities of the rheograms of A1 and A2. Thus, the conclusions drawn from the data on A1 above, equally well apply to A2. A comparison of CYM and PLM on sample A1 shows that CYM better correlates the rheology of sample A1. Equally, Figures 20 - 23 showed that CYM better correlated the rheology of sample A2.

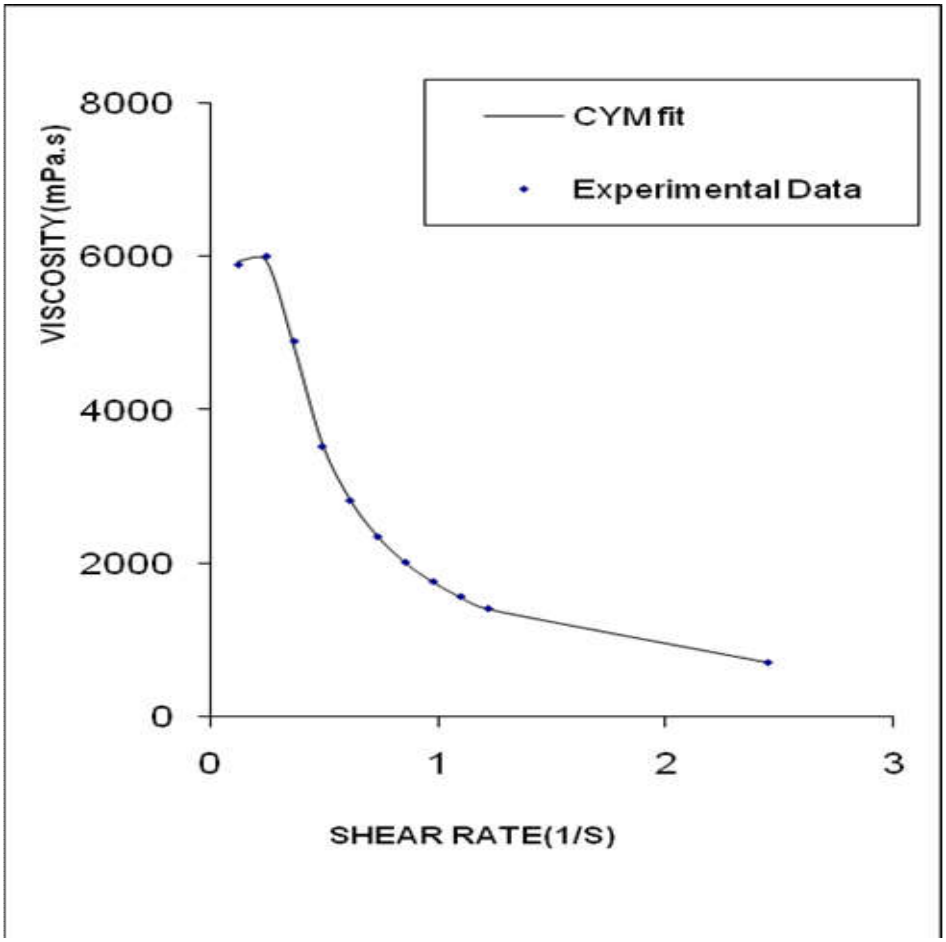

Figure 22. CYM Curvefit of Sample A2 (Ado-Ekiti) at 27˚C

The sum of the errors was found to be 0.000765 for CYM against 0.4541 for PLM at room temperature of 27 °C. The smaller the sum of errors is, the better the rheological correlation of samples (Morrison, 1999).

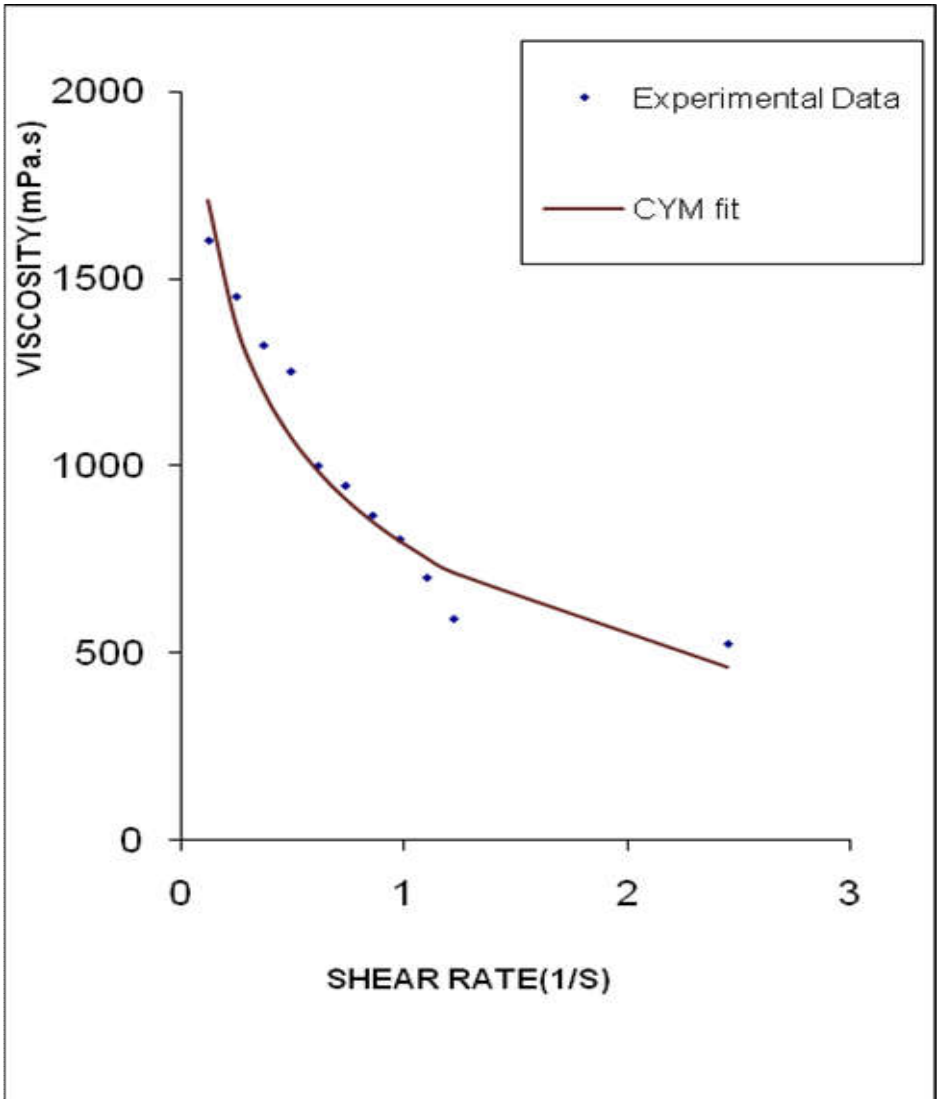

Figure 23. CYM Curvefit of Sample A2 (Ado-Ekiti) at 35˚C

Table 3, below, is the summary of rheological characterization results using PLM. The two parameter PLM utilizes only the behaviour index as its discriminative parameter while the zero shear viscosity contain information on the viscosity at the inception of deformation. Table 3 thus suggests that pure honey is a shear thinning fluid. It could also be observed that the behaviour index increases sequentially with increasing adulteration. Similarly, the zero shear viscosity of samples decreased sequentially with increasing adulteration of honey. The increase in temperature of honey to 35°C lead to increase in the behaviour index values, showing that at increased temperature, honey tends more towards Newtonian behaviour. This

is so because the hydrodynamic effect controls the rheology of honey under conditions of decreased apparent viscosity. The details of rheological curve fitting using the PLM are in Appendix 1.

Table 3. SUMMARY OF RHEOLOGICAL MODELING RESULTS USING PLM

S/N	Samples	n at27 °C	η_0 at 27°C	(∑Error)²at 27 °C	n at 35 °C	η_0 at 35 °C	(∑Error)² at 35°C
1	A1	0.28	1716.06	0.2746	0.59	796.80	0.1409
2	A2	0.23	1746.33	0.4184	0.58	778.84	0.1287
3	E1	1.22	1284.57	2.5841	1.31	1070.63	0.1087
4	E2	0.37	1664.03	0.3949	0.75	583.65	0.3157
5	E3	0.57	1661.21	0.8226	1.00	1181.41	0.6228
6	E4	0.88	1349.42	0.6992	1.03	879.63	0.1353
7	E5	1.10	1328.32	2.5930	1.18	1014.45	0.3217
8	B1	0.27	1741.74	0.4848	0.71	1556.73	0.6969
9	B2	-0.15	1245.78	15.7641	0.70	1540.34	0.7461
10	B3	0.60	1617.28	0.7258	1.00	1182.05	0.5260
11	B4	0.98	420.50	0.1311	0.88	293.22	0.0039
12	B5	0.69	1543.35	0.6932	1.00	1184.03	0.6218
13	B6	0.56	1511.52	0.7017	0.76	587.40	0.3270
14	B7	0.22	1744.32	0.3996	0.82	1413.96	0.6461
15	C1	-0.32	4916.29	1.8930	0.57	798.46	0.1469
16	C2	0.55	1681.90	0.7546	0.75	588.28	0.3231
17	C3	1.43	12814.25	3.3500	0.20	1772.40	0.2921
18	C4	0.17	1296.20	0.9460	0.59	618.71	0.0961
19	C5	0.64	1598.23	0.7590	0.58	777.94	0.1296
20	C6	0.55	1679.08	0.9206	0.93	1220.36	0.5333

In Tables 4 and 5, below, are the summaries of rheological curve fitting results using CYM at 27°C and 35°C respectively. Results presented in Table 4 shows that the behaviour index in the CYM increases with increasing adulteration of honey. Correspondingly, in Table 5, the behaviour index increased with increasing adulteration. The higher sample temperature is observed, in Table 5, to result in increases in the values of behaviour index from the CYM curve fit. This suggests that at the higher temperature, the structure of samples had been "stretched" and, thus, explains why the rheology of honey further tends towards Newtonian behaviour.

Table 4. SUMMARY OF RHEOLOGICAL CYM CORRELATION OF SAMPLES AT 27°C

S/N	Samples	n at 27 °C	λ(s)	$_o$ at 27 °C	a at 27 °C	∑(Error)^2
1	A1	0.00	3.62	5788.20	144.88	0.003412
2	A2	0.01	3.33	5943.96	74.60	0.000765
3	E1	1.07	1.87	702.28	13.80	3.168138
4	E2	0.13	3.90	5400.14	114.07	0.016016
5	E3	0.25	1.99	2818.87	217.71	0.084177
6	E4	0.50	1.19	1542.55	422.18	0.132526
7	E5	1.01	3.08	715.35	55.88	1.616931
8	B1	-0.03	3.06	5341.60	15.09	0.000835
9	B2	0.40	4.00	4637.92	10.00	5.861308
10	B3	0.28	1.82	2579.28	323.07	0.088440
11	B4	1.00	4.17	417.20	9.71	0.122842
12	B5	0.26	1.30	2164.79	238.83	0.002911
13	B6	0.14	1.72	2881.26	160.79	0.003019
14	B7	0.00	3.56	6138.99	106.36	0.00108
15	C1	0.01	5.82	55591.17	103.92	11.06954
16	C2	0.00	1.70	2944.43	103.87	0.007106
17	C3	0.26	9.57	16452.84	184.24	0.237377
18	C4	-.00	3.90	4941.43	166.78	0.410251
19	C5	0.27	1.40	2406.58	97.68	0.226462
20	C6	0.02	1.71	2955.68	56.29	0.019859

Table5. SUMMARY OF RHEOLOGICAL CYM CORRELATION OF SAMPLES AT 35°C

S/N	Samples	n at 35 °C	λ(s)	$_o$ at 35 °C	a at 35°C	(∑Error)^2
1	A1	0.69	3.62	13179.82	0.14	0.093775
2	A2	0.68	4.85	15569.99	0.13	0.099591
3	E1	1.70	0.01	845.08	5.74	0.668851
4	E2	0.71	18.00	1085.37	10.00	0.695125
5	E3	0.90	0.50	1214.83	34.48	0.559954
6	E4	1.00	26.30	804.82	49.45	0.131053
7	E5	1.66	0.00	833.73	1.87	0.774921
8	B1	0.40	1.27	2135.96	89.10	0.002393
9	B2	0.97	123.74	7397.98	0.28	1.288327
10	B3	0.93	0.70	1207.96	13.68	0.153539
11	B4	1.45	4.69	349.34	57.10	0.068475
12	B5	0.92	0.79	1220.83	405.25	0.922670
13	B6	0.72	18.13	1112.31	13.03	0.296078
14	B7	0.60	0.99	1691.76	275.00	0.006952
15	C1	0.67	0.12	2014.54	0.43	0.162941
16	C2	0.80	194.45	1729.88	51.25	0.309356
17	C3	-0.02	3.82	6765.38	7.65	0.000024
18	C4	0.69	2.64	1458.70	0.74	0.208878
19	C5	0.69	0.08	1569.54	0.54	0.230028
20	C6	0.83	0.51	1326.44	14.20	0.038380

The rheological curve fitting for pure honey, for different percentages of serially adulterated samples, and for samples gathered from different locations in Nigeria using both PLM and CYM all follow a consistent pattern. It appears justifiable, therefore, to extrapolate model parameters derived from the rheograms of the serially diluted samples to classify other samples according to the levels of their purity.

Table 6 below is the outcome of this suggested classification exercise for samples gathered from different locations across Nigeria. Thus, samples B1, B7, and C4 are considered pure. This is so because in the PLM curve fit at room temperature, the behaviour index which depends on the composition was found to be 0.23 for pure sample A1. The results of 0.28, 0.22, and 0.16 were obtained on this parameter for samples B1, B7 and C4, respectively, reflect acceptably low deviations from the result of the pure honey sample. Likewise, the behaviour index for pure sample A1 was found to be 0.59 at 35°C which is relatively closer to 0.70, 0.82 and 0.59 obtained for B1, B7 and C4 respectively than was observed for samples adjudged to be of poor quality.

Table 6. CLASSIFICATION OF SAMPLES BASED ON PLM AND CYM PARAMETERS (REFERENCE - DATA ON SERIAL DILUTION OF HONEY WITH SUCROSE)

Reference	Classification	Consistency of Sample	Samples
A1	Pure	Consistent	B1,B7,C4
E2	10% Adulteration	Consistent	B2,C1
E3	50% Adulteration	Consistent	B3,B5,B6,C2,C3,C5,C6
E4	70% Adulteration	Consistent	
E5	90% Adulteration	Consistent	
E1	100% Imitation	Consistent	B4

In the rheological curve fitting using CYM, the behaviour index value of 0.00 was obtained for the pure sample A1 which is quite close to -0.04, 0.00 and 0.00 obtained for B1(Gauraka,

Niger),B7 (Kabba, Kogi) and C4 (Nsukka, Enugu) respectively at 27 ˚C. Following the same trend, Table 6 suggests that samples B2 (Yola, Adamawa) and C1 (Sunshine, Ondo) conform closest to 10% adulteration. Also samples B3 (Zuru, Kebbi), B5 (Keffi, Nasarawa), B6 (Lokoja, Kogi), C2 (Real Oasis, Iworoko Ekiti), C6 (Lagos), C3 (Blessed ,Ado-Ekiti) and C5 (Abba Ibira, Ekiti) conform to about 50% adulteration while sample B4 (Orolu, Kwara) and conform to 100% fake or imitation sample. The consistency in colour and texture of the serially adulterated samples looked exactly the same like the pure samples but rheology was able to separate the pure from the adulterated. This supports the notion that rheology may serve as an index of quality in honey.

4.1.6 Extraction of Structural and Compositional Information from Rheological Data Using SKM and ACYM

The goal of this subsection is to extract the structural and additional compositional information from the rheological data. The SKM is used here to obtain both structural and compositional information from honey (see section 3.3.3). The structural information includes the order of deformation which reflects on the number of active components in a fluid undergoing deformation. Also the rate of deformation is obtained here as one of the structural information from the model. Lastly, the average molecular weight which is compositional information was obtained using the SKM. The ACYM was equally used to independently assess the molecular weight of honey using the method of Morrison (1999) (see section 3.3.4).

For the structural kinetic model, time resolved data on fluids' apparent viscosities at given constant rates of shear were extrapolated to zero times to obtain the zero shear viscosities.

The zero shear (zero time) viscosity was applied in Mark-Houwink equation to obtain the fluid's molecular weight at each shear rate. The average molecular weight was then determined for all shear rates studied. Since this work was done at low rates of shear, the fluid might not have deformed long enough to give values of the infinite time viscosity for the calculation of rate of deformation, k (see also section 3.3.3). From equation (3.11), the rate of deformation (k) is obtained explicitly from:

$$k = \left\{ \left[(\eta - \eta_\infty)/(\eta_o - \eta_\infty) \right]^{1-n} - 1 \right\} / t(n-1) \tag{3.14}$$

Also, if Γ is defined by, $\Gamma = \left(\frac{\eta - \eta_\infty}{\eta_o - \eta_\infty}\right)^{1-n}$ (4.2)

Then $\Gamma = tk(n-1) + 1$ (4.3)

Since k is expected to depend only on rate of shear rate (Abu-djayil, 2003) a scheme was developed by which an optimized value of k was determined for each rate of shear. The scheme associates optimum k with the set of parameters that yielded the least coefficient of variation. This coefficient of variation or relative standard deviation (RSD) is the standard deviation of k divided by its mean value calculated from the six different times of the experimental determination of apparent viscosities (10s, 20s, 30s, 40s, 50s and 60s). This value of k and the set of the other parameters that produced it are deemed as the parameters of the model and were found to also give the best fit, following equation (4.3), to Γ versus t data.

Figure 24 shows the viscosity-time rheogram of Imuwen Ijebu-Mushin honey (sample A4), used to obtain the zero shear viscosity at a shear rate of $0.01s^{-1}$.

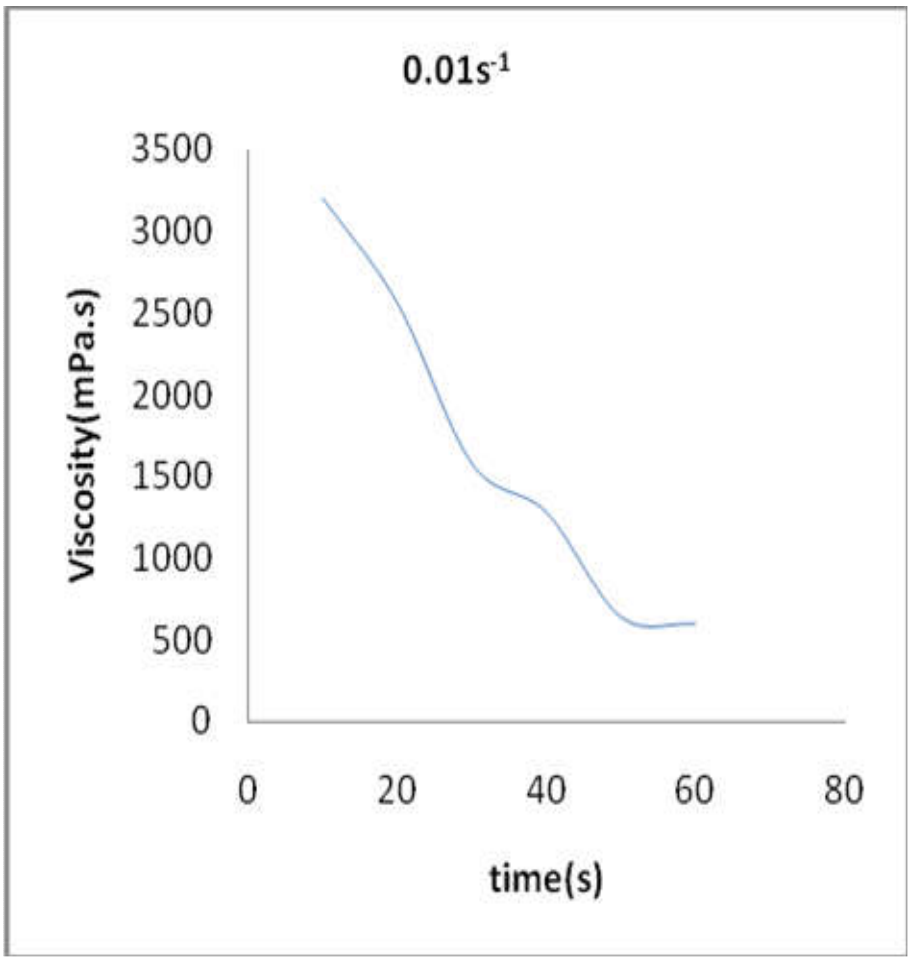

Figure 24.Viscosity vs time graph of Sample A4

The zero shear viscosity was applied in Mark-Houwink equation (equation 2.3) to obtain the molecular weight at that shear rate. The average molecular weight of the fluid was then determined for all the rates of shear used. Since this study was done at low shear rate, the fluid would not have deformed for a long time to obtain the infinite time viscosity. Figure 25 is the plot for optimization of infinite time viscosity at a shear rate of $0.01s^{-1}$.

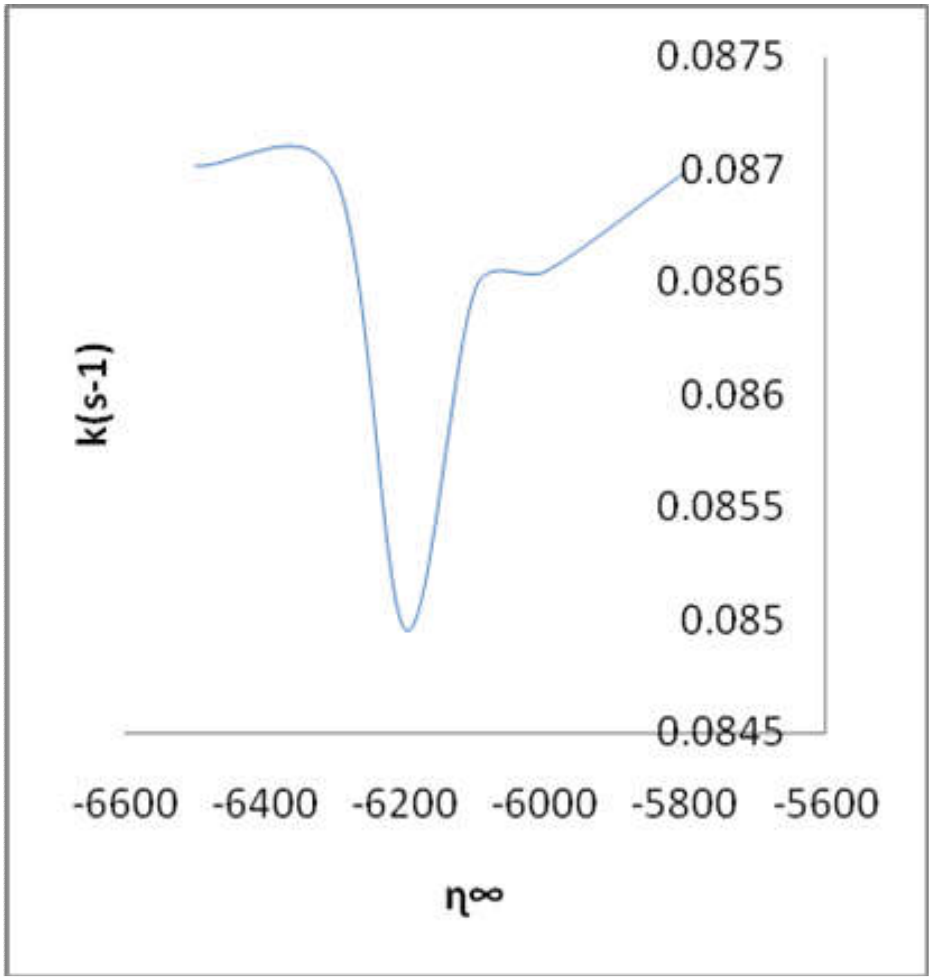

Figure25. Optimisation of *k* for Sample A4

From the plot, the minimum value (best value) of infinite time viscosity was obtained. The determined optimum infinite time viscosity with the model parameters that produced it gave explicit estimates of *k* from equation (4.1). The mean value of *k* for the constant rate of share data gave, as expected, the same value as was determined from the slope of the best linear fit to the data of Figure 26.

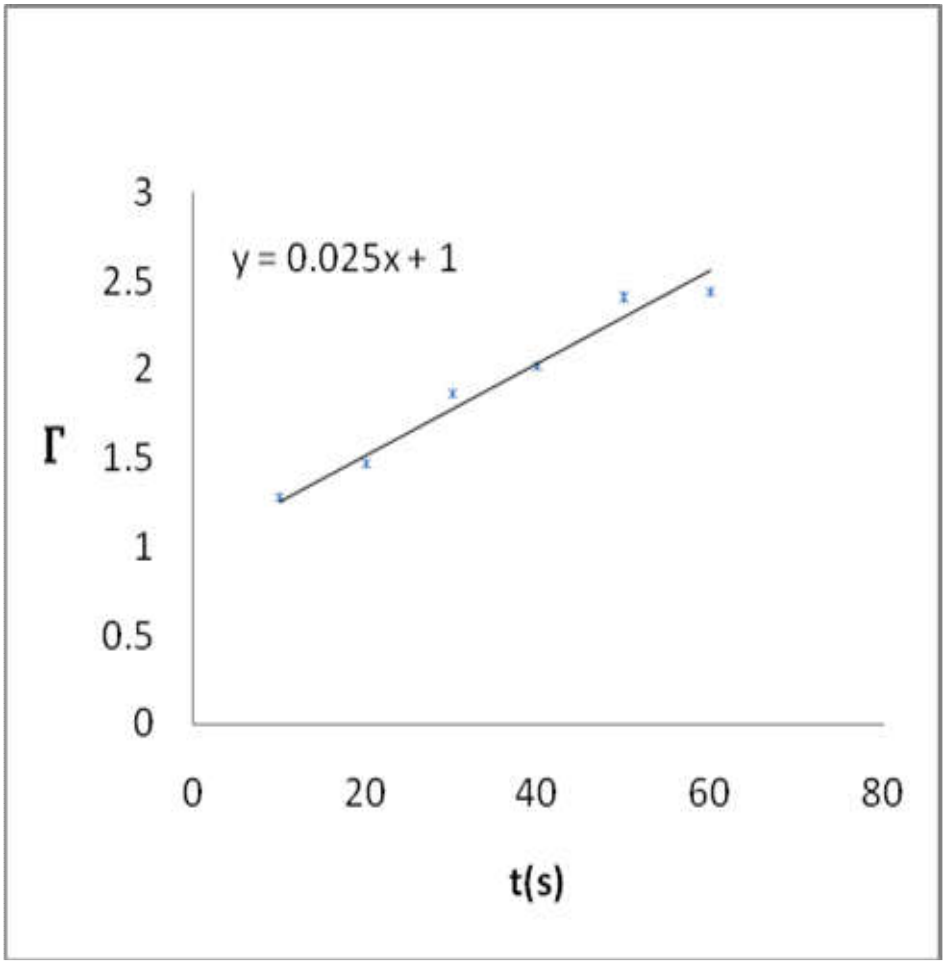

Figure 26. Plot of Γ against time

Figure 27 shows the dependence of rate of deformation for sample A4 on rate of shear. It is instructive to note, here, the goodness of linear fit of the rate of deformsation versus shear rate data (Figure 27). A different quality of fit was to be obtained on adulterated samples (see Figure 35).

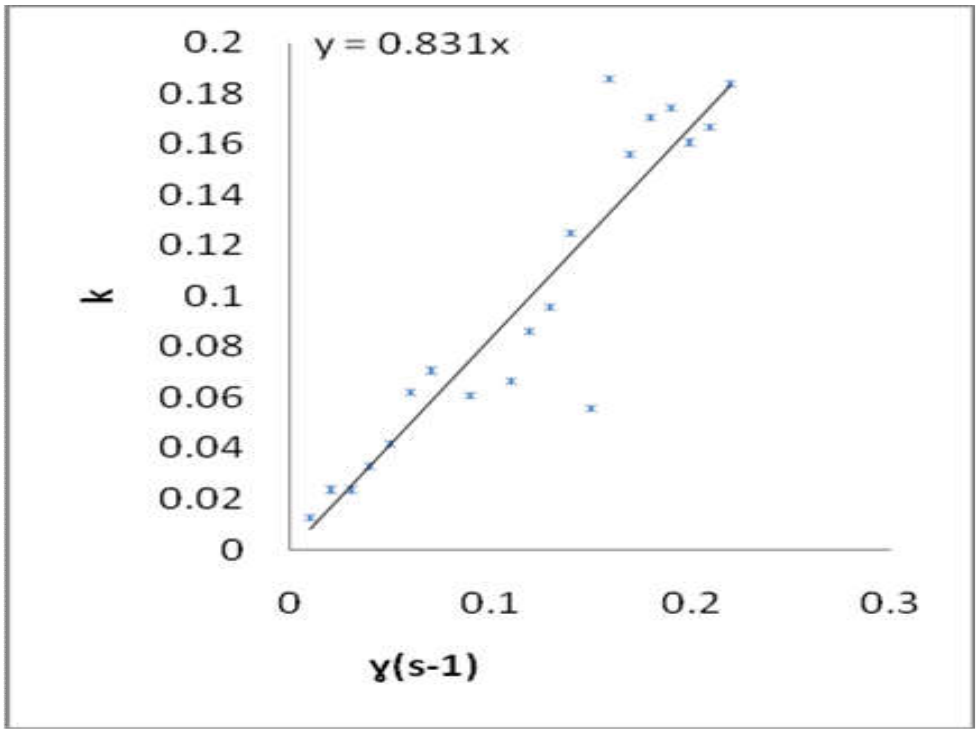

Figure 27. Plot of k against shear rate

Table 7 above is the summary of rheological curve fitting results using the new SKM. It was observed that the honeys from Imuwen Ijebu Mushin, Forever honey, Federal Polytechnic and Ayo bee farm Ado-Ekiti honey have their average molecular weights as 252 g/mol, 246 g/mol, 253 g/mol and 249 g/mol respectively. The molecular weight of samples decreased with increasing adulteration. The details of curve fitting using the SKM can be seen in Appendix 2. The results of the rate of deformation in Table 7 suggest that it increases with the adulteration of samples. There are sequential decreases in the average molecular weight of adulterated honey with increases in adulteration. This is expected because the molecular weights of the adulterating materials in this subsection are lower than that of pure honey.

TABLE 7. SUMMARY OF RHEOLOGICAL CURVE FITTING USING THE SKM AT 27°C

S/N	Sample Code	Sample Identity	Molecular Weight(g/mol)	n	*k*(S-1)
1.	A1	Ayo Bee Farm Ado-Ekiti	249	3.00	-
2.	A2	Fed Polytechnic Ado-Ekiti	253	3.00	-
3.	A3	Forever Honey	246	3.00	-
4.	A4	Ijebu Mushin	252	3.00	0.83
5.	G1	Glucose	146	1.50	3.69
6.	G2	10% Glucose Adulteration	232	2.50	10.69
7.	G3	50% Glucose Adulteration	189	2.00	13.16
8.	G4	70% Glucose Adulteration	174	2.00	2.83
9.	G5	90% Glucose Adulteration	160	1.50	3.29
10.	F1	Fructose	147	1.50	3.26
11.	F2	10% Fructose Adulteration	230	2.50	4.12
12.	F3	50% Fructose Adulteration	198	2.50	5.18
13.	F4	70% Fructose Adulteration	176	2.00	1.59
14.	F5	90% Fructose Adulteration	160	1.50	4.06
15.	H1	5% Water Adulteration	242	2.50	1.05
16.	H2	10% Water Adulteration	222	2.00	0.94
17.	H3	15% Water Adulteration	212	1.50	0.61
18.	H4	20% Water Adulteration	201	1.50	0.63
19.	H5	30% Water Adulteration	178	1.50	0.69
2.0.	H6	50% water Adulteration	132	1.50	0.75

The high molecular weight values (>180 g/mol) exhibited by pure samples in Tables 7 and Table 8 could be as a result of high melezitose, colloidal materials, polymerized and crystalised monosaccharides in honey. The addition of glucose, which has a molecular weight of 180g/mol, fructose which is an isomer of glucose with the same molecular weight and water with a molecular weight of 18g/mol lead to sequential decrease in the molecular weight of the resulting adulterated honeys. This could be attributed to the fact that all the materials used in the adulteration in this subsection have lower molecular weight than honey and reductions in the molecular weight of adulterated samples explain why their behaviour tends toward Newtonian. The lower molecular weight recorded for both glucose and fructose here is as a result of their water content. Similarly, the details of results on the effects glucose, fructose and water adulteration on the rate of deformation of honey are also in Tables A3.1-A3.3 of Appendix 2.3.

It was observed during the iterations, that the infinite time viscosities at different rates of shear that satisfied the SKM for pure honey were negative. Bacri and Perzynski, (1995) provided the very first evidence of negative viscosity of fluids. It suggests that when shear is applied, the fluid behaves in a negative manner as a result of stored up energy due to the shear history of the fluid. This could be an expression of time dependent behaviour of honey. A similar behaviour was also observed by Lemarchand *et al.,* (2015) in their study of Cooee bitumen. Earlier, Rao (2014) expressed frustration on the 'very low magnitude' of infinite time viscosities of food products and consequently suggest that it should be ignored. It was worthy to note that the adulterated samples all gave positive infinite time viscosities. It then suggests that honey when adulated became less time dependent.

The best results were obtained for the pure honey samples at third order deformation kinetics. The essence of this is that three components of the honey constituents are active during deformation. It suggests that melezitose and other oligosaccharides and polymerized materials serve as the first, water as the second, and monosaccharides as the third active component. In the study of effect of water adulteration in honey, the results of curve fitting were best at second order deformation. It again suggests that the kinetic model views the entire honey as one component and the water as another during deformation.

Table 8 below shows the summary of curve fitting results using the ACYM. The results show that Imuwen Ijebu Mushin honey has the average molecular weight of 250 g/mol. The two pure honeys from Ekiti, which are from Ayo bee farm and Federal Polytechnic Ado-Ekiti, have molecular weight of 260 g/mol and 260 g/mol respectively. It was also observed that Forever honey's average molecular weight is 253 g/mol. Similarly, the molecular weights obtained using the ACYM decreased with increasing adulteration of honey.

TABLE8. SUMMARY OF RHEOLOGICAL CURVE FIT RESULTS USING THE ACYM AT 27°C

S/N	Sample Code	Sample Identity	Molecular Weight(g/mol)	λ	n	∑(Error) ^{2}
1.	A1	Ayo Bee Farm Ado-Ekiti	261	3.63	0.00	0.0034
2.	A2	Fed Poly Ado	261	3.57	-0.07	0.0035
3.	A3	Forever Honey	254	3.63	-0.10	0.0416
4.	A4	Ijebu Mushin	250	1.60	-0.35	0.0279
5.	G1	Glucose	147	51.28	0.90	4.0771
6.	G2	10% Glucose Adulteration	244	1.47	0.37	0.3848
7.	G3	50% Glucose Adulteration	214	2881.38	0.56	2.2207
8.	G4	70% Glucose Adulteration	200	7.23	0.80	2.1296
9.	G5	90% Glucose Adulteration	187	2.32	0.94	2.4943
10.	F1	Fructose	150	1.92	1.00	0.2098
11.	F2	10% Fructose Adulteration	241	1.33	0.55	0.2642
12.	F3	50% Fructose Adulteration	217	0.90	0.79	0.0542
13.	F4	70% Fructose Adulteration	200	0.70	0.88	0.4967
14.	F5	90% Fructose Adulteration	187	0.49	0.89	0.7409
15.	H1	5% Water Adulteration	239	0.62	0.85	0.0135
16.	H2	10% Water Adulteration	227	3.44	0.99	0.0104
17.	H3	15% Water Adulteration	215	1.42	1.01	0.9847
18.	H4	20% Water Adulteration	200	8.34	0.51	0.7363
19.	H5	30% Water Adulteration	169	286.95	-1.69	0.9637
20.	H6	50% water Adulteration	130	0.00	0.14	3.6036

The sum of squares of errors for the ACYM were generally found to be less than that from new SKM for samples of pure honey, suggesting that the average molecular weight values obtained under this model conditions might be more accurate.

The high molecular weight values exhibited by most of the samples could be as a result of high melezitose, colloidal materials, polymerized and crystallized monosaccharides in honey (De Laney and Reilly, 2000 and Sunthar, 2008).

4.1.7 Comparism of ACYM and SKM

The two models used earlier in the rheological correlation were empirical. Both models encountered difficulties in correlating the effect of water adulteration on honey rheology, consequently the need to derive from first principle, a SKM.

Figures 28 to 31 are the ACYM curve fit of the effect of water adulteration on the rheology of honey. At first in Figure 28, the ACYM fitted the experimental data well when the percentage of water adulteration was only 5%. This was expected as ACYM was meant for viscous polymetric fluids (Bird *et al.,* 2006). However, as the percentage of water adulteration increases in Figures 29 to 31 in the direction of 20%, the model stoped following the experimental data, thereby suggesting the use of another model to study this manner of adulteration.

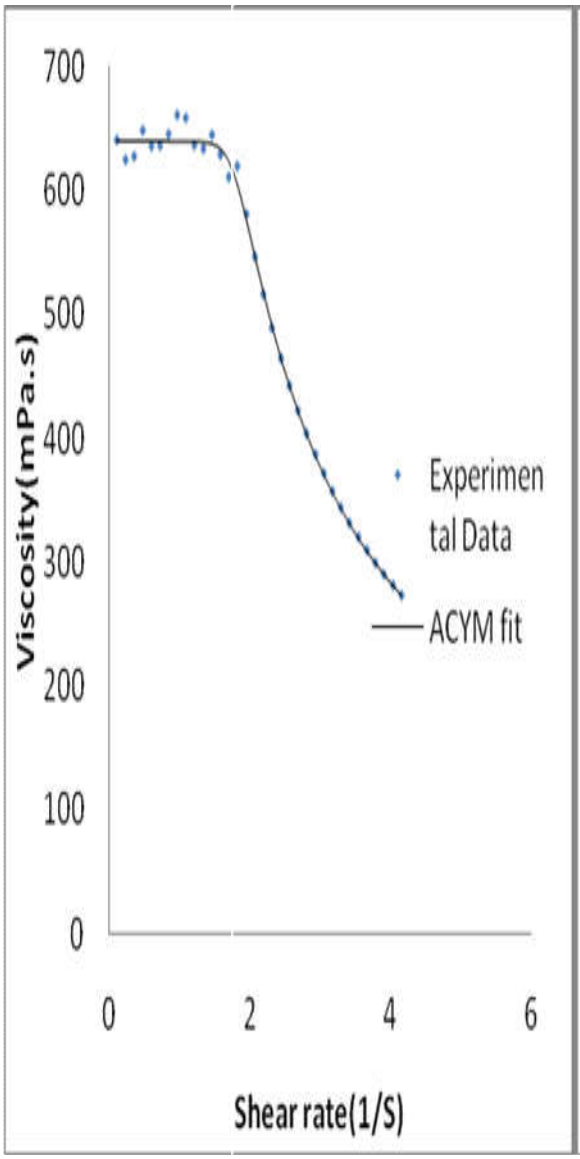

Figure 28. ACYM Curvefit of Sample H1 at 27˚C

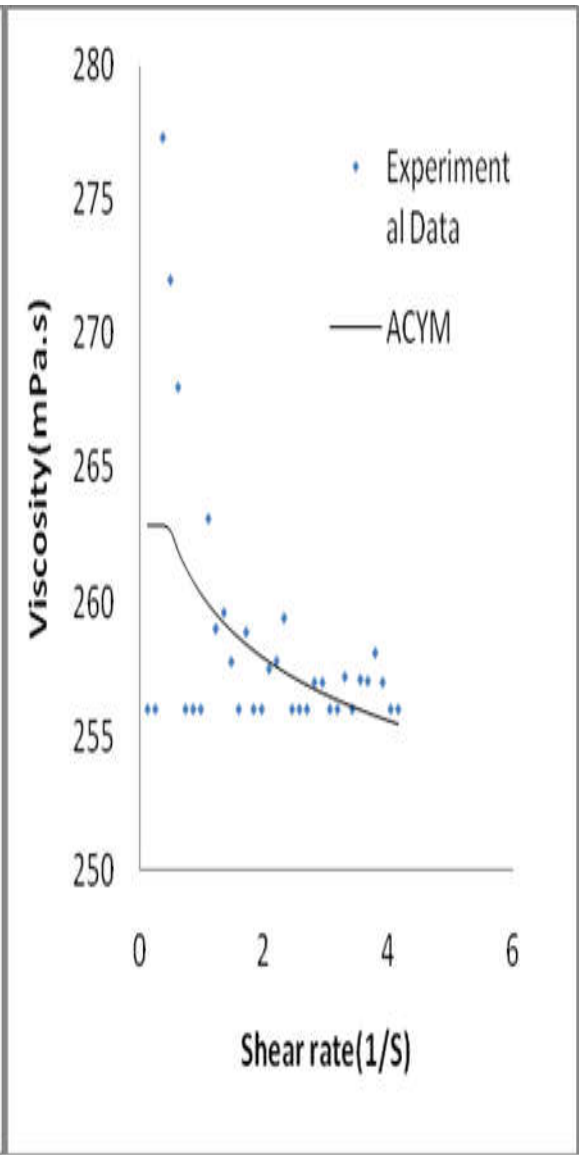

Figure 29. ACYM Curvefit of Sample H2 at 27˚C

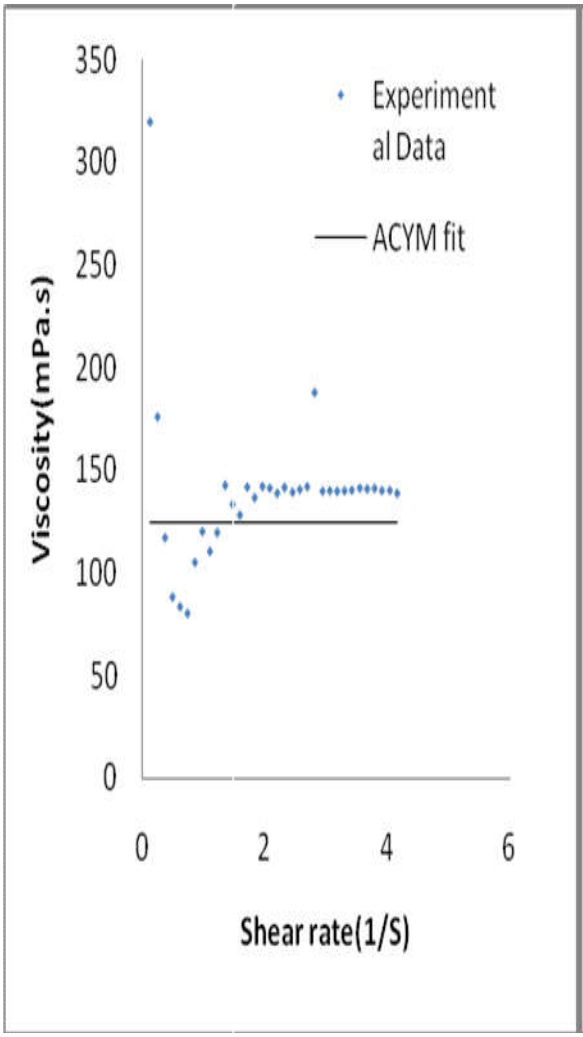

Figure 30. ACYM Correlation of Sample H3 at 27˚C

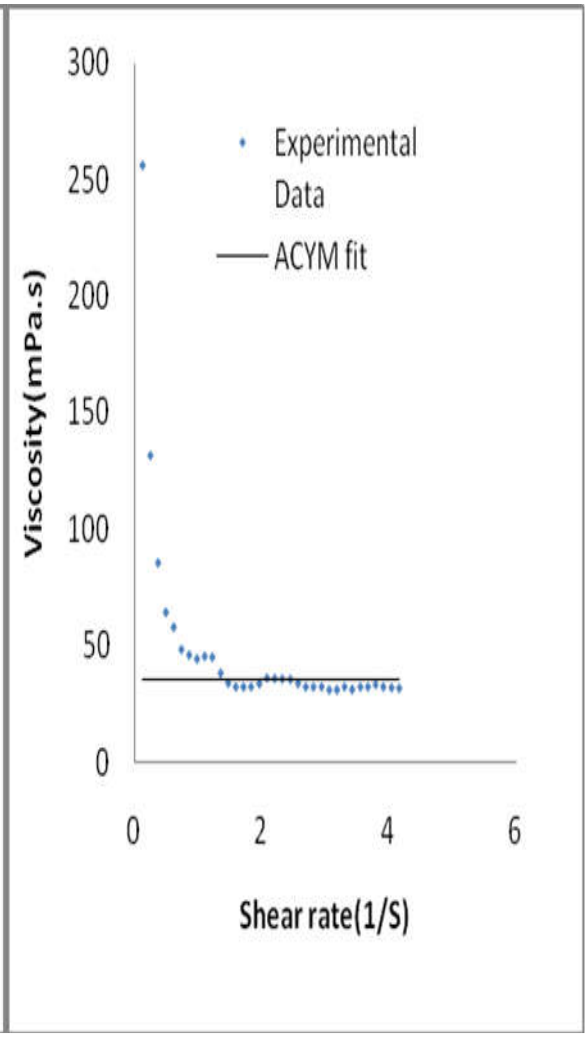

Figure 31. ACYM Curvefit of Sample H4 at 27˚C

The SKM was then used to extract both structural and compsitional information from the samples. It followed both the viscouse and the water adulterated samples. It handled both the sample types (pure and water adulterated) equally well.

The method of extracting data from the SKM had already been described earlier in subsection 4.1.6. Figures 32 to 35 are some of the rheograms used to obtain the structural and compositional information from sample H4 using the SKM.

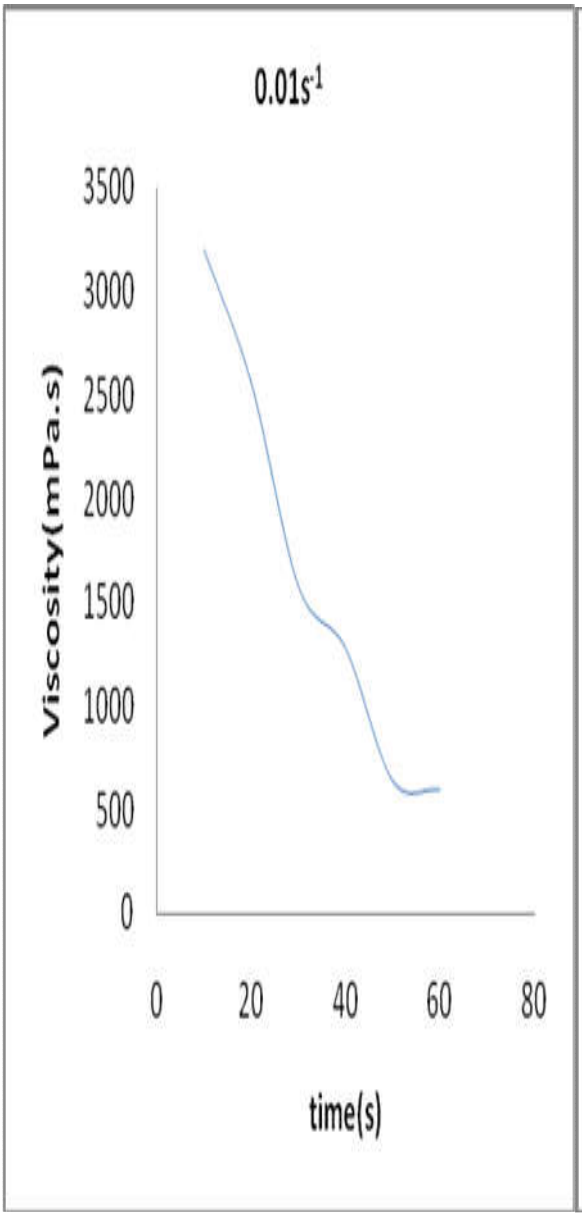

Figure 32. Viscosity vs time plot for H4 at =0.01s-1

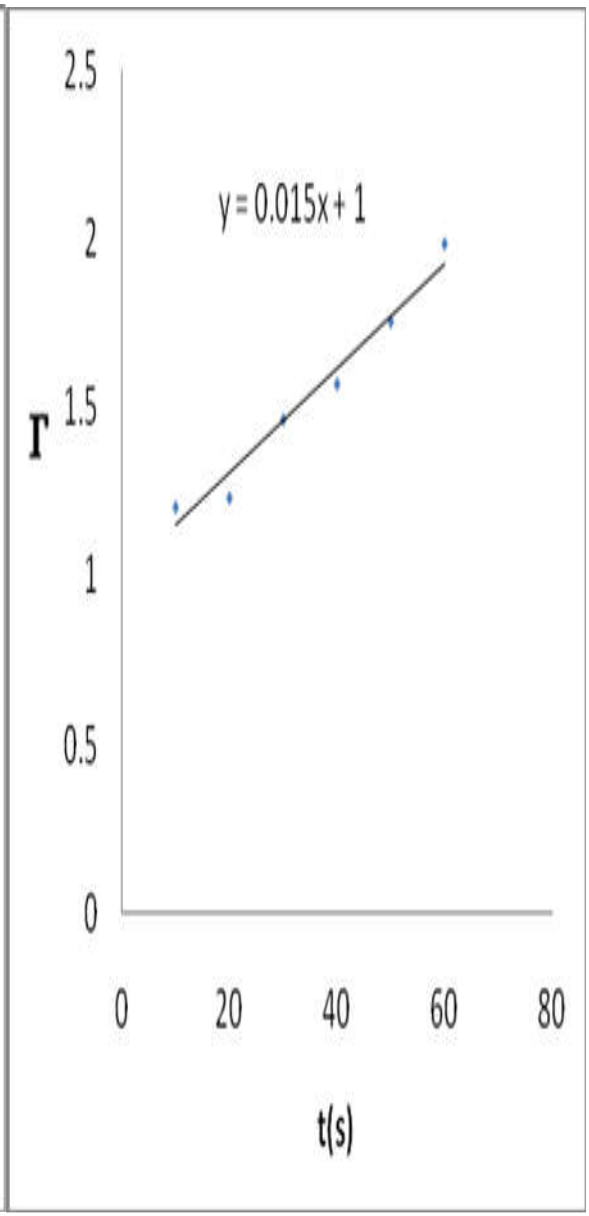

Figure 33. Plot of Γ against time for H4

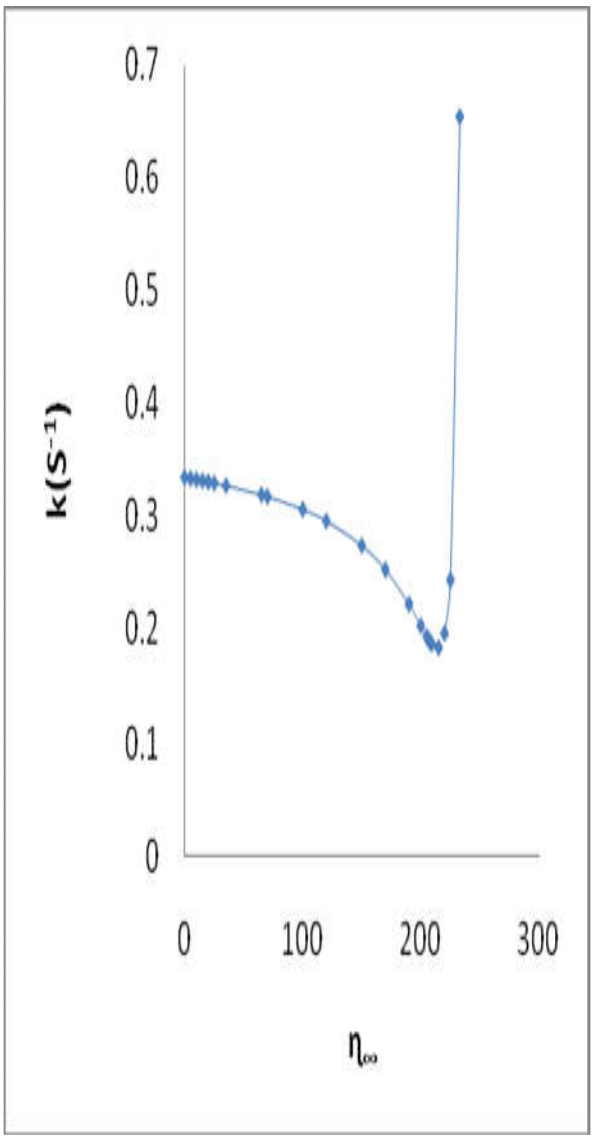

Figure 34. Plot of *k* against infinite time viscosity of H4

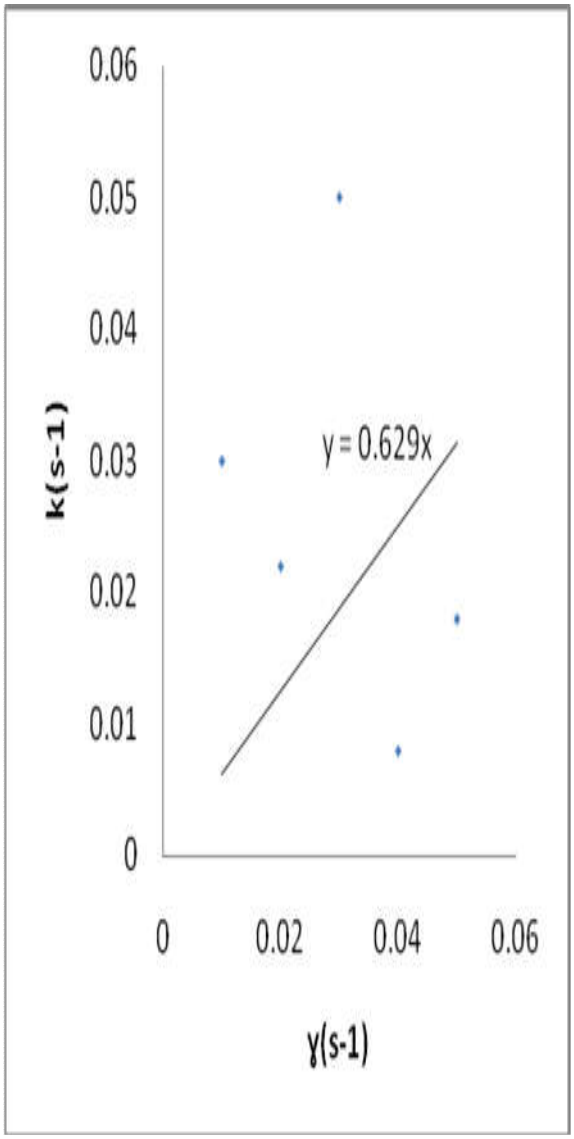

Figure 35. Plot of *k* against shear rate for H4

This distinction which appears to underlie a contrasting feature of the SKM for telling the adulterated fluid from pure honey could be suggested for practical tests of honey quality. See Appendix 2 for SKM analyses of other samples.

4.1.8 Hysteresis Loop of Honey

Figure 36 is the hysteresis loop observed on sample A1's apparent viscosities when the shear rate trajectory was reversed in the opposite direction. A loop was observed between the upper and the lower ramps. The loop suggests that the fluid flows at lower energy level when the shear rate was reversed. This can only be true for fluids that remember its shear history (see section 2.5).

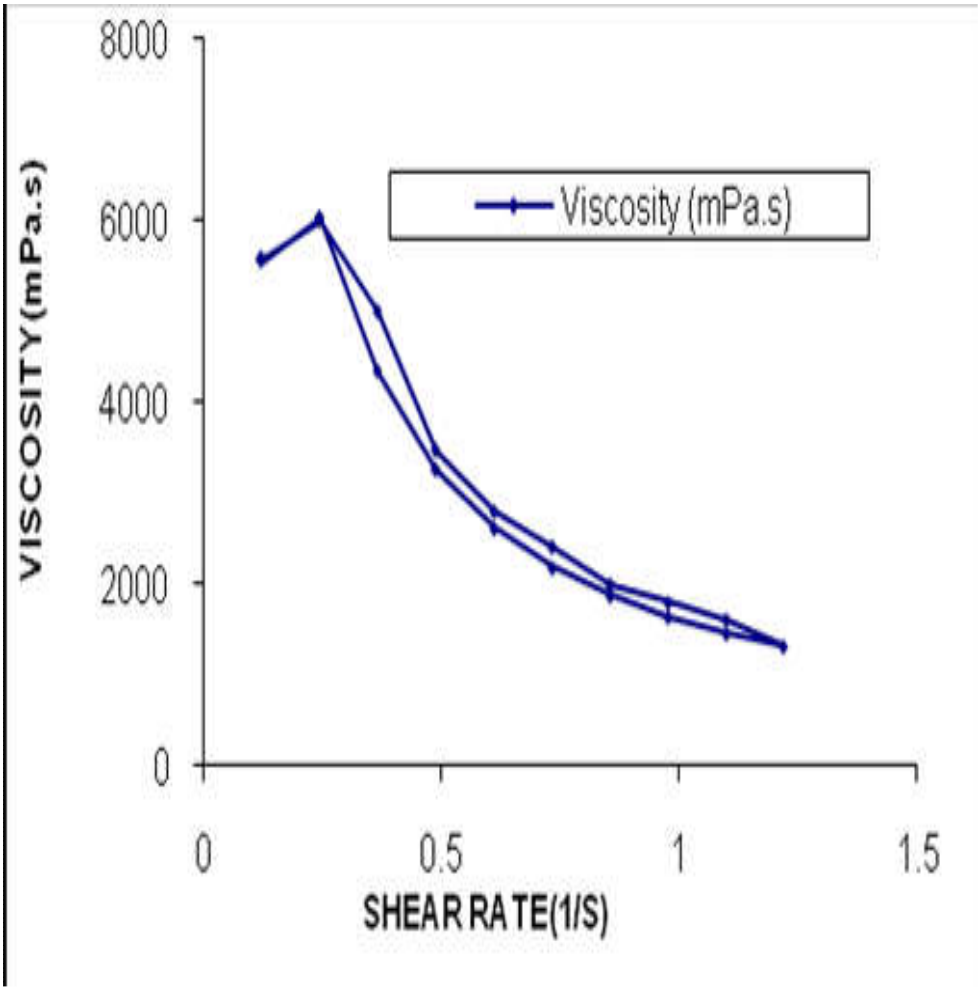

Figure .36 Hysteresis loop curve of of Sample A1 at 27°C

Figure 37 is the hysteresis loop of pure honey samples A1 and A2 at elevated temperature of 35°C. The Figure is the shear stress against shear rate rheogram of the two pure honeys showing a loop when the shear rate was reversed at low shear rate. At higher rates of shear

when the sample turned Newtonian, it was observed that the loop closed. The loops seen here are smaller than that observed in Figure 36 because the experiment was carried out at high temperature.

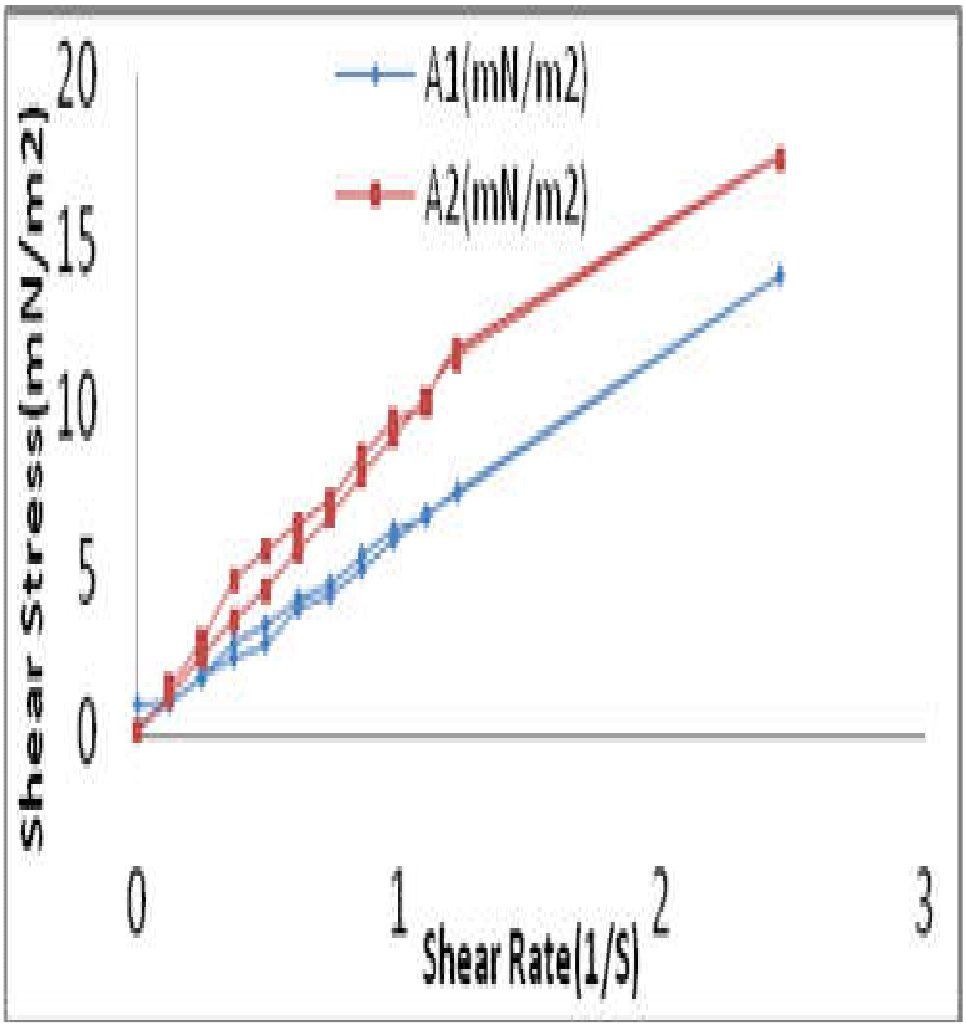

Figure .37 Hysteresis loop of A1 and A2 at 35˚C

At higher temperature, the structures of the fluid are stretched (see section 4.1.1). The loop quantifies the power loss during continuous input of energy into the fluid sample undergoing testing and it is independent of any thermal effects. It then suggests that honey exhibits thixotropic time dependent flow pattern. Thixotropy can be expressed as an isothermal, reversible reduction in apparent viscosities with shear rate. The amount of thixotropic

breakdown is sensitive to previous shear history of honey. For time independent fluids, the curves would have been superinposed.

4.2 Chromatographic Characterization of Honey

This phase of study seeks to establish a possible correlation of chromatographic characterization of honey with conclusions based on this study's rheological assessment of quality.

4.2.1 Calibration Data

HMF content of honey was determined using reverse phase HPLC equipped with a Diode Array Detector (DAD) set at 285 nm. The DAD spectrophotometer reads the absorbance of HMF at 285nm. Figure 38 is the chromatograph of pure HMF. The concentration of the HMF was 0.001mg/100ml of the mobile phase. The mobile phase used was 90% by volume of double distilled water and 10% by volume of methanol. The HMF elutes from the HPLC at a retention time of 4.073 minutes. The peak area was found to be 5,483,162 under this concentration. This chromatograph in Figure 38 below was generated as part of the calibration data for the experiment.

EZChrom Elite Custom Report

Sample ID: STD2
Filename: C:\EZChrom Elite\HONEY\Data\13-05-13\020dat-Rep1
Method: C:\EZChrom Elite\HONEY\Method\13-05-13\HMF13-05-13B.met
User: lab manager
Acquired: 5/14/2013 2:38:42 AM
Printed: 5/17/2013 12:16:42 AM

NAFDAC DAD REPORT

DAD-CH1 285 nm Results

Pk #	*Name*	*Retention Time*	*Area*	*Units*	*concentration*
4	***HMF***	**4.073**	5483162	mg/100ml	0.001 CAL

DILUTION FACTOR: 1
MULTIPIER: 1
VIAL: 1

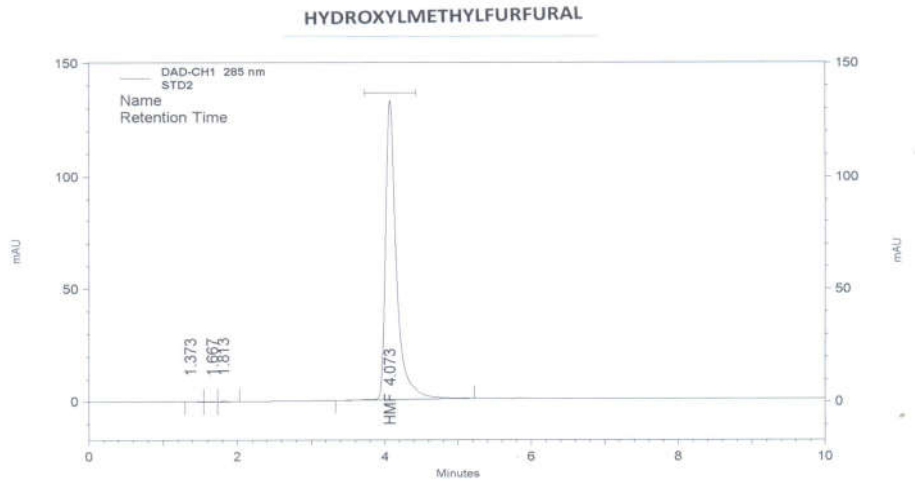

Scientific Software, Inc.

Figure 38. Chromatograph of Pure HMF

Calibration Report

Method: C:\EZChrom Elite\HONEY\Method\13-05-13\HMF13-05-13B.met
Print Time: 5/17/2013 12:18:10 AM
User: lab manager
Instrument: DAD HPLC

HMF (DAD-CH1)
Average RF: 5.45413e+009 RF StDev: 1.97127e+008 RF %RSD: 3.61427
Scaling: None LSQ Weighting: None Force Through Zero: On
Replicate Mode: Replace
Fit Type: Linear
y = 5.57341e+009x + 0.000000
Goodness of fit (r^2): 0.998911

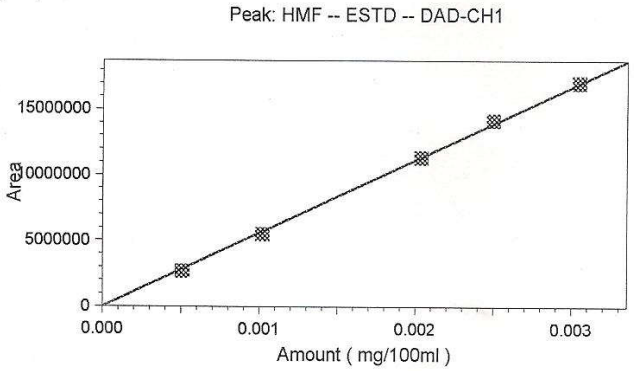

	Level 1	Level 2	Level 3	Level 4	Level 5
Amount	0.00051	0.00102	0.00204	0.0025	0.00305
Area	2637063	5446408	11274358	14150912	16998610
RF	5170711764.70588	5339615686.27451	5526646078.43137	5660364800	5573314754.09836
Last Area Residual	3.68492e-005	4.2787e-005	1.71165e-005	-3.90046e-005	5.17924e-008
Rep StDev	113928	25989	179749	242217	239989
Rep %RSD	4.45638	0.475572	1.61249	1.6912	1.39786
Rep 1 Area	2475945	5483162	11020155	14493458	17338005
Rep 1 User	lab manager	lab manager	lab manager	lab manager	lab manager
Rep 1 Data File	C:\EZChrom Elite\HONEY\Data\13-05-13\019dat-Rep1	C:\EZChrom Elite\HONEY\Data\13-05-13\020dat-Rep1	C:\EZChrom Elite\HONEY\Data\13-05-13\021dat-Rep1	C:\EZChrom Elite\HONEY\Data\13-05-13\022-Rep1.dat	C:\EZChrom Elite\HONEY\Data\13-05-13\023-Rep1.dat
Rep 1 Sample ID	STD1	STD2	STD3	STD4	STD5
Rep 1 Calib. Time	5/16/2013 9:56:55 PM	5/16/2013 9:57:02 PM	5/16/2013 9:57:10 PM	5/16/2013 9:57:17 PM	5/16/2013 9:57:23 PM
Rep 2 Area	2637063	5446408	11274358	14150912	16998610
Rep 2 User	lab manager	lab manager	lab manager	lab manager	lab manager

Figure 39. Calibration Report of the Test

Figure 39 is the calibration report of the test. As shown in the table under the graph above ,the concentration of 0.051mg/100ml, 0.102mg/100ml, 0.204mg/100ml, 0.25mg/100ml and 0.305mg/100ml of HMF were ran and plotted against the corresponding peak areas obtained from the respective concentration of the furfural. The plot gave a straight line graph with

goodness of fit, (R^2) 0.998911. This implies that the system can quantify with precision of 99.89%, the amount of the HMF in the samples.

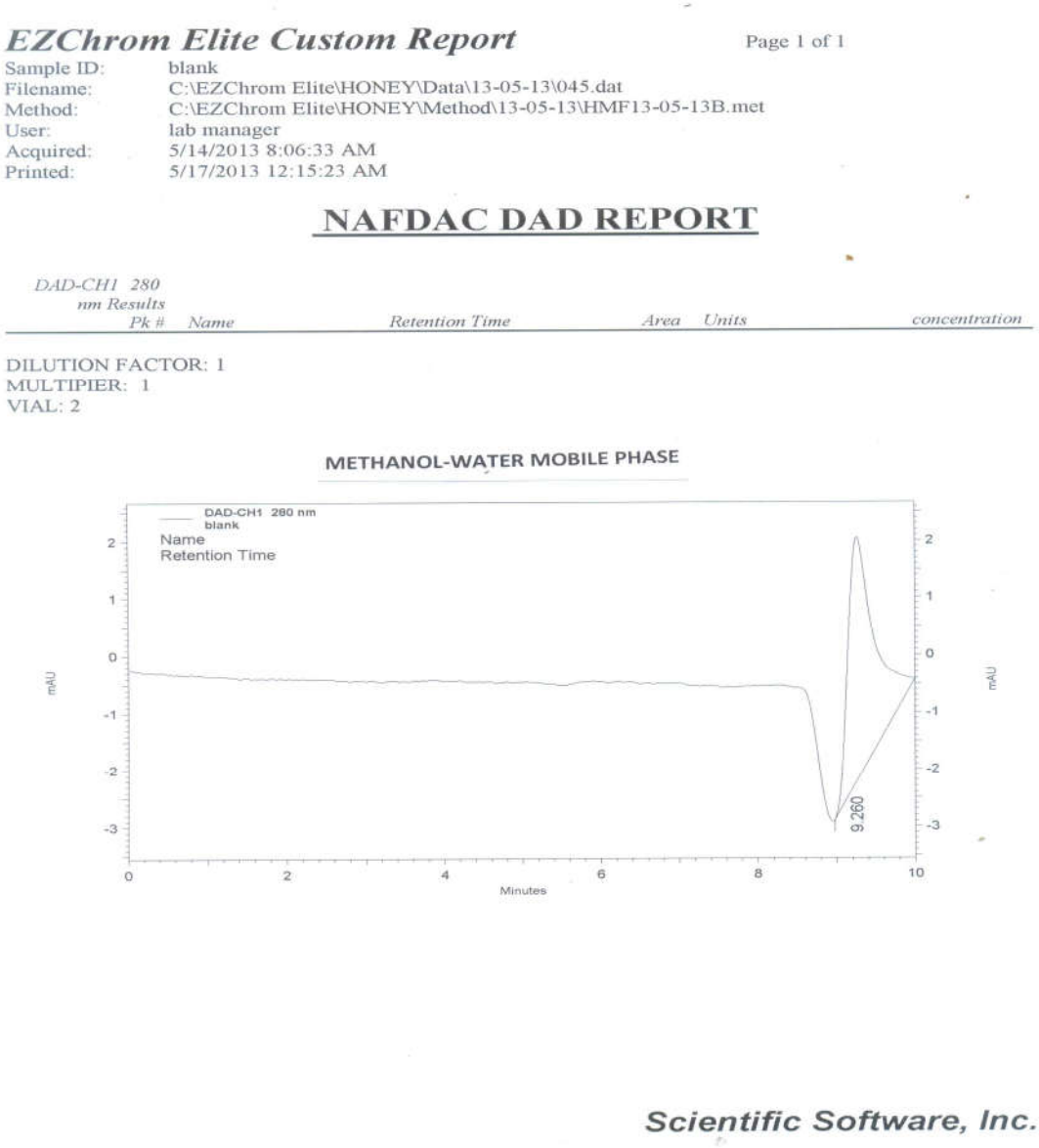

Figure 40. Blank Determination of the Test

Figure 40 is the blank determination of the mobile phase. As stated earlier, the mobile phase in this study was a mixture of metanol and water (10:90 by volume). The above chromatograph shows that this career fluid has insignificant absorption at the detection wavelength and so would not obscure absorption arising from the HMF content of samples.

4.2.2 Reference Pure Honey Samples

Figure 41 is the chromatograph of sample A4, pure honey from Imuwen, Ijubu Mushin in Ogun State. The HMF contents of the study's samples were quantified following the procedure described in section 3.4.1 from comparison of areas under the HMF peaks and those of the calibration data with corrections for sample dilutions.

A4

EZChrom Elite Custom Report Page 1 of 1

Sample ID: FCI3944
Filename: C:\EZChrom Elite\HONEY\Data\13-05-13\028.dat
Method: C:\EZChrom Elite\HONEY\Method\13-05-13\HMF13-05-13B.met
User: lab manager
Acquired: 5/14/2013 4:53:10 AM
Printed: 5/17/2013 12:12:23 AM

NAFDAC DAD REPORT

DAD-CH1 285 nm Results

Pk #	*Name*	*Retention Time*	*Area*	*Units*	*concentration*
6	***HMF***	**4.067**	319771	mg/L	0.287 x 50/10 = 1.435 mg/L

DILUTION FACTOR: 1
MULTIPIER: 4994.36
VIAL: 6

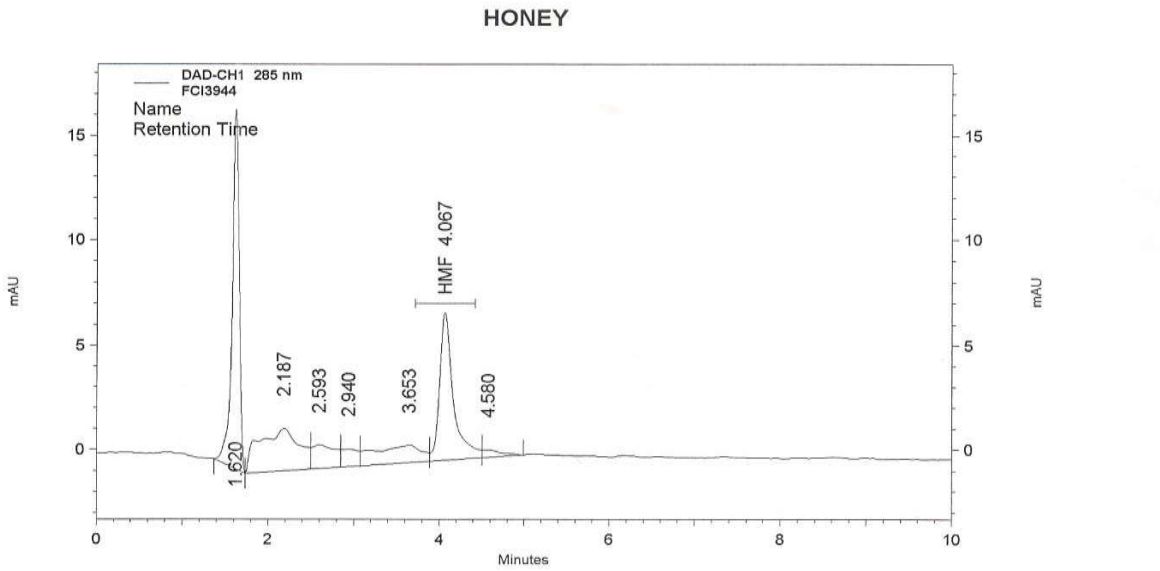

Figure 41. Chromatogram of Pure honey From Imuwen, Ijebu Mushin

The result of 1.435 mg/kg obtained on Imuwen Ijebu Mushin honey (sample A4) is below the Codex Alimentary threshold of 80mg/kg indicating compliance with the HMF standard for pure honey. The 5-hydroxyl methyl furfuraldehyde (HMF) content of honey samples is a measure of freshness, adulteration or heat treatment of honey. HMF is formed in honey during acid-catalyzed thermal dehydration of hexoses (fructose and glucose) occasioned by disequilibrium introduced by the adulterating material, storage or heat treatment of honey (Belitz and Grosch, 1999) (see section 2.7.1). Thus sample A4 is established, here, as unadulterated pure honey.

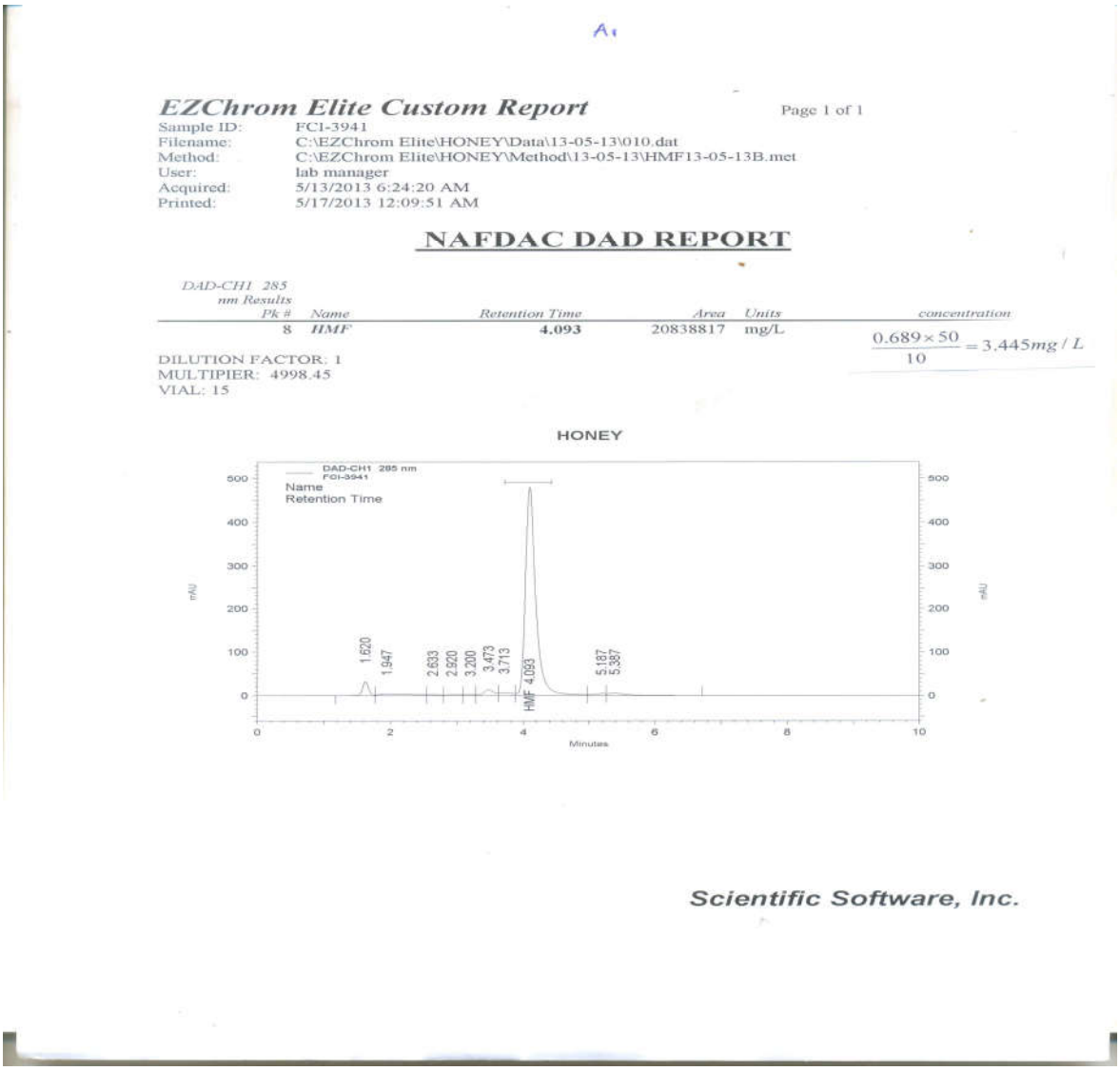
A1

EZChrom Elite Custom Report

Page 1 of 1

Sample ID: FCI-3941
Filename: C:\EZChrom Elite\HONEY\Data\13-05-13\010.dat
Method: C:\EZChrom Elite\HONEY\Method\13-05-13\HMF13-05-13B.met
User: lab manager
Acquired: 5/13/2013 6:24:20 AM
Printed: 5/17/2013 12:09:51 AM

NAFDAC DAD REPORT

DAD-CH1 285 nm Results

Pk #	Name	Retention Time	Area	Units	concentration
8	HMF	4.093	20838817	mg/L	$\frac{0.689 \times 50}{10} = 3.445 mg/L$

DILUTION FACTOR: 1
MULTIPIER: 4998.45
VIAL: 15

HONEY

Scientific Software, Inc.

Figure 42. Chromatograph of Honey from Ayo Bee Farm Ado-Ekiti

Figure 42 is the chromatograph of pure honey from from Ado-Ekiti (sample A1). In Figure 42, the amount of HMF in pure honey is quantified by comparing the peak areas of HMF content in pure honey and standard HMF used. The result of 3.455 mg/kg obtained is below the Codex Alimentary threshold of 80mg/kg confirming that sample A1 is pure honey judging by the HMF content. The 5-hydroxyl methyl furfuraldehyde content in honey samples is a measure of freshness, adulteration or heat treatment of honey. HMF is formed in honey during acid-catalyzed thermal dehydration of hexoses (fructose and glucose) occasioned by disequilibrium introduced by the adulterating material, storage or heat treatment of honey (Belitz and Grosch, 1999) (see section 2.7.1).

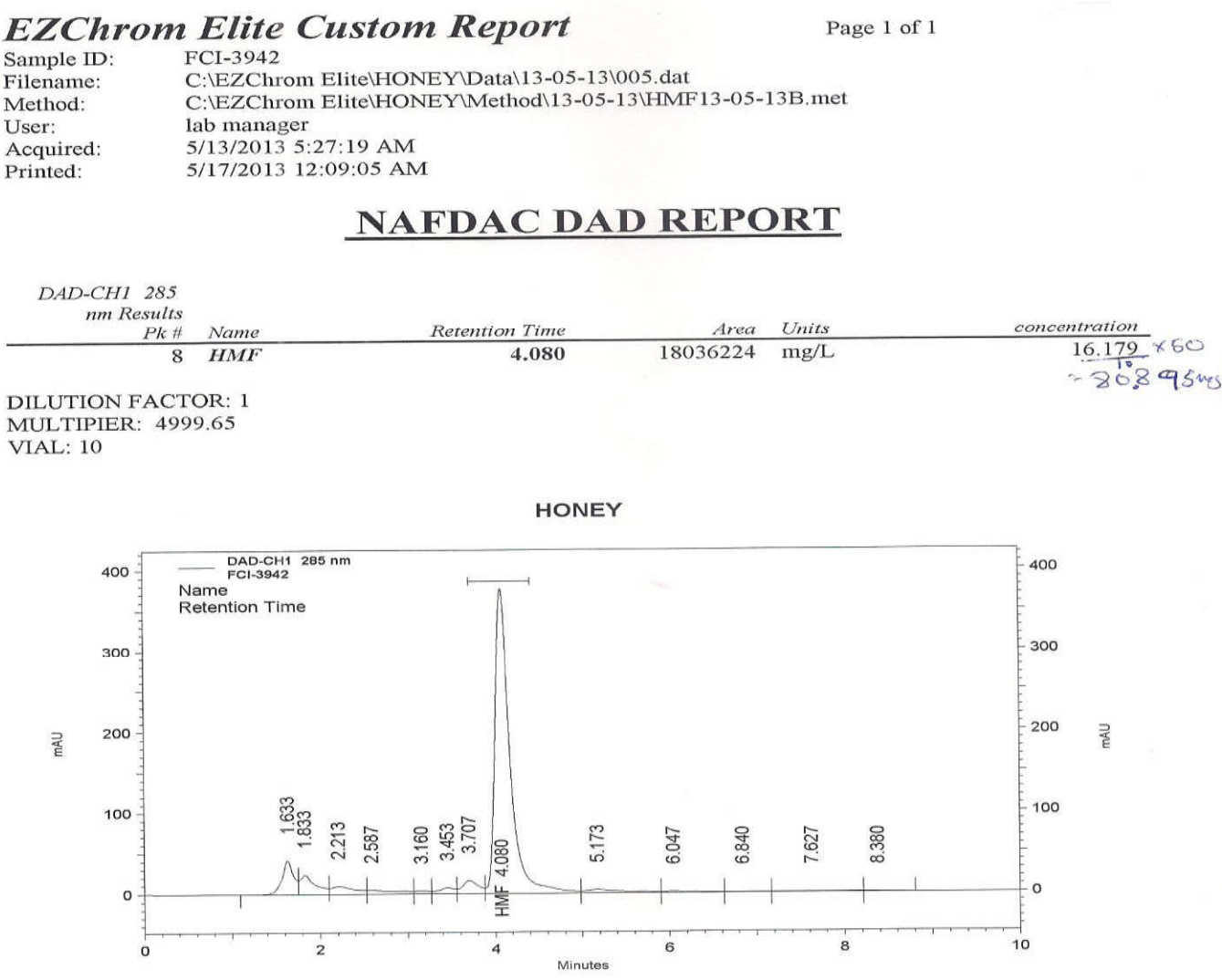

EZChrom Elite Custom Report Page 1 of 1

Sample ID: FCI-3942
Filename: C:\EZChrom Elite\HONEY\Data\13-05-13\005.dat
Method: C:\EZChrom Elite\HONEY\Method\13-05-13\HMF13-05-13B.met
User: lab manager
Acquired: 5/13/2013 5:27:19 AM
Printed: 5/17/2013 12:09:05 AM

NAFDAC DAD REPORT

DAD-CH1 285 nm Results

Pk #	*Name*	*Retention Time*	*Area*	*Units*	*concentration*
8	*HMF*	**4.080**	18036224	mg/L	16.179 ×60 = 308.95mg

DILUTION FACTOR: 1
MULTIPIER: 4999.65
VIAL: 10

HONEY

DAD-CH1 285 nm
FCI-3942
Name
Retention Time

mAU

400
300
200
100
0

1.633
1.833
2.213
2.587
3.160
3.453
3.707
HMF 4.080
5.173
6.047
6.840
7.627
8.380

0
2
4
6
8
10
Minutes

Figure 43. Chromatograph of Honey from Federal Polytechnic Ado-Ekiti

Figure 43 is the chromatograph of sample A2 (Federal Polytechnic Ado-Ekiti). The HMF quantified in this sample was 80.89ml/kg which is slightly above the codex alimentarius standard of 80ml/kg. This quantity is basically at the bother line of the HMF threshold for honey in the tropics.

A3

EZChrom Elite Custom Report Page 1 of 1

Sample ID: FCI3943
Filename: C:\EZChrom Elite\HONEY\Data\13-05-13\043.dat
Method: C:\EZChrom Elite\HONEY\Method\13-05-13\HMF13-05-13B.met
User: lab manager
Acquired: 5/14/2013 7:43:38 AM
Printed: 5/17/2013 12:15:01 AM

NAFDAC DAD REPORT

DAD-CH1 285 nm Results

Pk #	*Name*	*Retention Time*	*Area*	*Units*	*concentration*
8	***HMF***	**4.060**	33078199	mg/L	27.037 x 50 / 10 = 135.185 mg/L

DILUTION FACTOR: 1
MULTIPIER: 4555.6
VIAL: 21

HONEY

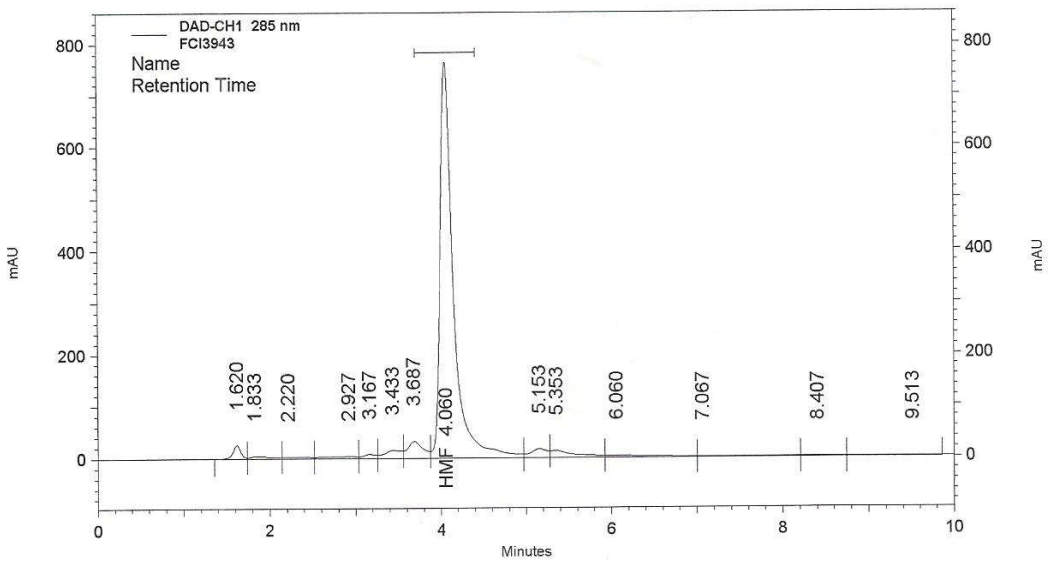

Figure 44. Chromatograph of Forever Living Product, USA

Figure 44 is the chromatogram of sample A3 (Forever Living Honey from Texas, United States). The HMF content of 135.185 ml/kg obtained from this sample clearly shows that the integrity of sample A3 is suspect because the value obtained is above the codex alimentarius standard of 80mg/kg. Perhaps during processing, the crystallized part of the sample may have been dissolved after experiencing high temperatures that fostered inordinate HMF formation in the sample. It will be recalled that the rheogram of this sample (see Figure 6) displayed curious deviations from characteristics of the reference pure honey samples A1 and A2 at the higher temperature (see Figure 5 also). This, again, is suggestive of certain correlation between rheological and chromatographic assessments of honey quality.

4.2.3 Honey Quality Analyses: Rheology versus Chromatographic HMF Assessment

Figure 45 is the chromatogram of sample B1, from Gauraka, Niger State. This sample was classified earlier using rheological method as a pure honey. The HMF value of 23.985 ml/kg obtained confirms this sample as pure, since its HMF content is within the standard specification of 80mg/kg.

EZChrom Elite Custom Report

Sample ID: FCI3945
Filename: C:\EZChrom Elite\HONEY\Data\13-05-13\033.dat
Method: C:\EZChrom Elite\HONEY\Method\13-05-13\HMF13-05-13B.met
User: lab manager
Acquired: 5/14/2013 5:50:01 AM
Printed: 5/17/2013 12:13:12 AM

NAFDAC DAD REPORT

DAD-CH1 285 nm Results

Pk #	*Name*	*Retention Time*	*Area*	*Units*	*concentration*
8	***HMF***	**4.060**	5368995	mg/L	4.797

4.797 x 50 / 10 = 23.985 mg/l

DILUTION FACTOR: 1
MULTIPIER: 4979.73
VIAL: 11

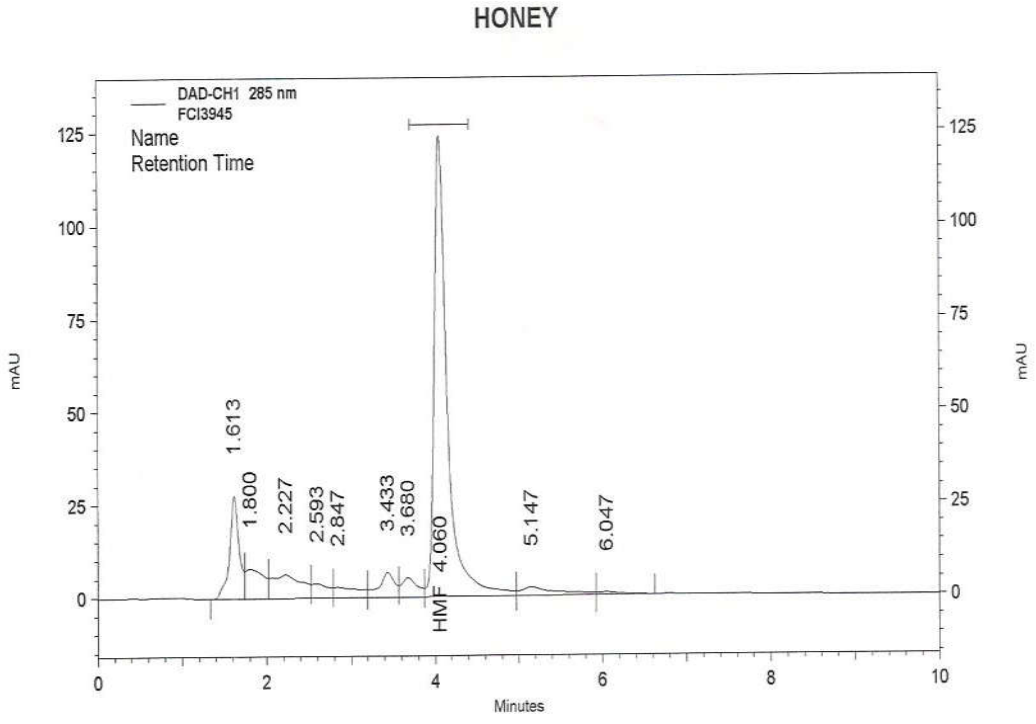

Figure 42. Chromatogram of Sample B1, from Gauraka, Niger State

The Figures 46 and 47 below are also the chromatograms of samples that exhibited rheological behaviour similar to that of pure honey. Their HMF content also corroborated the rheological characterization results on these samples. It may, thus, be concluded that rheological analyses reflect honey quality.

EZChrom Elite Custom Report Page 1 of 1

Sample ID: FCI3951
Filename: C:\EZChrom Elite\HONEY\Data\13-05-13\030.dat
Method: C:\EZChrom Elite\HONEY\Method\13-05-13\HMF13-05-13B.met
User: lab manager
Acquired: 5/14/2013 5:15:57 AM
Printed: 5/17/2013 12:12:42 AM

NAFDAC DAD REPORT

DAD-CH1 285 nm Results

Pk #	*Name*	*Retention Time*	*Area*	*Units*	*concentration*
7	***HMF***	**4.067**	7880382	mg/L	7.062 X 50 / 10 = 35.31 mg/L

DILUTION FACTOR: 1
MULTIPIER: 4994.61
VIAL: 8

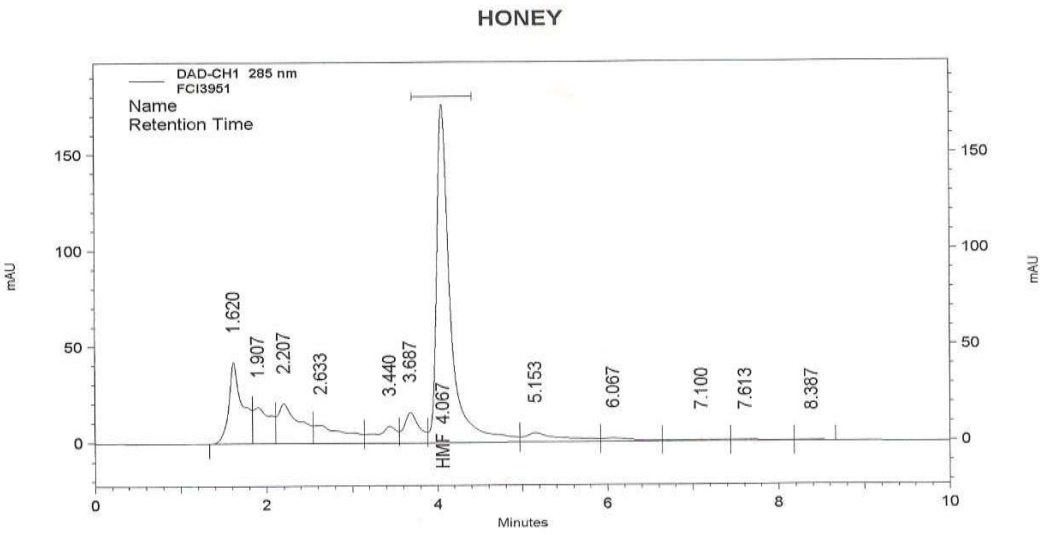

Figure 46. Chromatogram of Sample B7, From Kabba Kogi State

C4

EZChrom Elite Custom Report

Sample ID: FCI3956
Filename: C:\EZChrom Elite\HONEY\Data\13-05-13\026.dat
Method: C:\EZChrom Elite\HONEY\Method\13-05-13\HMF13-05-13B.met
User: lab manager
Acquired: 5/14/2013 4:30:28 AM
Printed: 5/17/2013 12:12:04 AM

NAFDAC DAD REPORT

DAD-CH1 285 nm Results

Pk #	*Name*	*Retention Time*	*Area*	*Units*	*concentration*
10	*HMF*	**4.060**	16961725	mg/L	15.148

15.148 × 66/10
75.74 mg/L

DILUTION FACTOR: 1
MULTIPIER: 4977.35
VIAL: 4

HONEY

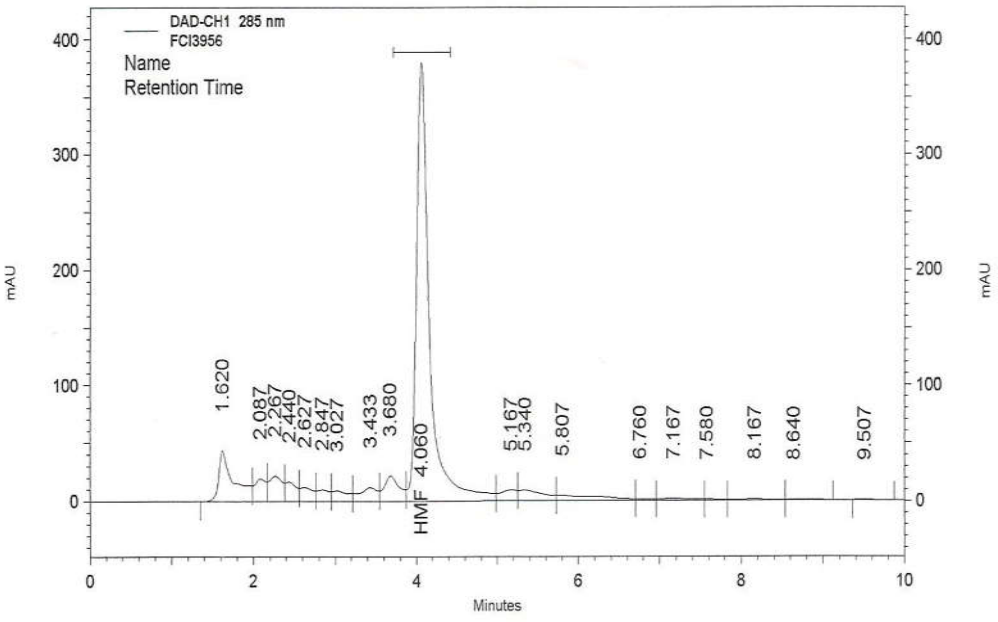

Figure 47. Chromatogram of Sample C4, From Nsukka Enugu State

4.2.4 Effect of Adulteration on Chromatographic HMF Content

Sucrose melt (E1) gave a high furfural content of 302.5mg/kg. When the reference pure honey (A1) was adulterated to 10% sucrose (sample E2) a furfural content of 88.91mg/kg resulted. Likewise at 50% adulteration the furfural content rose to 201.22mg/kg, and respectively to 220.34 and 288.75mg/kg at 70% and 90% adulteration. This, most likely, came from the rich HMF content of the sucrose melt, employed diluting A1. The high content of the furfural in the sucrose adulterant could be attributed to enzyme, invertase (Saccharase and α-glucosidase) which lead to decomposition of sucrose to glucose and fructose, thereby releasing HMF as by-product of further dehydration of glucose and fructose in the presence of good acidic medium and high temperature (see section 2.7.1). Glucose (Sample G1) has HMF content of 1.15mg/kg. The absence of furfural inducing enzymes explains why the HMF is less in the fluid. Imuwen Ijebu-Mushin honey adulterated with 10% glucose gave furfural content of only 8.85mg/kg. Similarly, 50% glucose adulteration gave HMF content of 4.0mg/kg. Correspondingly, the 70% glucose adulteration of honey gave furfural content of 4.1mg/kg while 90% glucose adulteration gave 0.4mg/kg. This suggests that adulteration of honey with glucose does not necessarily increase the furfural content of honey because glucose is a major component of honey.

In the case of fructose adulteration furfural content was only slightly altered from the pure honey level. Table 9 suggests that the adulteration with fructose does not overshoot the HMF international standard. This section concludes that HMF content tracking in honey may or may not indicate adulteration depending on the nature of the adulterant. This parameter alone fails to reflect adulteration and vice-versa when the adulterant is glucose or fructose and perhaps some other sugars. It is, therefore, not useful for validating an independent honey quality tracker. The chromatographs of samples are presented below.

F1

EZChrom Elite Custom Report

Sample ID: FCI3971
Filename: C:\EZChrom Elite\HONEY\Data\13-05-13\035.dat
Method: C:\EZChrom Elite\HONEY\Method\13-05-13\HMF13-05-13B.met
User: lab manager
Acquired: 5/14/2013 6:12:47 AM
Printed: 5/17/2013 12:13:32 AM

NAFDAC DAD REPORT

DAD-CH1 285 nm Results

Pk #	*Name*	*Retention Time*	*Area*	*Units*	*concentration*
9	***HMF***	**4.060**	7078781	mg/L	6.342 x50 to 31.71 mg/L

DILUTION FACTOR: 1
MULTIPIER: 4993.31
VIAL: 13

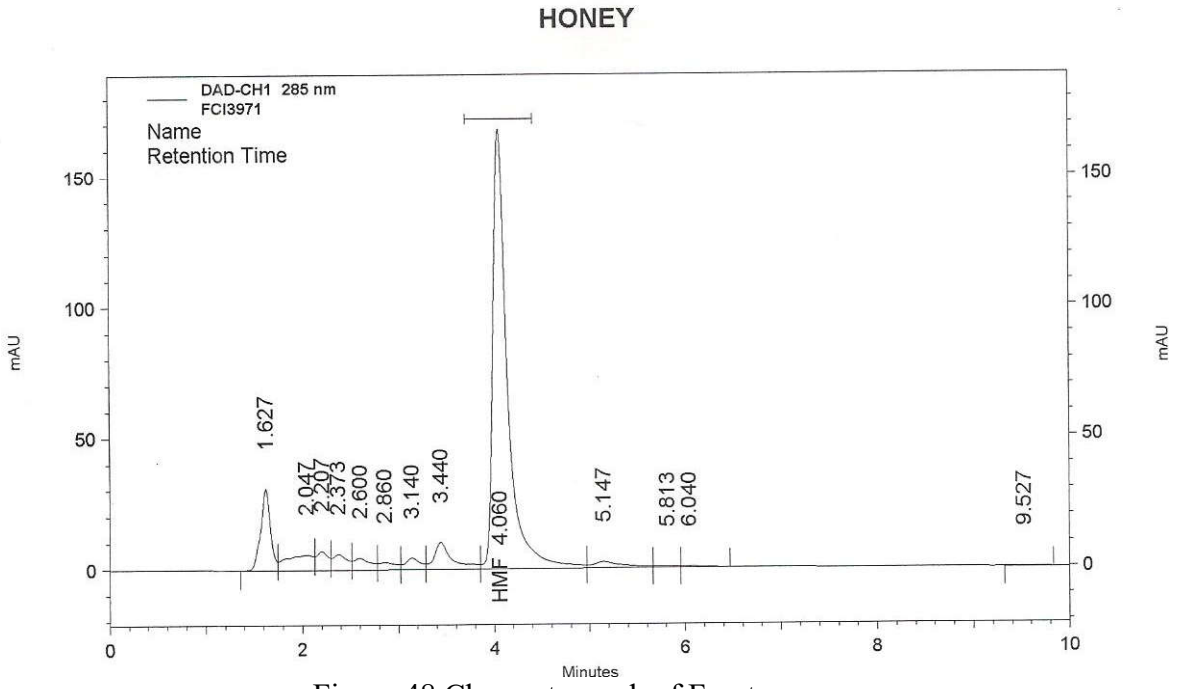

Figure 48 Chromatograph of Fructose

Hydroxylfurfural content of 31.77mg/l was obtained in Figure 48, from pure fructose which does not overshoot the Codex alimentary standard of 80mg/l.

Fr

EZChrom Elite Custom Report

Sample ID: FCI-3972
Filename: C:\EZChrom Elite\HONEY\Data\13-05-13\014.dat
Method: C:\EZChrom Elite\HONEY\Method\13-05-13\HMF13-05-13B.met
User: lab manager
Acquired: 5/13/2013 7:09:46 AM
Printed: 5/17/2013 12:11:04 AM

NAFDAC DAD REPORT

DAD-CH1 285 nm Results

Pk #	*Name*	*Retention Time*	*Area*	*Units*	*concentration*
7	***HMF***	**4.087**	708601	mg/L	0.633

3.165 mg/l

DILUTION FACTOR: 1
MULTIPIER: 4981.27
VIAL: 19

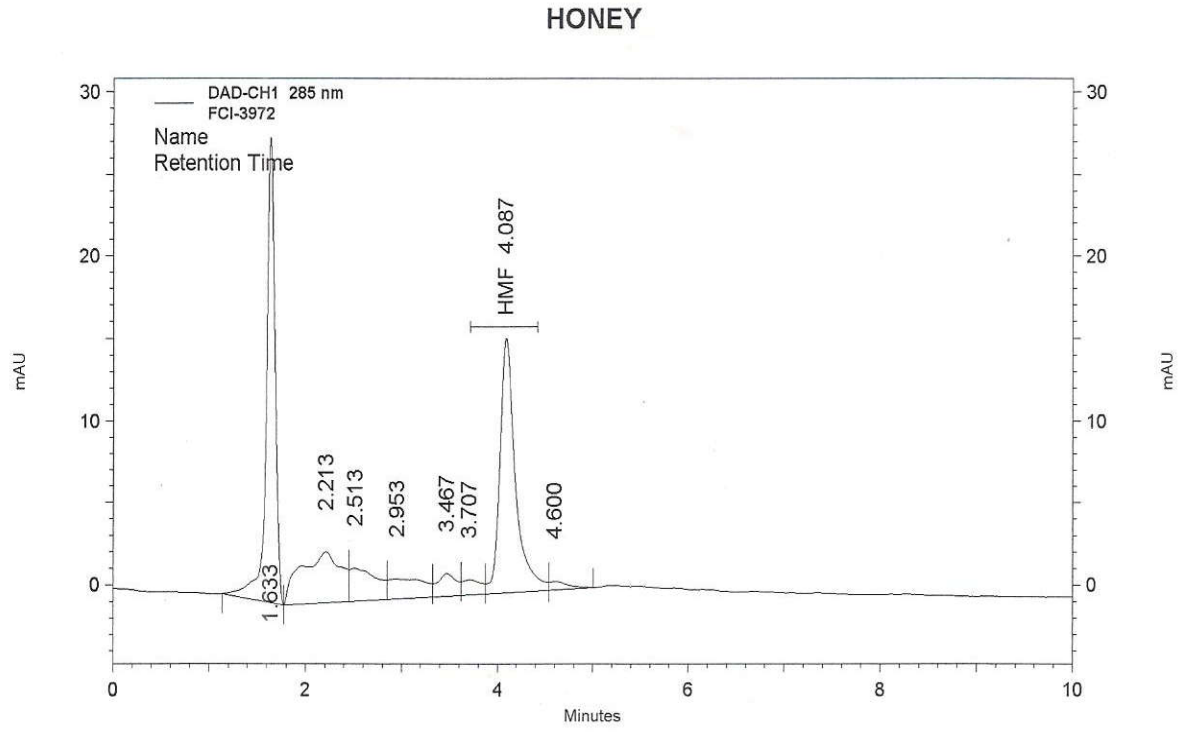

Figure 49 Chromatograph of 10% Adulteration of Honey with Fructose

Aulteration of pure honey sample A4 with 10% glucose in Figure 49, lead to a decrease in furfural content of the resulting sample from 31.77mg/l for pure glucoe to 3.165mg/l.

F3

EZChrom Elite Custom Report

Sample ID: FCI3773
Filename: C:\EZChrom Elite\HONEY\Data\13-05-13\044.dat
Method: C:\EZChrom Elite\HONEY\Method\13-05-13\HMF13-05-13B.met
User: lab manager
Acquired: 5/14/2013 7:55:00 AM
Printed: 5/17/2013 12:15:12 AM

NAFDAC DAD REPORT

DAD-CH1 285 nm Results

Pk #	*Name*	*Retention Time*	*Area*	*Units*	*concentration*
9	***HMF***	**4.067**	862519	mg/L	0.768 x 50/10

3.24 mg/l

DILUTION FACTOR: 1
MULTIPIER: 4960.56
VIAL: 22

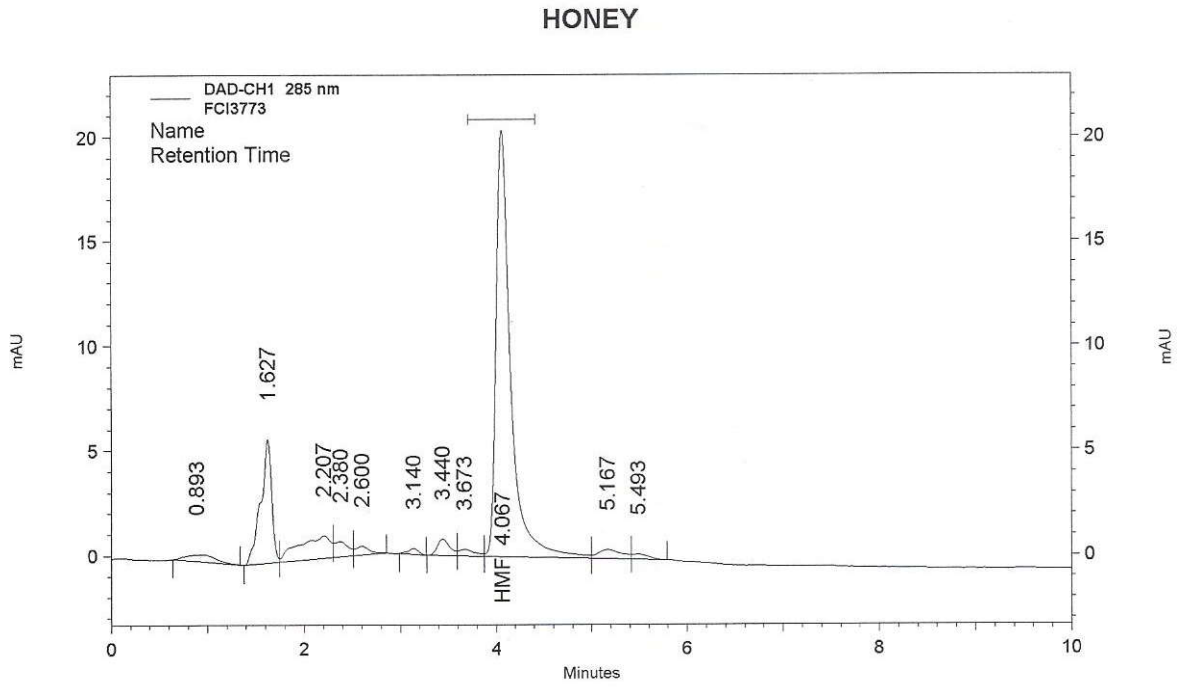

Figure 50 Chromatograph of 50% Adulteration of Honey with Fructose

Upon further aduleration of honey with 50% fructose in Figure 50, the hydroxylmethylfurfural content of the resulting fluid rose slightly to 3.24 ml/l which did not overshoot the Codex alimentarius standard for pure honey.

EZChrom Elite Custom Report

Sample ID: FCI-3974
Filename: C:\EZChrom Elite\HONEY\Data\13-05-13\007.dat
Method: C:\EZChrom Elite\HONEY\Method\13-05-13\HMF13-05-13B.met
User: lab manager
Acquired: 5/13/2013 5:50:11 AM
Printed: 5/17/2013 12:09:20 AM

NAFDAC DAD REPORT

DAD-CH1 285 nm Results

Pk #	*Name*	*Retention Time*	*Area*	*Units*	*concentration*
8	***HMF***	**4.087**	5148515	mg/L	4.581

4.581 X 50/10
229.05 mg/l

DILUTION FACTOR: 1
MULTIPIER: 4958.99
VIAL: 12

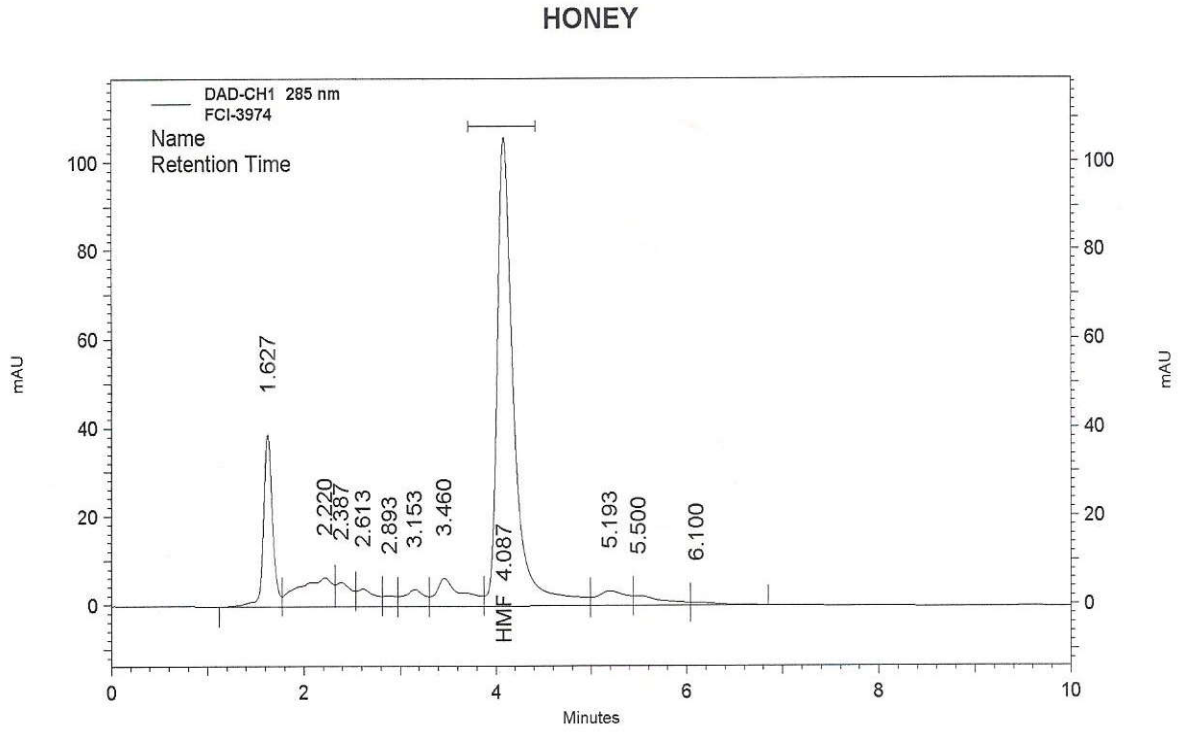

Figure 51 Chromatograph of 70% Adulteration of Honey with Fructose

F5

EZChrom Elite Custom Report

Sample ID: FCI-3975
Filename: C:\EZChrom Elite\HONEY\Data\13-05-13\012.dat
Method: C:\EZChrom Elite\HONEY\Method\13-05-13\HMF13-05-13B.met
User: lab manager
Acquired: 5/13/2013 6:47:05 AM
Printed: 5/17/2013 12:10:09 AM

NAFDAC DAD REPORT

DAD-CH1 285 nm Results

Pk #	*Name*	*Retention Time*	*Area*	*Units*	*concentration*
8	***HMF***	**4.093**	7017602	mg/L	6.296 x 50 / 10

31.48 mg/l

DILUTION FACTOR: 1
MULTIPIER: 4999.95
VIAL: 17

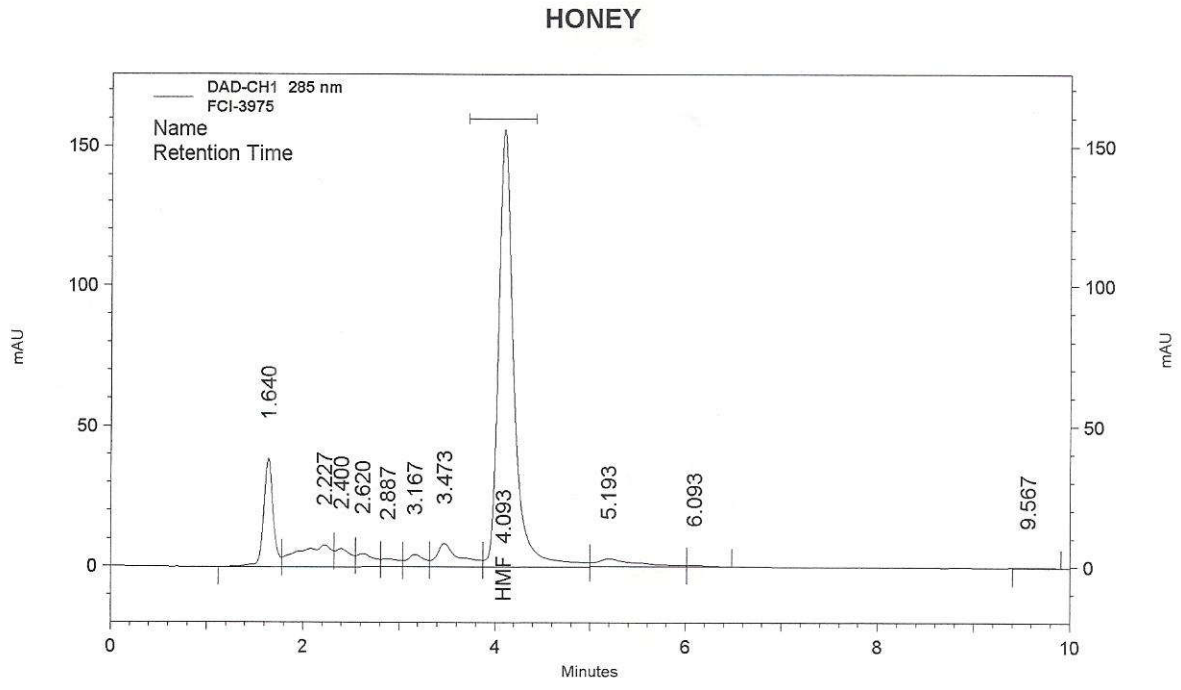

Figure 52 Chromatograph of 90% Adulteration of Honey with Fructose

Increaing the adulterant composition in honey to 90% significantly increased the furfural content of the fluid from 1.435 mg/l for pure honey to 31.48mg/l in Figure 52 ,without overshooting the

standard of 80mg/l. It therefore suggests that this chromatographic method cannot be used to track adulteration of honey with fructose.

The chrotographs of samples gathered from different sources in Nigeria are also presented .

B2

EZChrom Elite Custom Report Page 1 of 1

Sample ID: FCI-3946
Filename: C:\EZChrom Elite\HONEY\Data\13-05-13\006.dat
Method: C:\EZChrom Elite\HONEY\Method\13-05-13\HMF13-05-13B.met
User: lab manager
Acquired: 5/13/2013 5:38:44 AM
Printed: 5/17/2013 12:09:12 AM

NAFDAC DAD REPORT

DAD-CH1 285 nm Results

Pk #	*Name*	*Retention Time*	*Area*	*Units*	*concentration*
7	***HMF***	**4.093**	13289271	mg/L	11.843

11.843 x 50 / 10
592.15mg/L

DILUTION FACTOR: 1
MULTIPIER: 4966.97
VIAL: 11

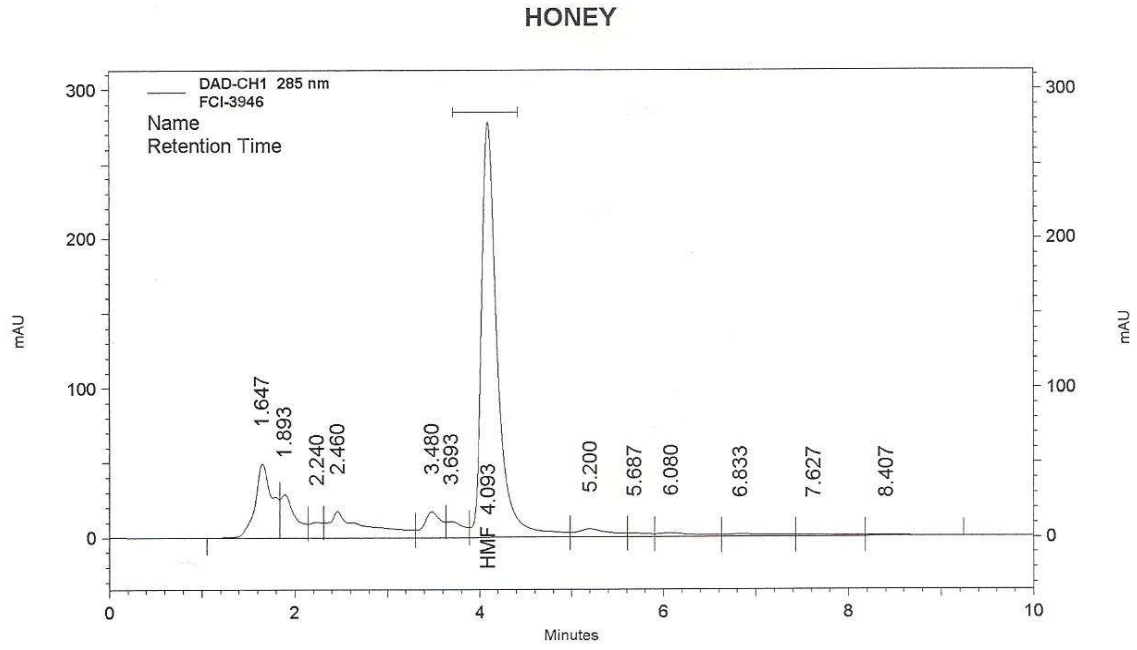

Figure 53 Chromatograph of Sample from Yola, Adamawa State.

B3

EZChrom Elite Custom Report

Sample ID: FCI-3947
Filename: C:\EZChrom Elite\HONEY\Data\13-05-13\004.dat
Method: C:\EZChrom Elite\HONEY\Method\13-05-13\HMF13-05-13B.met
User: lab manager
Acquired: 5/13/2013 5:15:56 AM
Printed: 5/17/2013 12:08:55 AM

NAFDAC DAD REPORT

DAD-CH1 285 nm Results

Pk #	*Name*	*Retention Time*	*Area*	*Units*	*concentration*
8	***HMF***	**4.087**	14746770	mg/L	13.219 X50 = 660.95 mg/L

DILUTION FACTOR: 1
MULTIPIER: 4995.9
VIAL: 9

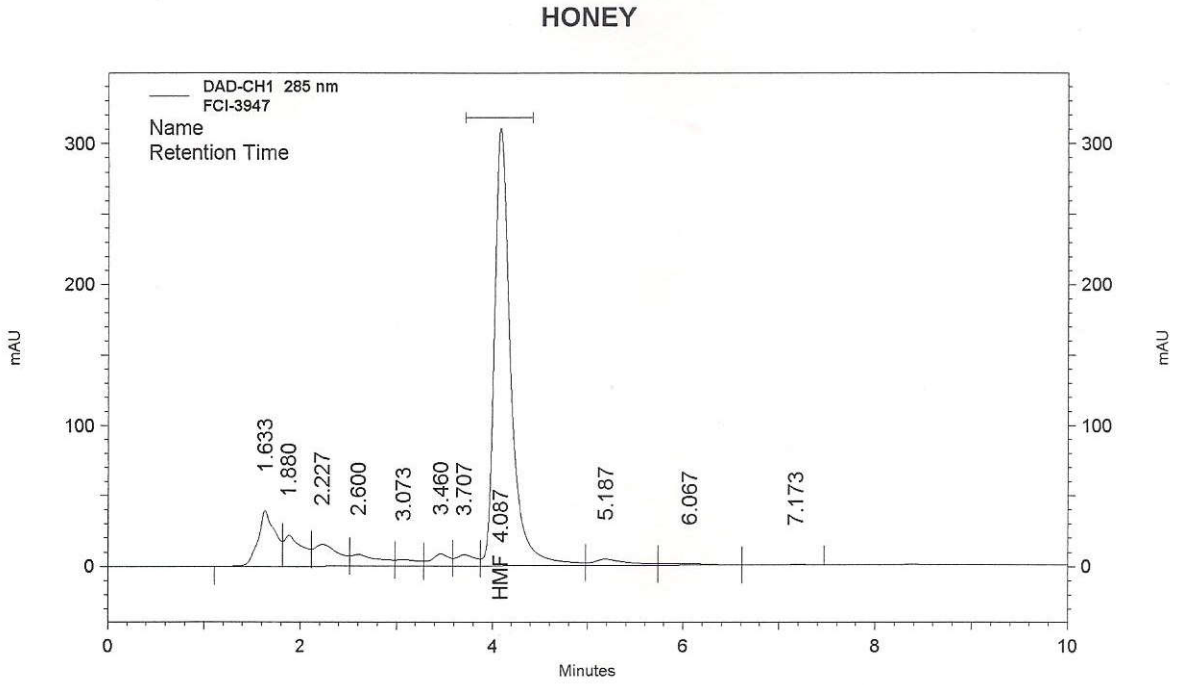

Figure 54 Chromatograph of Sample from Zuru, Kebbi State.

13 c4

EZChrom Elite Custom Report

Sample ID: FCI3948
Filename: C:\EZChrom Elite\HONEY\Data\13-05-13\049.dat
Method: C:\EZChrom Elite\HONEY\Method\13-05-13\HMF13-05-13c.met
User: Lab manager
Acquired: 5/23/2013 1:24:56 AM
Printed: 5/23/2013 10:45:06 PM

NAFDAC DAD REPORT

DAD-CH1 285 nm Results

Pk #	*Name*	*Retention Time*	*Area*	*Units*	*concentration*
8	*HMF*	**4.807**	6569037	mg/L	293.899 x 50/10

DILUTION FACTOR: 1
MULTIPIER: 249354
VIAL: 4

1469.495

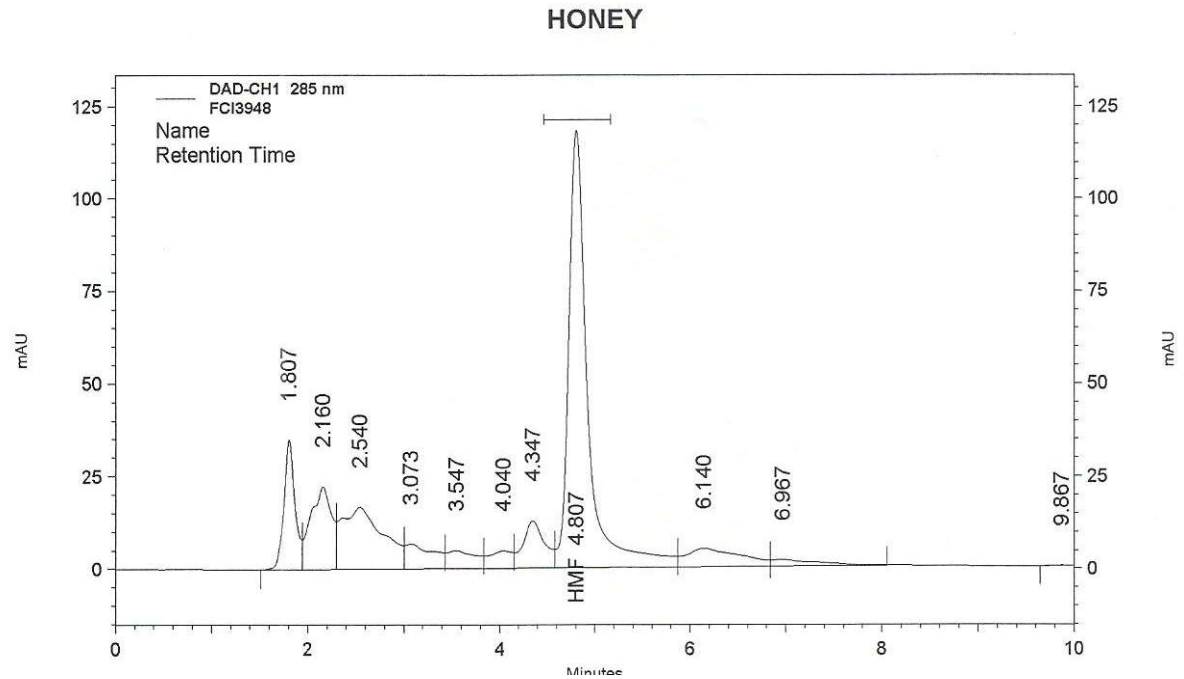

Figure 55 Chromatograph of Sample from Orolu, Kwara State.

This sample, B4 was earlier described as a fake honey using its rheological characterisation. The heavy build-up of hydroxylmethyl furfural in sample (more than eighteen times the acceptable standard) from Orolu in Kwara suggests that this sample was mainly made up of sucrose. In extension it also suggests a correlation between the rheological characterization of honey adulterated with sucrose and the hydroxylmethyl furfural content.

B5

EZChrom Elite Custom Report

Sample ID: FCI3949
Filename: C:\EZChrom Elite\HONEY\Data\13-05-13\025.dat
Method: C:\EZChrom Elite\HONEY\Method\13-05-13\HMF13-05-13B.met
User: lab manager
Acquired: 5/14/2013 4:19:06 AM
Printed: 5/17/2013 12:11:55 AM

NAFDAC DAD REPORT

DAD-CH1 285 nm Results

Pk #	*Name*	*Retention Time*	*Area*	*Units*	*concentration*
8	*HMF*	**4.060**	1550822	mg/L	1.385

x 60 = 69.25 mg/l

DILUTION FACTOR: 1
MULTIPIER: 4977.85
VIAL: 3

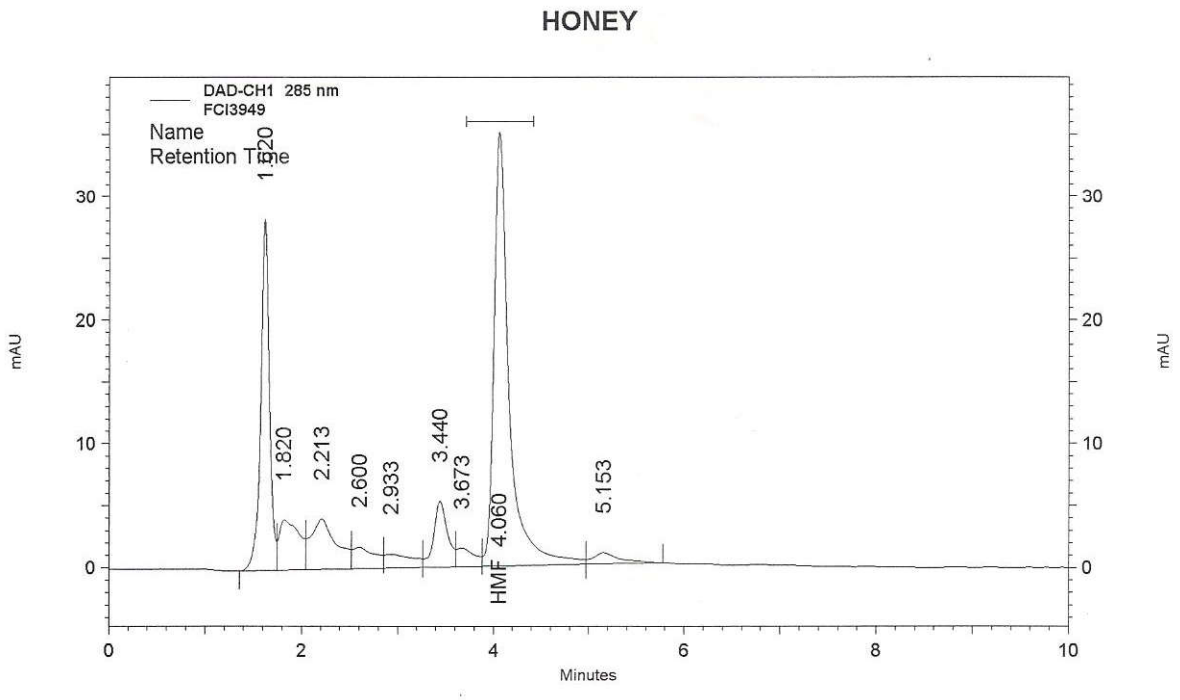

Figure 56 Chromatograph of Sample from Keffi, Nasarawa State.

EZChrom Elite Custom Report

Sample ID: FCI-3950
Filename: C:\EZChrom Elite\HONEY\Data\13-05-13\013.dat
Method: C:\EZChrom Elite\HONEY\Method\13-05-13\HMF13-05-13B.met
User: lab manager
Acquired: 5/13/2013 6:58:23 AM
Printed: 5/17/2013 12:10:18 AM

NAFDAC DAD REPORT

DAD-CH1 285 nm Results

Pk #	*Name*	*Retention Time*	*Area*	*Units*	*concentration*
6	***HMF***	**4.087**	12394392	mg/L	11.099

11.099 x 60 To = 554.95 mg

DILUTION FACTOR: 1
MULTIPIER: 4991.02
VIAL: 18

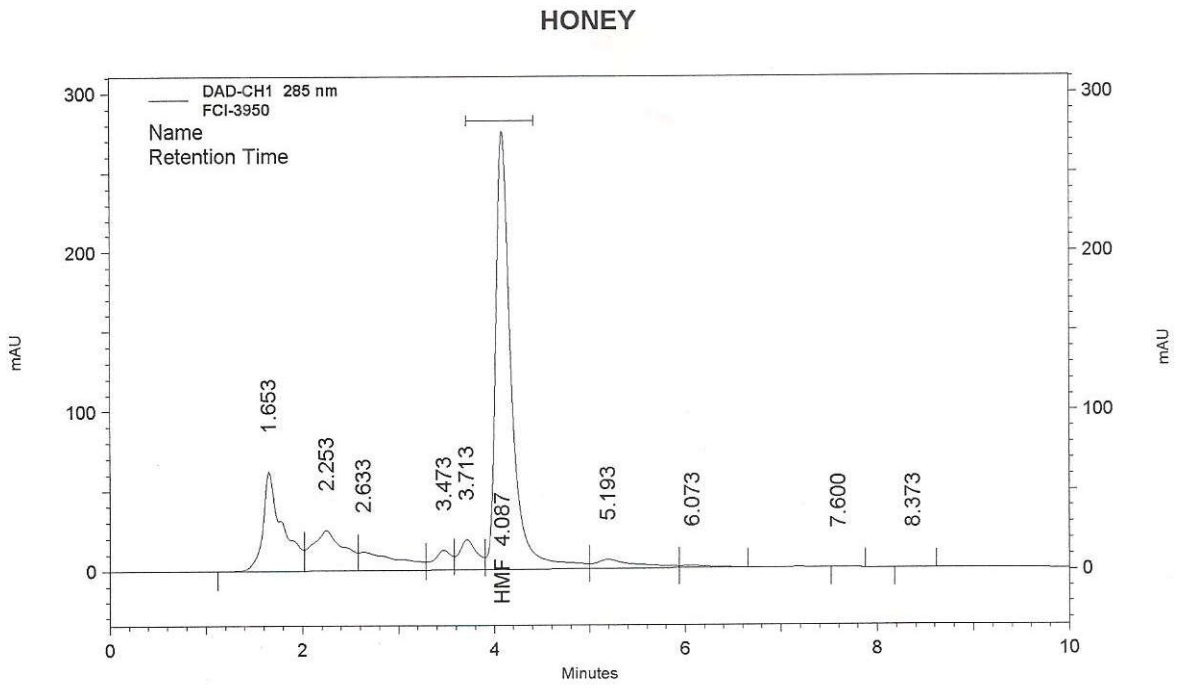

Figure 57 Chromatograph of Sample from Lokoja, Kogi State.

C1

EZChrom Elite Custom Report

Sample ID: FCI-3953
Filename: C:\EZChrom Elite\HONEY\Data\13-05-13\003.dat
Method: C:\EZChrom Elite\HONEY\Method\13-05-13\HMF13-05-13B.met
User: lab manager
Acquired: 5/13/2013 5:04:36 AM
Printed: 5/17/2013 12:08:47 AM

NAFDAC DAD REPORT

DAD-CH1 285 nm Results

Pk #	*Name*	*Retention Time*	*Area*	*Units*	*concentration*
8	***HMF***	**4.080**	4154798	mg/L	3.716

3.716 × 50 / 10 = 18.58 mg/l

DILUTION FACTOR: 1
MULTIPIER: 4984.9
VIAL: 8

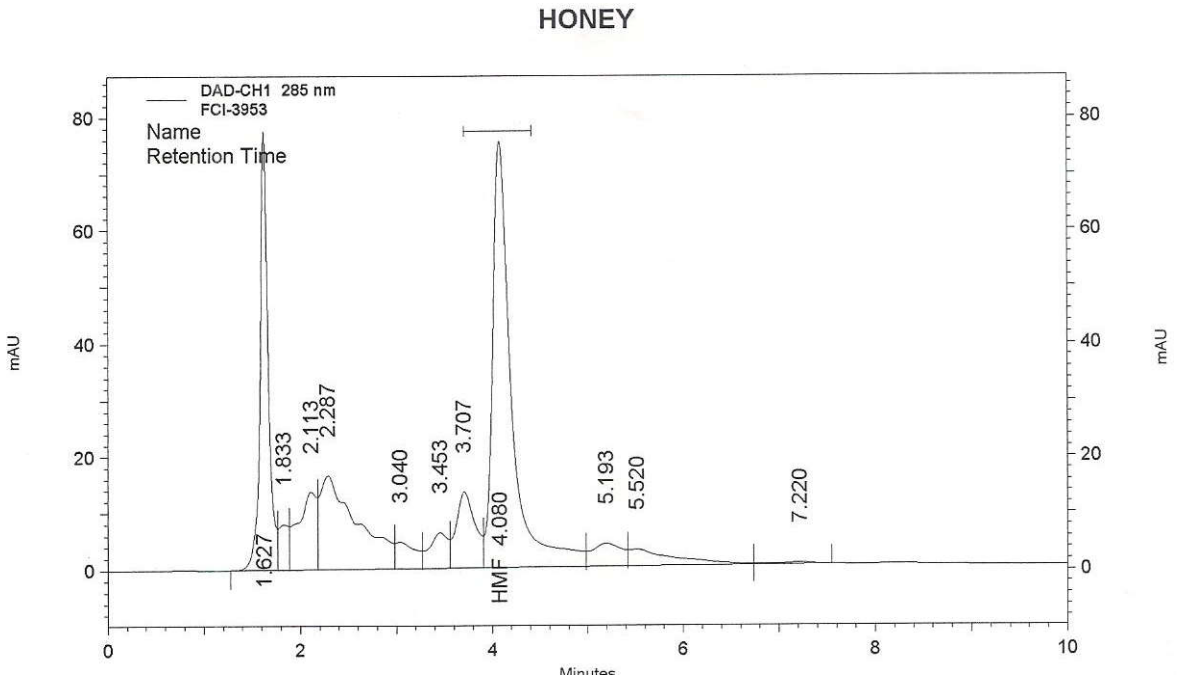

Figure 58 Chromatograph of Sample from Sunshine Ondo State.

C2

EZChrom Elite Custom Report

Sample ID: FCI3954
Filename: C:\EZChrom Elite\HONEY\Data\13-05-13\037.dat
Method: C:\EZChrom Elite\HONEY\Method\13-05-13\HMF13-05-13B.met
User: lab manager
Acquired: 5/14/2013 6:35:27 AM
Printed: 5/17/2013 12:13:53 AM

NAFDAC DAD REPORT

DAD-CH1 285 nm Results

Pk #	*Name*	*Retention Time*	*Area*	*Units*	*concentration*
8	***HMF***	**4.060**	1639930	mg/L	1.469

1.469 x 50/10
7.345 mg/L

DILUTION FACTOR: 1
MULTIPIER: 4992.26
VIAL: 15

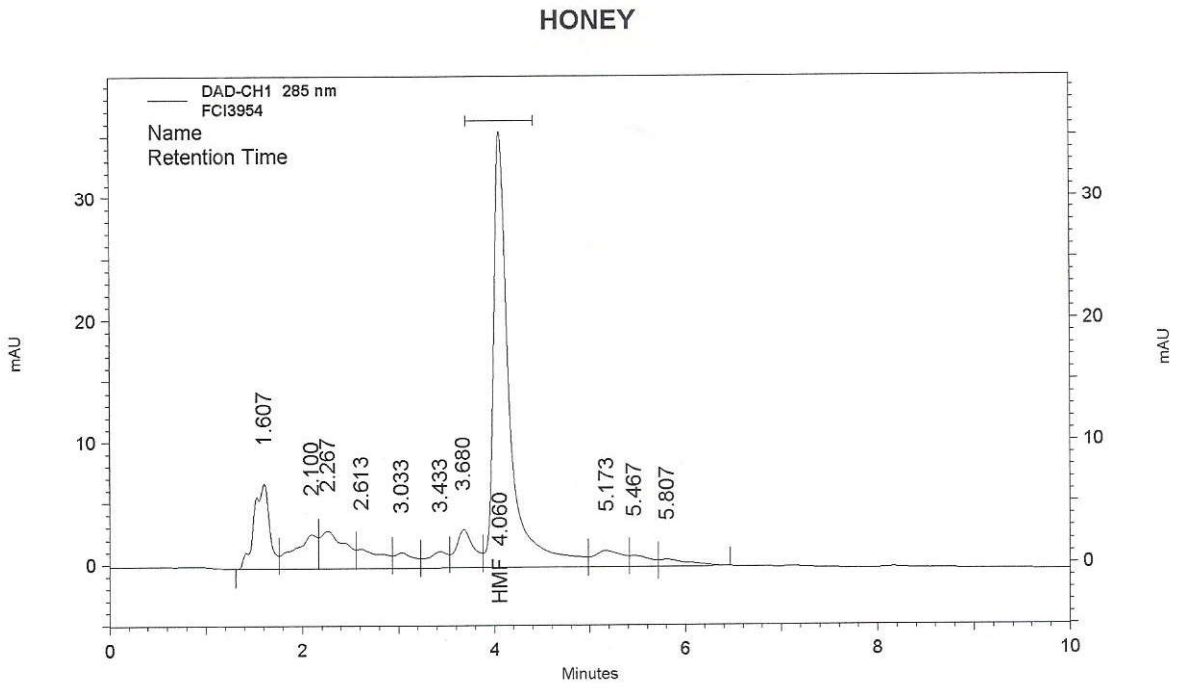

Figure 59 Chromatograph of Real Oasis Sample Iworoko Ekiti State.

C3

EZChrom Elite Custom Report

Sample ID: FCI3955
Filename: C:\EZChrom Elite\HONEY\Data\13-05-13\040.dat
Method: C:\EZChrom Elite\HONEY\Method\13-05-13\HMF13-05-13B.met
User: lab manager
Acquired: 5/14/2013 7:09:33 AM
Printed: 5/17/2013 12:14:30 AM

NAFDAC DAD REPORT

DAD-CH1 285 nm Results

Pk #	*Name*	*Retention Time*	*Area*	*Units*	*concentration*
7	***HMF***	**4.060**	24807082	mg/L	22.254 X50

111.27 mg/l

DILUTION FACTOR: 1
MULTIPIER: 4999.7
VIAL: 18

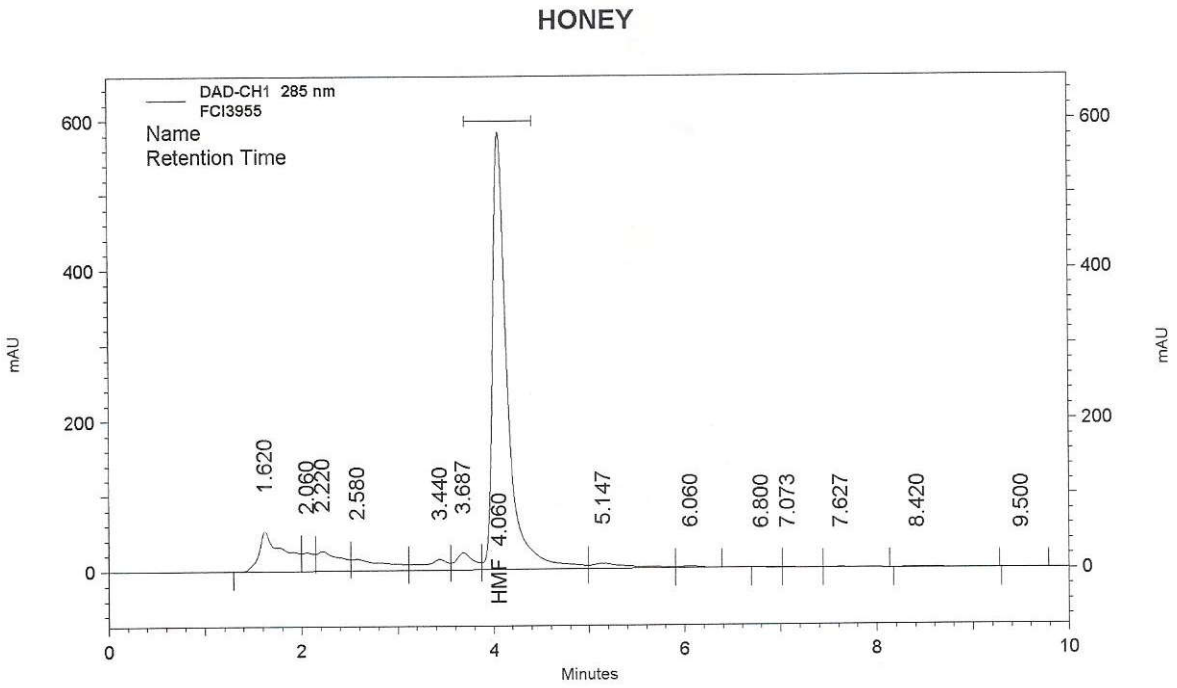

Figure 60 Chromatograph of Blessed Ado-Ekiti Sample from Ekiti State.

C5

EZChrom Elite Custom Report

Sample ID: FCI3957
Filename: C:\EZChrom Elite\HONEY\Data\13-05-13\041.dat
Method: C:\EZChrom Elite\HONEY\Method\13-05-13\HMF13-05-13B.met
User: lab manager
Acquired: 5/14/2013 7:20:53 AM
Printed: 5/17/2013 12:14:41 AM

NAFDAC DAD REPORT

DAD-CH1 285 nm Results

Pk #	*Name*	*Retention Time*	*Area*	*Units*	*concentration*
9	*HMF*	**4.067**	19410688	mg/L	17.274 x 50/10

863.7mg/L

DILUTION FACTOR: 1
MULTIPIER: 4959.87
VIAL: 19

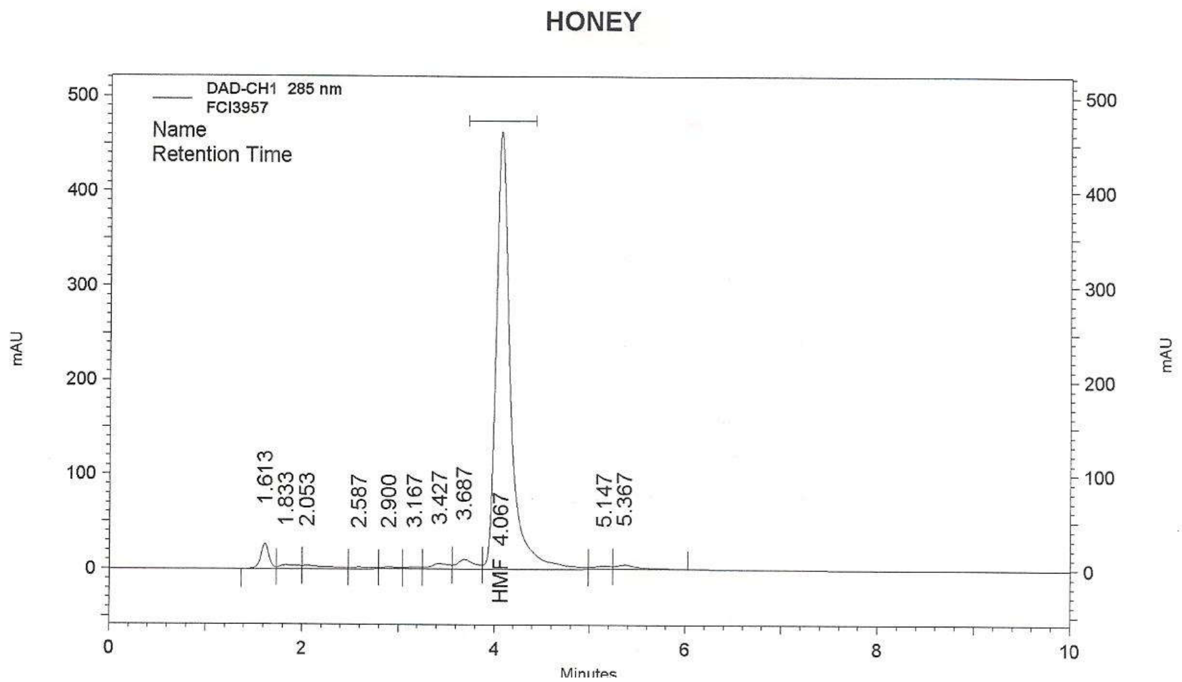

Figure 61 Chromatograph of Sample from Abba Igbira Ekiti State.

C6

EZChrom Elite Custom Report

Sample ID: FCI3958
Filename: C:\EZChrom Elite\HONEY\Data\13-05-13\031.dat
Method: C:\EZChrom Elite\HONEY\Method\13-05-13\HMF13-05-13B.met
User: lab manager
Acquired: 5/14/2013 5:27:17 AM
Printed: 5/17/2013 12:12:52 AM

NAFDAC DAD REPORT

DAD-CH1 285 nm Results

Pk #	*Name*	*Retention Time*	*Area*	*Units*	*concentration*
8	***HMF***	**4.060**	12064228	mg/L	10.748

10.748 × 50 / 10 = 53.74 mg/l

DILUTION FACTOR: 1
MULTIPIER: 4965.34
VIAL: 9

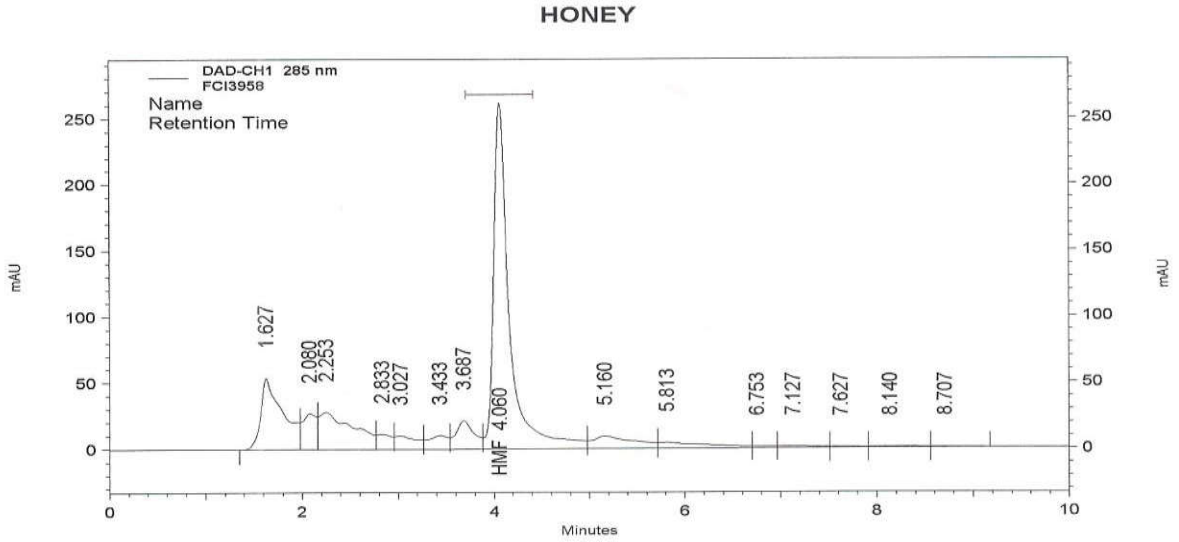

Figure 62 Chromatograph of Sample from Lagos, Lagos State.

Table 9. SUMMARY OF CHROMATOGRAPHIC HMF ANALYSES RESULTS

S/N	Sample Code	Sample Name	HMF (ml/kg)
1.	A1	Ayo Bee Farm Ado-Ekiti	3.45
2.	A2	Federal Poly Ado-Ekiti	80.90
3.	A3	Forever Honey	135.18
4.	A4	Imuwen Ijebu Mushin	1.44
5.	B1	Gauraka Niger State	23.98
6.	B2	Yola Adamawa	59.22
7.	B3	Zuru Sokoto	66.10
8.	B4	Oloru Kwara	1469.50
9.	B5	Keffi Nasarawa	6.93
10.	B6	Lokoja Kogi	55.50
11.	B7	Kabba Kogi	35.31
12.	C1	Sunshine honey Ondo	18.58
13.	C2	Real Oasis Ekiti	7.45
14.	C3	Blessed Ado-Ekiti	111.27
15.	C4	Nsukka Enugu	75.74
16.	C5	Abba Igbira	86.37
17.	C6	Lagos	53.74
18.	E1	Sucrose	302.50
19.	E2	10% Sucrose Adulteration	88.91
20.	E3	50% Sucrose Adulteration	201.22
21.	E4	70% Sucrose Adulteration	220.34
22.	E5	90% Sucrose Adulteration	288.75
23.	G1	Glucose	1.15
24.	G2	10% Glucose Adulteration	8.85
25.	G3	50% Glucose Adulteration	4.00
26.	G4	70% Glucose Adulteration	4.10
27.	G5	90% Glucose Adulteration	0.40
28.	F1	Fructose	31.71
29.	F2	10% Fructose Adulteration	3.17
30.	F3	50% Fructose Adulteration	3.24
31.	F4	70% Fructose Adulteration	22.91
32.	F5	90% Fructose Adulteration	31.48

4.3 Proximate and Some Physicochemical Analyses of honey

This section seeks to correlate the proximate and physicochemical analyses of honey with the rheological data. The Table 10 below presents the proximate and some physicochemical parameters of this study's samples.

Table10. PROXIMATE ANALYSES AND PHYSICOCHEMICAL PROPERTIES

S/N	Sample Code	Sample Name	**%Protein**	**%CHO**	**%Vit A**	**%Vit C**	**%H_2O**	**Density** (kg m^{-3})	**pH**
1.	A1	Ayo Bee Farm Ado-Ekiti	1.869	80.41	0.014	0.086	18.2	1420.0	3.3
2.	A2	Federal Poly Ado-Ekiti	1.825	78.63	0.019	0.112	20.9	1409.8	3.4
3.	A3	Forever Honey	1.863	80.22	0.088	0.109	19.2	1400.9	3.8
4.	A4	Imuwen Ijebu Mushin	1.944	81.31	0.032	0.096	18.2	1403.8	3.5
5.	B1	Gauraka Niger State	1.956	81.44	0.011	0.148	17.8	1403.8	3.9
6.	B2	Yola Adamawa	1.563	82.33	0.018	0.063	16.2	1410.4	3.9
7.	B3	Zuru Sokoto	1.237	81.21	0.014	0.106	18.2	1410.8	3.9
8.	B4	Oloru Kwara	0.256	74.33	0.027	0.021	24.6	1380.2	3.5
9.	B5	Keffi Nasarawa	1.094	79.34	0.022	0.084	19.4	1425.4	4.3
10.	B6	Lokoja Kogi	1.406	82.64	0.034	0.074	15.5	1400.0	3.9
11.	B7	Kabba Kogi	1.956	81.56	0.031	0.063	17.8	1435.0	4.0
12.	C1	Sunshine honey Ondo	1.563	79.33	0.018	0.253	19.8	1396.4	3.9
13.	C2	Real Oasis Ekiti	3.125	79.78	0.022	0.106	19.4	1396.4	3.7
14.	C3	Blessed Ado-Ekiti	1.169	79.88	0.031	0.232	17.8	1439.0	3.6
15.	C4	Nsukka Enugu	1.956	77.32	0.028	0.042	22.6	1408.7	3.7
16.	C5	Abba Igbira	1.093	80.78	0.041	0.232	18.6	1396.4	3.9
17.	C6	Lagos	1.244	79.33	0.026	0.155	20.2	1309.6	3.4
18.	E1	Sucrose	0.394	77.99	0.042	0.844	19.4	1398.0	*4.4*
19.	E2	10%SucroseAdulteration	1.250	79.40	0.019	0.200	19.4	1400.0	*3.9*
20.	E3	50% Sucrose Adulteration	0.919	78.75	0.028	0.337	19.4	1409.0	*3.9*
21.	E4	70% Sucrose Adulteration	0.575	78.23	0.034	0.529	19.4	1404.0	*4.1*
22.	E5	90% Sucrose Adulteration	0.444	78.09	0.039	0.785	19.4	1400.2	*4.2*
23.	G1	Glucose	0.313	63.39	0.005	0.045	*34.4*	1300.2	*5.1*
24.	G2	10% Glucose Adulteration	1.313	76.61	0.011	0.051	*21.8*	1386.2	*3.8*
25.	G3	50% Glucose Adulteration	1.181	73.44	0.019	0.054	*24.9*	1335.2	*4.0*
26.	G4	70% Glucose Adulteration	0.550	67.21	0.027	0.077	*30.4*	1330.6	*4.7*
27.	G5	90% Glucose Adulteration	0.344	65.62	0.030	0.090	*32.5*	1328.4	*4.8*
28.	F1	Fructose	0.450	74.25	0.006	0.011	24.2	1384.6	*5.0*
29.	F2	10% Fructose Adulteration	1.200	77.97	0.030	0.089	*20.2*	1398.4	*3.9*
30.	F3	50% Fructose Adulteration	0.619	75.83	0.028	0.077	*22.6*	1393.4	*4.2*
31.	F4	70% Fructose Adulteration	0.419	75.44	0.022	0.051	*23.0*	1382.8	*4.5*
32.	F5	90% Fructose Adulteration	0.125	74.65	0.008	0.049	*23.8*	1378.8	*4.7*

4.3.1 The Protein Content of Honey

The protein content of honey has been used for a long time as an index of quality in honey (Nazarian *et al.,* 2010 and Von De Ohe *et al.,* 1991). In the adulteration of honey with glucose, fructose corn syrup, sucrose and other carbohydrate based materials this infinitesimal trace amount of protein is not contended with. For this reason Food quality regulators like NAFDAC use this parameter to track quality. Bogdanov *et al.,* (2008) recommended a minimum protein content of 1.25 wt. % for pure honey. Looking at the results summerised in Table 10, pure sample from Ayo bee farm Ado-Ekiti (A1) has protein content value of 1.869 wt%. Other samples from Federal Polytechnic Ado-Ekiti(A2), Imuwen Ijebu Mushin (A4) and forever honey (A3) have protein content values of 1.825, 1.863 and 1.944 wt% respectively. These samples may be considered as pure honey on the basis only of their protein content and the assumption of that this parameter was not manipulated by deliberate addition of foreign substances. The above results, however, are in conformity with the data of Odeyemi *et al.,* (2013) which gave the protein concentration of the Nigerian honeys from 1.625 to 3.375 wt%. Agunbiade *et al.,* (2012) also gave the protein concentration of the Nigerian honeys as 1.43-2.72 wt. %. In the present study, samples B1, B7 and C4 were seen to behave rheologically like the reference pure samples. The above protein content results of these three samples coincidentally were 1.956 wt% which are within the standard recommended by Bogdanov *et al.,* (2008). On the other hand, honey samples B2 and C1 were adjudged to be 10% adulterated by rheological characterization. The results above show that samples B2 and C1 have protein content of 1.563%. These results are lower than the values the reference samples but, nonetheless, fall still within the protein content limit for pure honey. Here, perhaps, may be a suggestion that rheological characterization is a more sensitive tool than protein content for tracking adulteration of honey.

On samples B3, B5, C6, C3, and C5 which were adjudged to be 50% adulterated protein content values of 1.237, 1.094, 1.243, 1.168 and 1.094 wt. %, respectively, were off the minimum standard of 1.25wt. % recommended by Bogdanov. Here, perhaps, is another validation of the rheological characterizations of the present study. Similarly, it was suggested that sample B4 was an imitated honey. Therefore the protein content value of 0.256 wt. % obtained is similar to that of sucrose: 0.394, glucose: 0.313 and fructose: 0.313wt. %. In conclusion, this subsection suggests that protein content of honey correlated successfully with the rheological characterization of honey.

4.3.2 The Carbohydrate Content of Honey

The total carbohydrate content of samples did not follow any definite pattern and cannot be said on its own to be an index of quality in honey. Nevertheless, Codex Alimentarius recommended that reducing sugars in honey should be more than 60%. This cannot be used as an index of quality here since all the samples passed this test. Carbohydrate content is not suitable for tracking honey quality since most adulterants are carbohydrate based.

4.3.3 The Vitamin A, Vitamin C and Moisture Content of Honey

Like the carbohydrates, Vitamins A and C contents of samples did not follow a definite order and, thus, have no value as an index of quality. Water content of honey, on the other hand, has been used in this capacity. According to Codex Alimentarius, the moisture content of honey should not be above 21%. Almost all the samples conform to this specification with the exception of samples B4 (Oloru, Kwara) and C4 (Nsukka, Enugu). It will be recalled that B4 was earlier adjudged to be a fake honey. The moisture content value of 22.6% recorded for sample C4 suggests that it contains more water than it should have. It is good to point out that every case like this may not be that of water adulteration but may result from the

season of honey harvest which can have impact on the water content especially in situation where the bee hive was exposed to the rain.

4.3.4 The Density of Honey

Density of honey is another intrinsic quality of the sweetener capable of reflecting quality. The density of pure samples of honey, in this study is from 1403.8-1420 kg/m^3. A similar result was obtained for the Pakistani honey by Rehman *et al.,*(2008). From the results above, the adulteration of honey with glucose and fructose lowers the density of the resulting fluid. This trend was also observed in the work done by El-Bialee and Sorour, (2011). This could be attributed to the fact that honey contains some other heavier oligosaccharides and colloids which when substituted with these monomers (in this case, glucose and fructose) will naturally make the density of the resulting fluid lower. The results of density of samples therefore correlate with the earlier rheological characterization results. This is expected as relationship existed between density, dynamic and kinematic viscosities. When the density profile of honey in a particular region is noted, it may be easy to tell by aid of this instrument whether honey is adulterated or not. However one limitation of this method is water content which equally influences the density of samples.

4.3.5 The pH of Honey

The pH of our samples ranges from 3.3 to 5.1. This is similar to standard recommended by Codex Alimentarius which ranges from 3.2 to 5.5. Rehman *et al.,* (2008) also obtained similar results which is from 3 - 5 for the Pakistani honey. It can be seen that all the samples passed this test, including the suspected adulterated samples. However, it was also observed that the known pure samples have lower pH than the suspected adulterated ones. The low pH of honey contributes to its high antibacterial potency (Molan, 2001). Also, the higher the

levels of adulteration of honey with sweeteners, the higher the pH of the resulting fluids(Anidiobu, 2009). There is also need to look at the elemental analyses of honey.

4.4 Elemental Analyses of Honey

Table11. ELEMENTAL ANALYSES RESULTS : HEAVY METALS (mg/kg)

S/N	Sample Code	Sample Name	Zn	Cu	Pb	Cd	Ca	Mg	Fe
1.	A1	Ayo Bee Farm Ado-Ekiti	1.9702	5.1825	ND	ND	297.7292	29.6626	5.8202
2.	A2	Federal Poly Ado-Ekiti	2.2961	2.0378	ND	ND	293.7550	59.7878	4.2213
3.	A3	Forever Honey	0.6809	5.0190	ND	ND	195.5565	22.2785	20.4365
4.	A4	Imuwen Ijebu Mushin	2.2302	4.7178	ND	ND	18.0160	18.5091	3.5962
5.	B1	Gauraka Niger State	1.8418	4.6654	ND	ND	435.4856	61.4600	5.1311
6.	B2	Yola Adamawa	2.0925	1.9836	ND	ND	366.8750	70.6339	4.8478
7.	B3	Zuru Sokoto	7.5146	2.6313	ND	ND	494.3823	62.3200	5.7685
8.	B4	Oloru Kwara	0.8392	1.3506	ND	ND	273.2171	46.2378	5.5031
9.	B5	Keffi Nasarawa	3.5030	4.7889	ND	ND	610.2775	64.8702	4.9591
10.	B6	Lokoja Kogi	2.7678	1.9183	ND	ND	341.9230	65.8390	4.7188
11.	B7	Kabba Kogi	1.7293	3.6217	ND	ND	385.6717	68.5793	4.4794
12.	C1	Sunshine honey Ondo	2.8497	0.7568	ND	ND	242.0281	41.5222	1.0249
13.	C2	Real Oasis Ekiti	4.3305	4.6349	ND	ND	543.3992	27.2263	8.2451
14.	C3	Blessed Ado-Ekiti	7.6072	4.1306	ND	ND	536.9218	65.0660	15.6319
15.	C4	Nsukka Enugu	0.7823	1.6579	ND	ND	546.8797	50.2845	4.8849
16.	C5	Abba Igbira	2.0839	3.5661	ND	ND	181.7536	22.3537	8.8244
17.	C6	Lagos	0.6370	1.2312	ND	ND	498.5216	64.6908	10.9807
18.	E1	Sucrose	0.7012	5.034	ND	ND	173.1982	2.9856	5.8960
19.	E2	10% Sucrose Adulteration	1.5401	5.070	ND	ND	254.0999	13.6575	5.7765
20.	E3	50% Sucrose Adulteration	1.7508	5.1009	ND	ND	238.0166	15.0987	5.8034
21.	E4	70% Sucrose Adulteration	0.9126	5.0980	ND	ND	223.9887	12.8997	5.8900
22.	E5	90% Sucrose Adulteration	0.7299	5.0890	ND	ND	198.0886	4.8902	5.8809
23.	G1	Glucose	1.4918	5.2836	ND	ND	172.1798	3.5673	5.7925
24.	G2	10% Glucose Adulteration	2.5934	4.0579	ND	ND	116.3030	16.1687	2.7235
25.	G3	50% Glucose Adulteration	1.7250	4.8799	ND	ND	98.0050	9.7706	3.0897
26.	G4	70% Glucose Adulteration	0.8676	5.1189	ND	ND	98.9285	7.1230	2.3816
27.	G5	90% Glucose Adulteration	0.7612	1.6164	ND	ND	184.8838	4.5131	1.9130
28.	F1	Fructose	0.6897	4.9377	ND	ND	174.5307	15.9640	2.0509
29.	F2	10% Fructose Adulteration	2.1288	5.5468	ND	ND	162.5048	16.8972	3.1567
30.	F3	50% Fructose Adulteration	3.3886	2.9708	ND	ND	276.1376	17.1909	2.6953
31.	F4	70% Fructose Adulteration	1.1032	0.4476	ND	ND	115.5755	14.1152	1.1303
32.	F5	90% Fructose Adulteration	0.5772	2.1418	ND	ND	95.9454	13.1797	2.8000

ND — Not Detected

This section focuses on a possible linkage between metallic composition of honey and its purity and in extension seeks a correlation with its rheological properties. Table 11 above is the results of heavy metal analyses of samples. It shows that samples are rich in minerals. Heavy carcinogenic metals, lead and cadmium were undetected in all the samples which make them safe for consumption (FAO, 2012). The Zinc content of samples ranges from

0.6370 (C6-Lagos) to 7.6072 (C3-Blessed honey Ado-Ekiti). According to the works of Pisani *et al.,* (2008), Downey *et al.,* (2005), Fernandez-Torres *et al.,* (2005), Conti, (2000) and Latorre *et al.,* (1999), the Zinc content of honey range from 1.3 to 7.8mg/kg. It clearly shows that some of the samples are off the specification which suggests that they could have been adulterated. A look at the results of shows that sample A3 (Forever honey) failed this test. Likewise, fructose and sucrose have zinc values of 0.6897 and 0.7012 mg/kg. From the rheological characterization, we concluded that honey samples B1, B7 and C4 rheologically behaved like pure honey. While samples B1 and B7 passed the test, sample C4 has the Zinc value of 0.7823mg/kg which did not conform to the standard. Expectedly, samples B2 and C2 adjudged to be 10% adulterated both passed this test, because their level of adulteration was still modest. A thorough examination of serial adulterated samples E1-E5, F1-F5 and G1-G5 showed that the zinc content decreased with increasing adulteration in honey. However, this parameter cannot be used on its own to determine adulteration, but can be used in conjunction with other tests.

Also, according to Pisani *et al.,*(2008), Downey *et al.,*(2005), Fernandez-Torres *et al.,*(2005), Conti,(2000) and Latorre *et al.*,(1999) the Manganese content of honey is from 13.3 to 136mg/kg. Most of our samples conform to this standard except the imitation E1 (sucrose) that gave the value of 2.9856mg/kg and E5 (90% adulteration) that gave 4.8902mg/kg of the metal which are less. Like zinc, it could be observed that manganese content increases with the purity of honey.

Also the calcium content ranges from 47.7 to 341.0 mg/kg and most of the samples conform to this standard. Also, the standard for iron is that the content should be greater than 3.7 mg/kg. Forever honey (sample A3) and samples adulterated with fructose failed this test. This suggests that forever honey might have been stored with steel containers. In a similar

development, the standard for copper which is from 0.5 mg/kg saw all the samples passing the tests. There is a need to look at the antibacterial properties of honey.

4.5 Antibacterial Properties of Honey

This section seeks to establish a possible correlation between the rheological behaviour of honey and its medicinal value which is visible in its antibacterial properties. Tables 12 and 13 below are the summary of experimental results on the effect of fructose, glucose, sucrose and water adulteration on the antibacterial and healing properties of honey.

The results in Table 12 show that all the pure honey samples A1, A2 and A4 were effective against Staphylococcus *aureus* with the sample from Ijebu Mushin, A4, exhibiting the best activity. The Forever living honey, A3, also exhibited antibacterial activities against S. *aureus*. The implication of this is that S. *aureus* infected wounds that were not treated properly with antibiotics can be treated by topical application of honey (Chute *et al.,* 2010). The import of these results show that the antibacterial activities of pure honey correlate with the earlier rheological characterization of honey. Pure honey samples also showed decreasing activities upon dilution with water (Chute *et al.,* 2010) except for 5% and 10% water adulteration that gave high activities like pure honey itself (Rehman *et al.,* 2010). This could be attributed to hydrogen peroxide effect induced by the interaction of glucose oxidase in the presence of free water in honey (Molan, 2001) (see section 2.7.6). Surprisingly, 20% water adulteration showed no activity at all, meaning that the optimum concentration equilibrium for antibacterial property of standard honey sample A4 was between 5% and 10%. Also worthy of note are results from honey sample from Nsukka Enugu State, C4, which showed wide zones of inhibition against Staphylococcus *aureus* at different dilutions of honey as shown in Figure 45 below.

TABLE 12. THE ANTIBACTERIAL EFFECT OF HONEY ON *STAPHYLOCOCCUS AUREUS*

S/N	Samples	Sample Names	Concentration (%) Diameter of clear zone Inhibition(mm)				
			20%	40%	60%	80%	Net Honey
1.	A1	Ayo Bee Farm Ado-Ekiti	-	10	12	18	21
2.	A2	Fed Poly Ado	-	9	15	16	20
3.	A3	Forever Honey	-	10	14	18	22
4.	A4	Ijebu Mushin	-	10	16	20	25
5.	B1	Gauraka Niger State	-	-	8	9	15
6.	B2	Yola Adamawa	-	-	-	14	20
7.	B3	Zuru Sokoto	-	-	12	16	17
8.	B4	Oloru Kwara	-	-	-	-	-
9.	B5	Keffi Nasarawa	-	-	-	-	15
10	B6	Lokoja Kogi	-	-	-	-	12
11.	B7	Kabba Kogi	-	-	11	15	20
12	C1	Sunshine Ondo	-	-	-	8	10
13	C2	Real Oasis Ekiti	-	-	-	-	-
14	C3	Blessed Ado-Ekiti	-	-	-	-	15
15	C4	Nsukka Enugu	14	15	18	18	23
16	C5	Abba Igbira Ekiti	-	-	-	-	14
17	C6	Lagos	-	-	-	-	-
18	E1	Sucrose	-	-	-	-	-
19	E2	10% Sucrose Adulteration	-	-	-	-	10
20	E3	50% Sucrose Adulteration	-	-	-	-	8
21	E4	70% Sucrose Adulteration	-	-	-	-	-
22	E5	90% Sucrose Adulteration	-	-	-	-	-
23	F1	Fructose	-	-	-	-	-
24	F2	10% Fructose Adulteration	-	-	-	-	11
25	F3	50% Fructose Adulteration	-	-	-	-	9
26	F4	70% Fructose Adulteration	-	-	-	-	-
27	F5	90% Fructose Adulteration	-	-	-	-	-
28	G1	Glucose	-	-	-	-	-
29.	G2	10% Glucose Adulteration	-	-	-	-	11
30.	G3	50% Glucose Adulteration	-	-	-	-	10
31.	G3	70% Glucose Adulteration	-	-	-	-	-
32.	G5	90% Glucose Adulteration	-	-	-	-	-
33.	H1	5% Water Adulteration					24
34.	H2	10% Water Adulteration					25
35.	H3	15% Water Adulteration					22

Little wonder earlier in this report, this particular sample correlated rheologically as pure honey. Also, this result correlates with that of Chute,*et al.,* (2010). The honey samples from Gauraka Niger State, B1 and Kabba Kogi State, B7, also exhibited good antibacterial activities against S. *aureus*. It was as well observed that honey samples from Oloru Kwara

State (earlier adjudged to be fake through rheological characterization), Lagos State and Real Oasis honey Ado-Ekiti do not show any antibacterial activity against S. *aureus*.

TABLE 13. THE ANTIBACTERIAL EFFECT OF HONEY ON *PSEUDOMONAS AERUGINOSA*.

	Samples		Concentration (%) Diameter of clear zone Inhibition(mm)				
			20%	40%	60%	80%	Net Honey
1.	A1	Ayo Bee Farm Ado-Ekiti	-	8	12	17	20.7
2.	A2	Fed Poly Ado	-	7	12	15	20.4
3.	A3	Forever Honey	-	11	13	20	24.2
4.	A4	Ijebu Mushin	-	9	16	18	26
5.	B1	Gauraka Niger State	-	-	8	9	15
6.	B2	Yola Adamawa	-	-	-	15	20
7.	B3	Zuru Sokoto	-	-	8	9	10
8.	B4	Oloru Kwara	-	-	-	-	-
9.	B5	Keffi Nasarawa	-	-	10	12	18
10.	B6	Lokoja Kogi	-	-	-	-	18
11.	B7	Kabba Kogi	-	-	-	-	12
12	C1	Sunshine Ondo	-	-	10	15	20
13.	C2	Real Oasis Ekiti	-	-	-	-	15
14.	C3	Blessed Ado-Ekiti	-	-	-	-	10
15.	C4	Nsukka Enugu	-	-	13	10	20
16.	C5	Abba Igbira Ekiti	-	-	-	-	14
17.	C6	Lagos	-	-	-	-	-
18.	E1	Sucrose	-	-	-	-	-
19.	E2	10% Sucrose Adulteration	-	-	-	-	10
20.	E3	50% Sucrose Adulteration					8
21.	E4	70% Sucrose Adulteration	-	-	-	-	-
22.	E5	90% Sucrose Adulteration	-	-	-	-	-
23.	F1	Fructose	-	-	-	-	-
24.	F2	10% Fructose Adulteration	-	-	-	-	9
25.	F3	50% Fructose Adulteration	-	-	-	-	9
26.	F4	70% Fructose Adulteration	-	-	-	-	-
27.	F5	90% Fructose Adulteration	-	-	-	-	-
28.	G1	Glucose	-	-	-	-	-
29.	G2	10% Glucose Adulteration	-	-	-	-	11
30.	G3	50% Glucose Adulteration	-	-	-	-	8
31.	G3	70% Glucose Adulteration	-	-	-	-	-
32.	G5	90% Glucose Adulteration	-	-	-	-	-
33.	H1	5% Water Adulteration					25
34.	H2	10% Water Adulteration					26.2
35.	H3	15% Water Adulteration					21.9

The effect of adulteration on the antibacterial properties of honey was also studied against *Staphylococcus aureus*. Glucose, fructose and sucrose were also used as adulterants in the

experiment. Honey was adulterated using 10%, 50%, 70% and 90% of these materials (see section 3.1). It was observed in Table 12 that only 10% and 50% adulteration of honey in glucose, fructose and sucrose showed signs of antibacterial inhibition against S. *aureus* while higher concentration of adulteration showed no sign of inhibition. This is a direct reflection on what fake drugs do to patients.

Table 13 is the summary of the antibacterial effect of honey against *Pseudomonas aeruginosa*. Pure samples A1, A2 and A4 all exhibited good antibacterial properties against *Pseudomonas aeruginosa*. Forever honey, A3, also exhibited antibacterial activities. Upon dilution with 10% distilled water, a slight increase in diameter of the zone of inhibition was observed, signifying the peroxide activities in the pure honey. However, upon further addition of water, the antibacterial properties of the resulting fluids decrease sequentially. Samples from Gauraka Niger, B1, Nsukka Enugu, C4, and C1, Sunshine Ondo States exhibited antibacterial properties up to 60% and 80% dilution. In the study of the effect of adulteration on the antibacterial properties of honey, it was observed in Table 13 that only 10% and 50% adulteration of honey with glucose, fructose and sucrose showed signs of antibacterial inhibition against Pseudomonas *aeruginosa* while higher concentration of adulteration showed no sign of inhibition. This indicates the absence of healing properties of honey at higher concentration of adulterants (Chute *et al.,* 2010; Ndip *et al.,* 2007). Comparing the outcome of antibacterial properties with the rheological characterization of honey, it shows that antibacterial activities of samples correlated successfully with rheological characterization of honey. Thus, this study's rheological assessment of the quality of honey samples correlate with another independent index of honey quality – the antibacterial activity.

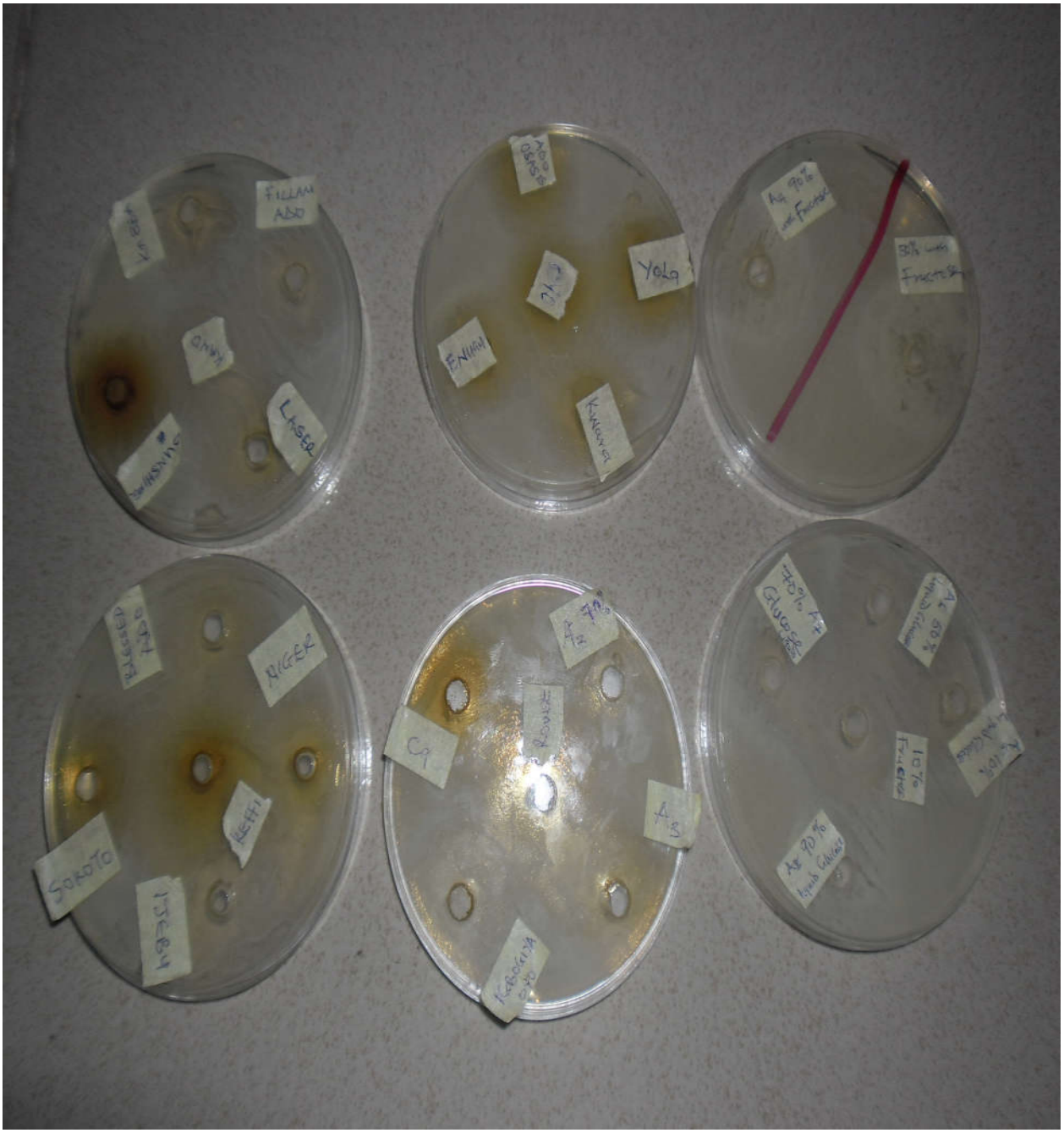

Figure 45 The Antibacterial Assay of Honey against *Staphyloccocus* Aereus

CHAPTER FIVE

5.1. SUMMARY OF FINDINGS

The findings of this study are summarized and aligned with the study's original objectives below.

Objective of the Work	**Summary of Findings**
i. To explore the efficacy of utilizing honey rheology to assess its purity.	Samples of pure honey from different sources were found to exhibit characteristic rheological line shapes on the apparent viscosity-rate of shear plane which changed with temperature. The viscosity generally decreases as shear rate increases but a peculiar shear thickening behaviour is observed at low rates of shear (0.01 to 0.245s^{-1}) and at temperatures around 25 ^{o}C leading to a maxima in the rheogram. In addition, hysteresis loops observed on pure honey rheograms for cyclic variations of rates of shear underscores the non-Newtonian nature of pure honey at low shear rates. The rheology of honey is a function of temperature with apparent viscosity decreasing as temperature increases and exhibiting a shift from non-Newtonian to Newtonian behaviour.
	Introduction of adulterants to samples of pure honey reflects on the sample's rheogram. Glucose, fructose, sucrose or water often employed to enhance mass of honey samples were found to drag the samples towards Newtonian behaviour even in the low shear rate zone. The degree of adulteration (mass % of adulterant

	in sample) was found to reflect on rheogram.
It may, thus, be concluded that rheograms of purported honey samples contain information on their quality.	
ii. To extract structural and compositional information from the rheological data.	PLM and CYM models were used to analyze the experimental data. The behaviour indexes in the two models were the distinguishing factor as they increased with the level of adulteration in honey. The results of graduated adulteration of a reference pure honey sample with glucose, fructose or sucrose were used as calibration data to quantify the level of adulteration of other samples from different locations in Nigeria. These two empirical models were found, however, unsatisfactory in tracking honey adulteration with water.
	The SKM was applied to honey rheology. This model, with the Mark-Houwink equation incorporated, was used to extract the average molecular weight of samples yielding data found cognate to distinguishing pure from adulterated honey. The SKM derived average molecular weights which better correlated with the composition of honey serially diluted with glucose, fructose, sucrose and water than was obtained from the empirical models. The order of the deformation kinetics in this model gives the number of active components or groups of active components taking part during the deformation. The best results were obtained for pure honey samples at third order deformation kinetics. This implies that three components of the honey

	constituents were active during deformation. It may be suggested that melezitose and other oligosaccharides and polymerized materials serve as the first, water as the second and mono-saccharides as the third active component. Very importantly, the SKM which employs time resolved data obtained at constant rates of share produces plots of rate of deformation versus rate of shear that display a remarkable contrast between pure honey and adulterated products. Equally remarkable is the negative infinite time viscosities which characterize pure honey data. These shift towards positive values with increasing degrees of adulteration.
	The CYM was improved upon by inserting the Mark-Houwink equation in place of zero shear viscosity to permitting its use for the determination of molecular weight of fluids from rheological data. The results from the ACYM compared relatively well with that of the SKM except for the effect of water adulteration on honey where the empirical model again failed.
Structural and compositional information have, through the deployment of empirical models and the SKM, been extracted from the rheological line shapes (rheograms) of this study.	

<table>
<tr><td rowspan="2">iii To establish rheological characterization as a testing method for honey quality</td><td>The results of physicochemical and chromatographic characterization of honey correlated well with conclusions of this new rheological method. The protein content of honey, a major index of its quality was found consistent with the suggestions from the rheological analyses. The HMF content of honey, another independent index of quality, corroborated the conclusions of this study's rheological characterization of the effect of sucrose adulterant on honey, but not with respect to glucose- and fructose-based adulteration.</td></tr>
<tr><td>The antibacterial activities or healing properties of samples against gram positive (Staphylococcus aureus) and gram negative (Pseudomonas aeruginosa) organisms correlated well with the rheological characterization of honey.</td></tr>
<tr><td colspan="2">A new way of testing honey for authenticity and quality has been established. This method was able to detect adulteration in purported honey samples and with a calibration data set obtained on simulated adulteration, produce their levels of adulteration. Such samples obtained from several locations across the country were classified according to levels of their purity. This classification was corroborated by data on independent honey quality checks.</td></tr>
</table>

5.2 CONCLUSION

The objectives of this study were achieved and from the results of the investigations conducted, the following conclusions can be made:

i. Pure Honey has a characteristic rheogram at a fixed condition of temperature. The viscosity generally decreases as shear rate increases but a peculiar shear thickening behaviour is observed at low rates of shear (0.01 to 0.245s^{-1}) and at temperatures around 25 ^{o}C leading to a maxima in the rheogram.

ii. The rheology of honey changes with temperature – the apparent viscosity decreasing as temperature increases and exhibiting a shift from non-Newtonian to Newtonian behaviour.

iii. Introduction of adulterants to samples of pure honey reflects on the sample's rheogram. Glucose, fructose, sucrose or water often fraudulently employed to enhance net product mass were found to drag the samples towards Newtonian behaviour even in the low shear rate zone. The degree of adulteration (mass % of adulterant in sample) was found to reflect on rheogram.

iv. Rheological data of purported honey samples contain information on their quality.

v. Structural and compositional information can be extracted with the deployment of empirical models and the SKM from the rheological data of this study. Very importantly, the SKM which employs time resolved data obtained at constant rates of shear produces plots of rate of deformation versus rate of share that display a remarkable contrast between pure honey and adulterated products. Equally remarkable is the negative infinite time viscosities which characterize pure honey data but which shift towards positive values with increasing degrees of adulteration.

vi. This study points to a new method of testing honey for authenticity and quality. It was possible, by this method and with a calibration data set obtained on simulated

adulteration, to detect adulteration in purported honey samples and to produce their levels of adulteration. Such samples obtained from several locations across the country were classified according to levels of their purity. This classification was corroborated by data on established independent indices of honey quality. The latter included Protein Content, HMF Content, and Antibacterial activity. The new method may, thus, be considered as validated.

5.3 CONTRIBUTIONS TO KNWOLEDGE

i. A novel test method has been devised for rheological authentication of honey and classification of honey adulterated with glucose, fructose, sucrose and water.

ii. The Structural Kinetic Model has, for the first time, been deployed for the extraction of structural and average molecular weight information on purported honey samples from rheological data. Also this study's Structural Kinetic Model analyses produce palpable contrasting plots which tell pure honey from the adulterated product.

iii. This study for the first time suggests that a 3^{rd} order breakdown kinetics adequately describes honey deformation under shear which perhaps accounts for the three main constituents of the fluid.

iv. This work to the best of my knowledge is the first to successfully link the antibacterial activities, proximate and physicochemical properties of honey with its rheological parameters.

5.4 RECOMMENDATIONS

In view of the limited number and source distribution of samples used in this study, the conclusions drawn can be augmented to a more general applicability by including and analyzing more samples from locations outside Nigeria and from more locations within the country.

The results of this study should inspire the design and manufacture of a simple test apparatus for the rheological screening of samples of honey for authenticity and quality.

REFERENCES

Abu-Jdayil, B. (2003). Modeling the time-dependent rheological behavior of semisolid foodstuffs. *Journal of Food Engineering* **57**: 97–102.

Adebiyi, F.M., Akpan, I., Obiajunwa, E.I. and Olaniyi, H.B. (2004). Chemical/physical characterisation of Nigerian honey. *Pakistan journal of nutrition* **3**(5): 278-281.

Agunbiade, S.O., Arojojoye, O.A. and Alao, O.O. (2012). Evaluation of some biochemical, microbiological and Organoleptic characteristics of some honey samples in Nigeria. *Academia Arena* **4**(8):41-45.

Ajibola, A., Chamunorwa, J.P. and Erlwanger, K.H. (2012). Nutraceutical values of natural honey and its contribution to human health and wealth. *Nutrition & Metabolism* **9**: 61.

Allen, K.L., Molan, P.C and Reid, G.M. (1991): A survey of the antibacterial activity of some New Zealand honeys. *Journal of Pharmacy and Pharmacology* **43**(12): 817-822.

Alqurashi, A. M., Masoud, E. A. and Alamin, M. A. (2013): Antibacterial activity of Saudi honey against Gram negative bacteria. *Journal of Microbiology and Antimicrobials* **5**(1), 1-5.

Anidiobu, V.O.(2009). Rheological Analysis of Honey Samples in Nigeria. *Journal of Research in Bioscience* **5**(1):46-51

Ayansola, A.A. and Banjo, A.D. (2011). Physicochemical evaluation of authenticity of honey marketed in Southwestern Nigeria. *Journal of Basic Applied Sciences* **1**(12):3339-3344.

AOAC (1990). Official Methods of Analysis of the Association of Analytical Chemists15th Edn., Wasinton, DC.

Bacri, J.C and Perzynski, R. (1995). Negative Viscosity:Effect in a magnetic fluid. *Physical Review Letters* **75**(11):2128-2131.

Bakier, S. (2007). Influence of Temperature and water content on the Rheological Properties of Polish Honey. *Polish Journal of Food and Nutrition Sciences* **57**(2):17-23.

Batsoulis, A. N., Siatis, N. G., Kimbaris, A. C., Alissandrakis, E. K., Pappas, C. S. and Tarantilis, P. A. (2005). FT -Raman spectroscopic simultaneous determination of fructose and glucose in honey. *Journal of Agricultural and Food Chemistry* **53**, 207–210.

Bera, A., Almeida-Muradian, M., and Sabato, S.F. (2008). Study of physicochemical and rheological properties of Irradiated honey. *NUKLEONIKA Journal* **2**:85-8.

Belitz, H.D., and Grosch, W. (1999). *Food Chemistry*. Berlin : *Sprnger Verlag* 412-421.

Bird, R.B., Stewart, W.E, and Lightfoot, E.N. (2006). *Transport Phenomena*. John Wiley & sons, Incorporated 1- 31 & 232-251.

Bogdanov, S., Jurendic, T., and Sieber, R. (2008). Honey for nutrition and health: A review. *American Journal of the College of Nutrition* **27**:677-689.

Bose, B. (1982). Honey or sugar in treatment of infected wounds. *Lancet* **1**(8278):963.

Brookfield (2002). "Ultra programmable rheometer: Operating instructions manual" Serial number: RY6511496 No.

Candon, R .E. (1993). Curious interaction of bugs and bees. *Surgery* **113** (2):234-5.

Chauhan, A., Pandey, V., Chacko, K.M., and Khandal, R.K. (2010). Antibacterial activity of raw and processed honey. *Electronic Journal of Biology* **5**:58-66.

Chavez, T.T. and Decker, C.F. (2008). Health care-associated MRSA versus community-associated MRSA. Dis. Mon. **54**: 763-768.

Cheesbrough, M. (2006). *District Laboratory Practice in Tropical Countries. Cambridge*:Cambridge University Press.

Chenlo, F., Chaguri, L., Santos, F., and Moreira, R. (2006). Osmotic dehydration/impregnation kinetics of padron pepper (*capsicum annml Longum*) with sodium chloridoe solution: Process modeling and colour Analysis. *International Journal of Food Science and Techonlogy* **12**(3):221-227.

Chirife, J., .Scarmato,G, and Herszage, L. (1983). Scientific basis for use of granulated sugar in treatment of infected wounds. *Journal of Antimicrobial Agents and Chemotherapy* **23**(5): 766–773.

Chute, R.K, Deogade. N.G and Kawale. M (2010). Antibacterial activity of Indian honey against clinical isolates. *Asiatic Journal of Biotechnology Resources* **1**:35-38.

CLSI (2012). Performance Standards for Antimicrobial Disk Susceptibility Tests; Approved Standard—Eleventh Edition. CLSI document M02-A11. Wayne, PA: Clinical and Laboratory Standards Institute.

Conti, M. E. (2000). Lazio region (central Italy) honeys: A survey of mineral content and typical quality parameters. *Food control* **11**:459-463.

Cooper, R.A., Molan, P.C. and Harding, K.G. (2002). Honey and gram positive cocci of clinical significance in wounds. *Journal of Applied Microbiology* **93**: 857-863.

Coussot, P., Lennov, A.I, and Piau, J.M. (1992). Rheological modeling and peculiar properties of some debris flow, Eurosin Debris flows and Environment in Mountain Regions. Proceedings of Chengdu symposium 234-239.

Da Costa, C.C, and Pereira, R.G. (2012). Rheological Analysis of Honey and Propolis Mixtures, 13th International Symposium on Food Rheology and Structure 435-436.

De la Funte, E., Sanz, M.L.,Martinez-Castro, I., J. and Ruiz-Matute, A.I. (2007). Volatile and carbohydrate composition of rare unifloral honeys from Spain. *Food Chemistry* **105**:84-93.

De laney, D.,and Reilly, M. (2000). A New Approach to Polymer Rheology for Process and Quality Control, *Kayeness Intruments*.

Dold, H., Du, D.H., and Dziaos, T (1937). Nachweis antibacterieller, hitze und Lichtempfind licher hemmungsstoffe (inhibine) in Naturhonig Blutechonig, *Z. Hyg. Infektion Skrankh* **120**: 155-167.

Downey, G., Hussey, K., Jelly, J.D., Walshe, T.F. and Martin, P.G. (2005). Preliminary contribution to the characterization of artisanal honey produced on the island of Ireland by palynological and physicochemical data. *Food chemistry* **91**:347-354.

Dreywood, R. (1946). Qualitative test for carbohydrate materials. *Industrial and Engineering Chemistry Analytical Edition* **18**:499-504.

Dustmann, J.H (1979): Antibacterial effect of honey. *Apiacta* **14**: 7-11.

Efem, S.E (1988): Clinical observations on the wound healing properties of honey. *British Journal of Surgery* **75**(7): 679-810.

Einstein, A., (1906): A new determination of molecular dimensions. *Analytical Physics***19**:289-306.

El-Bialee, N.M and Sorour, M.A. (2011). Effect of adulteration on honey properties. International Journal of Applied Sciences and Technology **1**(6) 122-133.

El-Bialee, N.M., Ramia, K., Ibrahim, A.M., El-Bialee, G., Harth, M.A., and Darwish, N.E.M. (2013). Discrimination of honey adulteration using Laser technique. *Australian Journal of Basic and Applied Sciences* 7(11):132-138.

Fan, Y., Jiang, W., and Zou, Y. (2009). Numerical Simulation of Pulsatile non-Newtonian flow in the Carotid bifurcation. Acta Mechanica **2**(25): 249-255.

Fallico, B., Zappala, M., Arena, E and Verzera, A. (2004). Effects of conditioning on HMF content in unifloral honeys. *Food Chemistry*, **85**:305–313.

Fernandez-Torres, R., Perez-Bernal, J.L., Bello-Lopez, M.A., Callejon-Mochon, M., Jimenez-Sanchez, J.C., and Guiraum-Perez, A. (2005). Mineral content and botanical origin of Spanish honeys. *Journal of Food Science* **2**(72):11-20.

Franck, A.J. (2004). *Understanding Rheology of Structured Fluids*. An Instrument Publication.

Food and Agriculture Organisation of United Nations Rome, 2012.

Genovese, D.B., Lozano, J.E and Roa, M.A. (2001). Rheology of colloidal and non-colloidal dispersions. Journal of Food Science **2**(72):11-20.

Green, A.E. (1988). Wound healing properties of honey. *British Journal of Surgery* **75**(12):1278

Gunther, R. T.(1959). *The Greek Herbal Dioscorides*. New Yoork: Hafner.

Havesteen, B.(1983). Flavonoids: Class of natural products of high pharmacological potency. *Journal of Biochemistry and Pharmacology* **32**: 1141-1148.

James,O.O., Mesubi, M.A.,Usman,.L.A., Yeye, S.O., Ajanaku.K.O.,Ogunniran.K.O., Ajani.O.O., and Siyanbola,T.O. (2009). Physical Characterisation of Some honey samples from North-Central Nigeria. *International Journal of Physical sciences* **4**(9):464-470.

Jeuring, J., and Kuppers, F. (1980). High performance Liquid chromatography of furfural and hydroxymethylfurfural in spirits and honey. *Journal of the Association of Official Analytical chemists* **63**:1215-1218.

Kalabova, K., Vorlova, L., Borkovcova, I., Smutna, M., and Vecerek, V. (2003). Hydroxylmethylfurfural in Czech honeys. *Czech Journal of Animal Science* **12**:551-557.

Kaskoniene, V., Venskutonis, P.R., and Ceksteryte, V. (2010). Carbohydrate composition and electrical conductivity of different origin honeys from Lithuania. *Food science and technology* **43**:801-807.

Kamal, A., Raza, S., Rashid, N., and Hameed, T. (2002). Comparative study of honey collected from different flora of Pakistan. *Online Journal of Biological Sciences* **2**(9):626-627.

Kavanagh, K.T., Calderon, L.E., Saman, D.M. and Abusalem, S.K. (2014). The use of surveillance and preventative measures for methicillin-resistant Staphylococcus aureus infections in surgical patients. *Antimicrobial Resistance and Infection Control* **3**(18):1-7.

Klevens, R.M., Morrison, M.A., Nadle, J., Petit, S., Gershman, K., Ray, S., Harrison, L.H., Lynfield, R., Dumyati, G., Townes, J.M., Craig, A.S., Zell, E.R., Fosheim, G.E., McDougal, L.K., Carey, R.B. and Fridkin, S.K. (2007). Invasive methicillin-resistant Staphylococcus aureus infectious in the United States. *Journal of the American Medical Association* **298**:1763.

Khonik. V.A. (2001). The kinetics of irreversible structural relaxation and rheological behaviour of metallic glasses under quasi-static loading. *Journal of Non-crystalline solids* **269**:147-157.

Kokuti, Z., Kokavecz. J., Czirakak. A., Holczer, I., Danyi, A., Gabor, Z., Szabo, G., Pezsa, N., Ailer, P., and Palkovics, L. (2011). Nonlinear viscosity and thixotropy of silicon fluid. *International Journal of Engineering* **2**:177-180.

Kurzbeck, S., Oster, F., Mu¨nstedt, H., Nguyen, T.Q., and Gensler, R., (1999). Rheological properties of two polypropylenes with different molecular structure. *Journal of Rheology* ***43***:359–374.

Latorre, M.J., Pena, R., Pita, C., Botana, A., Galcia, S., Herrero, C. (1999). Chemomeric classification of honeys according to their type.II. metal content data. *Food chemistry* **66**:263-268.

Launay, B., Doublier, J. R., and Cuvelier, G. (1986). Flow properties of aqueous solutions and dispersions of polysaccharides. In J. R. Mitchell & D. A. Ledward (Eds.), Functional properties of food macromolecules 1–78. London: *Elsevier Applied Science*.

Lawal, R.A., Lawal, A.K., and Adekalu, J.B. (2009). Physico-chemical studies on adulteration of honey in Nigeria. *Pakistan Journal of Biosciences* **12**(15):1080-1084.

Lazaridou, A., Biliaderis C.G., Bacandritsos, N., Sabatini, A.G. (2004). Composition, thermal and rheological behaviour of selected Greek Honeys. *Journal of Food Engineering* **64**:9-21.

Lemarchand, C.A., Bailey, N.P.,Todd, B.D , Daivis, P.J and Hansen, J.S.(2015). Non-Newtonian behaviour and molecular structure of cooee bitumen under shear flow: a non-equilibrium molecular dynamic study. Physics.chem-ph.

Lewkowski, J. (2001). Synthesis, chemistry and applications of 5-hydroxymethylfurfural and its derivatives. *ARKIVOC Journal*. **1**:17-54.

Makawi SZA ,Taha MI, Zakaria BA, Siddig B, Mahmod H, Elhussein AR, Elrasheed AGK (2009). Identification and Quantification of 5- Hydroxymethyl Furfural HMF in Some Sugar-Containing Food Products by HPLC. *Pakistan Journal of Nutrition* **8**:1391-1396.

Molan, P.C. (1992). The Antibacterial activity of honey: The nature of the antibacterial activity. *Bee world* **73**(1): 5-8.

Molan, P.C. (2001). Potential of honey in the treatment of wounds and burns. *American Journal of Clinical Dermatology* **2**(1)13-19.

Morrison, F.A. (1999). Using the solver Add-in in Microsoft Excel.www.google.com/rheological modeling.

Mullai, V. and Menon, T. (2007). Bactericidal activity of different types of honey against clinical and environmental isolates of Pseudomonas aeruginosa. Journal *of Alternate Complementary Medicine* **13**:439-441.

Nazarian, H., Taghavizad, R., and Majid, A. (2010). Origin of honey proteins and method for its quality control. *Pakistan Journal of Botany* **42**(5):3221-3228.

Ndip, R. N.,Takang, E.A.M., Echakachi, C.M., Malongue, A. , Akoachere, J.T.K. ,Ndip,L.M., and Luma, H.N. (2007). In-vitro antimicrobial activity of selected honeys on clinical isolates of Helicobacter pylori. *African Health Science*. **7** (4):228-232.

Nguyen, Q. D., Jensen, C. T. B., and Kristensen, P. G. (1998). Experimental and modelling studies of the ow properties of maize and waxy starch pastes. Chemical Engineering Journal, **70**, 165–171.

Nozal, M.J.D., Bernal, J L., Marinero, P., Diego, J.C, Frechilla, J.I., Higes, M., Llorente, J. (1998). High performance liquid chromatographic determination of organic acids in honey from different botanical origin. Journal *of Liquid Chromatography and Related Technologies* **21**(20): 3197-3214.

Nwalor, J.U, Babalola, F.U & Anidiobu, V.O .(2014,July 15). *Rheological Characterization of Honey: Application as an Index of Quality.* In P. Scales & P. Ranganthan (Eds.), Abstract Proceedings of the 6th Pacific Rim Conference on Rheology 211-212. Melbourne, Australia.

Odeyemi, A.T., Odefemi, S.O., and Adebayo, A.A. (2013). Antimicrobial and Proximate properties of some processed honey in Ado-Ekiti. *International Journal of Aquatic Science* **1**(4): 36-43.

Owayss, A.A., (2005). Physicochemical analysis for standardizing quality criteria of Libyan (Eucalyptus sp.) honey. *Egypt Journal of Applied Science* **20** (6A):247-255.

Pisani, A., Protano, G., and Riccobono, F. (2008). Minor and trace elements in different honey types produced in Siena County (Italy). *Food Chemistry* **107**:1553-1560.

Quemada, D. (1998). Rheological modeling of complex fluids: The concept of effective volume revisited. *The European Journal of Applied Physics* **1**:119-127.

Razavi, S.M.A., Taghizadeh, M., and Ardekani, S. (2010). Modeling the time dependent rheological properties of Pistachio butter. *International Journal of Nuts Related Sciences.* **1**(1):41-48.

Rehman, S.U., Khan, Z.F., and Maqbool, T. (2008). Physical and spectroscopic characterisation of Pakistani honey. *Crecia e Investigacion Agreria* **35**(2):199-204.

Revanasiddappa, H. D., and Veena, M. A. (2008). Sensitive spectrophotometric methods for the determination of ascorbic acid. *E-Journal of Chemistry* **1**(5):10-15,

Roa, M.A. (1997). Rheology of liquid foods: a review. *Journal of Texture Studies* **8**:135-168.

Rao, M.A., and Steffe, J.F. (1992). Measurement of Viscoelastic properties of fluid and semisolid Foods, in ‘‘Viscoelastic properties of food,’’, 207-232, Elsevier Applied Science Publishers, New York.

Rao, M.A. (2006*).* Influence of Food Microstructure on Food Rheology, in understanding and controlling the microstructure of complex foods, ed. D.J. McClements, Woodhead publishing Ltd., Cambridge, U.K.

Rao, M. A. (2014).Rheology of Fluid, Semisolid, and Solid Foods, Food Engineering Series, Springer Science, Business Media New York .

Sabato, S.F. (2004). Rheology of irradiated honey from Parana region. *Radiation Physics and Chemistry.* **71**:99-102.

Saissy, J. M., Guignar, B., Pats, B., Guiavarch, M, and Rouvier, B.(1995).Pulmonary edema after hydrogen peroxide irrigation of a war wound. *Intensive care Medical Journal* **21**(3): 287-288

Salahudeen, A.K., Clark, E.C., Nath, K.A. (1991). Hydrogen peroxide-induced renal injury: A protective role for pyruvate in vitro and in vivo. *Journal of Clinical Investigation* **88**(6): 1886-1893.

Staudinger, H.and Heuer, W., (1930) High Polymeric Compounds, 33. Announcement: Relationship between viscosity and molecular weight in polysterols.Ber. Disch. Ges **63**:222-234.

Steffe, J.F. (1996). *Rheological Methods in Food Process Engineering* 2nd ed. ISBN 0-9632036-1-4.

Story, P.J. (1953). *Principles of polymer chemistry*. Cornel University Press, Ithca, New York 24-45.

Sopade, P.A., Halley, P.J., D'Arcy, B.R., Bhandari, B., and Caffin, N. (2004). Dynamic and steady-state rheology of Australian honeys at subzero temperatures. *Journal of Food Process Engineering* **27**:284-309.

Sunthar, P. (2008). Polymer Rheology. Department of Chemical Engineering, Indian Institute of Technology (IIT) Bombay, Mumbai 400076 India. (www.google/polymerheology.com).

Triantafillopoulos, N. (1988). Measurement of Fluid Rheology and Interpretation of Rheograms second edition. Kaltech Scientific, Inc. 22425 Heslip Drive Novi, Michigan 48375 USA.

Turian, R.M., and Bird, R.B. (1963). Viscous heating in the cone-and-plate viscometer.2. Newtonian fluids with temperature-dependent viscosity and thermal conductivity. *Chemical Engineering Science* **18**(11):689-696.

Tuzen, M., and Soylak, M. (2005). Trace metal level in microwave digested honey samples from Middle Anatolia, Turkey. J. Food Drug Analysis **13**(14) 344-347.

Venugopal, K.N., and Abhilash, M. (2010). Study of hydration kinetics and rheological behaviour of guar gum. *International Journal of Pharmaceutical Sciences and Research* **1**(1):28-39.

Von Der Ohe, W., Dustmann, J.H., and Von Der Ohe, K. (1991). Prolin als Kriterium der Reif des Honigs. Deutsche Lebensmittel-Rundschau **87**(12):383-386.

White, J.W. Jr. (1992). Quality evaluation of honey: Role of HMF and diastase assays. *American Bee Journal* **132** (11 & 12):737-743, 792-794.

White, J.W.,(1975). "Physical characteristics of Honey"in: Honey A Comprehensive Survey (Ed. Crane E);Heinemann, London 207-239.

White. J.W.(1979). Spectrophotometric Method for Hydroxymethylfurfural in Honey, *Journal Association Of Analytical Chemistry* **62**: 509.

Winkler,O.(1955) Beitrag zum Nachweis und zur Bestimmung von Oxymethylfurfural in Honig und Kunsthonig. Z.Lebensm.Unters.Forsch **102**: 160-167.

Witczak, M., Jus zczak, L., and Gałko wska, D. (2011). Non-Newtonian behaviour of heather honey. *Journal of Food Engineering* **104**:532–537.

Yasuda, K. (1979). *Investigation of the analogies between viscometric and linear viscoelastic properties of polystyrene fluids*. Ph.D. thesis, Massachusetts Institute of Technology, Department of Chemical Engineering.

Yung-Yi, L. (1974). *Coal Tar Autoxidation Kinetic Studies by viscometric and refractometric methods*. Ph.D.Thesis, University of Utah, Department of Mining, Metallurgical and Fuel Engineering.

Zappala M, Fallico B, Arena E, Verzera A (2005). Methods for the determination of HMF in honey: A comparison. *Food Control* **16**:273-277.

APPENDICES

APPENDIX 1

POWER LAW CURVE FIT TO SAMPLE RHEOGRAMS

The rheological parameters of PLM in chapter three were extracted using the least square method.

The principles and details of the calculations are shown below.

Least Square Models

For two variables: $Y = bX + C$ (A1.1)

At a point on a plot of (A1.1), $X=Xi$, $Y= Yi$, we have, $Y=a + bXi$. The difference between two points in the line gives: $Yi-a-bXi$. Therefore, the sum of square of these differences for all n such points is given by:

$$S = \sum_{i=k}^{n}(Y = a + bXi)^2$$

We have to determine the values of a and b so that S shall be minimum. The right hand side contains two unknowns a and b. Therefore, for the sum of squares to be minimum

$$\frac{\partial S}{\partial a} = 0 \text{ and } \frac{\partial S}{\partial b} = 0$$

$$\frac{\partial S}{\partial a} = -2\sum_{i=k}^{n}(Yi - a - bXi) = 0, \quad \frac{\partial S}{\partial b} = -2\sum_{i=k}^{n} Xi(Yi - a - bXi) = 0$$

The first gives:

$$\sum_{i=1}^{n} Yi = na + b\sum_{i=1}^{n} Xi \quad \text{(A1.2)}$$

The second gives:

$$\sum_{i=1}^{n} XiYi = a\sum_{i=1}^{n} Xi + b\sum_{i=1}^{n} Xi^2 \quad \text{(A1.3)}$$

For Three parameter Variables:

$$Yi=a + a_1X_{ij} + a_2 X_{2j} \quad \text{(A1.4)}$$

$$\sum_{i=1}^{n} Yi = na_o + a_1\sum_{i=1}^{n} X_{1j} + a_2\sum_{i=1}^{n} X_{2j} \quad \text{(A1.5)}$$

$$\sum_{i=1}^{n} YiXj = a_o \sum_{i=1}^{n} X_{ij} + a_1 \sum_{i=1}^{n} X_{ij}^{\ 2} + a_2 \sum_{i=1}^{n} X_{ij} X_{2j} \quad \text{(A1.6)}$$

$$\sum_{i=1}^{n} Y_1 X_2 = a_o \sum_{i=1}^{n} X_{2j} + a_1 \sum_{i=1}^{n} X_{ij} X_{2j} + a_2 \sum_{i=1}^{n} X^2{}_{2j} \quad \text{(A1.7)}$$

When the PLM is linearised in the form of equation (A1.1), equations (A1.2) and (A1.3) can be used to obtain the parameters using the least square method.

Table A1.1. PLM Curve Fit of Sample A1 at 27°C

S/N	η(mMPa.s)	(1/S)	Y=Lnη	X=Ln	XY	X^2
1.	5568	0.122	8.624791	-2.10373	-18.1443	4.425698
2.	6048	0.245	8.707483	-1.4065	-12.247	1.978234
3.	4352	0.367	8.378391	-1.00239	-8.39844	1.004793
4.	3264	0.489	8.090709	-0.71539	-5.78803	0.511787
5.	2611	0.612	7.867489	-0.49102	-3.86312	0.241104
6.	2176	0.734	7.685244	-0.30925	-2.37663	0.095633
7.	1865	0.856	7.531016	-0.15548	-1.17096	0.024176
8.	1632	0.978	7.397562	-0.02225	-0.16456	0.000495
9.	1451	1.100	7.280008	0.09531	0.693859	0.009084
10.	1306	1.220	7.174724	0.198851	1.4267	0.039542
SUM			78.73742	-5.91186	-50.0325	8.330544

Applying equations (A1.2) and (A1.3) we have the following

$$78.73742 = 10a - 5.91186b \quad \text{(A1.8)}$$

$$-50.0325 = -5.91186\,a + 8.33054b \quad \text{(A1.9)}$$

the results of simultaneous equations (A1.8) and (A1.9) were obtained as follows:

a=7.44779 and b= -0.7205

$Ln\ \eta$ = 7.44779, Taking the exponential of both sides of the equations,

$$e^{Ln\,\eta} = e^{7.44779}$$

Therefore, η = 1716.066 mPa.s

Likewise, $b = n-1 = -0.7205$

$n = 0.2795$

Using the values of n and η above, the curve fit in figure 16 was obtained.

Table A1.2. PLM Curve Fit of Sample A1 at 35°C

S/N	η(MPa.s)	(1/S)	Y=Lnη	X=Ln	XY	X^2
1.	1560	0.122	7.352441	-2.10373	-15.4676	4.425698
2.	1478	0.245	7.298445	-1.4065	-10.2652	1.978234
3.	1301	0.367	7.170888	-1.00239	-7.18805	1.004793
4.	1275	0.489	7.150701	-0.71539	-5.11556	0.511787
5.	1109	0.612	7.011214	-0.49102	-3.44267	0.241104
6.	988	0.734	6.895683	-0.30925	-2.13246	0.095633
7.	845	0.856	6.739337	-0.15548	-1.04787	0.024176
8.	799	0.978	6.683361	-0.02225	-0.14868	0.000495
9.	712	1.1	6.568078	0.09531	0.626005	0.009084
10.	625	1.22	6.437752	0.198851	1.280152	0.039542
11.	522	2.45	6.257668	0.896088	5.607421	0.802974
SUM			75.56557	-5.01577	-37.2945	9.133518

Applying equations (A1.2) and (A1.3) we have the following

$$75.56557 = 11a - 5.01577b \quad \text{(A1.10)}$$

$$-37.2945 = -5.01577\,a + 9.133518b \quad \text{(A1.11)}$$

a=6.6806 and b= -0.4145

$Ln\ \eta = 6.6806$, Taking the exponential of both sides of the equations,

$$e^{Ln\,\eta} = e^{6.6806}$$

Therefore, $\eta = 796.7970$ mPa.s

Likewise, $b = n-1 = -0.4145$

$n = 0.5855$

Using the values of n and η above, the curve fit in figure 17 was obtained.

SUMMARY ON POWER LAW CURVE FIT TO SAMPLE RHEOGRAMS

PLM followed the rheological signature of pure honey, but necessarily devoid of low shear rate characteristic turning point at the inception of deformation. The model parameters reflected the serial dilution of honey with sucrose and can be said to be a good tracker of adulteration and imitation in honey. Least square method was used to extract the parameters of PLM. The sum of square errors of the analyses generally increased with increasing adulteration of honey. This model having two parameters experience difficulties in following the rheograms of some samples but serves as a good initial guess to use in Carreau-Yasuda model curve fit.

APPENDIX 2

2.1 STRUCTURAL KINETIC MODEL CURVE FITS TO SAMPLE RHEOGRAMS

The SKM was used in this section to extract the data on structure and composition of samples. The data were obtained at constant shear rate over variable time.

The SKM is given as follows:

$$\eta = \eta_\infty + (KM^A - \eta_\infty)\left[kt\ (n-1)+1\right]^{1/1-n} \tag{3.11}$$

If the molecular weight, Mark-Houwink constants are replaced with zero shear viscosity we have:

$$\left(\frac{\eta-\eta_\infty}{\eta_o-\eta_\infty}\right)^{1-n} - 1 = tk(n-1) \tag{B1.1}$$

For the structural kinetic model, time resolved data on fluids' apparent viscosities at given constant rates of shear were extrapolated to zero times to obtain the zero shear viscosities. The zero shear (zero time) viscosity was applied in Mark-Houwink equation to obtain the fluid's molecular weight at each shear rate. The average molecular weight was then determined for all shear rates studied. Since this work was done at low rates of shear, the fluid might not have deformed long enough to give values of the infinite time viscosity for the calculation of rate of deformation, k (see also section 3.3.4). From equation (6.1), the rate of deformation (k) is obtained explicitly from:

$$k = \left\{\left[(\eta-\eta_\infty)/(\eta_o-\eta_\infty)\right]^{1-n} - 1\right\}\ /t(n-1) \tag{3.14}$$

Also, if Γ is defined by, $\Gamma = \left(\frac{\eta-\eta_\infty}{\eta_o-\eta_\infty}\right)^{1-n}$ (4.2)

Then $\Gamma = tk(n-1)+1$ (4.3)

Since k is expected to depend only on rate of shear rate (Abu-djayil, 2003) a scheme was developed by which an optimized value of k was determined for each rate of shear. The scheme associates optimum k with the set of parameters that yielded the least coefficient of variation. This coefficient of variation or relative standard deviation (RSD) is the standard deviation of k divided by its mean value calculated from the six different times of the experimental determination of apparent viscosities (10s, 20s, 30s, 40s, 50s and 60s). This value of k and the set of the other parameters that produced it are deemed as the parameters of the model and were found to also give the best fit, following equation (4.3), to Γ versus t data (see sections 3.3.4 and 4.1.6). The details of the calculations are given below:

Sample A4 at Shear rate of 0.01(s^{-1})

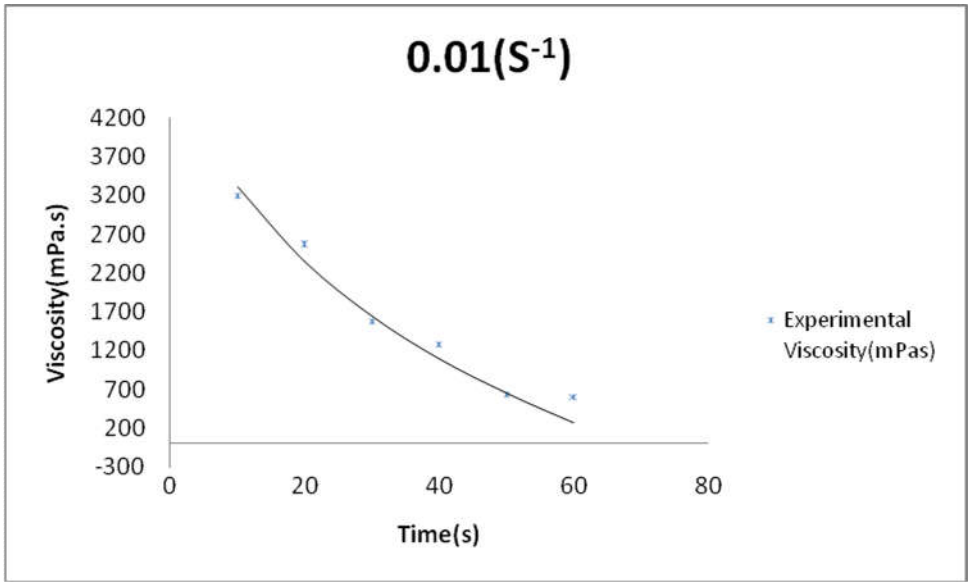

Figure A-1 Viscosity time graph of Sample A4 at shear rate of 0.01(S-1)

From the curve, η = 4422.49161

From equation (1.3), $\eta_o = KM^A$

$$\left(\frac{\eta_o}{k}\right)^{1/A} = M$$

Taking A=0.5635 and K= 165

M= 342.3626 g/mol

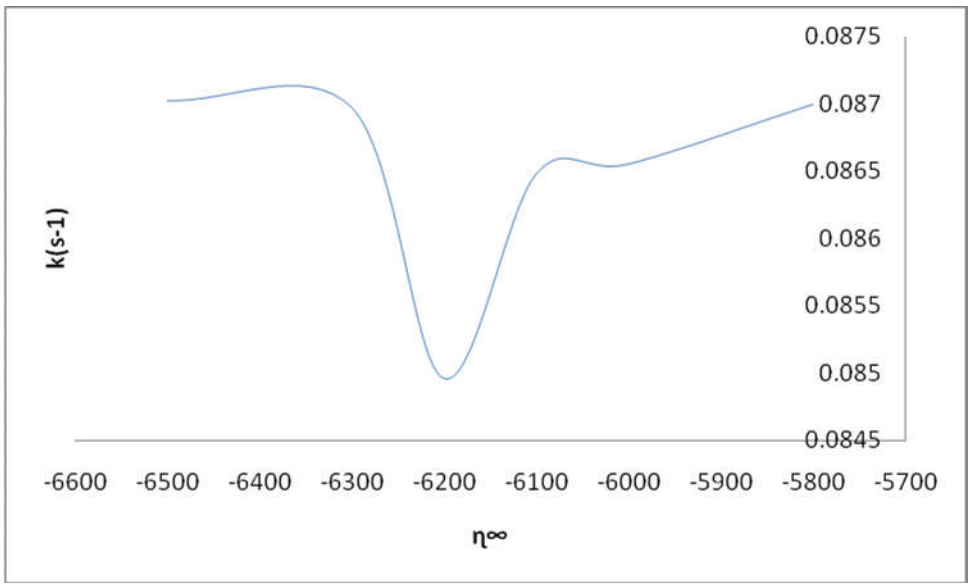

Figure A-2 Optimisation of *k* for Sample A4 at shear rate of 0.01(s^{-1})

From Figure A-2 above, the infinite time viscosity, η_∞, was found to be -6200mPa.s.

From equation (3.17):

$$\text{Let } \Gamma = \left(\frac{\eta - \eta_\infty}{\eta_o - \eta_\infty}\right)^{1-n} \tag{4.2}$$

$$\text{Therefore } \Gamma = tk(n-1)+1 \tag{4.3}$$

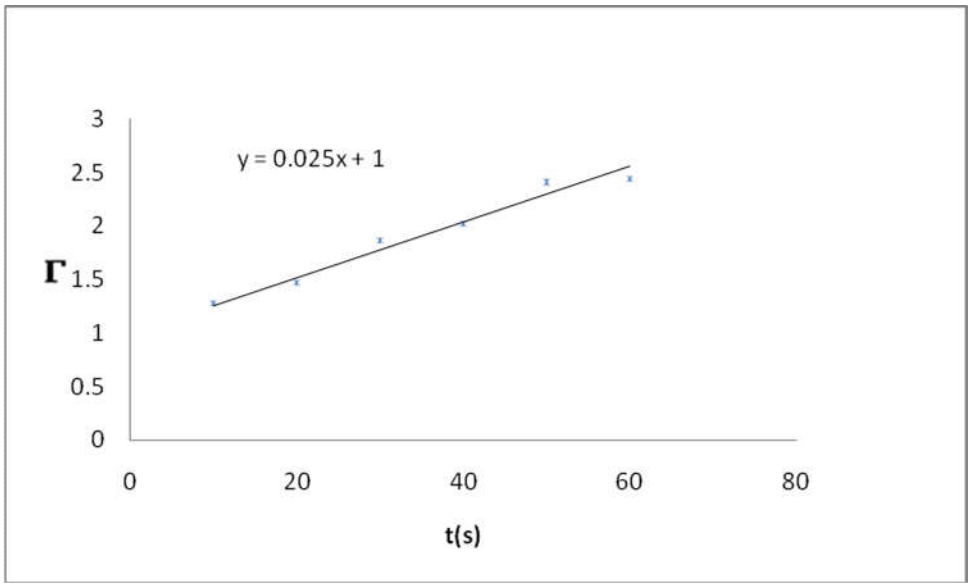

A3- Plot of Γ against t at shear rate of 0.01s^{-1}

From the slope of Figure A3, $0.025 = k(n-1)$. When n=3, then k=0.0125 s^{-1}

At Shear Rate of 0.02 (s^{-1})

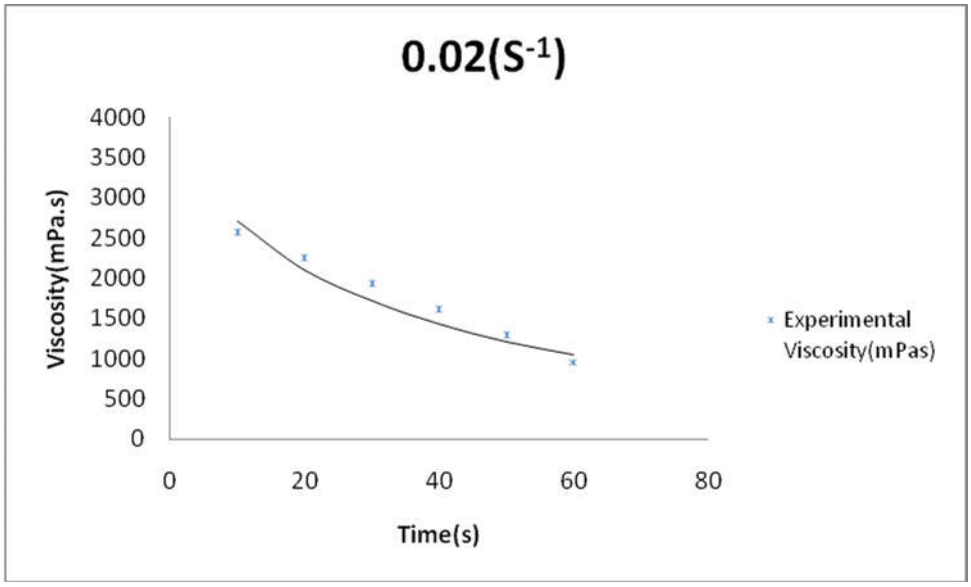

Figure A4-Viscosity time graph of Sample A4 at Shear rate of 0.02 s^{-1}

From the curve, η = 3662.8081

From equation (1.3), $\eta_o = KM^A$

$$\left(\frac{\eta_o}{K}\right)^{1/A} = M$$

Taking A=0.5635 and *K*= 165

M= 245.0352g/mol

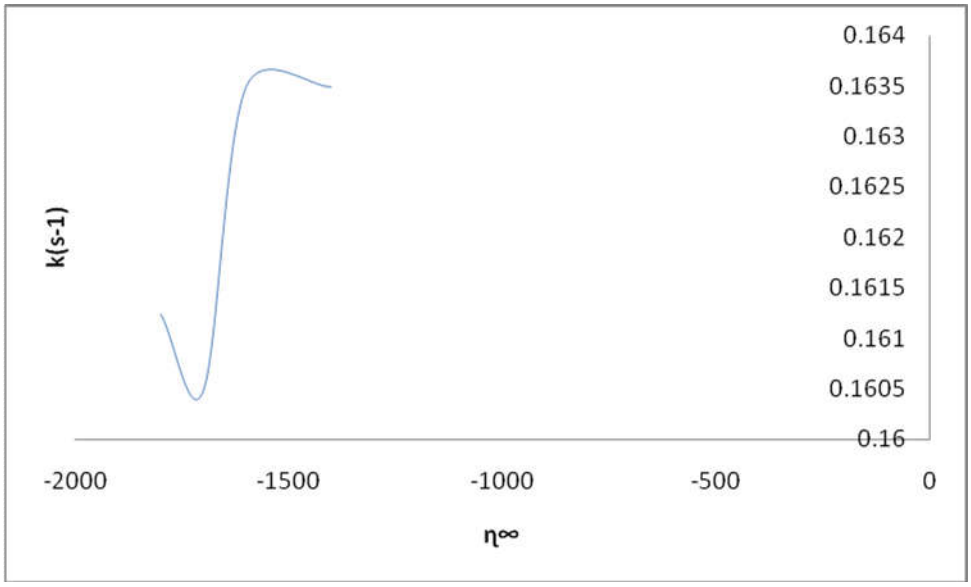

Figure A-5 Optimisation of k for Sample A4 at shear rate of 0.02(s^{-1})

From Figure A-2 above, the infinite time viscosity, η_∞,was found to be -1700 mPa.s.

From equation (3.17):

$$\text{Let } \Gamma = \left(\frac{\eta - \eta_\infty}{\eta_o - \eta_\infty}\right)^{1-n} \tag{4.2}$$

$$\text{Therefore } \Gamma = tk(n-1)+1 \tag{4.3}$$

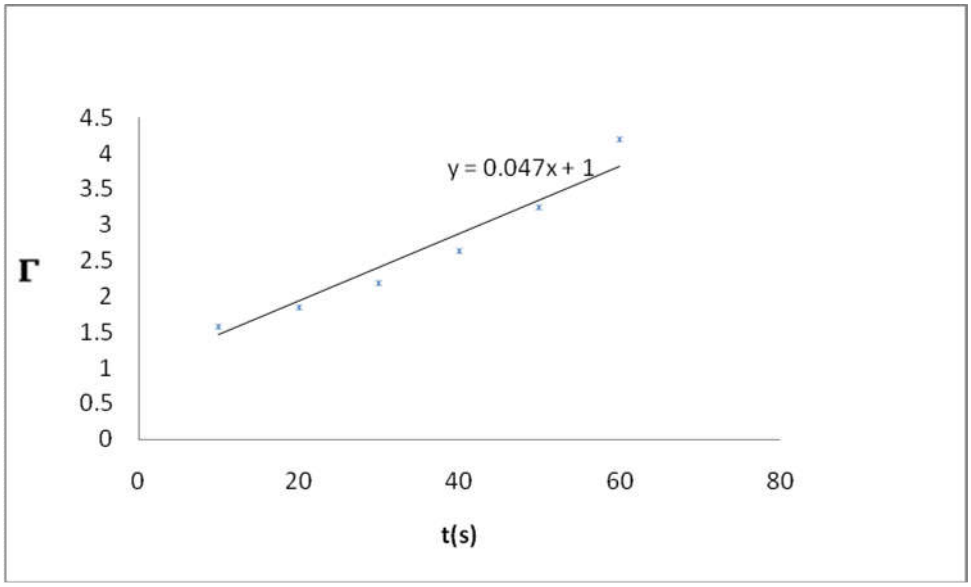

A6- Plot of Γ against t at shear rate of 0.02s-1

From the slope of Figure A6, $0.047 = k(n-1)$. When n=3, then k=0.0235 s^{-1}

At Shear Rate of 0.03 (s^{-1})

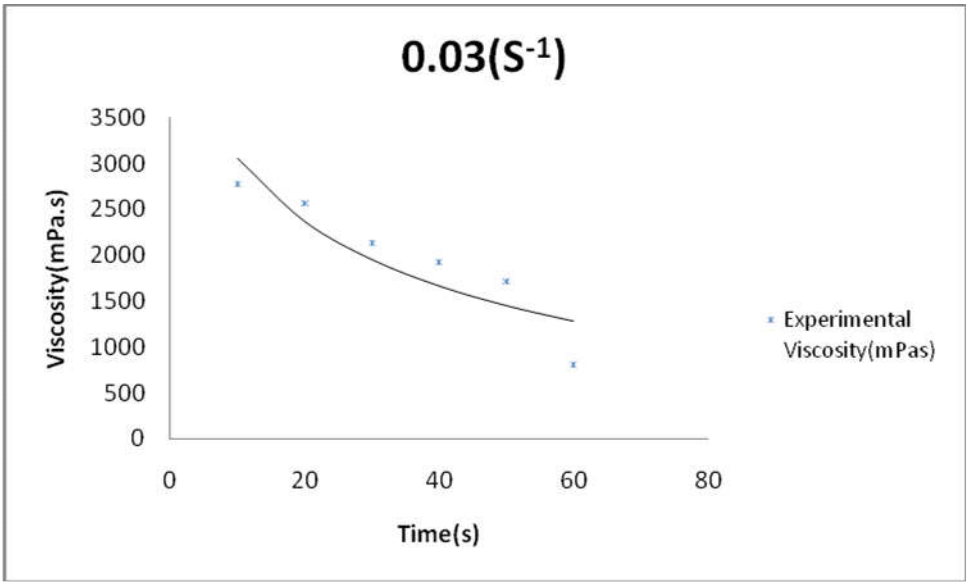

Figure A7-Viscosity time graph of Sample A4 at Shear rate of 0.03S-1

Therefore η = 4329.2921

From equation (1.3), $\eta_o = KM^A$

$$\left(\frac{\eta_o}{k}\right)^{1/A} = M$$

Taking A=0.5635 and *K*= 165

M= 329.6635g/mol

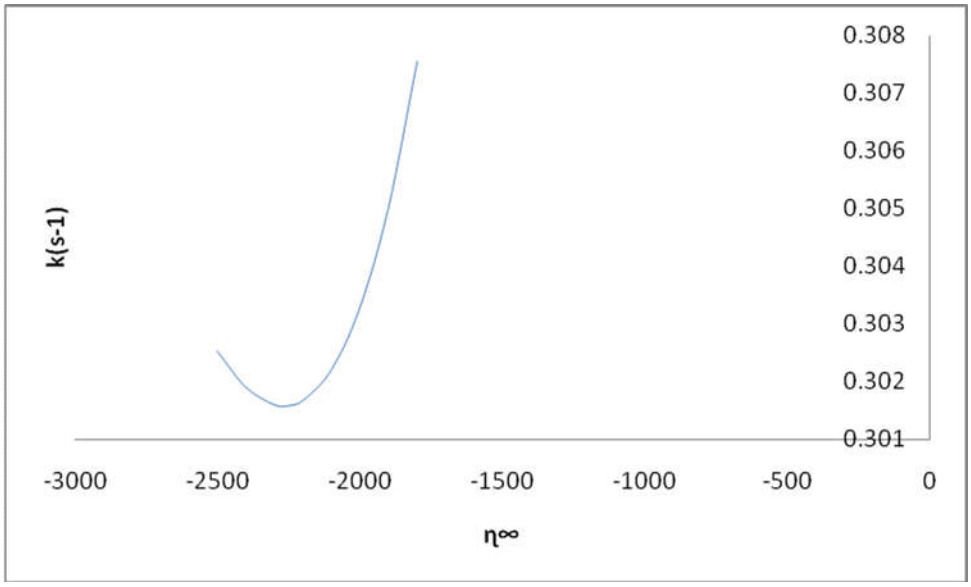

Figure A-8 Optimisation of k for Sample A4 at shear rate of 0.03(s^{-1})

From Figure A-8 above, the infinite time viscosity, η_∞,was found to be -2250 mPa.s.

From equation (3.17):

$$\text{Let } \Gamma = \left(\frac{\eta - \eta_\infty}{\eta_o - \eta_\infty}\right)^{1-n} \tag{4.2}$$

$$\text{Therefore } \Gamma = tk(n-1)+1 \tag{4.3}$$

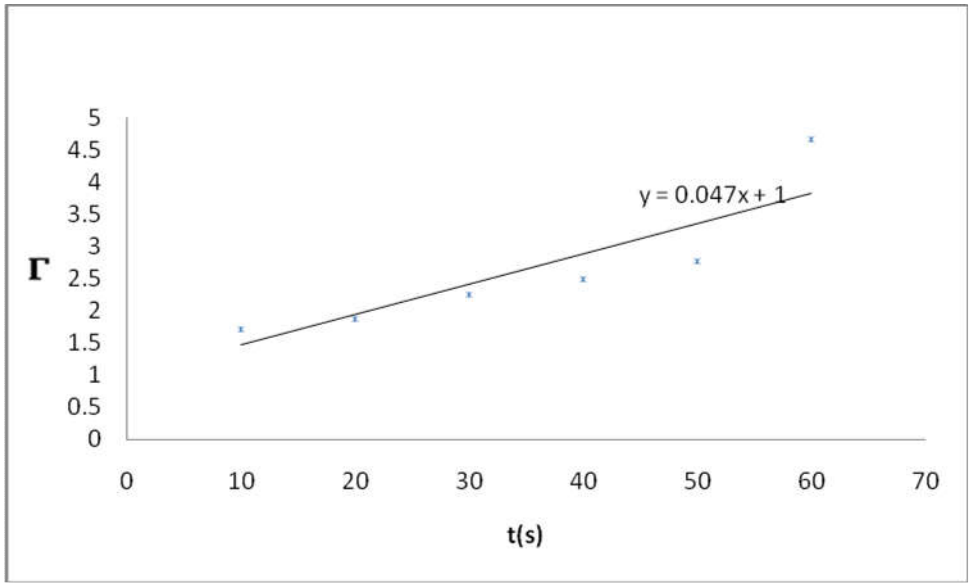

A9- Plot of Γ against t at shear rate of 0.03s^{-1}

From the slope of Figure A9, $0.047 = k(n-1)$. When n=3, then k=0.0235 s^{-1}

At Shear Rate of 0.04 (s^{-1})

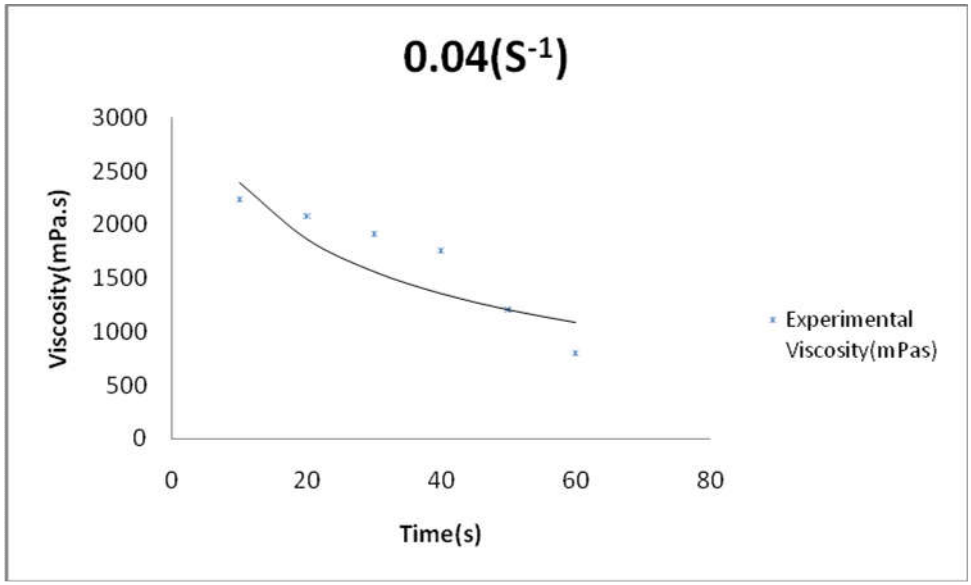

Figure A10-Viscosity time graph of Sample A4 at Shear rate of 0.04s^{-1}

Therefore η = 3669.97135

From equation (1.3), $\eta_o = KM^A$

$$\left(\frac{\eta_o}{k}\right)^{1/A} = M$$

Taking A=0.5635 and *K*= 165

M= 245.8862g/mol

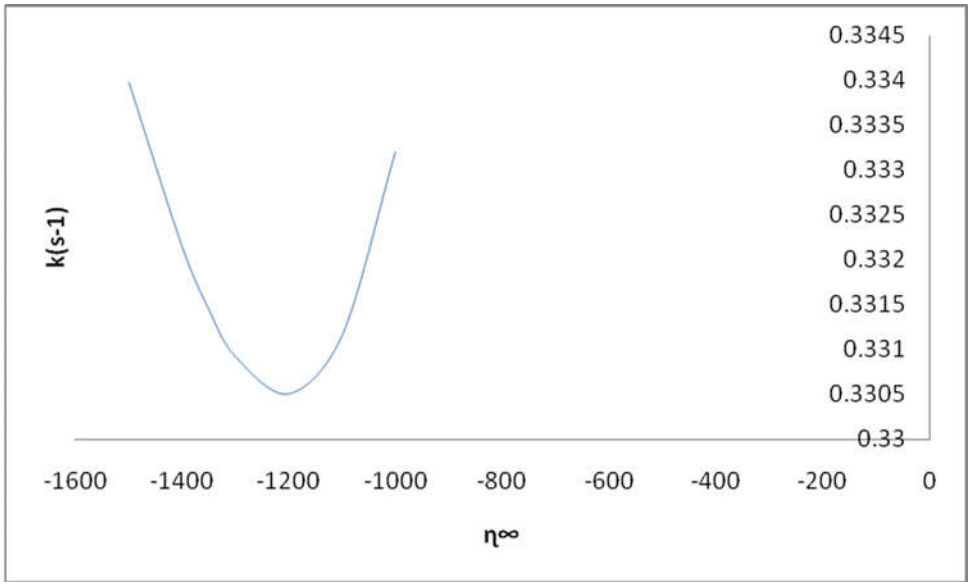

Figure A-11 Optimisation of k for Sample A4 at shear rate of 0.04(s^{-1})

From Figure A-2 above, the infinite time viscosity, η_∞,was found to be -1200 mPa.s.

From equation (3.17), let

$$\text{Let } \Gamma = \left(\frac{\eta - \eta_\infty}{\eta_o - \eta_\infty}\right)^{1-n} \tag{4.2}$$

$$\text{Therefore } \Gamma = tk(n-1)+1 \tag{4.3}$$

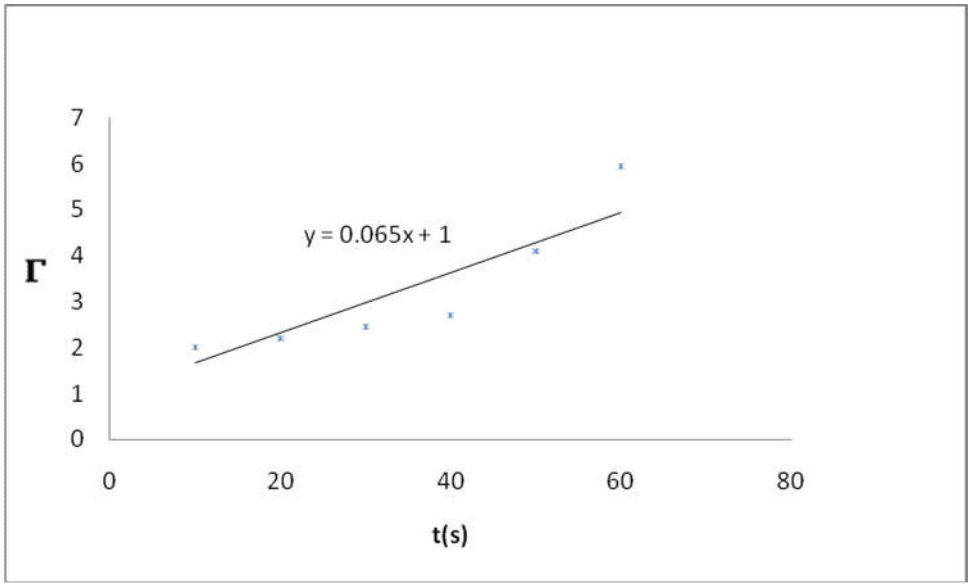

A12- Plot of Γ against t at shear rate of 0.04s^{-1}

From the slope of Figure A3, $0.065 = k(n-1)$. When n=3, then k=0.0325s^{-1}

At Shear Rate of 0.05 (s^{-1})

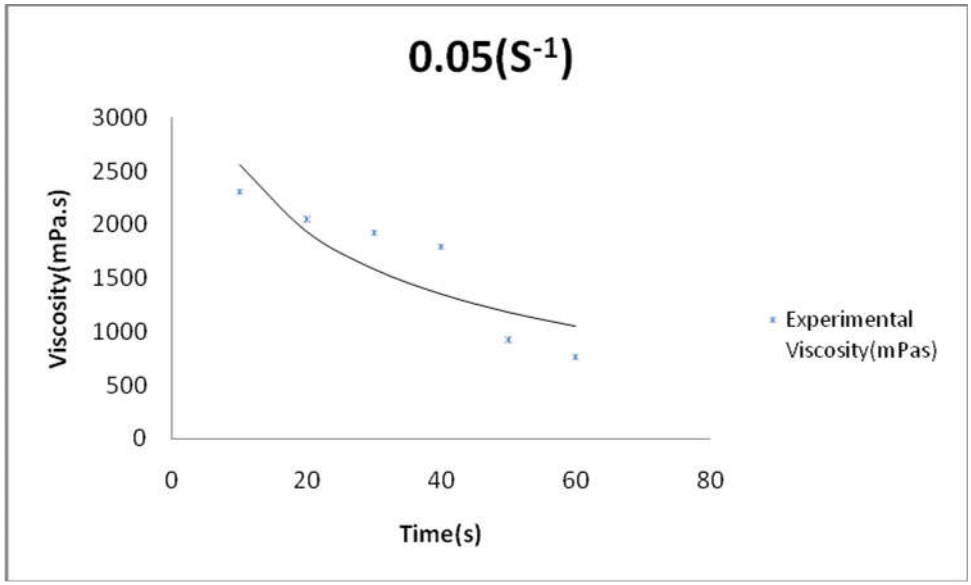

Figure A13-Viscosity time graph of Sample A4 at Shear rate of 0.05s^{-1}

Therefore η = 4102.323189

From equation (1.3), $\eta_o = KM^A$

$$\left(\frac{\eta_o}{k}\right)^{1/A} = M$$

Taking A=0.5635 and *K*= 165

M= 299.6179g/mol

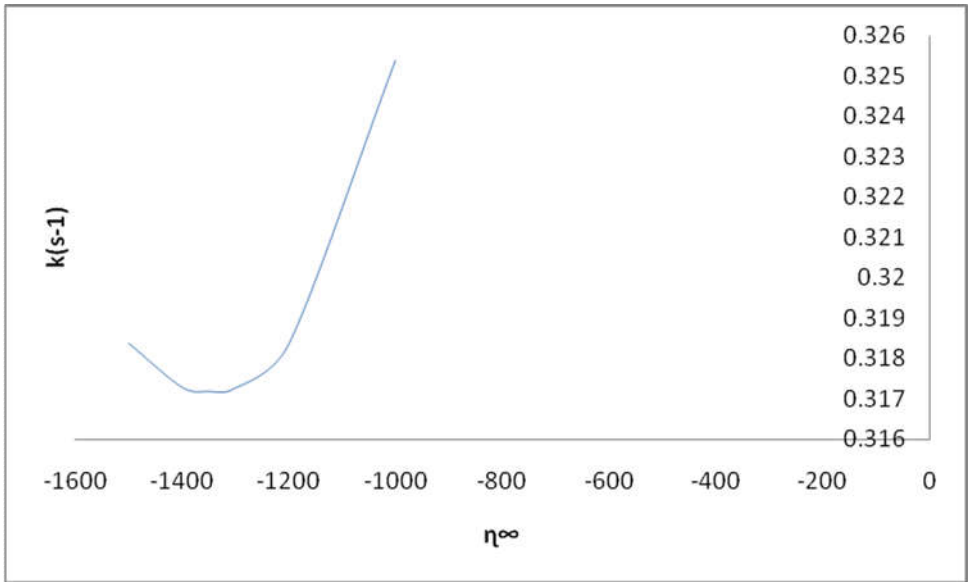

Figure A-14 Optimisation of k for Sample A4 at shear rate of 0.05(s^{-1})

From Figure A-14 above, the infinite time viscosity, η_∞,was found to be -1350 mPa.s.

From equation (3.17):

$$\text{Let } \Gamma = \left(\frac{\eta - \eta_\infty}{\eta_o - \eta_\infty}\right)^{1-n} \tag{4.2}$$

$$\text{Therefore } \Gamma = tk(n-1)+1 \tag{4.3}$$

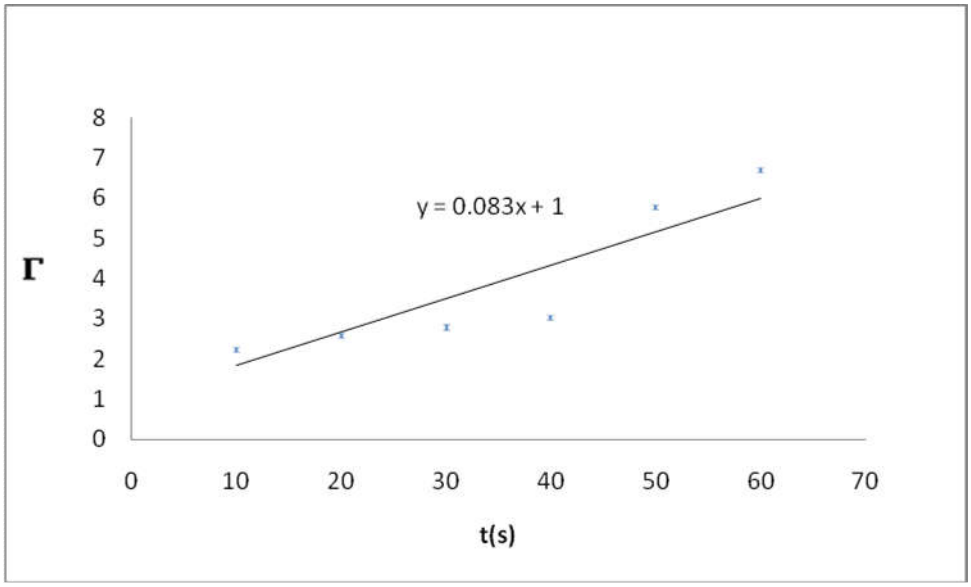

B15- Plot of Γ against t at shear rate of 0.05s^{-1}

From the slope of Figure A15, $0.083 = k(n-1)$. When n=3, then k=0.0415S-1

At Shear Rate of 0.06(s-1)

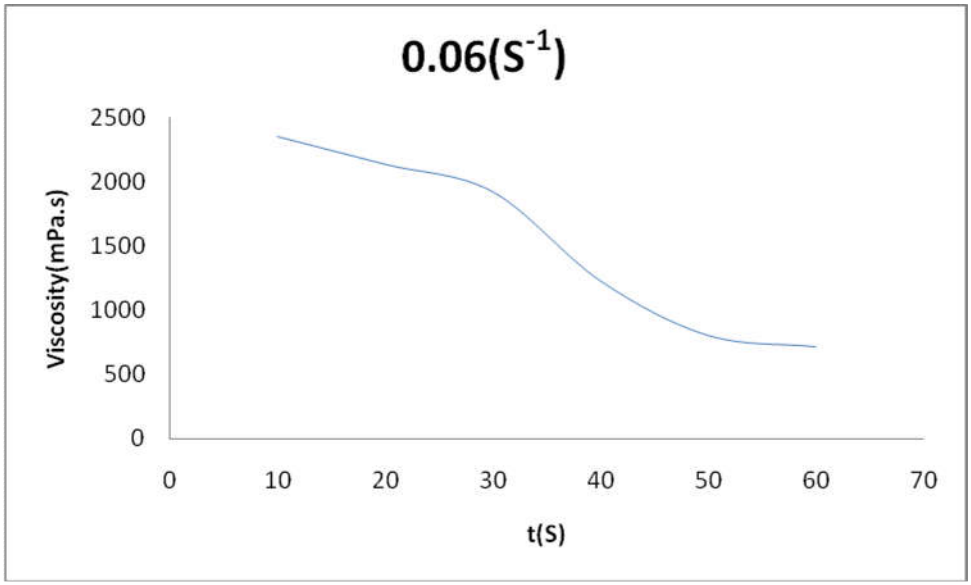

Figure A16-Viscosity time graph of Sample A4 at Shear rate of 0.06s-1

Therefore η = 4683.402

From equation (1.3), $\eta_o = KM^A$

$$\left(\frac{\eta_o}{k}\right)^{1/A} = M$$

Taking A=0.5635 and *K*= 165

M= 379.0221g/mol

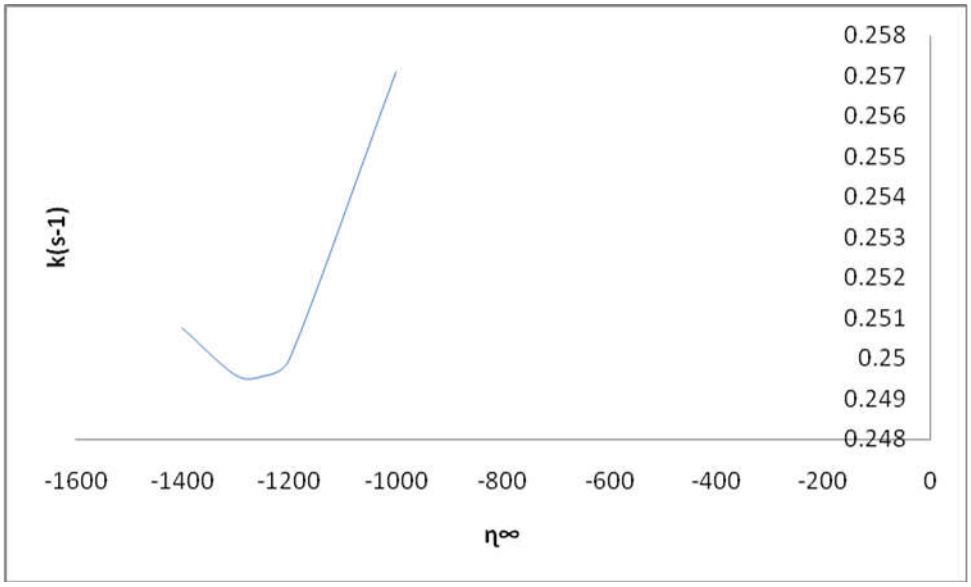

From Figure A-17 above, the infinite time viscosity, η_∞,was found to be -1300 mPa.s.

From equation (3.17), let

$$\text{Let } \Gamma = \left(\frac{\eta - \eta_\infty}{\eta_o - \eta_\infty}\right)^{1-n} \tag{4.2}$$

$$\text{Therefore } \Gamma = tk(n-1)+1 \tag{4.3}$$

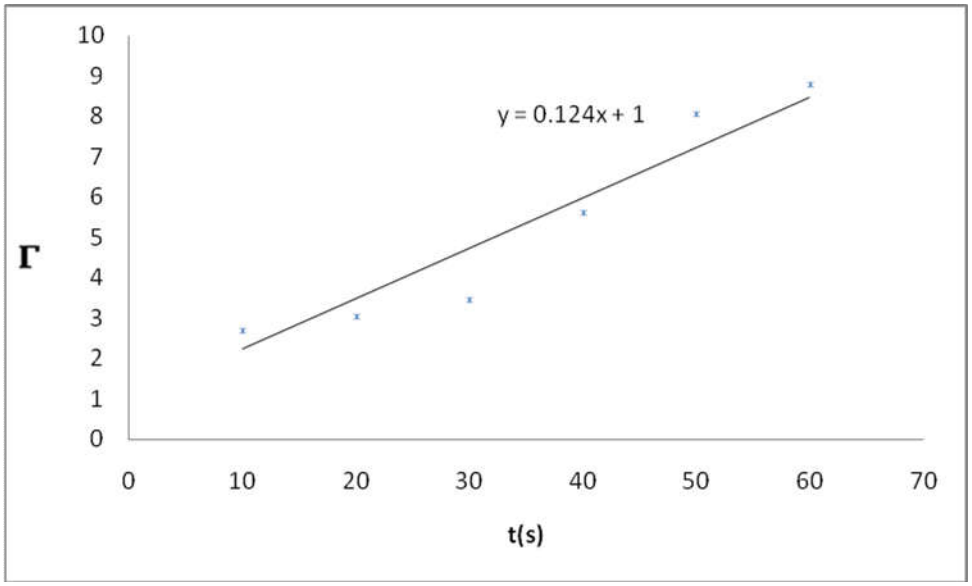

A18- Plot of Γ against t at shear rate of 0.06s s^{-1}

From the slope of Figure A18, $0.124 = k(n-1)$. When n=3, then k=0.062s^{-1}

At Shear Rate of 0.07(s^{-1})

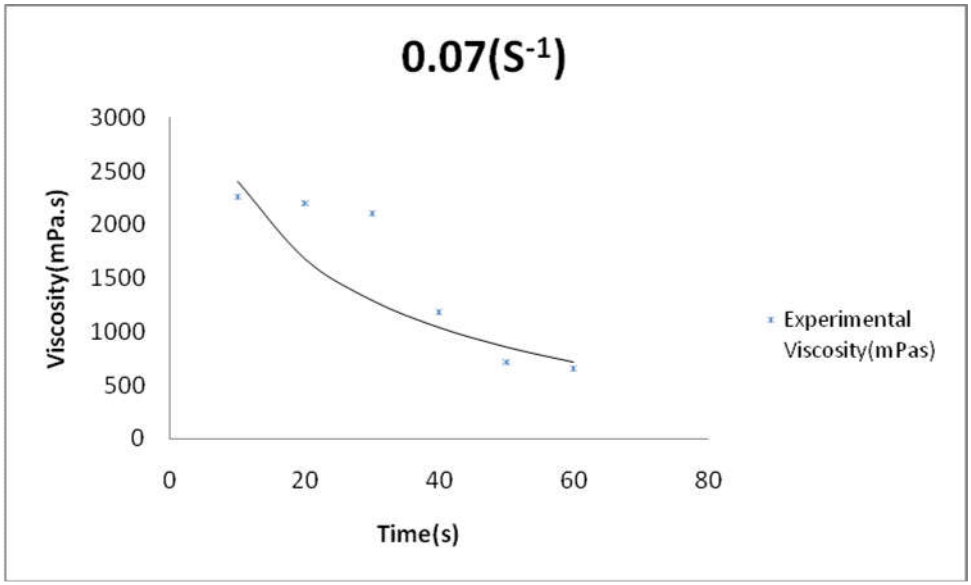

Figure A19-Viscosity time graph of Sample A4 at Shear rate of 0.07s^{-1}

Therefore η = 4916.544809

From equation (1.3), $\eta_o = KM^A$

$$\left(\frac{\eta_o}{k}\right)^{1/A} = M$$

Taking A=0.5635 and *K*= 165

M= 413.1489g/mol

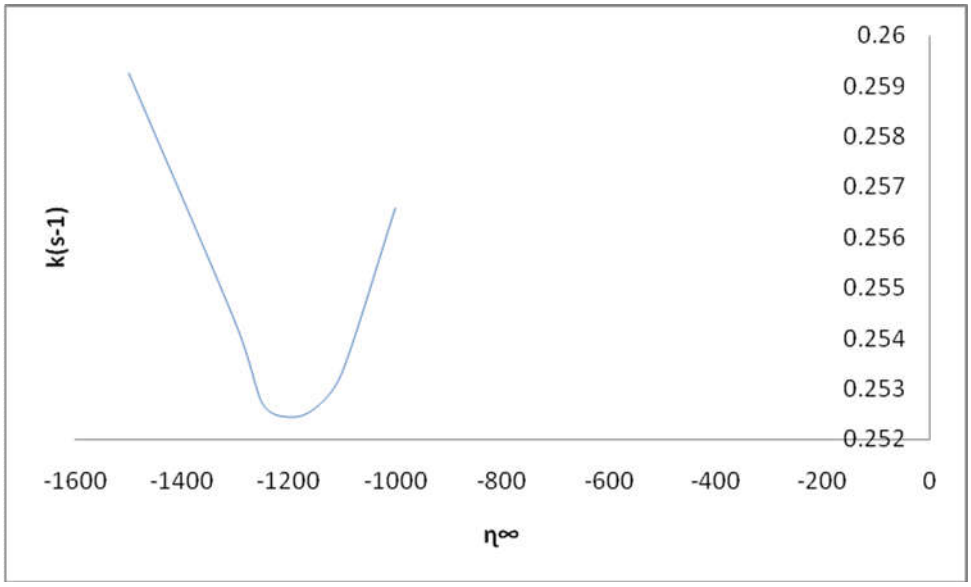

Figure A-20 Optimisation of k for Sample A4 at shear rate of 0.07(s^{-1})

From Figure A-2 above, the infinite time viscosity, η_∞,was found to be -1250 mPa.s.

From equation (3.17):

$$\text{Let } \Gamma = \left(\frac{\eta - \eta_\infty}{\eta_o - \eta_\infty}\right)^{1-n} \tag{4.2}$$

$$\text{Therefore } \Gamma = tk(n-1)+1 \tag{4.3}$$

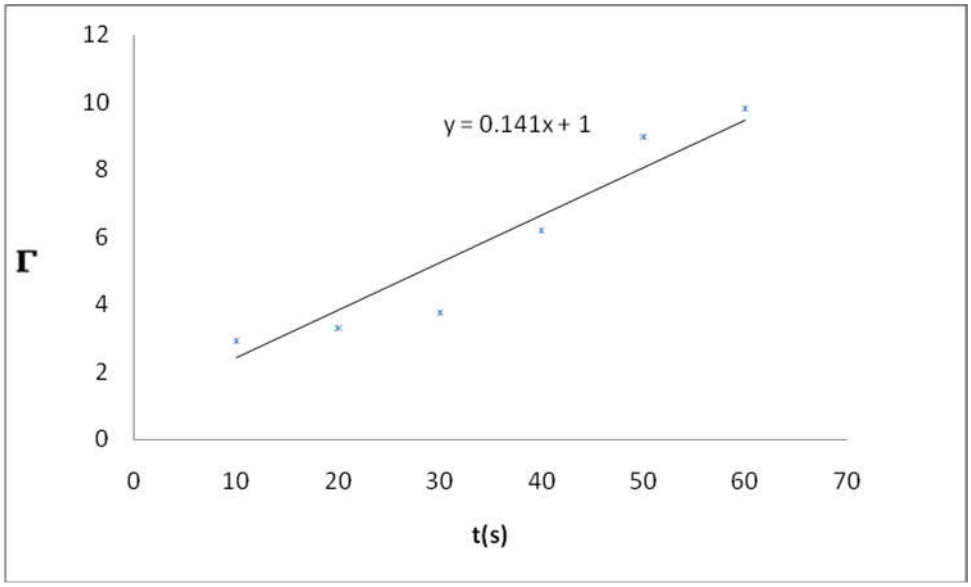

A21- Plot of Γ against t at shear rate of 0.07s^{-1}

From the slope of Figure A3, $0.141 = k(n-1)$. When n=3, then k=0.0705s^{-1}

At Shear Rate of 0.09 (s^{-1})

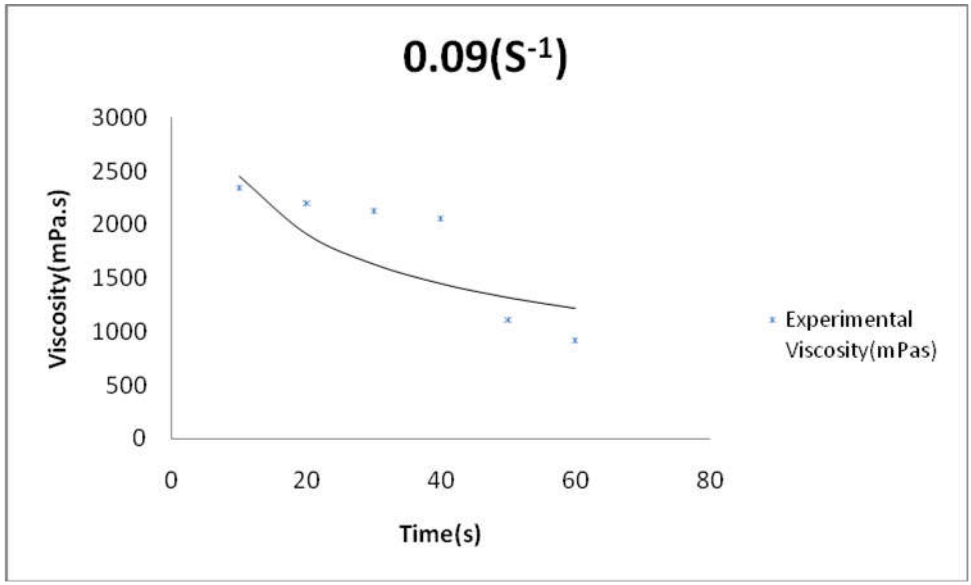

Figure A22-Viscosity time graph of Sample A4 at Shear rate of 0.09s^{-1}

Therefore η = 4609.49986

From equation (1.3), $\eta_o = KM^A$

$$\left(\frac{\eta_o}{k}\right)^{1/A} = M$$

Taking A=0.5635 and *K*= 165

M= 368.4734g/mol

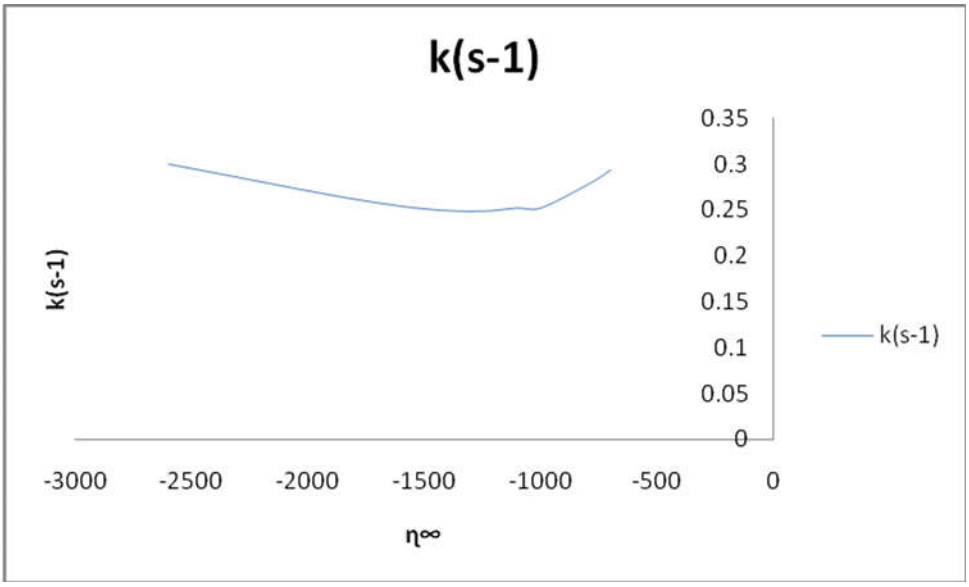

Figure A-23 Optimisation of k for Sample A4 at shear rate of 0.09(s^{-1})

From Figure A-23 above, the infinite time viscosity, η_∞,was found to be -1300 mPa.s.

From equation (3.17):

$$\text{Let } \Gamma = \left(\frac{\eta - \eta_\infty}{\eta_o - \eta_\infty}\right)^{1-n} \tag{4.2}$$

$$\text{Therefore } \Gamma = tk(n-1)+1 \tag{4.3}$$

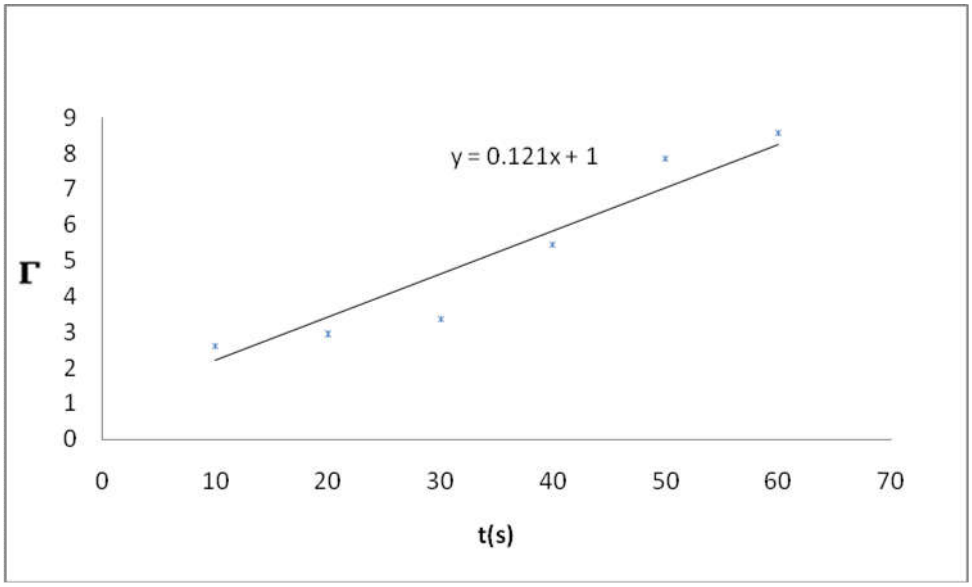

A24- Plot of Γ against t at shear rate of 0.09s^{-1}

From the slope of Figure A24, $0.121 = k(n-1)$. When n=3, then k=0.0605s^{-1}

At Shear Rate of 0.11(s^{-1})

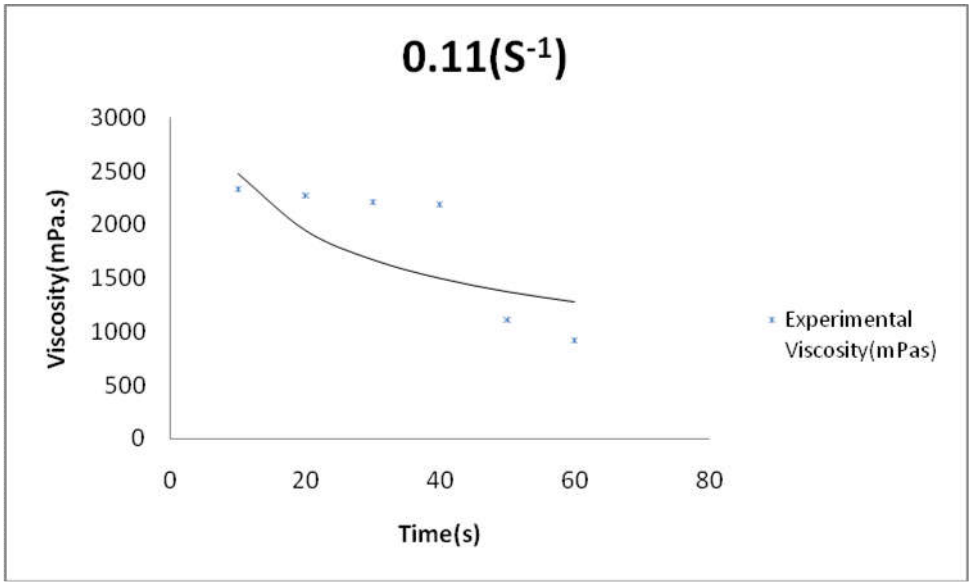

Figure A25-Viscosity time graph of Sample A4 at Shear rate of 0.011s^{-1}

Therefore η = 4821.142454

From equation (1.3), $\eta_o = KM^A$

$$\left(\frac{\eta_o}{k}\right)^{1/A} = M$$

Taking A=0.5635 and *K*= 165

M= 399.0290g/mol

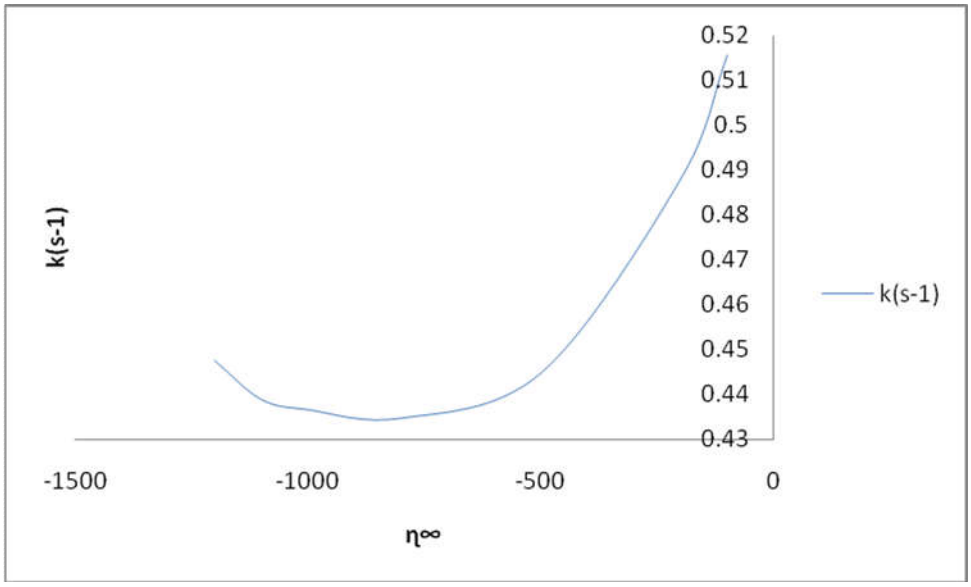

Figure A-26 Optimisation of *k* for Sample A4 at shear rate of 0.11(s^{-1})

From Figure A-26 above, the infinite time viscosity, η_∞,was found to be -800 mPa.s.

From equation (3.17):

$$\text{Let } \Gamma = \left(\frac{\eta - \eta_\infty}{\eta_o - \eta_\infty}\right)^{1-n} \tag{4.2}$$

$$\text{Therefore } \Gamma = tk(n-1)+1 \tag{4.3}$$

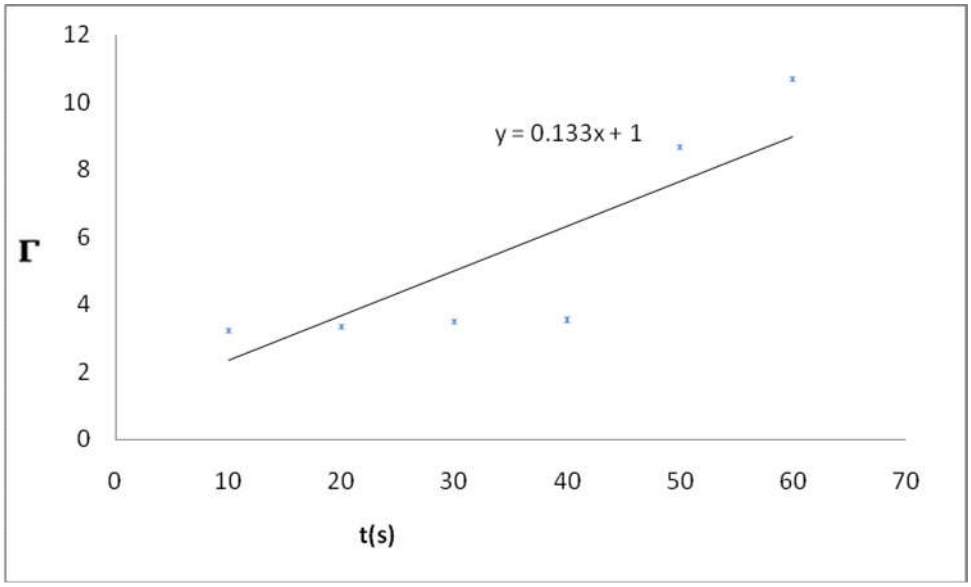

B27- Plot of Γ against t at shear rate of 0.11s^{-1}

From the slope of Figure A27, $0.133 = k(n-1)$. When n=3, then *k*=0.0665 s^{-1}

At Shear Rate of 0.12 (s^{-1})

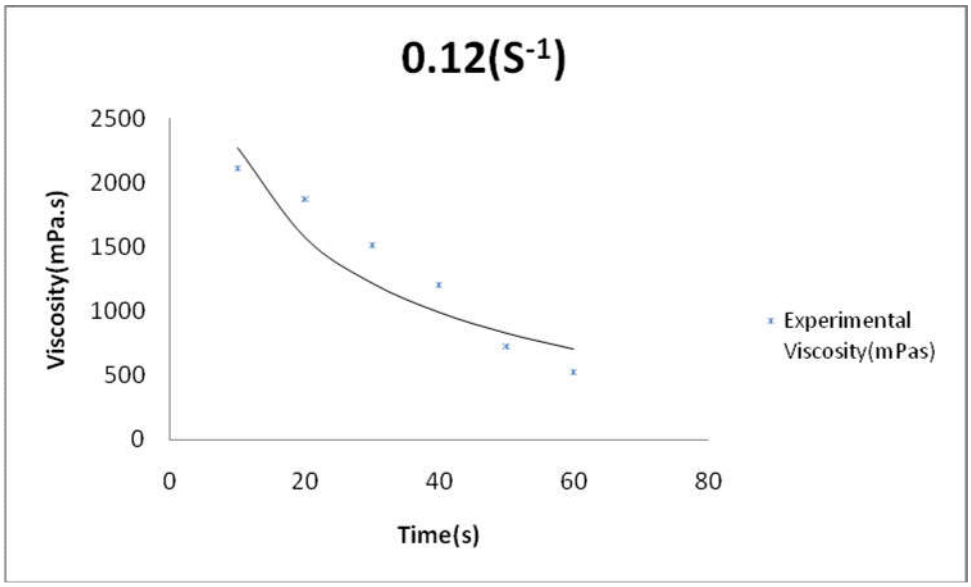

Figure A28-Viscosity time graph of Sample A4 at Shear rate of 0.12 s^{-1}

Therefore η = 5218.161531

From equation (1.3), $\eta_o = KM^A$

$$\left(\frac{\eta_o}{K}\right)^{1/A} = M$$

Taking A=0.5635 and *K*= 165

M= 459.1915 g/mol

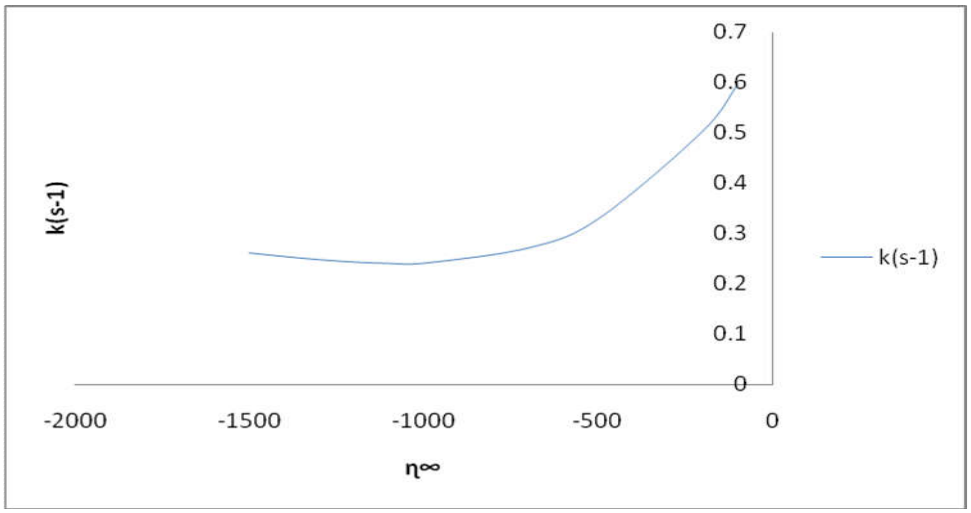

Figure A-29 Optimisation of *k* for Sample A4 at shear rate of 0.12(s^{-1})

From Figure A-29 above, the infinite time viscosity, η_∞,was found to be -1350 mPa.s.

From equation (3.17):

$$\text{Let } \Gamma = \left(\frac{\eta - \eta_\infty}{\eta_o - \eta_\infty}\right)^{1-n} \tag{4.2}$$

$$\text{Therefore } \Gamma = tk(n-1)+1 \tag{4.3}$$

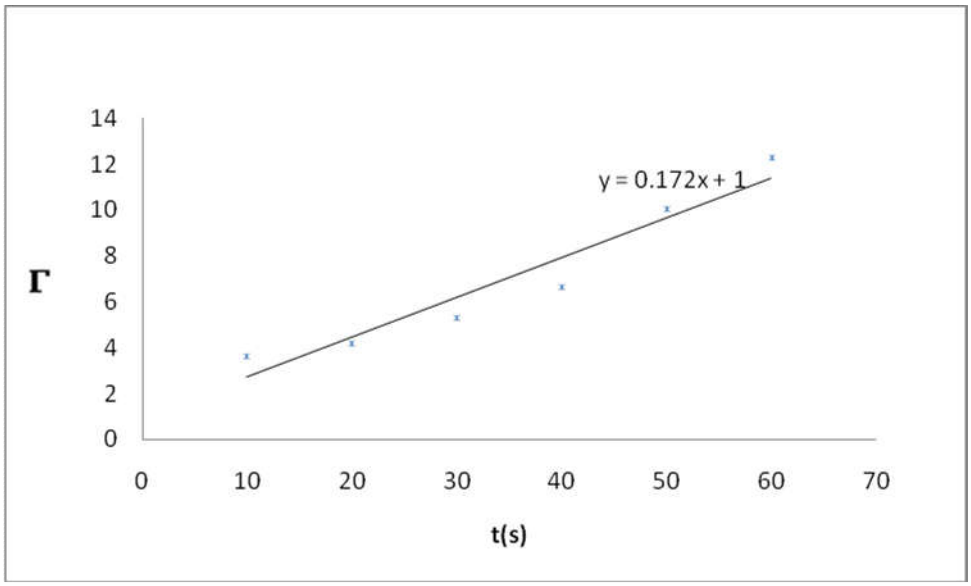

B30- Plot of Γ against t at shear rate of 0.12 s^{-1}

From the slope of Figure A30, $0.172 = k(n-1)$. When n=3, then k=0.086 s^{-1}

At Shear Rate of 0.13 (S-1)

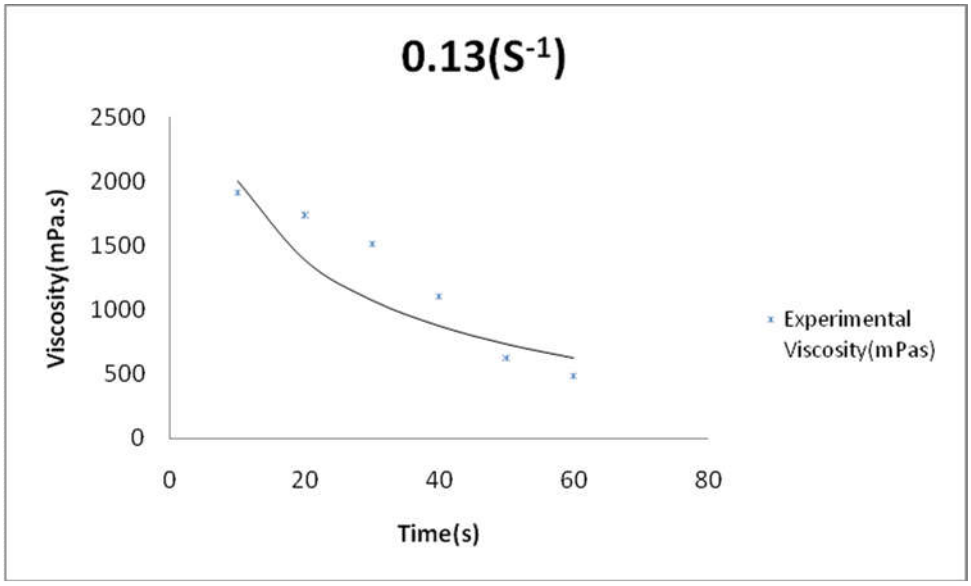

Figure A31-Viscosity time graph of Sample A4 at Shear rate of 0.13 s^{-1}

Therefore η = 4883.177709

From equation (1.3), $\eta_o = KM^A$

$$\left(\frac{\eta_o}{K}\right)^{1/A} = M$$

Taking A=0.5635 and *K*= 165

M= 408.1861 g/mol

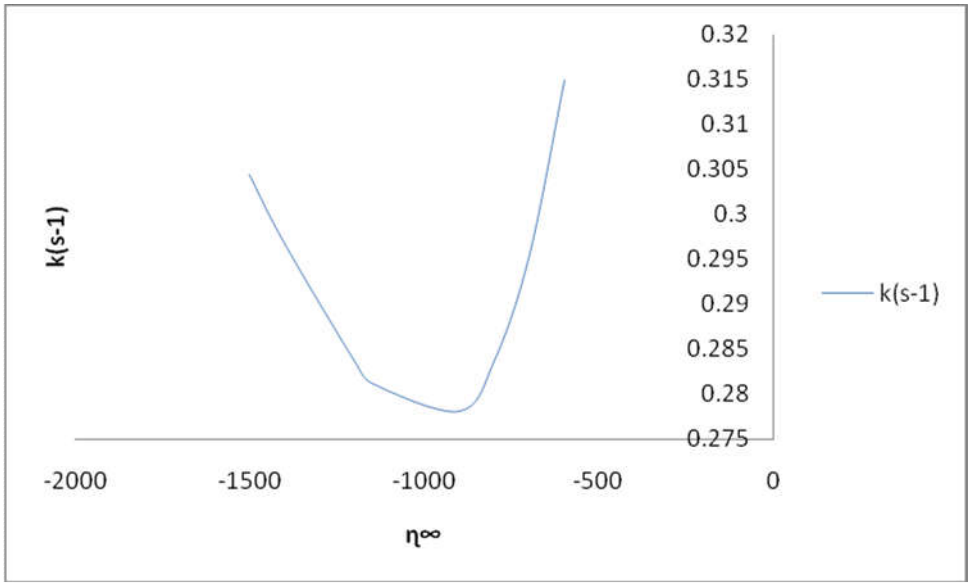

Figure A-32 Optimisation of *k* for Sample A4 at shear rate of 0.13 (s^{-1})

From Figure A-32 above, the infinite time viscosity, η_∞ ,was found to be -1150 mPa.s.

From equation (3.17), let

$$\text{Let } \Gamma = \left(\frac{\eta - \eta_\infty}{\eta_o - \eta_\infty}\right)^{1-n} \tag{4.2}$$

$$\text{Therefore } \Gamma = tk(n-1)+1 \tag{4.3}$$

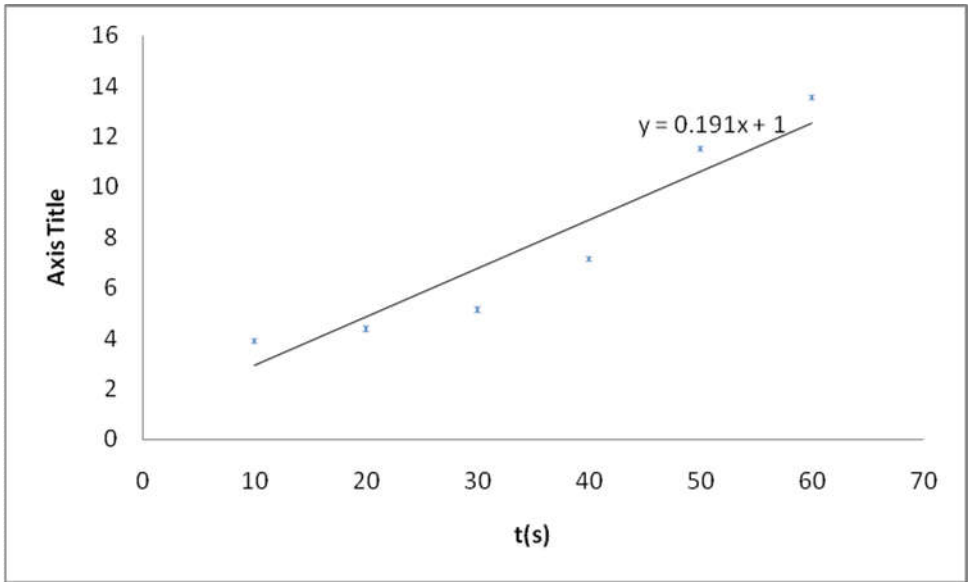

B33- Plot of Γ against t at shear rate of 0.01s^{-1}

From the slope of Figure A33, $0.191 = k(n-1)$. When n=3, then k=0.0955s^{-1}

At Shear Rate of 0.14(S-1)

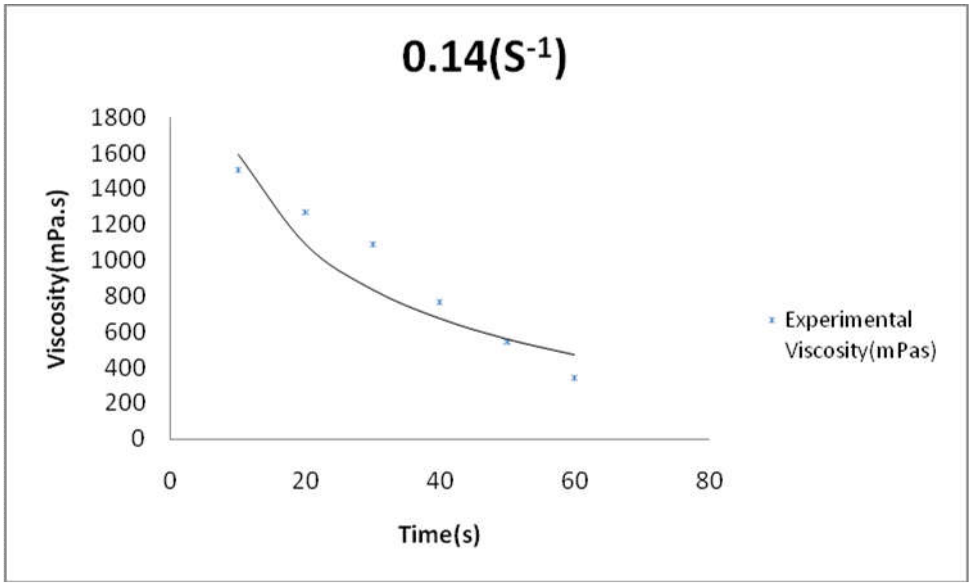

Figure A34-Viscosity time graph of Sample A4 at Shear rate of 0.14 s^{-1}

Therefore η = 3929.255323

From equation (1.3), $\eta_o = KM^A$

$$\left(\frac{\eta_o}{k}\right)^{1/A} = M$$

Taking A=0.5635 and *K*= 165

M= 277.5540 g/mol

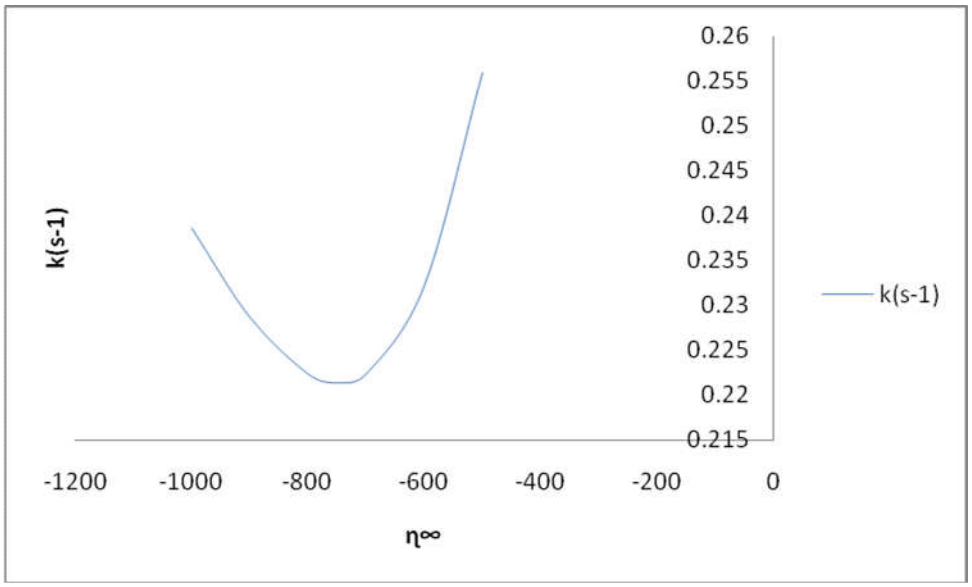

Figure A-35 Optimisation of *k* for Sample A4 at shear rate of 0.14 (S^{-1})

From Figure A-35 above, the infinite time viscosity, η_∞,was found to be -750 mPa.s.

From equation (3.17):

Let $\Gamma = (\frac{\eta - \eta_\infty}{\eta_o - \eta_\infty})^{1-n}$ (4.2)

Therefore $\Gamma = tk(n-1)+1$ (4.3)

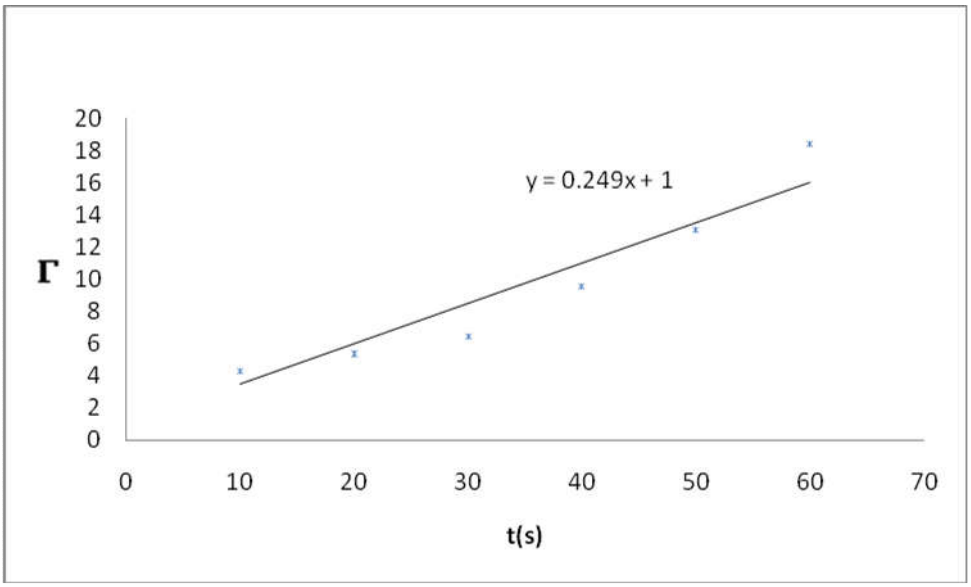

B36- Plot of Γ against t at shear rate of 0.14 s^{-1}

From Figure A-38 above, the infinite time viscosity, η_∞,was found to be -1000 mPa.s.

From equation (3.17), let

$$\text{Let } \Gamma = \left(\frac{\eta - \eta_\infty}{\eta_o - \eta_\infty}\right)^{1-n} \tag{4.2}$$

$$\text{Therefore } \Gamma = tk(n-1)+1 \tag{4.3}$$

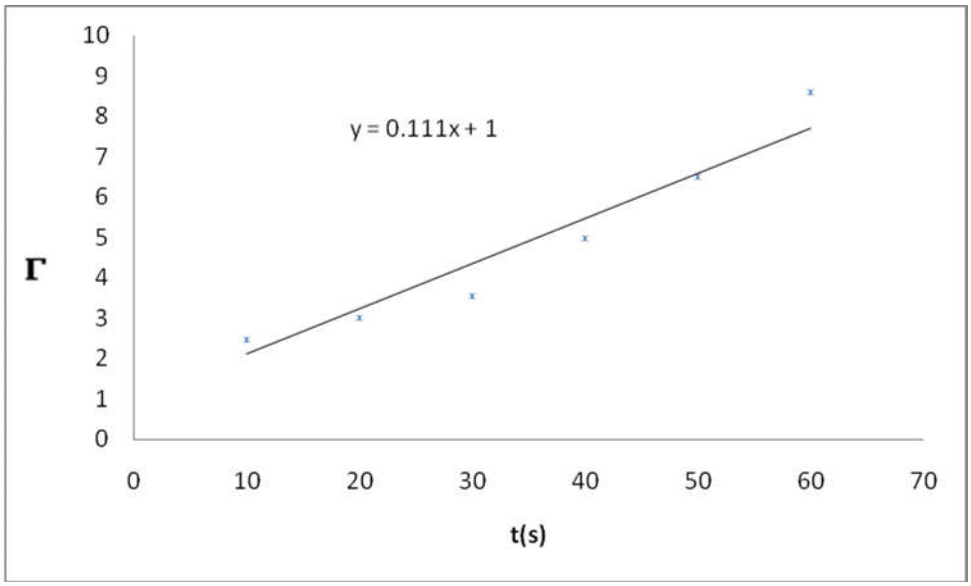

B39- Plot of Γ against *t* at shear rate of 0.15 s^{-1}

From the slope of Figure A3, $0.111 = k(n-1)$. When n=3, then *k*=0.0555 s^{-1}

At Shear Rate of 0.16(s^{-1})

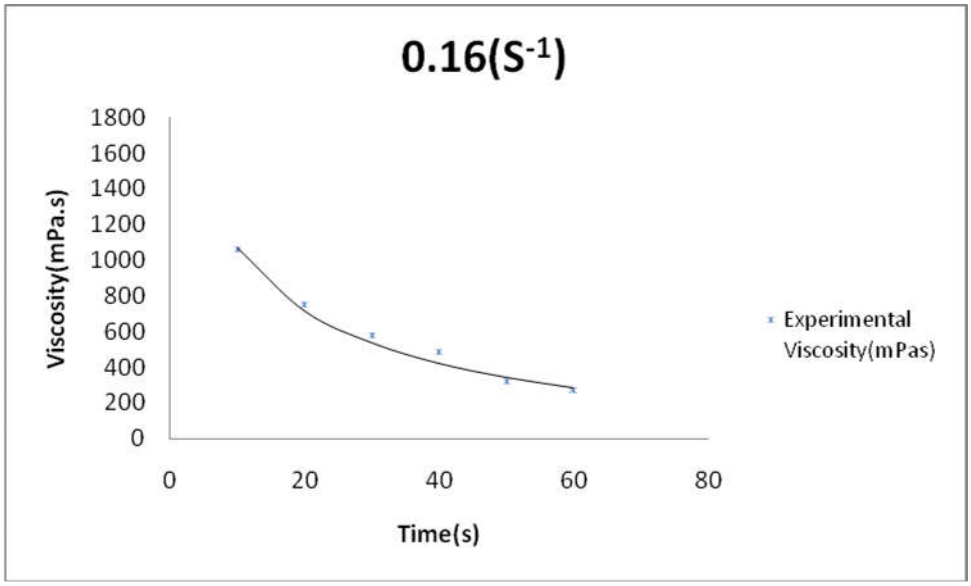

Figure A40-Viscosity time graph of Sample A4 at Shear rate of 0.16 s^{-1}

Therefore η = 2894.654942

From equation (1.3), $\eta_o = KM^A$

$$\left(\frac{\eta_o}{K}\right)^{1/A} = M$$

Taking A=0.5635 and *K*= 165

M= 161.3731g/mol

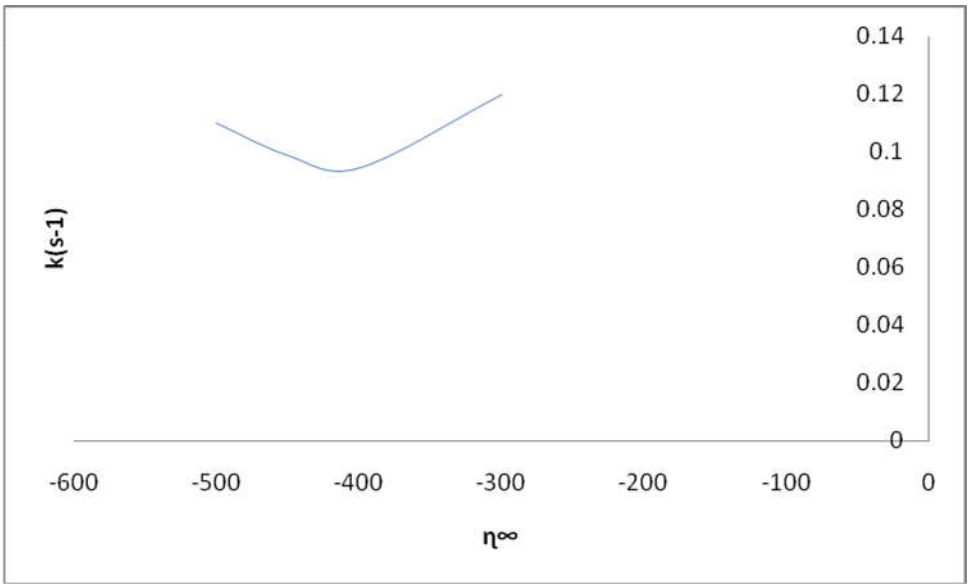

Figure A-41 Optimisation of *k* for Sample A4 at shear rate of 0.16(s^{-1})

From Figure A-41 above, the infinite time viscosity, η_∞,was found to be -400 mPa.s.

From equation (3.17):

$$\text{Let } \Gamma = \left(\frac{\eta - \eta_\infty}{\eta_o - \eta_\infty}\right)^{1-n} \qquad (4.2)$$

$$\text{Therefore } \Gamma = tk(n-1)+1 \qquad (4.3)$$

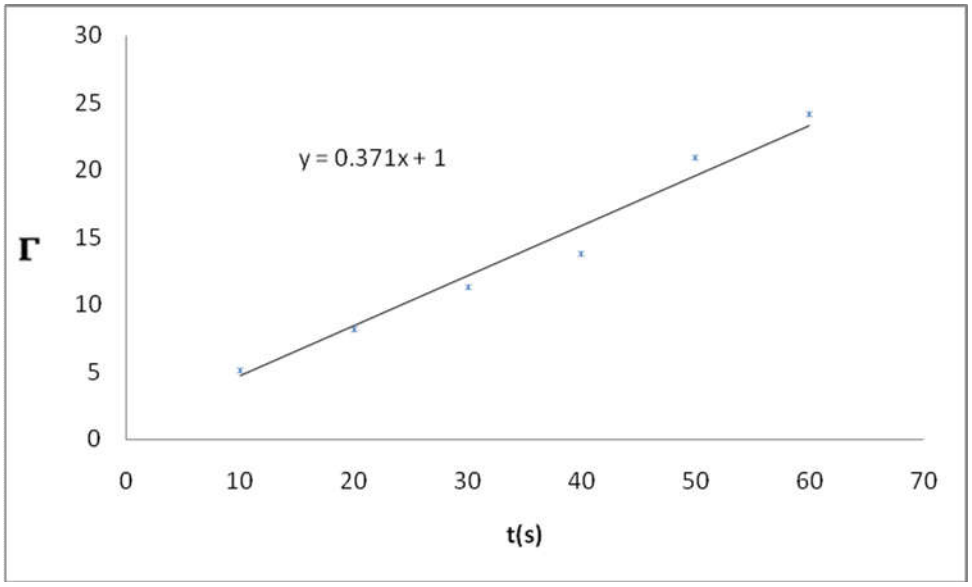

B42- Plot of Γ against t at shear rate of 0.16 s^{-1}

From the slope of Figure A42, $0.371 = k(n-1)$. When n=3, then k=0.1855 s^{-1}

At Shear Rate of 0.17(S-1)

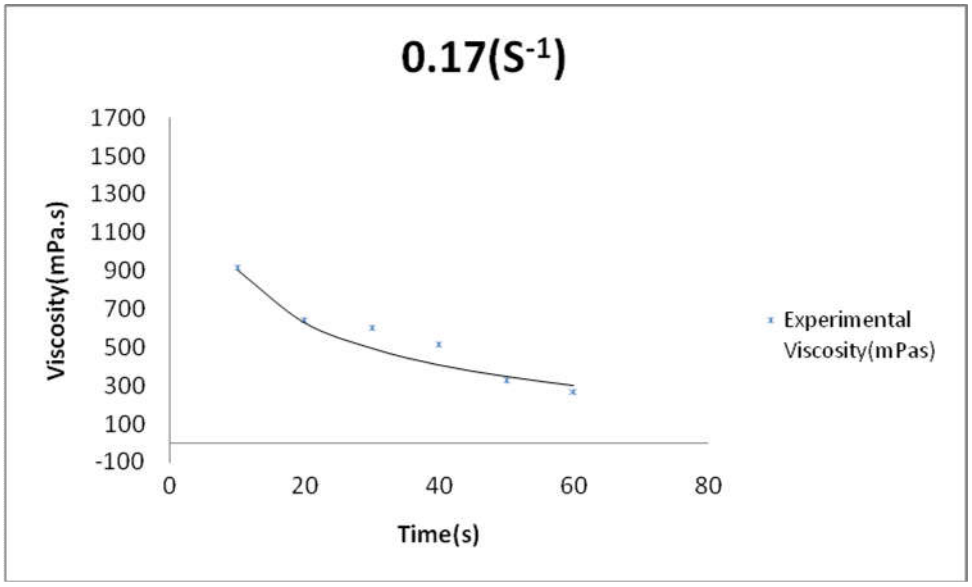

Figure A43-Viscosity time graph of Sample A4 at Shear rate of 0.17 s^{-1}

Therefore η = 2332.230799

From equation (1.3), $\eta_o = KM^A$

$$\left(\frac{\eta_o}{k}\right)^{1/A} = M$$

Taking A=0.5635 and *K*= 165

M= 109.9833g/mol

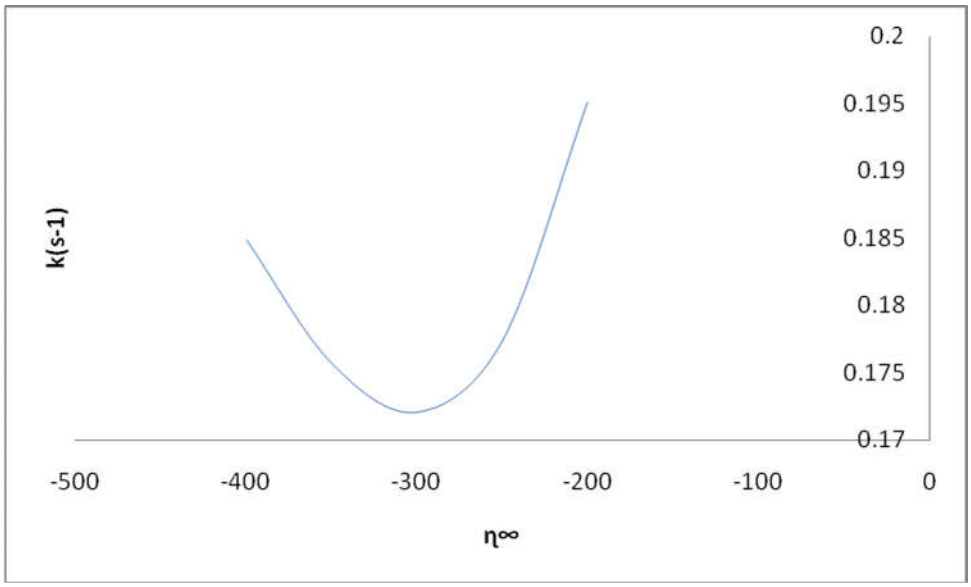

Figure A-44 Optimisation of *k* for Sample A4 at shear rate of 0.17(s^{-1})

From Figure A-44 above, the infinite time viscosity, η_∞,was found to be -300mPa.s.

From equation (3.17):

Let $\Gamma = (\frac{\eta - \eta_\infty}{\eta_o - \eta_\infty})^{1-n}$ (4.2)

Therefore $\Gamma = tk(n-1)+1$ (4.3)

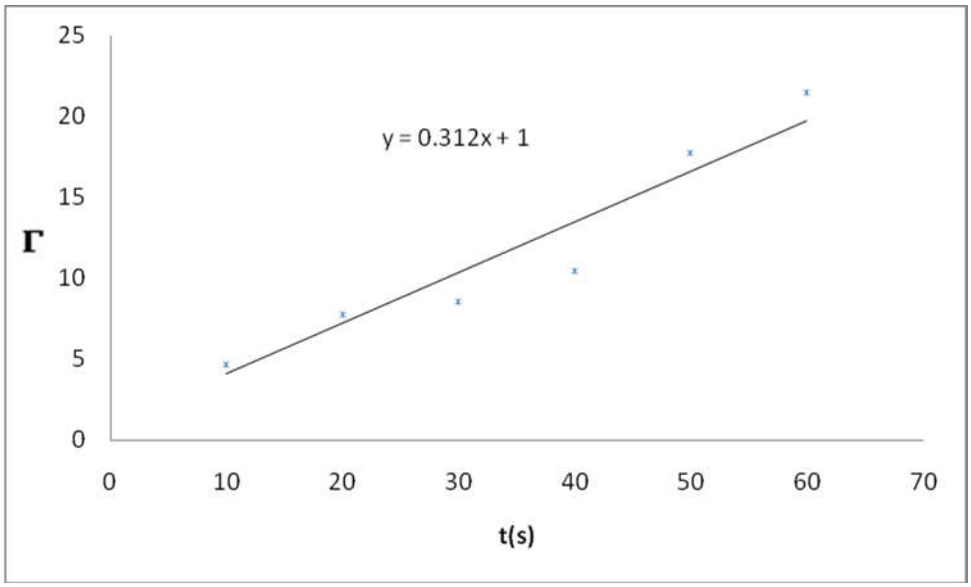

B45- Plot of Γ against *t* at shear rate of 0.17 s^{-1}

From the slope of Figure A45, $0.312 = k(n-1)$. When n=3, then k=0.156 s^{-1}

At Shear Rate of 0.18 s^{-1}

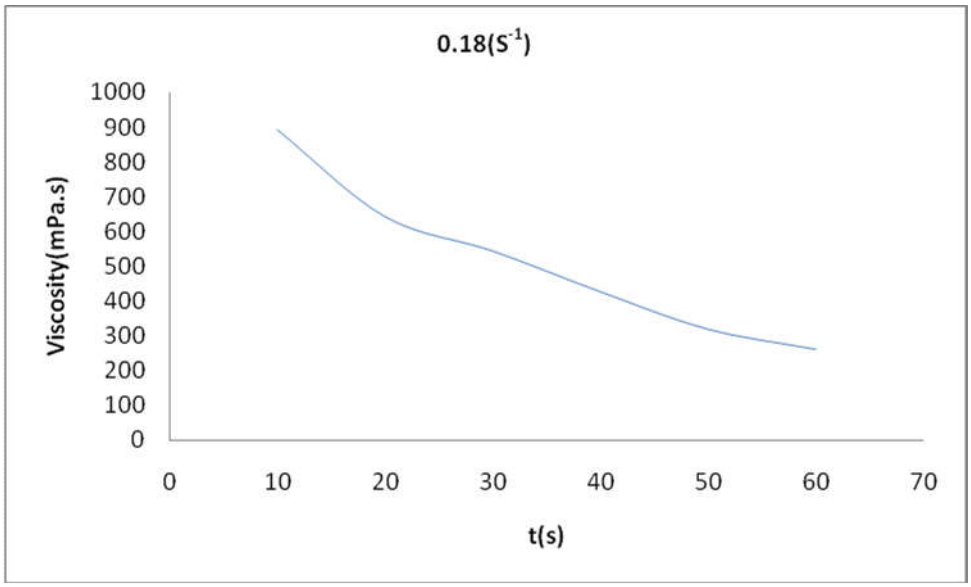

Figure A46-Viscosity time graph of Sample A4 at Shear rate of 0.18 s^{-1}

Therefore η = 2365.151

From equation (1.3), $\eta_o = KM^A$

$$\left(\frac{\eta_o}{k}\right)^{1/A} = M$$

Taking A=0.5635 and *K*= 165

M= 112.7533g/mol

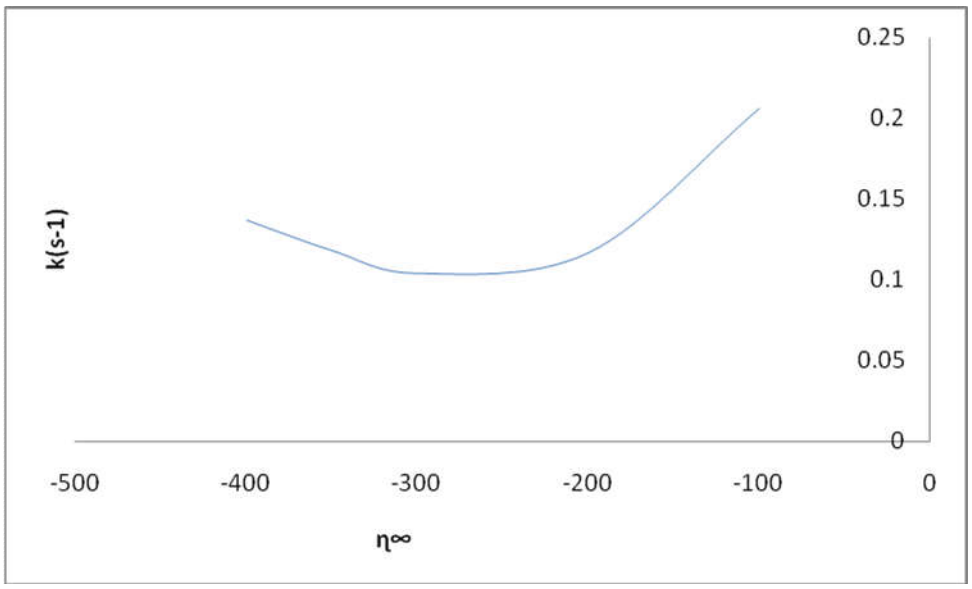

From Figure A-47 above, the infinite time viscosity, η_∞,was found to be -300 mPa.s.

From equation (3.17):

$$\text{Let } \Gamma = \left(\frac{\eta - \eta_\infty}{\eta_o - \eta_\infty}\right)^{1-n} \tag{4.2}$$

$$\text{Therefore } \Gamma = tk(n-1)+1 \tag{4.3}$$

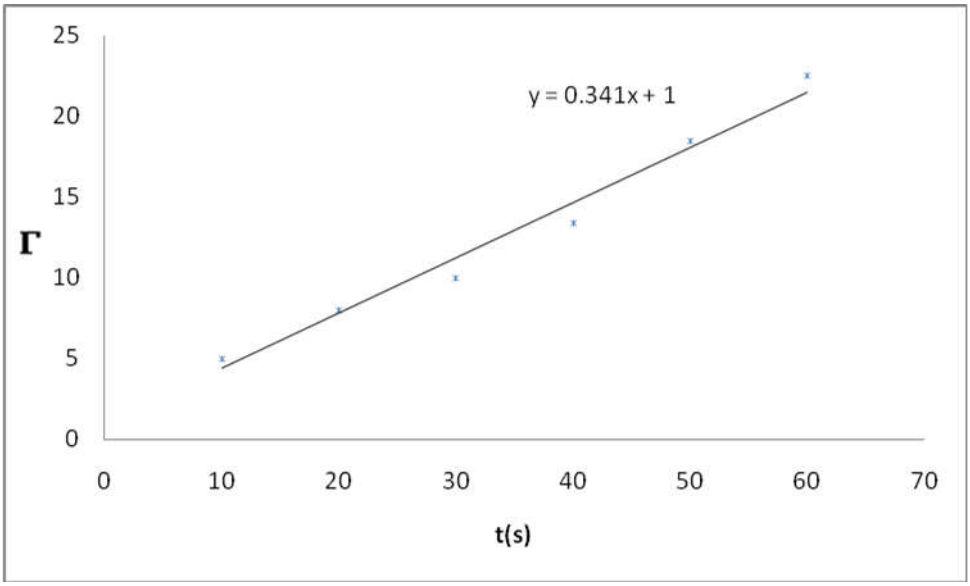

B48- Plot of Γ against t at shear rate of 0.18 s^{-1}

From the slope of Figure A48, $0.341 = k(n-1)$. When n=3, then k=0.1705 s^{-1}

At Shear Rate of 0.19 (s^{-1})

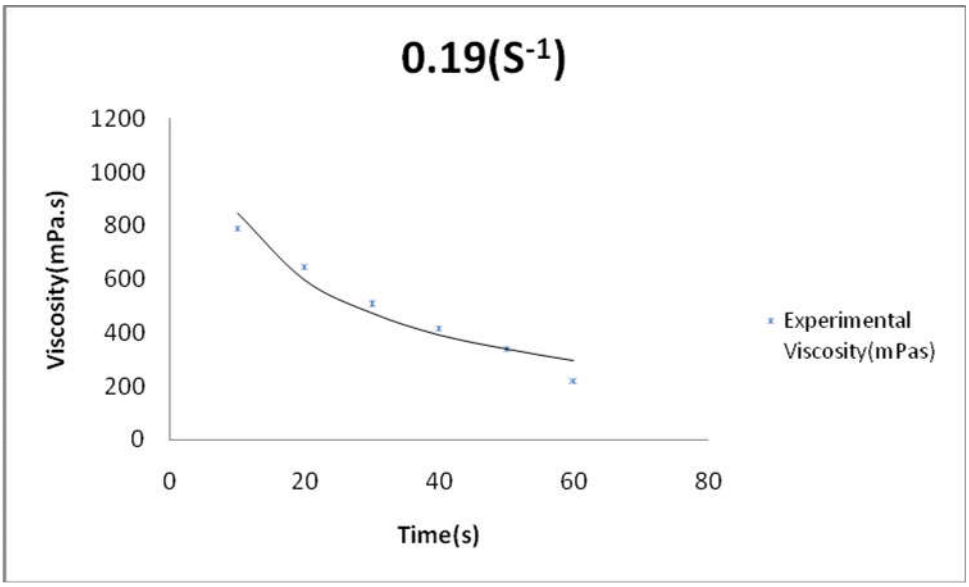

Figure A49-Viscosity time graph of Sample A4 at Shear rate of 0.19 s^{-1}

Therefore η = 2139.19743

From equation (1.3), $\eta_o = KM^A$

$$\left(\frac{\eta_o}{K}\right)^{1/A} = M$$

Taking A=0.5635 and *K*= 165

M= 94.3499g/mol

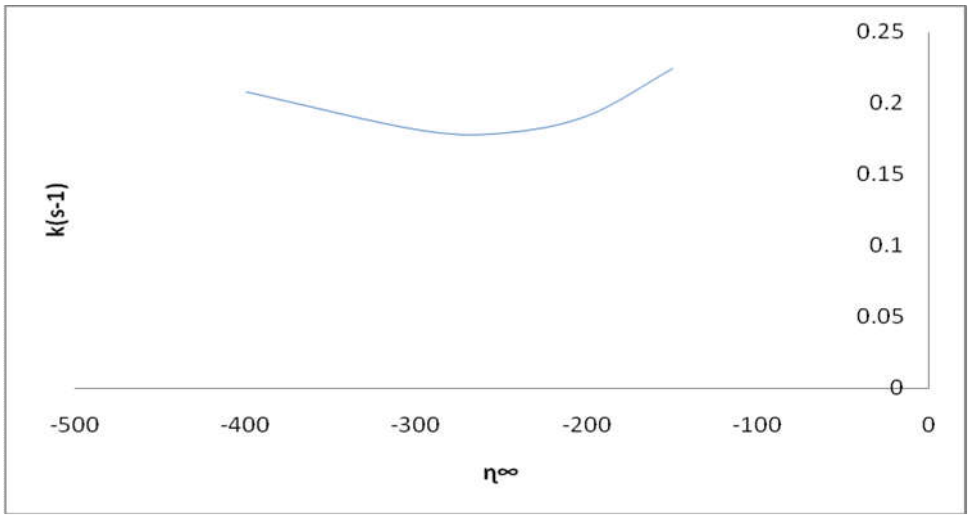

Figure A-50 Optimisation of *k* for Sample A4 at shear rate of 0.19(s^{-1})

From Figure A-50 above, the infinite time viscosity, η_∞,was found to be -250 mPa.s.

From equation (3.17):

$$\text{Let } \Gamma = \left(\frac{\eta - \eta_\infty}{\eta_o - \eta_\infty}\right)^{1-n} \tag{4.2}$$

$$\text{Therefore } \Gamma = tk(n-1)+1 \tag{4.3}$$

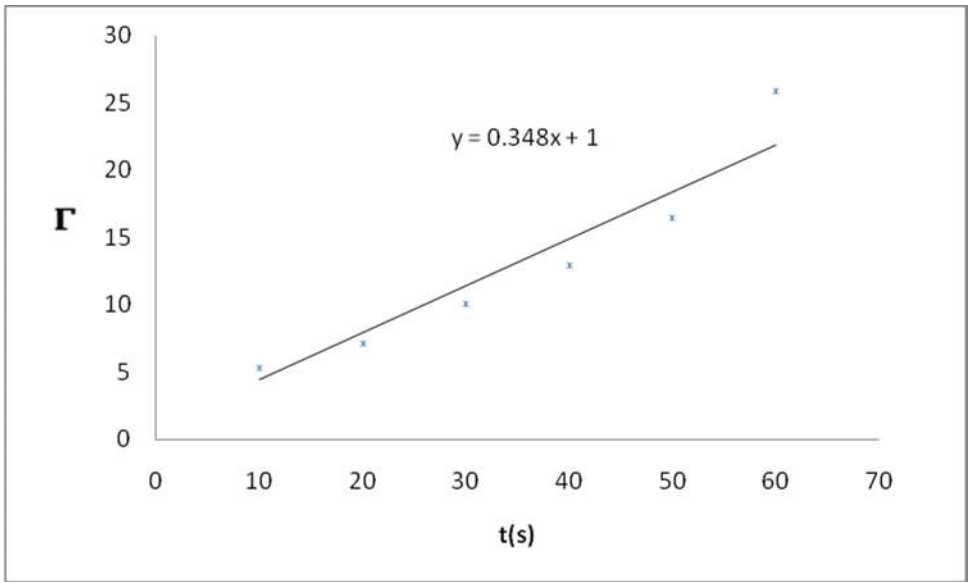

B51- Plot of Γ against t at shear rate of 0.19 s^{-1}

From the slope of Figure A3, $0.348 = k(n-1)$. When n=3, then k=0.174 s^{-1}

At Shear Rate of 0.20 (S-1)

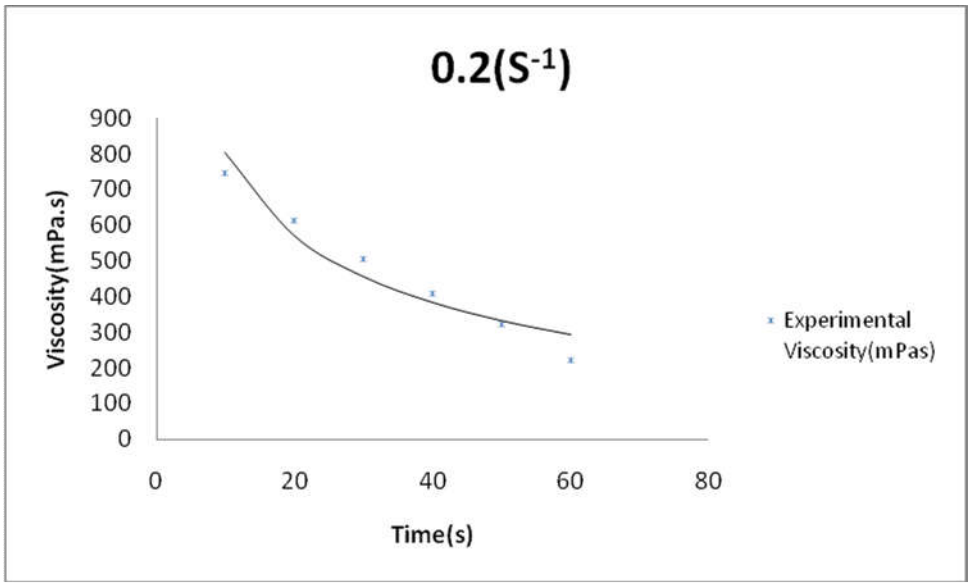

Figure A52-Viscosity time graph of Sample A4 at Shear rate of 0.2 s^{-1}

Therefore η = 2027.630784

From equation (1.3), $\eta_o = KM^A$

$$\left(\frac{\eta_o}{K}\right)^{1/A} = M$$

Taking A=0.5635 and *K*= 165

M= 85.7947g/mol

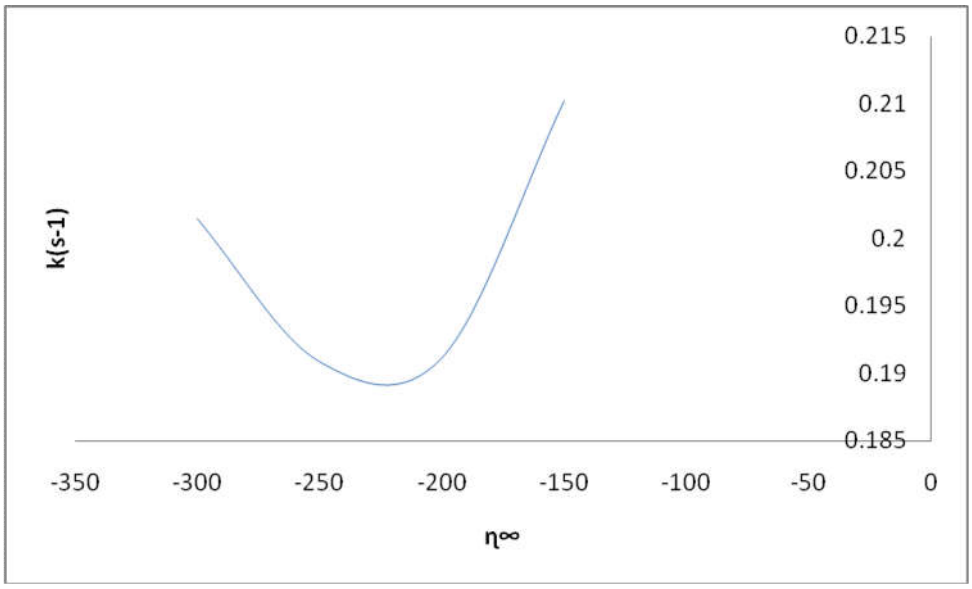

Figure A-53 Optimisation of *k* for Sample A4 at shear rate of 0.2(s^{-1})

From Figure A-53 above, the infinite time viscosity, η_∞,was found to be -250 mPa.s.

From equation (3.17):

$$\text{Let } \Gamma = \left(\frac{\eta - \eta_\infty}{\eta_o - \eta_\infty}\right)^{1-n} \qquad (4.2)$$

$$\text{Therefore } \Gamma = tk(n-1)+1 \qquad (4.3)$$

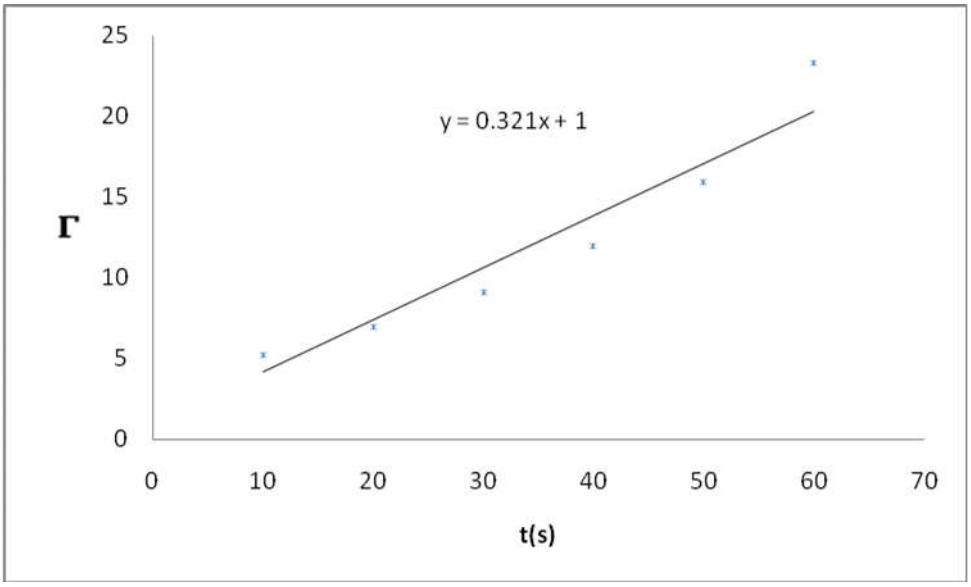

B54- Plot of Γ against t at shear rate of 0.2 s^{-1}

From the slope of Figure A54, $0.321 = k(n-1)$. When n=3, then k=0.1605 s^{-1}

At Shear Rate of 0.21(s^{-1})

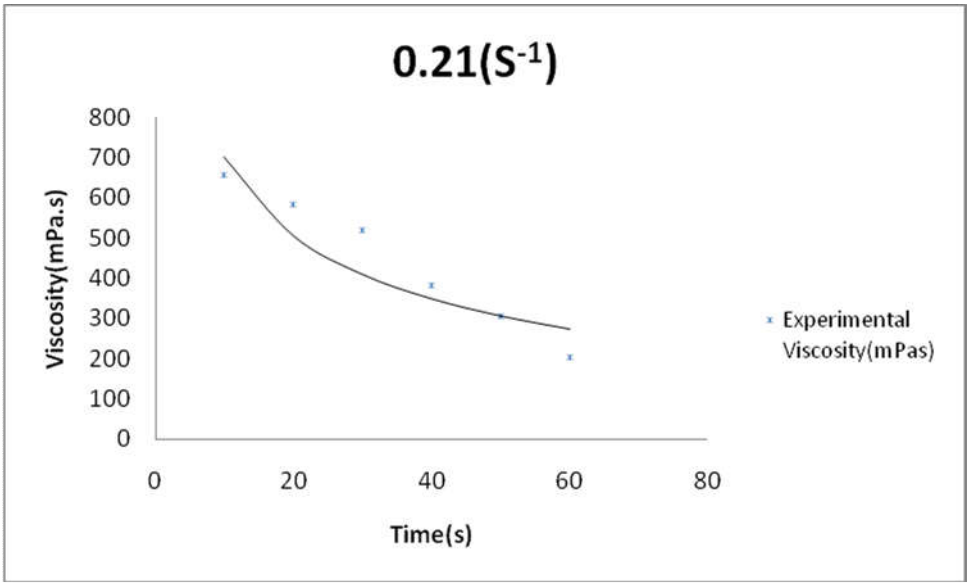

Figure A55-Viscosity time graph of Sample A4 at Shear rate of 0.21s^{-1}

Therefore η = 1827.127114

From equation (1.3), $\eta_o = KM^A$

$(\frac{\eta_o}{k})^{1/A} = M$

Taking A=0.5635 and *K*= 165

M= 71.3201g/mol

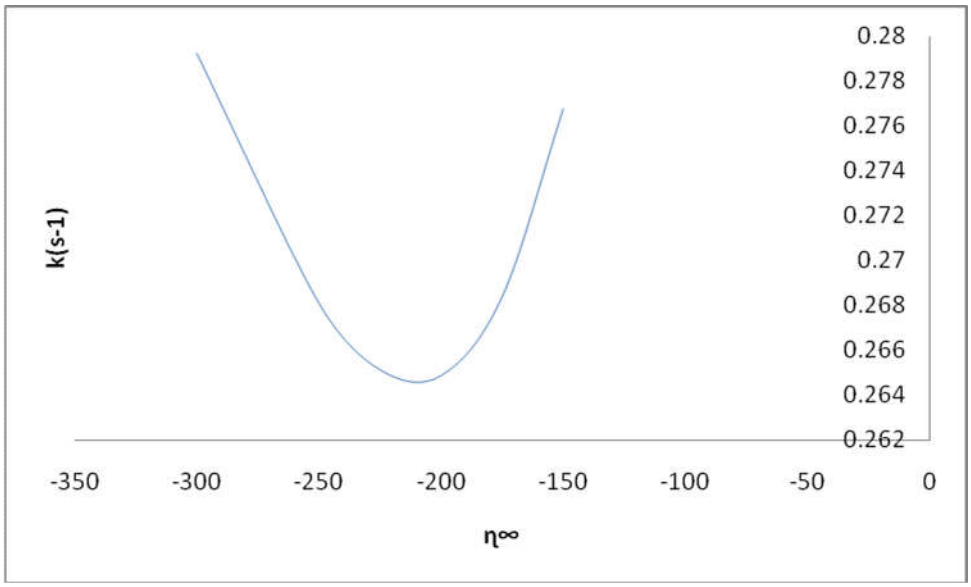

Figure A-56 Optimisation of *k* for Sample A4 at shear rate of 0.21(s^{-1})

From Figure A-56 above, the infinite time viscosity, η_∞, was found to be -200 mPa.s.

From equation (3.17):

$$\text{Let } \Gamma = \left(\frac{\eta - \eta_\infty}{\eta_o - \eta_\infty}\right)^{1-n} \tag{4.2}$$

$$\text{Therefore } \Gamma = tk(n-1)+1 \tag{4.3}$$

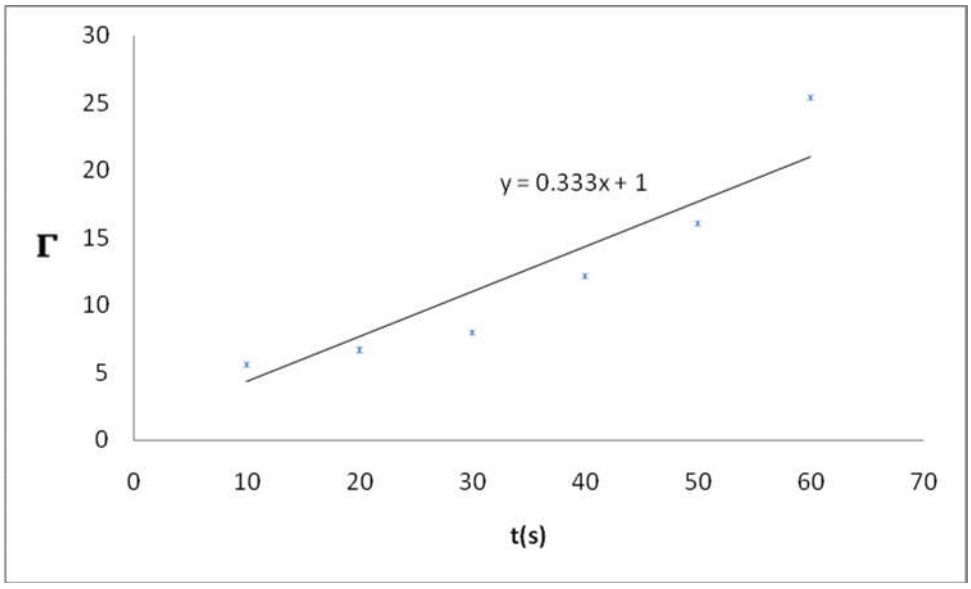

B57- Plot of Γ against t at shear rate of 0.21 s^{-1}

From the slope of Figure A3, $0.333 = k(n-1)$. When n=3, then k=0.1665S-1

At Shear Rate of 0.22 (S-1)

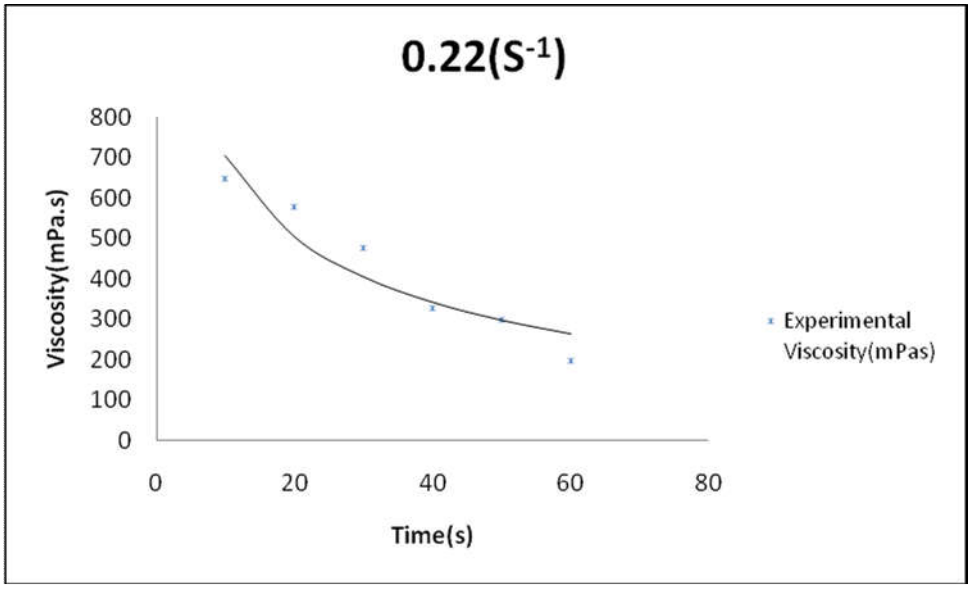

Figure A58-Viscosity time graph of Sample A4 at Shear rate of 0.22S-1

Therefore η = 1864.231982

From equation (1.3), $\eta_o = KM^A$

$$\left(\frac{\eta_o}{k}\right)^{1/A} = M$$

Taking A=0.5635 and *K*= 165

M= 73.9105g/mol

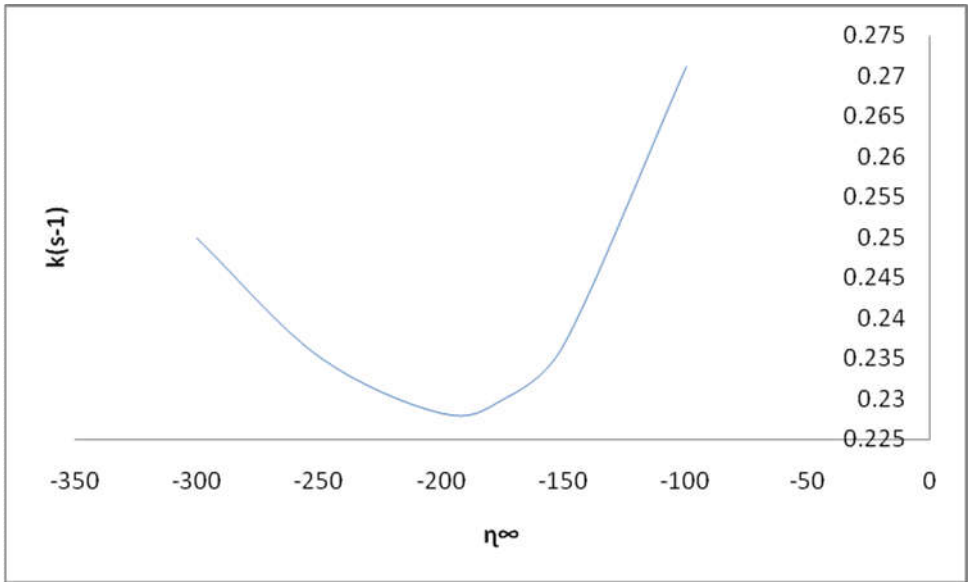

Figure A-59 Optimisation From Figure A-2 above, the infinite time viscosity, η_∞ ,was found to be -200mPa.s.

From equation (3.17):

$$\text{Let } \Gamma = (\frac{\eta - \eta_\infty}{\eta_o - \eta_\infty})^{1-n} \tag{4.2}$$

$$\text{Therefore } \Gamma = tk(n-1)+1 \tag{4.3}$$

n of k for Sample A4 at shear rate of 0.01(s^{-1})

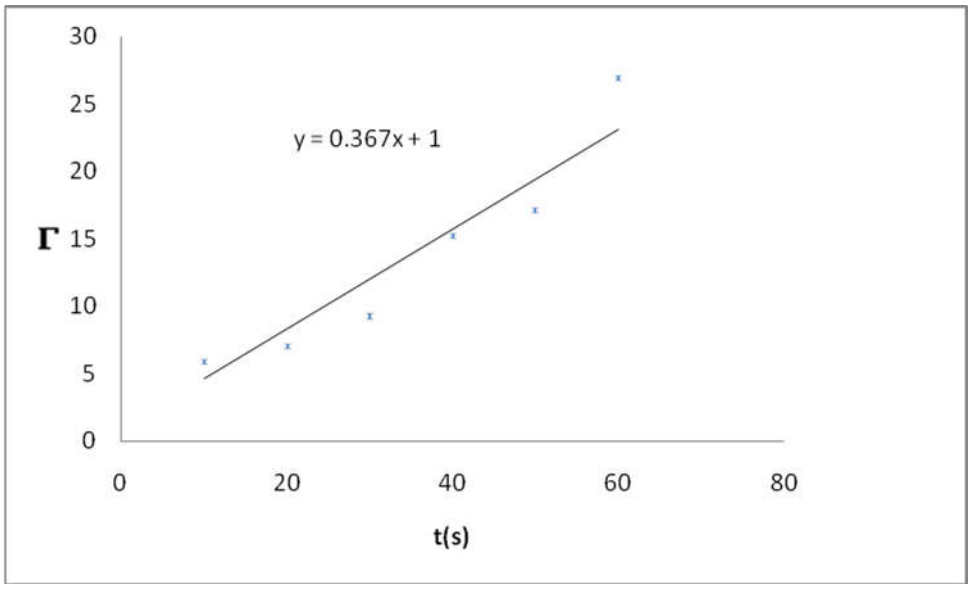

Figure A-60 Plot of Γ against t at shear rate of 0.22 s^{-1}

From the slope of Figure A3, $0.367 = k(n-1)$. When n=3, then k=0.1835 s^{-1}

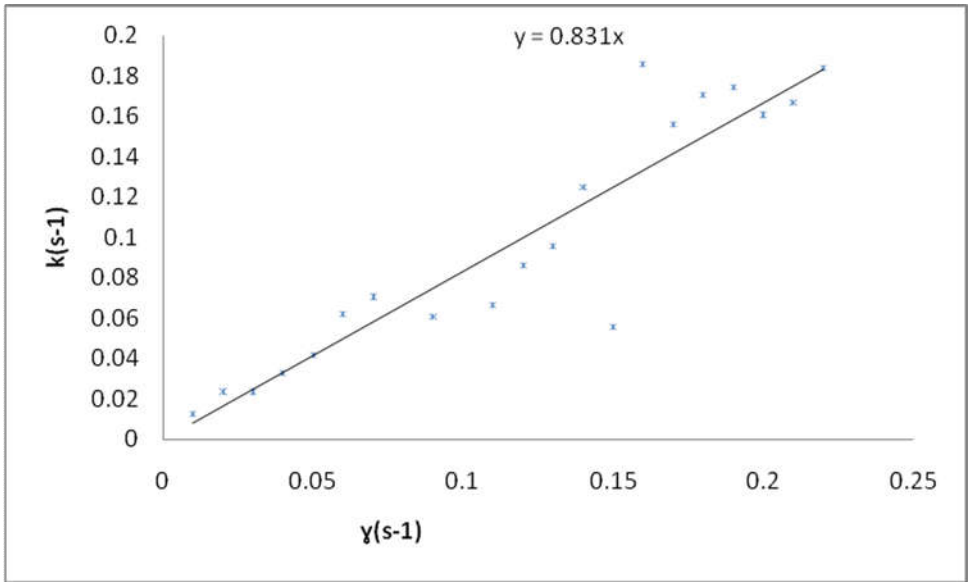

Figure 44- Plot of k against shear rate of Sample A4

From Figure 44, the overall rate of deformation of Sample A4=**0.831** s^{-1}

Therefor, the average molecular weight=252.07g/mol

APPENDIX 2.2

PANORAMA VIEW OF SAMPLES

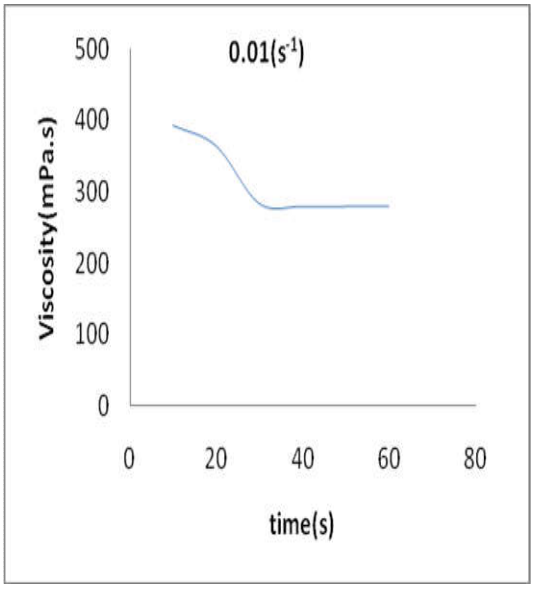

Figure A-61 Viscosity vs time plot of G1

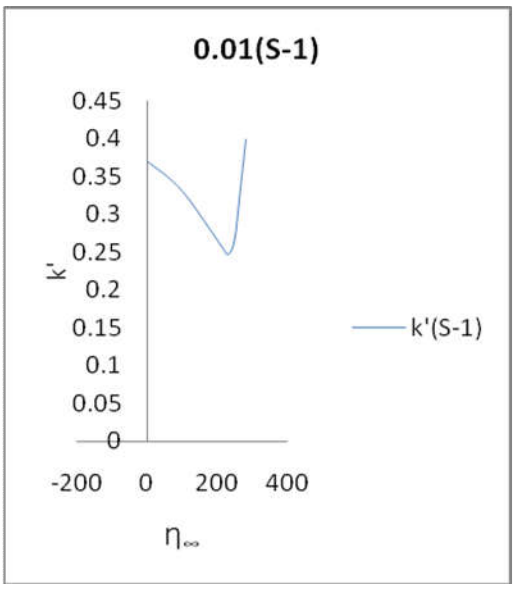

Figure A-62 Optimization of *k* for Sample G1

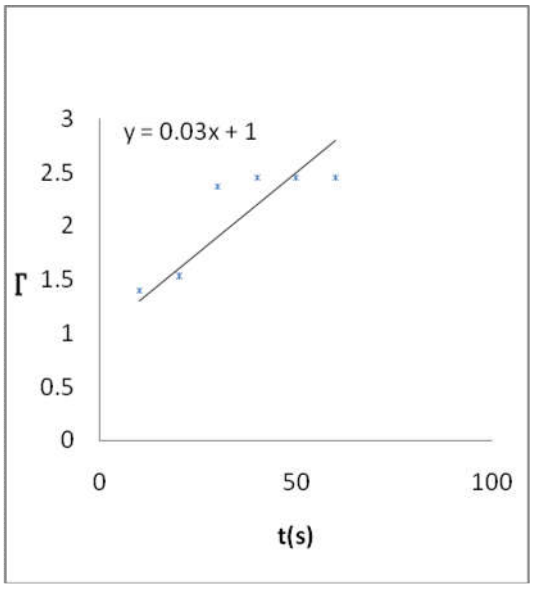

Figure A-63 Plot of Γ against time for G1

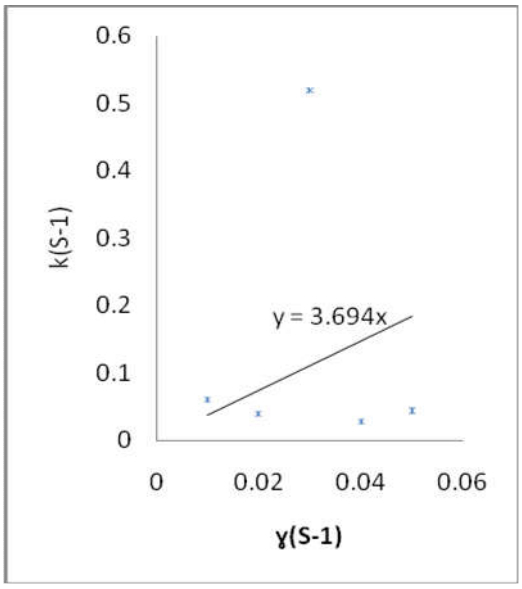

Figure A-64 Plot of k vs shear rate for G1

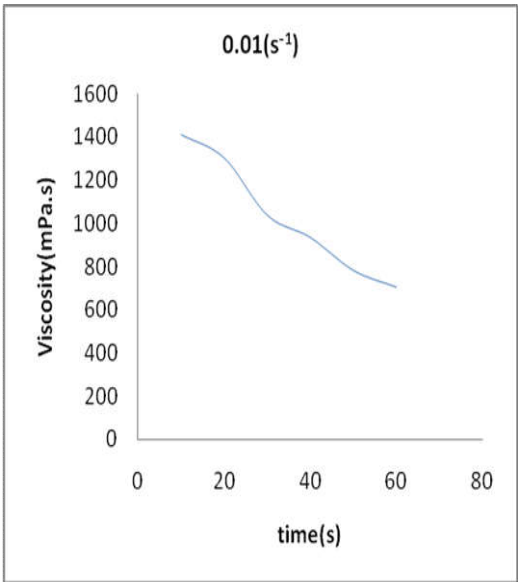

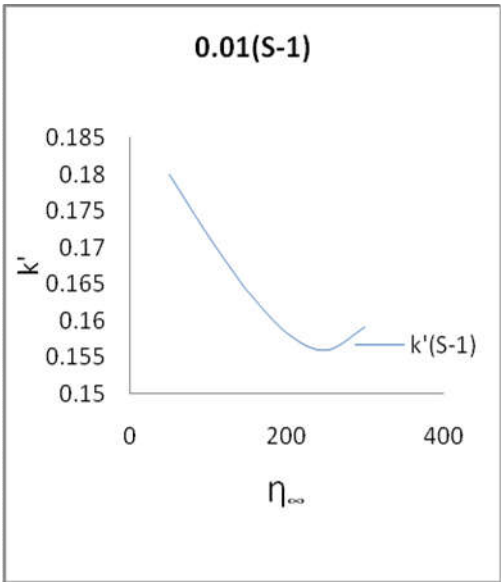

Figure A-65 Viscosity vs time plot of G2 Figure A-66 Optimization of *k* for Sample G2

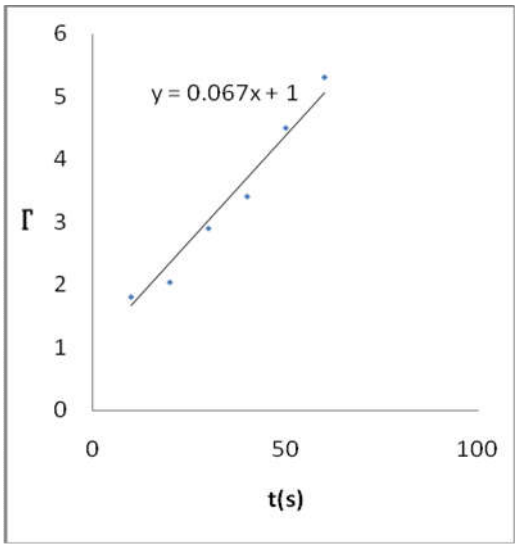

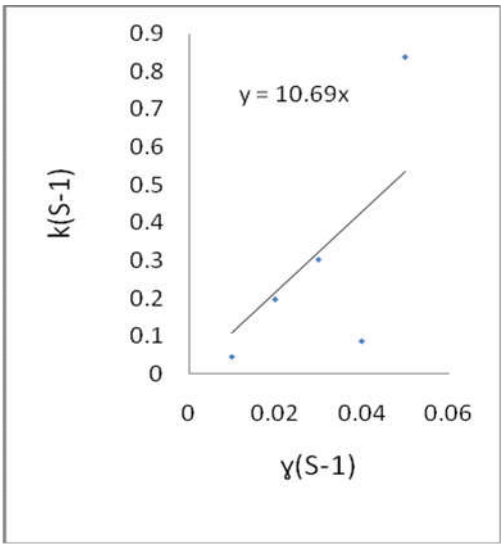

Figure A-67 Plot of Γ against time Figure A-68 Plot of k vs shear rate for G2

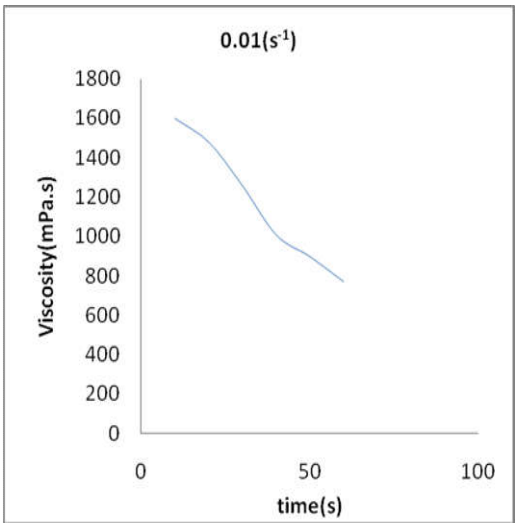

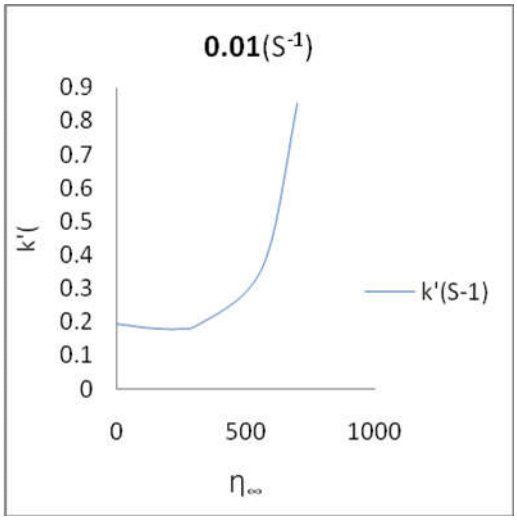

Figure A-69 Viscosity vs time plot of G3 Figure A-70 Optimization of *k* for Sample G3

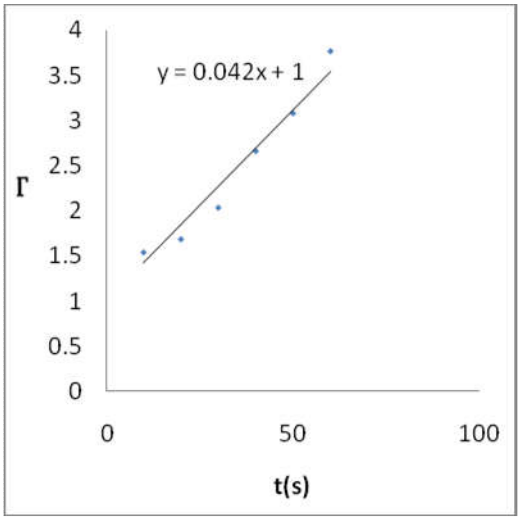

Figure A-71 Plot of Γ against time for G3

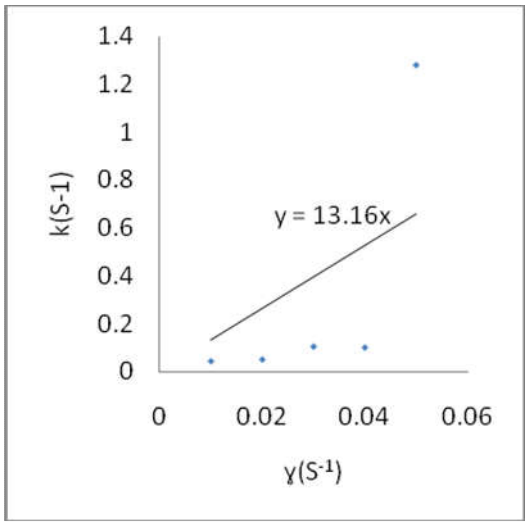

Figure A-72 Plot of k vs shear rate for G3

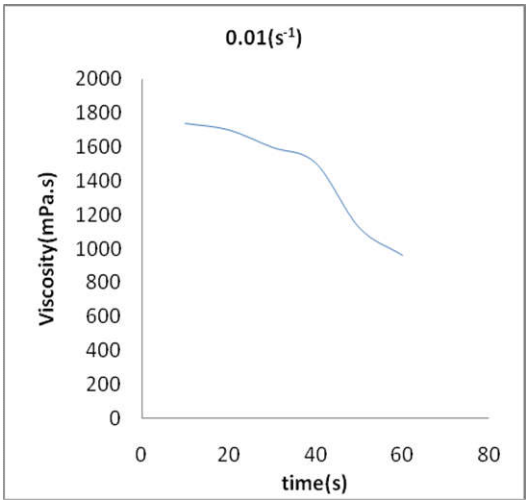

Figure A-73 Viscosity vs time plot of G4

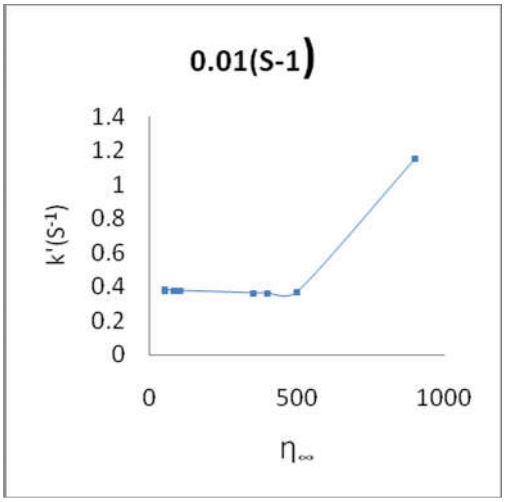

Figure A-74 Optimization of *k* for Sample G4

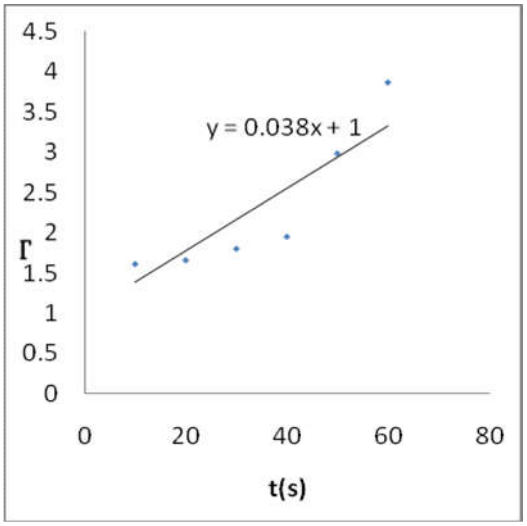

Figure A-75 Plot of Γ against time for G4

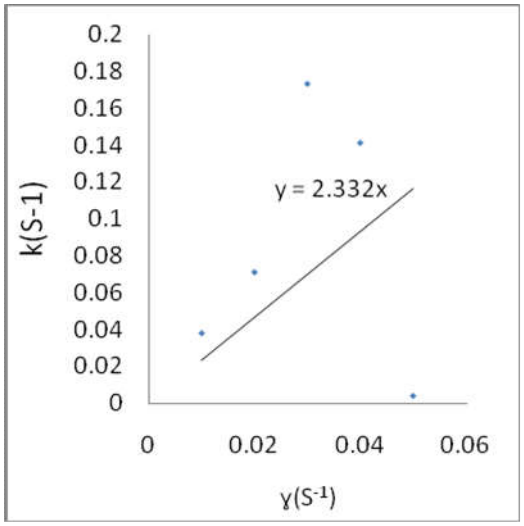

Figure A-76 Plot of k vs shear rate for G4

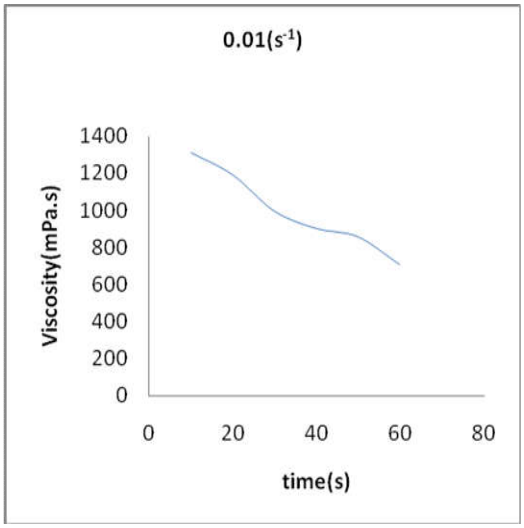

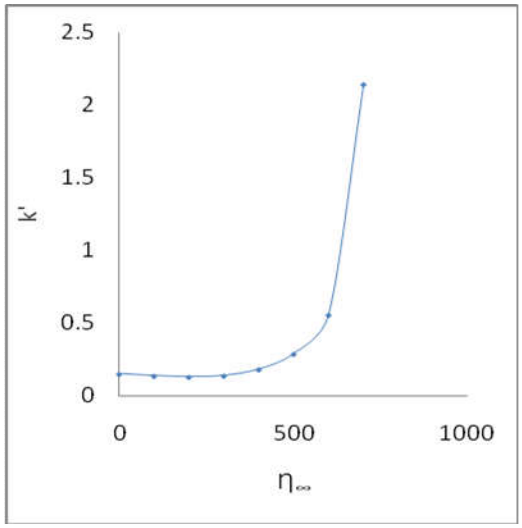

Figure A-77 Viscosity vs time plot of G5 Figure A-78 Optimization of *k* for Sample G5

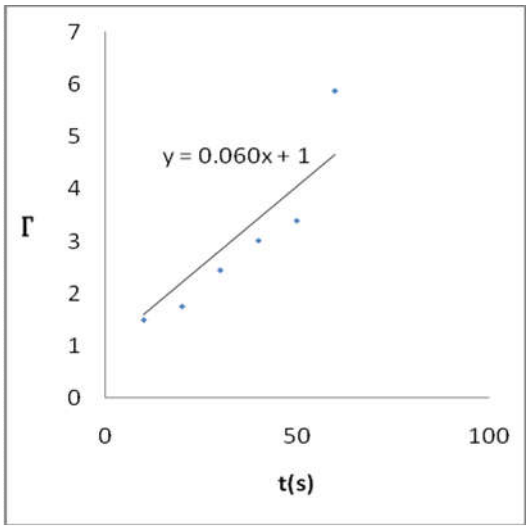

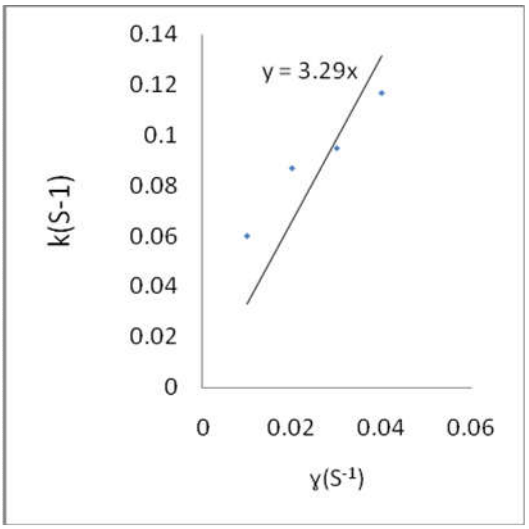

Figure A-79 Plot of Γ against time for G5 Figure A-80 Plot of k vs shear rate for G5

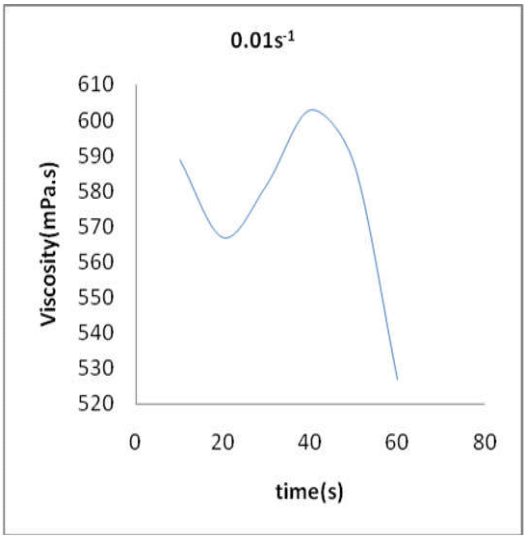

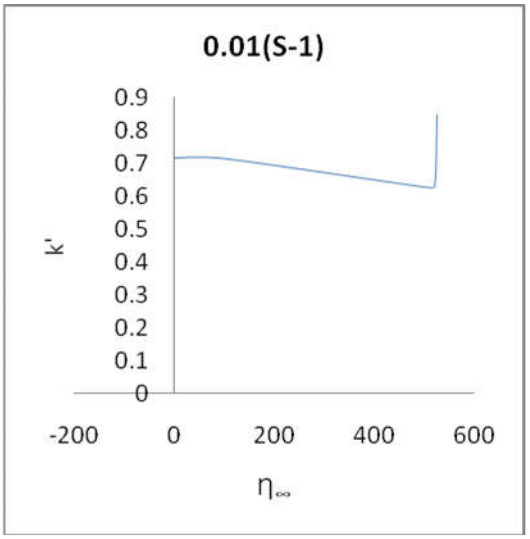

Figure A-81 Viscosity vs time plot of F1 Figure A-82 Optimization of *k* for Sample F1

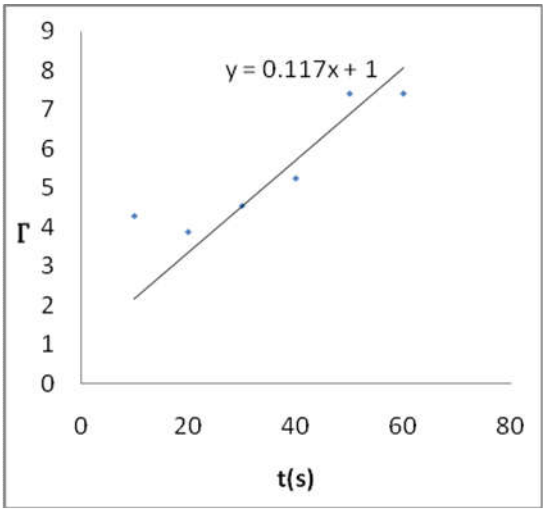

Figure A-83 Plot of Γ against time for F1

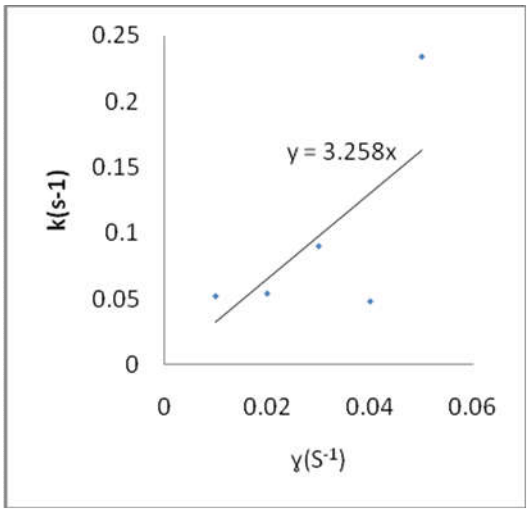

Figure A-84 Plot of k vs shear rate for F1

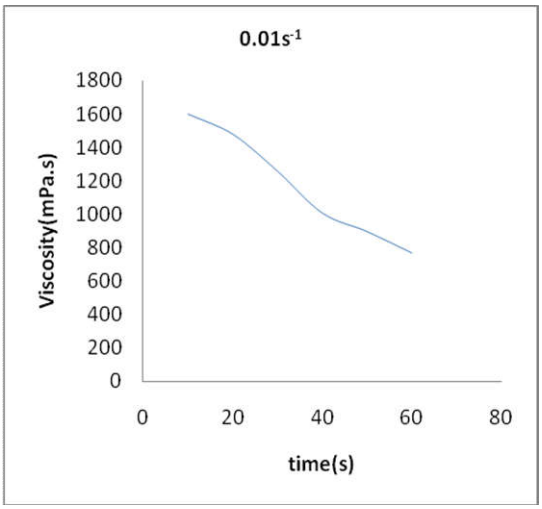

Figure A-85 Viscosity vs time plot of F2

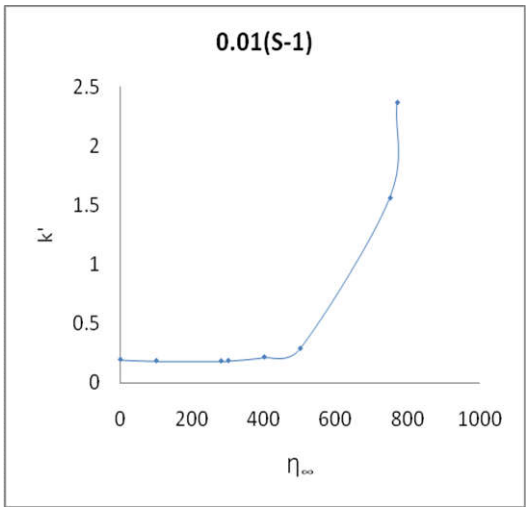

Figure A-86 Optimization of *k* for Sample F2

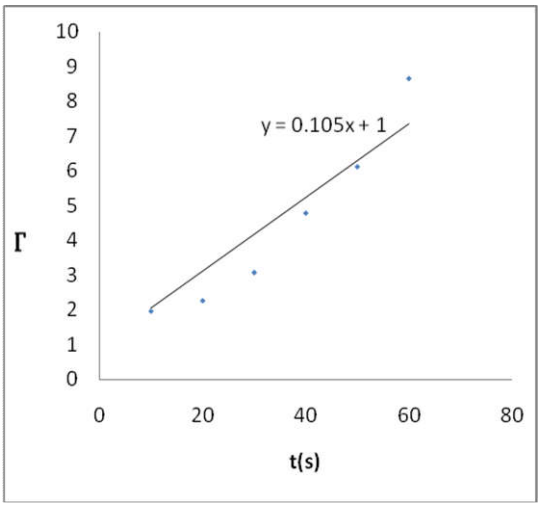

Figure A-87 Plot of Γ against time for F2

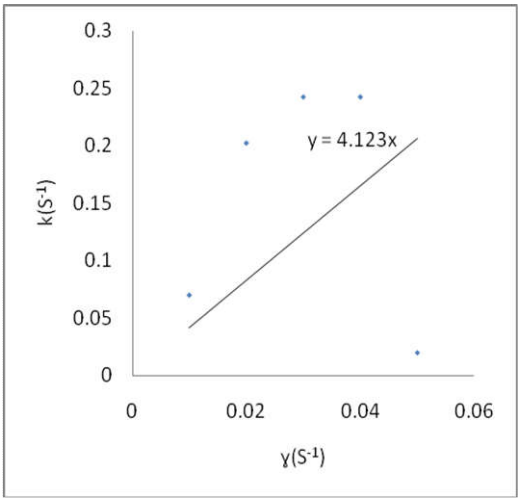

Figure A-88 Plot of *k* vs shear rate for F2

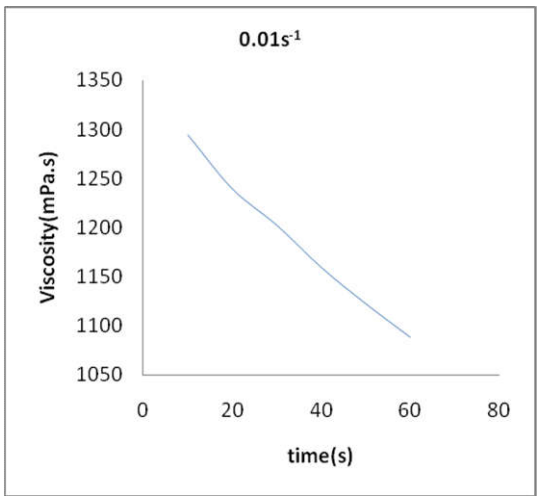

Figure A-89 Viscosity vs time plot of F3

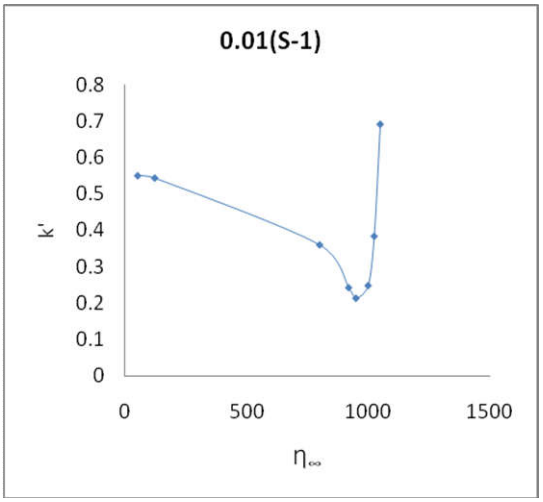

Figure A-90 Optimization of *k* for Sample F3

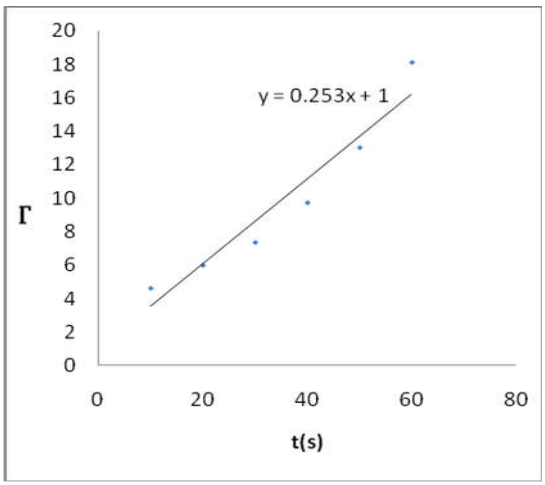

Figure A-91 Plot of Γ against time for F3

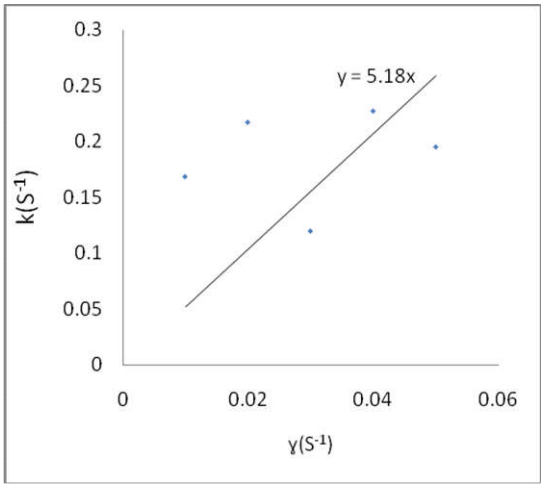

Figure A-92 Plot of k vs shear rate for F3

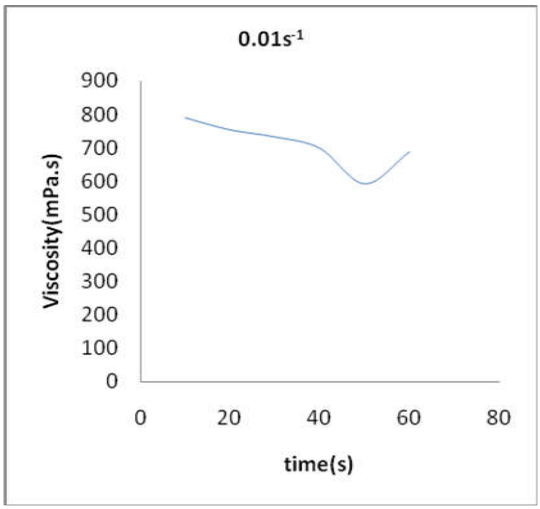

Figure A-93 Viscosity vs time plot of F4

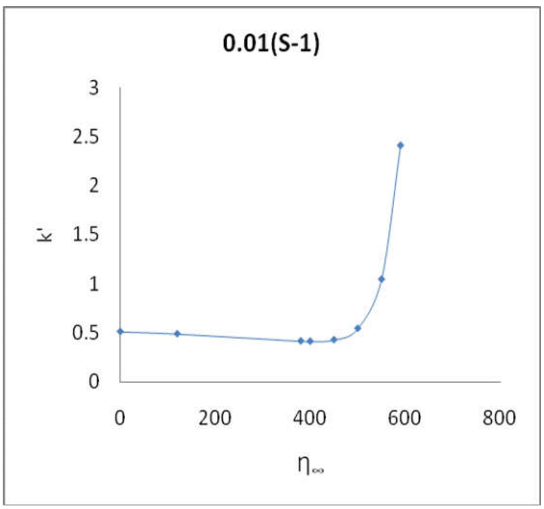

Figure A-94 Optimization of *k* for Sample F4

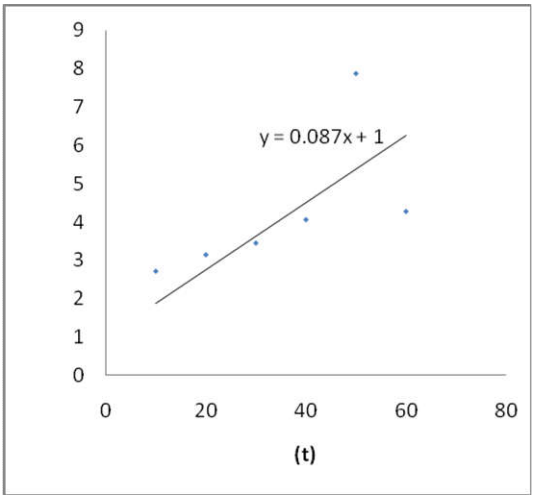

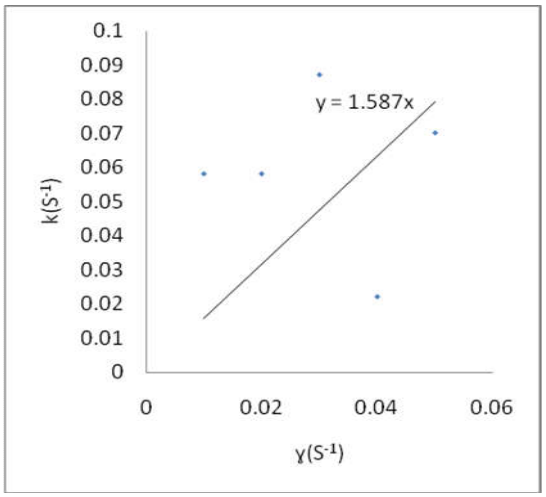

Figure A-95 Plot of Γ against time for F4 Figure A-96 Plot of k vs shear rate for F4

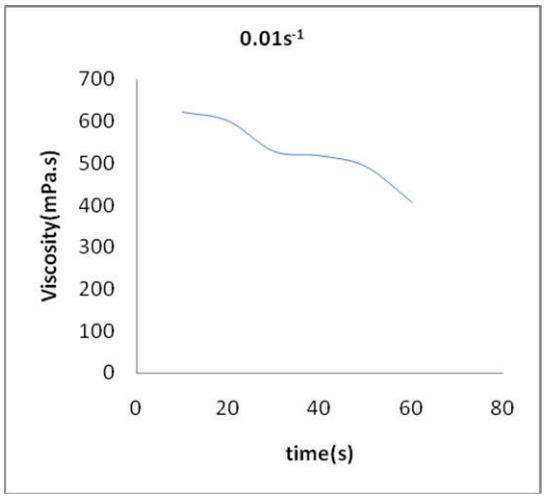

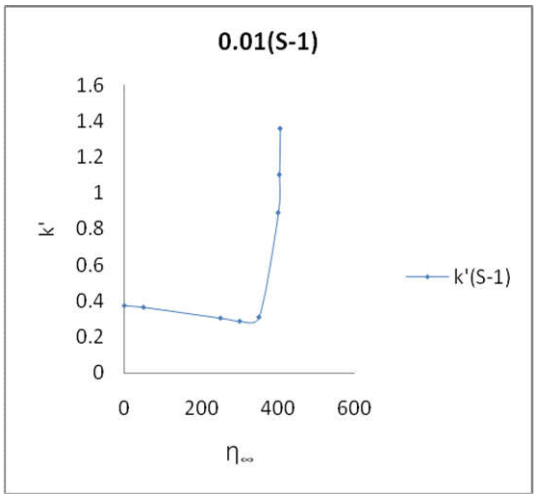

Figure A-97 Viscosity vs time plot of F5 Figure A-98 Optimization of *k* for Sample F5

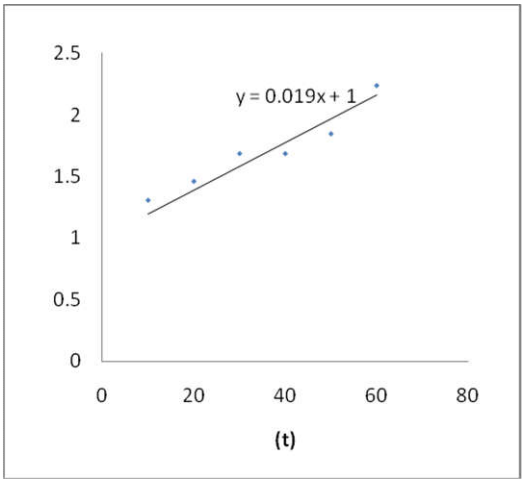

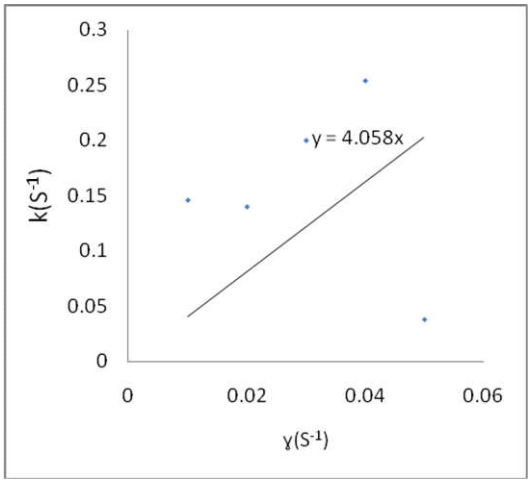

Figure A-99 Plot of Γ against time for F5 Figure A-100 Plot of k vs shear rate for F5

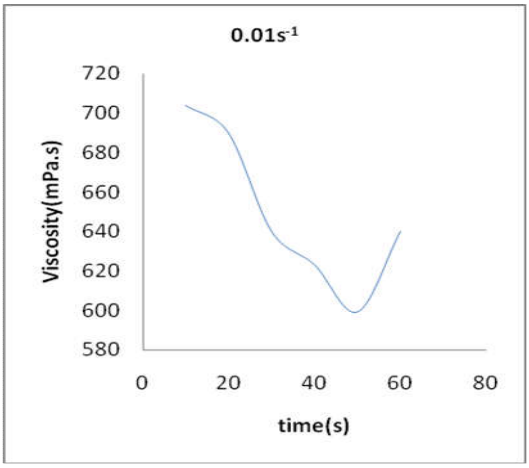

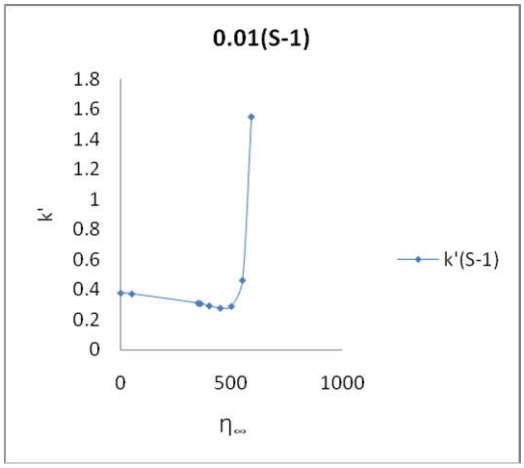

Figure A-101 Viscosity vs time plot of H1 Figure A-102 Optimization of *k* for Sample H1

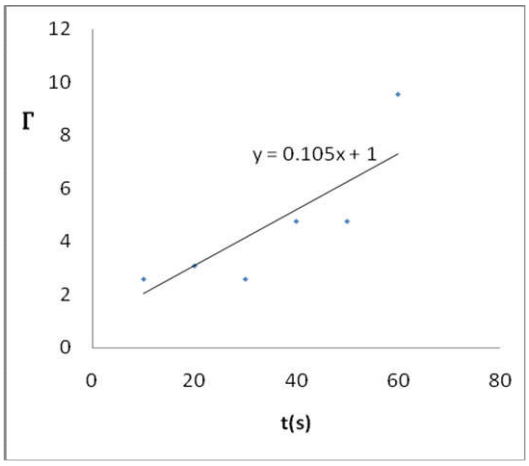

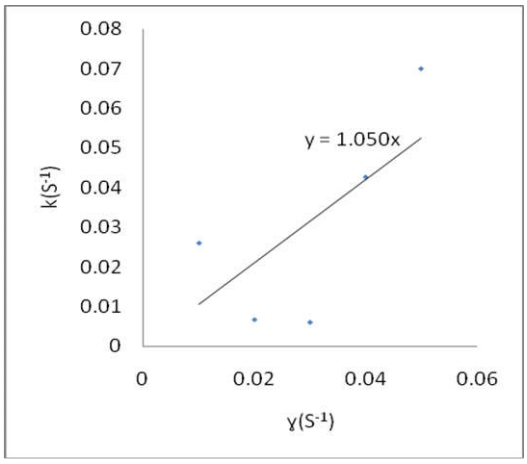

Figure A-103 Plot of Γ against time for H1 Figure A-104 Plot of k vs shear rate for H1

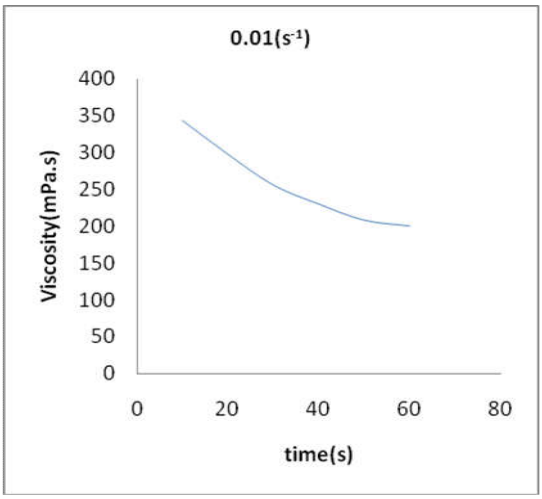

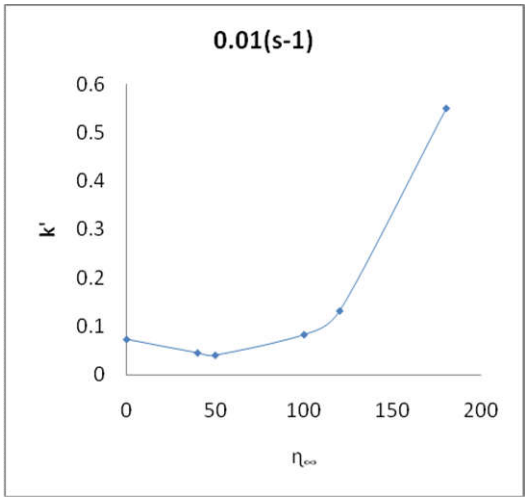

Figure A-105 Viscosity vs time plot of H2 Figure A-106 Optimization of *k* for Sample H2

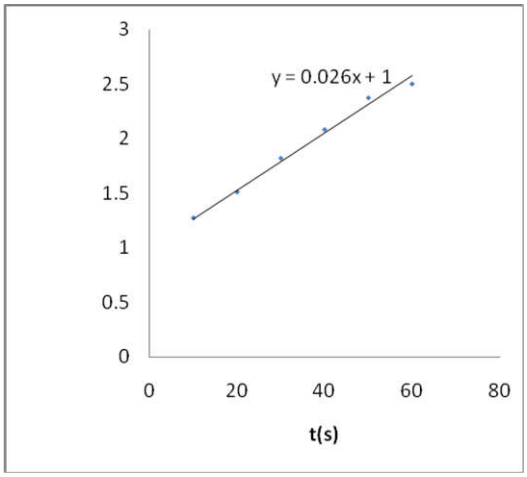

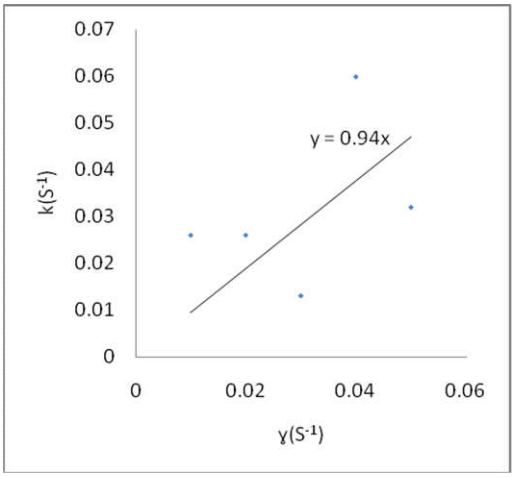

Figure A-107 Plot of Γ against time for H2 Figure A-108 Plot of k vs shear rate for H2

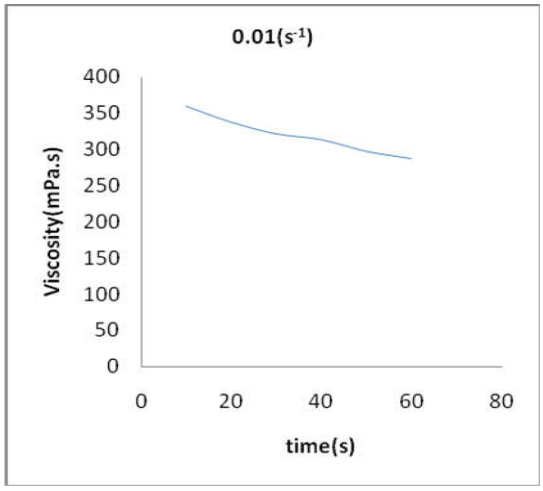

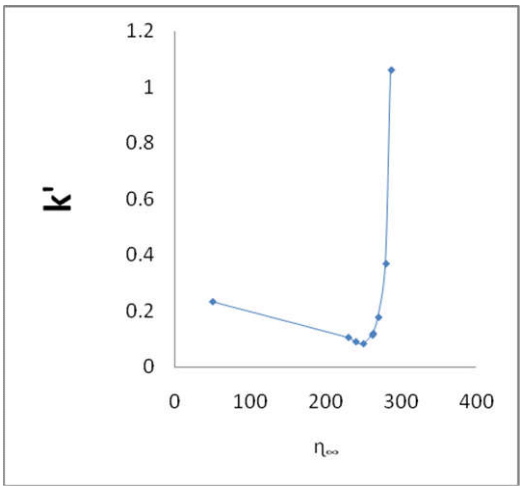

Figure A-109 Viscosity vs time plot of H3 Figure A-110 Optimization of *k* for Sample H3

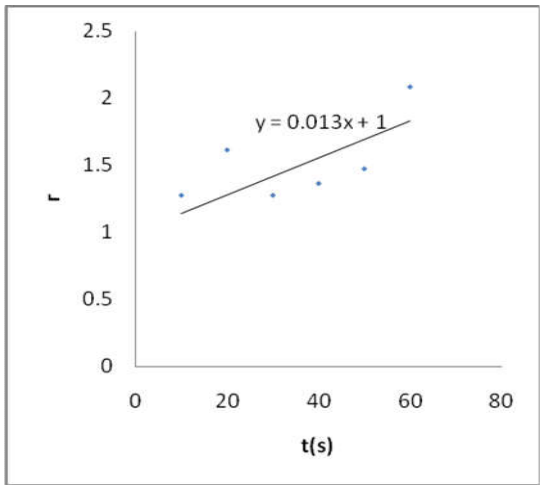

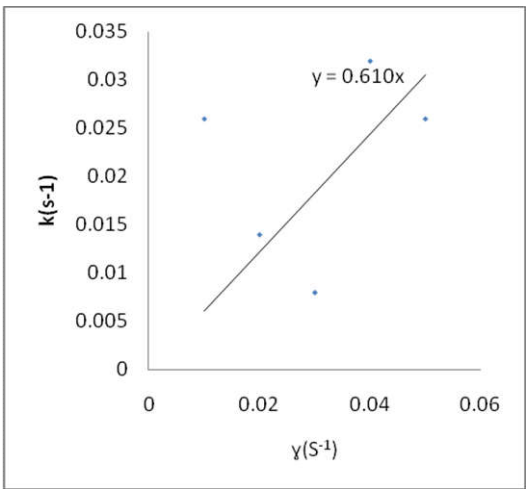

Figure A-111 Plot of Γ against time for H3 Figure A-112 Plot of k vs shear rate for H3

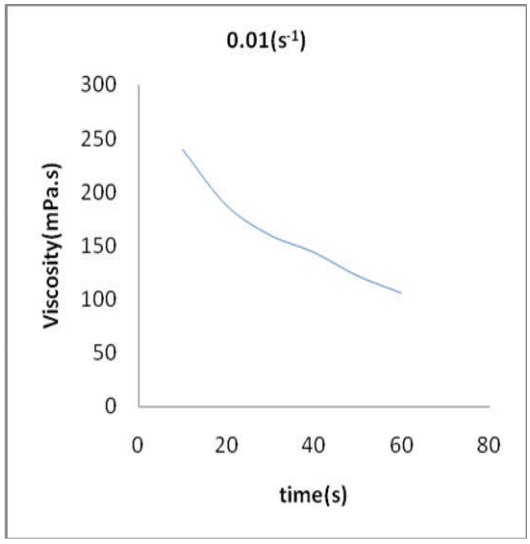

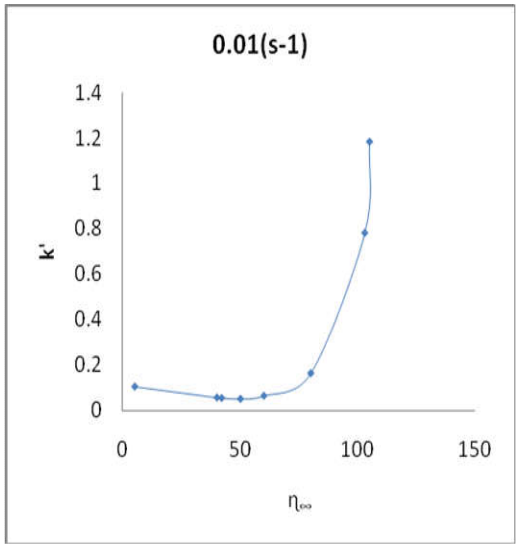

Figure A-113 Viscosity vs time plot of H5 Figure A-114 Optimization of *k* for Sample H5

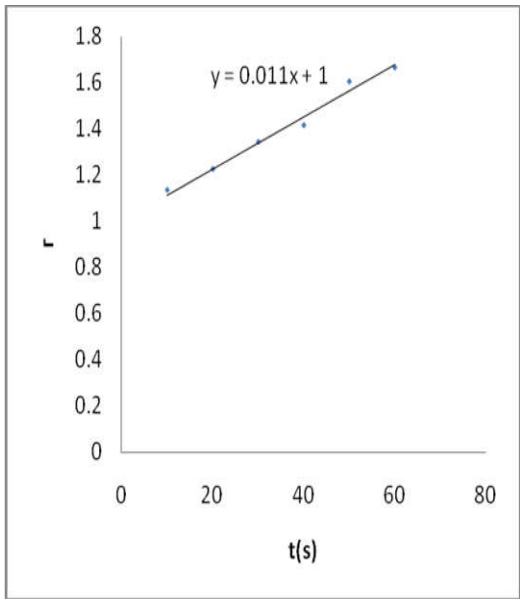

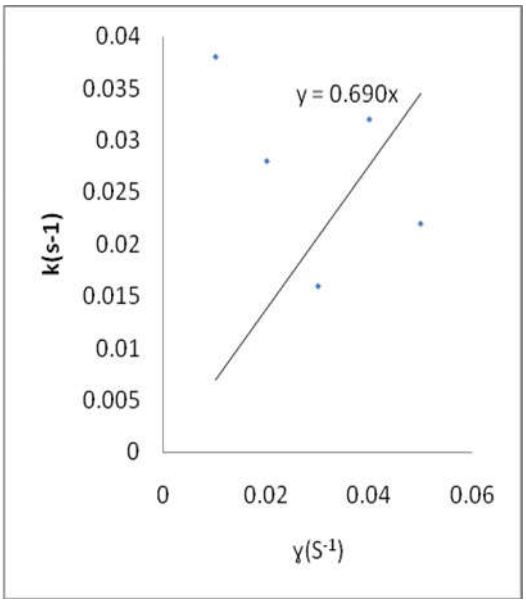

Figure A-115 Optimization of *k* for Sample H5 Figure A-116 Plot of Γ against time for H5

APPENDIX 2.3

DETAILED SKM RESULTS ON ADULTERATED SAMPLES

Table A2.1. Details of SKM Results of the Effect of Glucose Adulteration on Honey Rheology

Sample	Shear rate (S-1)	η_o	η_∞	n	k^-	k
G1	0.01	550	226	1.5	0.060	1.141
	0.02	600	365	1.5	0.040	
	0.03	750	415	1.5	0.052	
	0.04	700	370	1.5	0.028	
	0.05	300	282	1.5	0.404	
G2	0.01	2071	40	2.5	0.045	10.690
	0.02	2800	1450	2.5	0.197	
	0.03	2195	1200	2.5	0.302	
	0.04	3011	250	2.5	0.086	
	0.05	2761	1800	2.5	0.839	
G3	0.01	2352	200	2.0	0.042	13.160
	0.02	2451	1000	2.0	0.049	
	0.03	1942	1200	2.0	0.103	
	0.04	1026	450	2.0	0.099	
	0.05	673	448	2.0	1.279	
G4	0.01	2561	400	2.0	0.038	2.332
	0.02	1383	600	2.0	0.071	
	0.03	557	317	2.0	0.173	
	0.04	228	120	2.0	0.141	
	0.05	210	180	2.0	0.004	
G5	0.01	1702	200	1.5	0.060	3.290
	0.02	754	80	1.5	0.087	
	0.03	243	145	1.5	0.095	
	0.04	224	140	1.5	0.117	

Table A2.2. Details of SKM Results of the Effect of Fructose Adulteration on HoneyRheology

Sample	Shear rate (S-1)	η_o	η_∞	*n*	k^-	k
F1	0.01	766	500	1.5	0.052	3.258
	0.02	754	350	1.5	0.054	
	0.03	471	290	1.5	0.090	
	0.04	400	389	1.5	0.048	
	0.05	675	510	1.5	0.234	
F2	0.01	2351	280	2.5	0.070	4.123
	0.02	3094	2100	2.5	0.202	
	0.03	3384	2200	2.5	0.242	
	0.04	3384	2200	2.5	0.242	
	0.05	1900	1885	2.5	0.020	
F3	0.01	1902	950	2.0	0.169	5.18
	0.02	1823	1000	2.0	0.217	
	0.03	1604	680	2.0	0.120	
	0.04	1620	1000	2.0	0.227	
	0.05	1250	1205	2.0	0.193	
F4	0.01	1160	400	20.	0.041	2.360
	0.02	1160	400	2.0	0.052	
	0.03	2349	800	2.0	0.076	
	0.04	1240	1220	2.0	0.018	
	0.05	1200	1175	2.0	0.160	
F5	0.01	808	300	1.5	0.032	3.421
	0.02	1350	300	1.5	0.220	
	0.03	1178	840	1.5	0.200	
	0.04	1209	905	1.5	0.254	
	0.05	420	403	1.5	0.038	

TableA2.3. Details of SKM Results of the Effect of Water Adulteration on Honey Rheology

Sample	Shear rate (s-1)	η_o	η_∞	*n*	k^-	k
H1	0.01	800	450	2.5	0.026	0.105
	0.02	600	450	2.5	0.007	
	0.03	750	5	2.5	0.006	
	0.04	660	638	2.5	0.043	
	0.05	645	628	2.5	0.070	
H2	0.01	425	50	2.0	0.026	0.940
	0.02	425	50	2.0	0.026	
	0.03	325	155	2.0	0.013	
	0.04	280	268	2.0	0.060	
	0.05	272	263	2.0	0.032	
H3	0.01	400	240	1.5	0.026	0.610
	0.02	225	70	1.5	0.014	
	0.03	130	70	1.5	0.008	
	0.04	95	83	1.5	0.032	
	0.05	90	77	1.5	0.026	
H4	0.01	309	210	1.5	0.030	0.629
	0.02	180	70	1.5	0.022	
	0.03	120	68	1.5	0.050	
	0.04	65	60	1.5	0.008	
	0.05	60	54	1.5	0.018	
H5	0.01	320	50	1.5	0.038	0.690
	0.02	185	70	1.5	0.028	
	0.03	90	20	1.5	0.016	
	0.04	45	36	1.5	0.032	
	0.05	53	35	1.5	0.022	

SUMMARY OF STRUCTURAL KINETIC MODEL CURVE FITS TO SAMPLE RHEOGRAMS, PANORAMA VIEW OF SAMPLES AND DETAILED RESULTS ON ADULTERATED SAMPLES

Appendix 2 was divided into three segments. The first deals with the SKM curve fit of pure honey. The second covers the panorama view of adulterated samples at at shear rate of 0.01(s-1) and the third displays the detailed SKM results obtained from the curve fit. The SKM was used to obtain both structural and compositional information from honey. The structural information includes the order of deformation which reflects on the number of active components in a fluid undergoing deformation. During the adulteration of honey with hexoses and water in tables A3.1 to A3.3, the order of deformation was found to have decreased with increasing adulteration of honey. Also the rate of deformation was obtained as one of the structural information from the model. It increased with increasing adulteration of honey. Lastly, the average molecular weight which is compositional information was obtained using the SKM. The molecular weight of honey decreased with its increasing adulteration.

APPENDIX 3

NAFDAC LETTER OF

APPROVAL

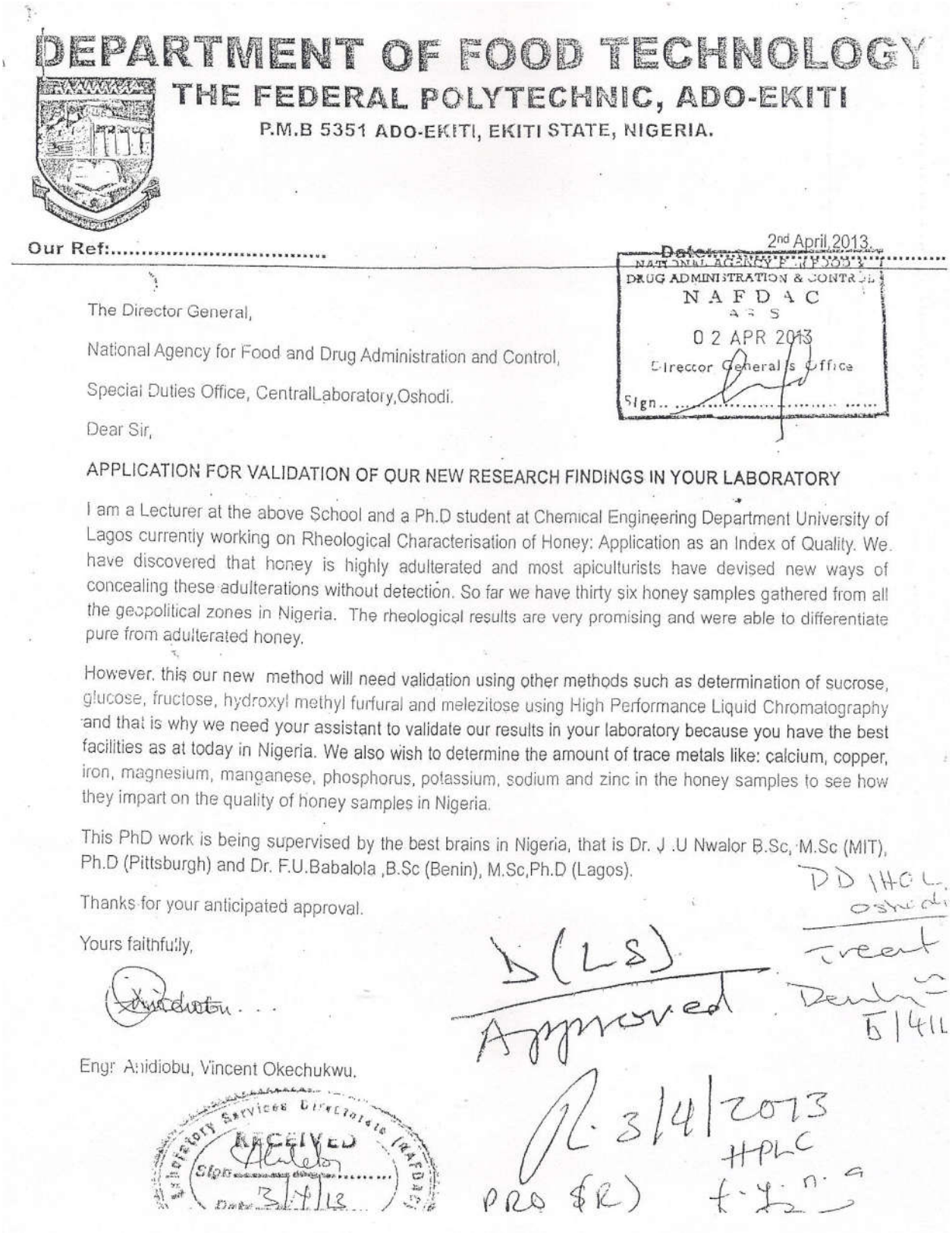

DEPARTMENT OF FOOD TECHNOLOGY

THE FEDERAL POLYTECHNIC, ADO-EKITI

P.M.B 5351 ADO-EKITI, EKITI STATE, NIGERIA.

Our Ref:.....

Date: 2nd April 2013

NATIONAL AGENCY FOR FOOD DRUG ADMINISTRATION & CONTROL
NAFDAC
A & S
02 APR 2013
Director General's Office
Sign.....

The Director General,

National Agency for Food and Drug Administration and Control,

Special Duties Office, CentralLaboratory,Oshodi.

Dear Sir,

APPLICATION FOR VALIDATION OF OUR NEW RESEARCH FINDINGS IN YOUR LABORATORY

I am a Lecturer at the above School and a Ph.D student at Chemical Engineering Department University of Lagos currently working on Rheological Characterisation of Honey: Application as an Index of Quality. We have discovered that honey is highly adulterated and most apiculturists have devised new ways of concealing these adulterations without detection. So far we have thirty six honey samples gathered from all the geopolitical zones in Nigeria. The rheological results are very promising and were able to differentiate pure from adulterated honey.

However, this our new method will need validation using other methods such as determination of sucrose, glucose, fructose, hydroxyl methyl furfural and melezitose using High Performance Liquid Chromatography and that is why we need your assistant to validate our results in your laboratory because you have the best facilities as at today in Nigeria. We also wish to determine the amount of trace metals like: calcium, copper, iron, magnesium, manganese, phosphorus, potassium, sodium and zinc in the honey samples to see how they impart on the quality of honey samples in Nigeria.

This PhD work is being supervised by the best brains in Nigeria, that is Dr. J .U Nwalor B.Sc, M.Sc (MIT), Ph.D (Pittsburgh) and Dr. F.U.Babalola ,B.Sc (Benin), M.Sc,Ph.D (Lagos).

Thanks for your anticipated approval.

Yours faithfully,

Engr Anidiobu, Vincent Okechukwu.

Safety Services Directorate (NAFDAC)
RECEIVED
Sign.....
Date 3/4/13

DD (HCL)
Oshodi
Treat
Approved
Dealt
5/4/13
3/4/2013
HPLC
PRO (SR)